
Doctoral Dissertations

Student Theses and Dissertations

Summer 2020

Experimental study on a novel EOR method -- polymeric nanogel combined with surfactant and low salinity water flooding to enhance oil recovery

Mustafa M. Almahfood

Follow this and additional works at: https://scholarsmine.mst.edu/doctoral_dissertations



Part of the [Petroleum Engineering Commons](#)

Department: Geosciences and Geological and Petroleum Engineering

Recommended Citation

Almahfood, Mustafa M., "Experimental study on a novel EOR method -- polymeric nanogel combined with surfactant and low salinity water flooding to enhance oil recovery" (2020). *Doctoral Dissertations*. 2905.
https://scholarsmine.mst.edu/doctoral_dissertations/2905

This thesis is brought to you by Scholars' Mine, a service of the Missouri S&T Library and Learning Resources. This work is protected by U. S. Copyright Law. Unauthorized use including reproduction for redistribution requires the permission of the copyright holder. For more information, please contact scholarsmine@mst.edu.

EXPERIMENTAL STUDY ON A NOVEL EOR METHOD – POLYMERIC NANOGEL
COMBINED WITH SURFACTANT AND LOW SALINITY WATER FLOODING TO
ENHANCE OIL RECOVERY

by

MUSTAFA ALMAHFOOD

A DISSERTATION

Presented to the Graduate Faculty of the

MISSOURI UNIVERSITY OF SCIENCE AND TECHNOLOGY

In Partial Fulfillment of the Requirements for the Degree

DOCTOR OF PHILOSOPHY

in

PETROLEUM ENGINEERING

2020

Approved by

Dr. Baojun Bai, Advisor

Dr. Parthasakha Neogi, Co-Advisor

Dr. Ralph Flori

Dr. Mingzhen Wei

Dr. Waleed Albazzaz

Copyright 2020
MUSTAFA ALMAHFOOD
All Rights Reserved

PUBLICATION DISSERTATION OPTION

This dissertation consists of the following five articles which have been submitted for publication, or will be submitted for publication as follows:

Paper I: Pages 7-55 have been published by Journal of Petroleum Science and Engineering.

Paper II: Pages 56-83 have been submitted to Journal of Petroleum Science.

Paper III: Pages 84-126 are intended for submission to FUEL Journal.

Paper IV: Pages 127-171 are intended for submission to Journal of Petroleum Science and Engineering.

Paper V: Pages 172-203 are intended for submission to Nature Nanotechnology Journal.

ABSTRACT

Extracting higher amounts of oil from current reservoirs is a necessity for the oil industry to enhance their profitability and sustainability. The desire to recover more oil from the existing reservoirs has led to a growing interest of nanoparticle application in enhanced oil recovery (EOR). However, most researchers have focused on the evaluation and surface modification of non-deformable nanoparticles. This dissertation evaluates the potential of deformable nanogel particles as an EOR material when they are combined with two other promising technologies - surfactant and low salinity water floodings. The particle size distribution, ζ -potential and interfacial tension were measured for a newly developed nanogel when dispersed in brine with different salinities. The core flooding experiments, using sandstone and carbonate rocks, have indicated the ability of nanogel-surfactant flooding to emulsify crude oil in-situ and produce it as oil-in-water emulsion. The results have also revealed that substantial oil recovery, up to 27%, beyond conventional seawater flooding can be obtained by nanogel combined with SDS injections and assisted with altering salinity and ionic content of post water injections. Surfactant injection has shown to reduce nanogel adsorption density on rock surfaces. The injectivity and plugging performance induced by nanogel injection through sandstone and carbonate reservoir rocks were elucidated to assess their potential as oil recovery improvement agents. Emulsification is believed to be a major recovery mechanism of nanogel-assisted surfactant flooding. Here, oil-in-water Pickering emulsions stabilized by nanogel and surfactants using different brine salinities, pH, homogenizing time were evaluated for the formulation of a stable oil droplets. The confocal microscopy images have shown that stable oil-in-water Pickering emulsions are formed by nanogel combined with anionic surfactant and low brine salinity. The results presented in this dissertation promote the effect of nanogel assisted-surfactant flooding combined with low salinity water as a promising method for enhancing oil recovery.

ACKNOWLEDGMENTS

In the Name of God, the Most Gracious, the Most Merciful. Thanks to Almighty God for giving me the opportunity, patience and strength to complete this journey.

I would like to express my sincere gratitude to my advisor Prof. Baojun Bai for the continuous support during my Ph.D study and related research, for his patience, motivation, and immense knowledge. His guidance helped me in all the time of research and writing of this dissertation. I could not have imagined having a better advisor and mentor for my Ph.D study.

I also would like to thank my co-advisor Dr. Parthasakha Neogi for his guidance and valuable discussions during my research.

I would also like to thank the rest of my committee members: Dr. Ralph Flori, Dr. Mingzhen Wei, and Dr. Waleed Albazzaz for their insightful comments and encouragement.

My sincere appreciation also goes to Dr. Ali Alhuraishawy and Dr. Jaming Geng, who have helped me during the early stages of my research. I am also very thankful for our research group colleagues: Ali Albrahim, Yandong Zhang, Yifu Long, Jianqiao Leng, Haifeng Ding, Adriane Melnyczuk and Yang Zhao for their help and support.

A special thanks goes to my parents: Mohammed Almahfood and Zahraa Alsaif for their continuous support, encouragement and prayers throughout these years. This would have never been accomplished without their guidance and help. I would also like to thank my sisters: Ebtahal, Batoool and Hawraa for their continuous love.

Last but not least, I would like to thank my lovely wife, Eithar, and my son, Mohammed, for their love, support and patience throughout this journey. You made this journey memorable. You are without a doubt part of this accomplishment.

TABLE OF CONTENTS

	Page
PUBLICATION DISSERTATION OPTION	iii
ABSTRACT	iv
ACKNOWLEDGMENTS	v
LIST OF ILLUSTRATIONS	xiii
LIST OF TABLES	xx
 SECTION	
1. INTRODUCTION.....	1
1.1. STATEMENT AND SIGNIFICANCE OF THE PROBLEM.....	1
1.2. POTENTIAL IMPACT AND CONTRIBUTIONS.....	4
1.3. STATEMENT OF WORK.....	4
1.3.1. Objectives	4
1.3.2. Scope of Work.....	5
 PAPER	
I. LITERATURE REVIEW: THE SYNERGISTIC EFFECTS OF NANOPARTICLE-SURFACTANT NANOFLUIDS IN EOR APPLICATIONS	7
ABSTRACT	7
1. INTRODUCTION	8
2. TYPES OF NANOPARTICLES.....	12
3. RECOVERY MECHANISMS OF NANOPARTICLE FLOODING	12

3.1.	NANOFLUIDS	14
3.1.1.	Disjoining Pressure	14
3.1.2.	IFT Reduction	16
3.1.3.	Wettability Modification	17
3.1.4.	Discussion of Nanofluid Recovery Mechanisms	19
3.2.	NANOEMULSION	20
3.3.	NANO-CATALYSTS	22
4.	COMBINATION OF NANOPARTICLES AND SURFACTANTS	22
4.1.	ROCK WETTABILITY MODIFICATION	24
4.2.	OIL-WATER INTERFACIAL TENSION (IFT) REDUCTION	29
4.2.1.	Silica Nanoparticles	29
4.2.2.	Metallic Oxide Nanoparticles	36
4.3.	OIL VISCOSITY REDUCTION AND CONFORMANCE CONTROL	37
4.4.	DISCUSSION OF SURFACTANTS-NANOPARTICLES RECOVERY MECHANISMS	39
5.	CHALLENGES AND LIMITATIONS	40
6.	CONCLUSION	44
	NOMENCLATURE	45
	REFERENCES	45
II.	CHARACTERIZATION AND OIL RECOVERY ENHANCEMENT BY A POLYMERIC NANO GEL COMBINED WITH SURFACTANT FOR SANDSTONE RESERVOIRS	56
	ABSTRACT	56
1.	INTRODUCTION	57
2.	EXPERIMENT	59
2.1.	MATERIALS	59
2.2.	NANO GEL SYNTHESIS	59

2.3.	NANOGEL SIZE DISTRIBUTION AND ZETA POTENTIAL	60
2.4.	RHEOLOGICAL PROPERTIES	61
2.5.	INTERFACIAL TENSION MEASUREMENTS	61
2.6.	POROUS MEDIA	61
2.7.	CORE FLOODING EXPERIMENTS.....	62
2.7.1.	Experimental Procedure.....	62
2.7.2.	Injection Scheme	64
3.	RESULTS AND DISCUSSION.....	65
3.1.	SIZE DISTRIBUTION OF NANOGEL	65
3.2.	RHEOLOGICAL PROPERTIES	66
3.3.	INTERFACIAL TENSION MEASUREMENTS	68
3.4.	CONCENTRATION OF NANOGEL DISPERSIONS.....	73
3.5.	CONFIRMATION OF ENHANCED OIL RECOVERY BY CORE FLOODING	74
3.5.1.	Injection Scheme	75
4.	CONCLUSION	79
	NOMENCLATURE.....	80
	REFERENCES	81
III. EXPERIMENTAL INVESTIGATION OF POLYMERIC NANOGEL COM- BINED WITH SURFACTANT AND LOW SALINITY WATER FLOODING FOR SANDSTONE RESERVOIRS		84
	ABSTRACT	84
1.	INTRODUCTION	85
2.	EXPERIMENT.....	87
2.1.	MATERIALS	87
2.2.	NANOGEL SYNTHESIS.....	87
2.3.	BRINE	88

2.4.	CRUDE OIL	89
2.5.	RHEOLOGICAL PROPERTIES	89
2.6.	SANDSTONE ROCK	89
2.7.	EXPERIMENTAL SETUP AND PROCEDURE.....	90
2.8.	NANO GEL SIZE DISTRIBUTION AND ZETA POTENTIAL	92
2.9.	DYNAMIC ADSORPTION AND DESORPTION MEASUREMENTS	92
2.10.	INJECTIVITY AND PLUGGING PERFORMANCE OF NANO GEL IN SANDSTONE.....	93
3.	RESULTS AND DISCUSSION	94
3.1.	SIZE DISTRIBUTION OF NANO GEL	94
3.2.	CONFIRMATION OF ENHANCED OIL RECOVERY BY CORE FLOODING	96
3.2.1.	Validation of Nanogel and SDS Injection Sequence	97
3.2.2.	Effect of Nanogel Concentration.....	100
3.2.3.	Evaluation of Nanogel and SDS One-Slug Injection Mode	104
3.2.4.	Effect of Diluted Seawater Salinity	106
3.2.5.	Effect of Nanogel Concentration Combined with Diluted Waterflooding.....	109
3.2.6.	Evaluation of Nanogel and SDS One-Slug Injection Mode	111
3.3.	DYNAMIC ADSORPTION AND DESORPTION MEASUREMENTS	113
3.4.	INJECTIVITY AND PLUGGING PERFORMANCE OF NANO GEL IN SANDSTONE.....	117
3.5.	DISCUSSION	119
4.	CONCLUSIONS	122
	NOMENCLATURE	124
	REFERENCES	124

IV. EXPERIMENTAL EVALUATION OF POLYMERIC NANOGEL COMBINED WITH SURFACTANT AND LOW SALINITY WATER FLOODING FOR CARBONATE RESERVOIRS	127
ABSTRACT	127
1. INTRODUCTION	128
2. EXPERIMENT	131
2.1. MATERIALS	131
2.2. NANOGEL SYNTHESIS	132
2.3. BRINE	132
2.4. CRUDE OIL	133
2.5. CARBONATE ROCK	134
2.6. NANOGEL SIZE DISTRIBUTION AND ZETA POTENTIAL	135
2.7. RHEOLOGICAL PROPERTIES	135
2.8. CORE FLOODING EXPERIMENTAL SETUP AND PROCEDURE	135
2.9. NANOGEL DYNAMIC ADSORPTION AND DESORPTION MEASUREMENTS	138
2.10. INJECTIVITY AND PLUGGING PERFORMANCE OF NANOGEL ON CARBONATE CORES	139
3. RESULTS AND DISCUSSION	140
3.1. SIZE DISTRIBUTION OF NANOGEL	140
3.2. CONFIRMATION OF ENHANCED OIL RECOVERY BY CORE FLOODING	142
3.2.1. Base Cases	143
3.2.2. Validation of Nanogel Potential	146
3.2.3. Validation of Nanogel Coupled with SDS Potential	149
3.2.4. Effect of Nanogel and SDS Concentration	152
3.2.5. Evaluation of Nanogel and SDS One-Slug Injection Mode	155
3.3. DYNAMIC ADSORPTION AND DESORPTION MEASUREMENTS	158

3.4.	INJECTIVITY AND PLUGGING PERFORMANCE OF NANOGEL	161
3.5.	DISCUSSION	163
4.	CONCLUSION	164
	NOMENCLATURE	165
	REFERENCES	166
V.	STABILITY OF OIL-IN-WATER PICKERING EMULSION IN THE PRESENCE OF POLYMERIC NANOGELS AND SURFACTANTS	172
	ABSTRACT	172
1.	INTRODUCTION	173
2.	EXPERIMENT	175
2.1.	MATERIALS	175
2.2.	NANOGEL SYNTHESIS	176
2.3.	SURFACTANTS	176
2.4.	BRINE PROPERTIES	178
2.5.	CRUDE OIL	179
2.6.	VISCOSITY MEASUREMENTS	179
2.7.	PREPARATION OF PICKERING EMULSION SYSTEMS	179
2.8.	CHARACTERIZATION OF NANOGEL AND SURFACTANTS ...	181
2.9.	PICKERING EMULSION CHARACTERIZATION	181
2.9.1.	Methodology	181
3.	RESULTS AND DISCUSSION	183
3.1.	CHARACTERIZATION OF NANOGEL AND SURFACTANTS ...	183
3.2.	PICKERING EMULSION CHARACTERIZATION	185
3.3.	EFFECT OF BRINE SALINITY ON NANOGEL-SURFACTANT PICKERING EMULSION	186
3.4.	EFFECT OF PH ON NANOGEL-SURFACTANT PICKERING EMULSION	189

3.5. EFFECT OF HOMOGENIZING TIME ON NANOGEL - SUR- FACTANT PICKERING EMULSION	192
4. CONCLUSIONS	196
NOMENCLATURE	201
REFERENCES	201
SECTION	
2. CONCLUSIONS AND RECOMMENDATIONS	204
2.1. CONCLUSIONS	204
2.2. RECOMMENDATIONS	206
APPENDIX	207
REFERENCES	209
VITA	227

LIST OF ILLUSTRATIONS

Figure	Page
SECTION	
1.1. Research Scope.	6
PAPER I	
1. EOR target for different hydrocarbons.....	9
2. Microscopic images of (a) Titanium oxide, (b) aluminum oxide, (c) Nickel oxide, and (d) silicon oxide. Figure was obtained from Alomair <i>et al.</i> (2014). ...	10
3. Nanoscale comparison. Figure was obtained from Lau <i>et al.</i> (2017).	11
4. An illustration of the huge surface area of nanoparticles.	12
5. Nanofluid wedge-film structure. The figure was obtained from Lau <i>et al.</i> (2017). ...	16
6. Typical Pendant Drop Apparatus. The figure was obtained from Arashiro and Demarquette (1999).	17
7. IFT measurement of oil-brine/nanofluid system at various nanoparticle concentrations. Data were obtained from Li <i>et al.</i> (2013a).....	18
8. A schematic diagram of rock wettability systems. Figure was obtained from Ogunberu and Ayub (2005).	19
9. Contact angle measurements of SiO_2 nanoparticles in air and oil as a function of concentration. Figure was obtained from Al-Anssari <i>et al.</i> (2016).	20
10. Nano-emulsions observed during nano-flooding process. Figure was obtained from Li <i>et al.</i> (2013b).	21
11. Optical micrographs of emulsions stabilized with 1% silica nanoparticles (NP)+0.05% CAPB at (a) pH 4; (b) pH 6; and (c) pH 8. Micrographs taken 1 day after emulsion formation. Figure was obtained from Worthen <i>et al.</i> (2013)..	24
12. Contact angle measurement of non-ionic surfactant (TX-100) and silica nanoparticles. The data were obtained from Hunter <i>et al.</i> (2009).	26
13. Interfacial tension of the oil-water system at different surfactant concentrations. The data were obtained from Ravera <i>et al.</i> (2008).	31
14. The change in interfacial tension due to the change in NP concentration. The plot was obtained from Jiang <i>et al.</i> (2016).	32

15. Interfacial tension changes with surfactant concentration. The plot was obtained from Jiang <i>et al.</i> (2016).	33
16. Heavy oil viscosity reduction using surfactant-based <i>CuO</i> nanofluid. The plot was obtained from Srinivasan <i>et al.</i> (2014).	40

PAPER II

1. (A) Dried Na-AMPS nanogel. (B) Na-AMPS nanogel dispersed in seawater.	60
2. Schematic of the experimental setup.	63
3. Hydrodynamic diameter distribution of Na-AMPS nanogel in seawater and diluted seawater measured at a concentration of 1 gram/liter and a temperature of 25° C.	66
4. Nanogel stability evaluation in seawater for a two-week time period.	67
5. The change in zeta potential in the mixed nanogel-SDS solutions dispersed in seawater and measured at a temperature of 25° C. SDS concentration is kept constant at 1,000 ppm.	68
6. Viscosity of varying concentration of nanogel dispersions combined with SDS at different shear rates. SDS concentration is kept constant at 1,000 ppm.	69
7. Relative viscosity η_r of different concentrations of nanogel dispersions combined with SDS in seawater at shear rate of 120 s ⁻¹ . SDS concentration is kept constant at 1,000 ppm.	70
8. Surface tension between air and varying concentration of nanogel dispersions combined with SDS at a temperature of 25° C. SDS concentration is kept constant at 1,000 ppm.	71
9. Dynamic interfacial tension between mineral oil and varying concentrations of nanogel dispersions combined with SDS. SDS concentration is kept constant at 1,000 ppm.	72
10. Equilibrium interfacial tension of nanogel dispersions combined with SDS. SDS concentration is kept constant at 1,000 ppm.	73
11. Oil recovery factor and water cut results of core A-3.	75
12. Oil recovery factor and water cut results of core A-2.	76
13. Injection pressure results of core A-3 using sequential injections of nanogel and SDS followed by seawater flooding.	77

14.	Injection pressure results of core A-8 using one-slug injection of nanogel-SDS (500 ppm each) followed by alternating seawater and 10-times diluted seawater injections.	78
15.	Resistance factor calculated at the end of NG/SDS injection and residual resistance factor calculated using stabilized pressure of last water slug of all employed cores.	79

PAPER III

1.	(A) Dried Na-AMPS nanogel. (B) Na-AMPS nanogel dispersed in seawater. ...	88
2.	Schematic of the experimental setup.	92
3.	Calibration curve of nanogel standards at the peak wavelength of 209 nm.	93
4.	Particle size distribution of nanogel dispersed in several brine types at a concentration of 1 gram/liter and a temperature of 25° C.	95
5.	Nanogel stability evaluation in different water types for a two-week time period.	96
6.	Oil recovery factor and water cut of Core B-1.	98
7.	Injection pressure of Core B-1.	99
8.	Oil recovery factor and water cut of Core B-2.	100
9.	Injection pressure of Core B-2.	101
10.	Oil recovery factor and water cut of Core B-3.	102
11.	Injection pressure of Core B-3.	103
12.	Oil recovery factor and water cut of Core B-4.	104
13.	Injection pressure of Core B-4.	105
14.	Oil recovery factor and water cut of Core B-5.	106
15.	Injection pressure of Core B-5.	107
16.	Oil recovery factor and water cut of Core B-6.	108
17.	Injection pressure of Core B-6.	109
18.	Oil recovery factor and water cut of Core B-7.	110
19.	Injection pressure of Core B-7.	111
20.	Oil recovery factor and water cut of Core B-8.	112
21.	Injection pressure of Core B-8.	113

22.	Oil recovery factor and water cut of Core B-9.	114
23.	Injection pressure of Core B-9.	115
24.	Oil recovery factor and water cut of Core B-10.	116
25.	Injection pressure of Core B-10.....	117
26.	Oil recovery factor and water cut of Core B-11.	118
27.	Injection pressure of Core B-11.....	119
28.	Effluent nanogel concentration and injection pressure as a function of injection volume of dynamic adsorption using Core B-12.	120
29.	Effluent nanogel concentration and injection pressure as a function of injection volume of dynamic desorption using Core B-12.....	121
30.	Resistance factor calculated at the end of NG/SDS injection and residual resistance factor calculated using stabilized pressure of last water slug of all cores used in core flooding experiments.....	122

PAPER IV

1.	(A) Dried Na-AMPS nanogel. (B) Na-AMPS nanogel dispersed in seawater. ...	133
2.	Schematic of the experimental setup.	137
3.	Calibration curve of nanogel standards at the peak wavelength of 207 nm.	138
4.	Particle size distribution of nanogel dispersed in several brine types at a concentration of 1 gram/liter and a temperature of 25° C.	141
5.	Nanogel stability evaluation in different water types for a two-week time period.	142
6.	Oil recovery factor and water cut of core C-1.	144
7.	Injection pressure profile of core C-1.....	144
8.	Oil recovery factor and water cut of core C-2.	145
9.	Injection pressure profile of Core C-2.	146
10.	Oil recovery factor and water cut of Core C-3.	147
11.	Injection pressure profile of Core C-3.	147
12.	Oil recovery factor and water cut of Core C-4.	148
13.	Injection pressure profile of Core C-4.	149
14.	Oil recovery factor and water cut of Core C-5.	150

15.	Injection pressure profile of Core C-5.	150
16.	Oil recovery factor and water cut of Core C-6.	151
17.	Injection pressure profile of Core C-6.	152
18.	Oil recovery factor and water cut of Core C-7.	153
19.	Injection pressure profile of Core C-7.	153
20.	Oil recovery factor and water cut of Core C-8.	154
21.	Injection pressure profile of Core C-8.	155
22.	Oil recovery factor and water cut of Core C-9.	156
23.	Injection pressure profile of Core C-9.	156
24.	Oil recovery factor and water cut of Core C-10.	157
25.	Injection pressure profile of Core C-10.	158
26.	Effluent nanogel concentration and injection pressure profile as a function of injection volume of dynamic adsorption using Core C-11.	160
27.	Effluent nanogel concentration and injection pressure profile as a function of injection volume of dynamic desorption using Core C-11.	160
28.	Resistance factor calculated at the end of NG/SDS injection and residual resistance factor calculated using stabilized pressure of last water slug of all cores used in core flooding experiments.	161
29.	Pressure profile of core C-12 used to evaluate the injectivity and plugging performance caused by nanogel.	162

PAPER V

1.	(A) Dried Na-AMPS nanogel. (B) Na-AMPS nanogel dispersed in seawater. ...	176
2.	Surface tension of a surfactant solution with increasing concentration leading to forming micelles.	177
3.	Processes of Emulsion Breakage.	180
4.	An illustration of emulsified oil droplet stabilized by nanogel and surfactant. 3-D confocal images show oil droplets in green and nanogel-surfactant clusters in white.	182
5.	Particle size distribution of nanogel dispersed in several brine types at a concentration of 1 gram/liter and a temperature of 25° C.	184

6. ζ potential of cationic, anionic, and neutral surfactants combined with anionic nanogel at various brine salinities. 185
7. Confocal microscopy images of emulsions stabilized by 0.1 wt.% nanogel dispersed in (A) 100-times diluted seawater, and (B) seawater. Emulsified oil drops are shown in green color. Scale bars are 5 μm . Particle size distribution of emulsified oil droplets stabilized by nanogel in (C) 100-times diluted seawater, and (D) seawater. 187
8. Confocal microscopy images of emulsions stabilized by 0.1 wt.% Tween[®] 60 dispersed in (A) 100-times diluted seawater, and (B) seawater. Emulsified oil drops are shown in green color. Scale bars are 5 μm . Particle size distribution of emulsified oil droplets stabilized by Tween[®] 60 in (C) 100-times diluted seawater, and (D) seawater. 188
9. Confocal microscopy images of emulsions stabilized by 0.1 wt.% CTAB dispersed in (A) 100-times diluted seawater, and (B) seawater. Emulsified oil drops are shown in green color. Scale bars are 5 μm . Particle size distribution of emulsified oil droplets stabilized by CTAB in (C) 100-times diluted seawater, and (D) seawater. 189
10. Confocal microscopy images of emulsions stabilized by 0.1 wt.% SDS dispersed in (A) 100-times diluted seawater, and (B) seawater. Emulsified oil drops are shown in green color. Scale bars are 5 μm . Particle size distribution of emulsified oil droplets stabilized by SDS in (C) 100-times diluted seawater, and (D) seawater. 190
11. Confocal microscopy images of Pickering emulsions stabilized by 0.1 wt.% nanogel and Tween[®] 60 dispersed in 100-times diluted seawater at pH from 1 to 13. Scale bars are 5 μm . (H) the average diameter of emulsified oil droplets. . 192
12. Confocal microscopy images of Pickering emulsions stabilized by 0.1 wt.% nanogel and Tween[®] 60 dispersed in seawater at pH from 1 to 13. Scale bars are 5 μm . (H) the average diameter of emulsified oil droplets. 193
13. Confocal microscopy images of Pickering emulsions stabilized by 0.1 wt.% nanogel and CTAB dispersed in 100-times diluted seawater at pH from 1 to 13. Scale bars are 5 μm . (H) the average diameter of emulsified oil droplets. 194
14. Confocal microscopy images of Pickering emulsions stabilized by 0.1 wt.% nanogel and CTAB dispersed in seawater at pH from 1 to 13. Scale bars are 5 μm . (H) the average diameter of emulsified oil droplets. 195
15. Confocal microscopy images of Pickering emulsions stabilized by 0.1 wt.% nanogel and SDS dispersed in 100-times diluted seawater at pH from 1 to 13. Scale bars are 5 μm . (H) the average diameter of emulsified oil droplets. 196

16. Confocal microscopy images of Pickering emulsions stabilized by 0.1 wt.% nanogel and SDS dispersed in seawater at pH from 1 to 13. Scale bars are 5 μm . (H) the average diameter of emulsified oil droplets. 197
17. Confocal microscopy images of Pickering emulsions stabilized by 0.1 wt.% nanogel and Tween[®] 60 dispersed in 100-times diluted seawater at several homogenizing times from 30 to 240 seconds. Scale bars are 5 μm . (E) the average diameter of emulsified oil droplets. 198
18. Confocal microscopy images of Pickering emulsions stabilized by 0.1 wt.% nanogel and Tween[®] 60 dispersed in seawater at several homogenizing times from 30 to 240 seconds. Scale bars are 5 μm . (E) the average diameter of emulsified oil droplets. 198
19. Confocal microscopy images of Pickering emulsions stabilized by 0.1 wt.% nanogel and CTAB dispersed in 100-times diluted seawater at several homogenizing times from 30 to 240 seconds. Scale bars are 5 μm . (E) the average diameter of emulsified oil droplets. 199
20. Confocal microscopy images of Pickering emulsions stabilized by 0.1 wt.% nanogel and CTAB dispersed in seawater at several homogenizing times from 30 to 240 seconds. Scale bars are 5 μm . (E) the average diameter of emulsified oil droplets. 199
21. Confocal microscopy images of Pickering emulsions stabilized by 0.1 wt.% nanogel and SDS dispersed in 100-times diluted seawater at several homogenizing times from 30 to 240 seconds. Scale bars are 5 μm . (E) the average diameter of emulsified oil droplets. 200
22. Confocal microscopy images of Pickering emulsions stabilized by 0.1 wt.% nanogel and SDS dispersed in seawater at several homogenizing times from 30 to 240 seconds. Scale bars are 5 μm . (E) the average diameter of emulsified oil droplets. 200

LIST OF TABLES

Table	Page
PAPER I	
1. Types of nanoparticles.....	13
2. Summary of nanoparticle flooding experiments.	15
3. Summary of wettability modification of nanoparticle-surfactant flooding experiments.....	30
4. Summary of interfacial tension reduction of silica nanoparticle-surfactant flooding experiments.	35
5. Summary of interfacial tension reduction of metallic nanoparticle-surfactant flooding experiments	41
6. Summary of viscosity reduction of nanoparticle-surfactant flooding experiments	42
PAPER II	
1. Typical seawater composition in Saudi Arabia.....	59
2. Petrophysical properties of core plugs.	62
3. Injection schedules for each core used in the experiments.	64
4. Physiochemical properties of the synthesized nanogel with a concentration of 0.1 wt% dispersed in seawater.	65
5. Surface and interfacial tension measurements of nanogel dispersions.....	70
6. Summary of sequential injection core flooding experiments.	77
7. Comparison between sequential and one-slug injection schemes.	78
PAPER III	
1. Composition of all employed brine types with different salinities.	89
2. Density and viscosity of different brine types at room temperature of 25° C.	90
3. Petrophysical properties of core plugs employed in core flooding experiments... ..	91
4. Physiochemical properties of different nanogel dispersions in several water types.	95
5. Injection schedules for core plugs employed in core flooding experiments.....	97

PAPER IV

1. Composition of all employed brine types with different salinities. 134
2. Density and viscosity of different brine types at room temperature of 25° C. 135
3. Petrophysical properties of core plugs employed in core flooding experiments... 137
4. Petrophysical properties of core plugs employed for dynamic adsorption-desorption measurements and injectivity evaluation..... 139
5. Physiochemical properties of different nanogel dispersions in several water types.141
6. Injection schedules for core plugs employed in core flooding experiments..... 143

PAPER V

1. Properties of surfactants..... 177
2. Composition of all employed brine types with different salinities. 178
3. Density and viscosity of different brine types at room temperature of 25° C. 179
4. Physiochemical properties of the employed nanogel dispersed in different brines. 183

SECTION

1. INTRODUCTION

1.1. STATEMENT AND SIGNIFICANCE OF THE PROBLEM

Maximizing the amount of crude oil extracted from current reservoirs is a necessity for the oil and gas industry to increase its profitability and sustainability. However, multiple studies have concluded that about 70% of global oil reserves cannot be extracted using conventional oil recovery techniques (Kokal and Al-Kaabi, 2010). Improving the global oil recovery factor by only 1% has the potential to produce an extra 88 billion barrels of oil, which is equal to three years of annual oil production at current rates (Sheng, 2013). In principle, oil recovery methods involve three mechanisms. During the primary oil recovery mechanism, the reservoir pressure pushes the oil out of the well. This mechanism can only extract an average of 10% of the available oil reserves in the reservoir, depending on the reservoir conditions and development strategies. During the secondary oil recovery mechanism, water flooding is injected to the reservoir to provide pressure support and improve the sweep efficiency (Thomas, 2008). Both primary and secondary oil recovery methods can extract only 40% of the available oil at best, often much less than that, and leave the rest of the oil underground. The desire to recover more oil from the existing wells leads to a growing use of tertiary enhanced oil recovery EOR methods. During this mechanism, chemical flooding (polymers, surfactants, and alkaline), miscible flooding (carbon dioxide, nitrogen, methane, and liquefied gases), microbial flooding (micro-organisms), thermal flooding (steam), or combination of them are introduced to the reservoir which help the flow of the trapped oil in reservoir rocks by decreasing the surface tension and viscosity of the crude oil (Green *et al.*, 1998; Lake, 1989; Lyons and Plisga, 2011; Thomas, 2008). The

application of each enhanced oil recovery technique depends on the reservoir conditions, such as brine salinity, crude oil viscosity, average rock permeability, and average reservoir temperature. Enhanced oil recovery processes can extract an additional 5-20% of the original oil in-place (OOIP), thus the total oil recovery after EOR processes can reach 50-70% depending on reservoir conditions (Green *et al.*, 1998; Thomas, 2008).

Nowadays, nanoparticles are widely employed to improve the overall performance of chemical and physical processes in many fields including the oil industry. Materials having a dimension of 1-100 nm are called 'nanoparticles' (Das *et al.*, 2007). Previous studies proposed enhanced features of nanoparticles including their ability to modify the wetting behavior of reservoir rocks, high surface to volume ratio and the rheological properties of drilling fluids (Almahfood and Bai, 2018; Ayatollahi *et al.*, 2012; Li *et al.*, 2016; Pourafshary *et al.*, 2009; Zhang *et al.*, 2010). Structural disjoining pressure is one of the main recovery mechanisms of nanoparticle-assisted flooding (Chengara *et al.*, 2004; Wasan and Nikolov, 2003). This mechanism is explained as the energy existing between nanoparticles that leads to Brownian motion and electrostatic repulsion (Chengara *et al.*, 2004). The electrostatic repulsion and Brownian motion increase as nanoparticle size becomes smaller (Mcelfresh *et al.*, 2012a). In order to regain the equilibrium of the system caused by disjoining pressure, some of the properties including IFT and wettability are modified which leads to extra oil recovery (Mcelfresh *et al.*, 2012a).

Nanosized cross-linked polymeric particles known as nanogels are newly developed particles in EOR applications. They are known for their easy injection process due to their small size, which is much smaller than the diameter of the pore throats in oil reservoirs (Qiu *et al.*, 2010b). They are also characterized by low viscosity, especially at low concentrations (Almahfood and Bai, 2020a,c; Moraes *et al.*, 2011). Also, nanogels can reduce the interfacial tension by adsorbing at the oil-water interface, which stabilizes oil-in-water emulsions, leading to improvement of the recovered oil from reservoirs (Geng *et al.*, 2018a). They are able to mobilize residual oil, which enhances oil recovery by mainly reducing the interfacial

tension (Almahfood and Bai, 2020a,c; Lenchenkov *et al.*, 2016). In addition, surfactant flooding has played an essential role in enhanced oil recovery processes over the years due to its effectiveness in reducing oil-water interfacial tension, modifying the wettability of the oil phase towards a water-wet state and mobilizing the residual oil (Green *et al.*, 1998; Johannessen and Spildo, 2013).

Low salinity water flooding, which is also known in the literature as smart water flooding, designer waterflood, and ion tuned waterflood, injects brines with controlled ionic composition and concentration (Gupta *et al.*, 2011; Ligthelm *et al.*, 2009). The revised brine formulations destabilize the equilibrium of the initial oil-brine-rock system, which results in altering the wettability condition and improving the capillary pressure (Sheng, 2013). During low salinity water flooding, no expensive chemicals are added, which makes this method cheap and environmentally friendly. Compared to conventional water flooding, low salinity water flooding can extract additional 10% of original oil in place (Kokal and Al-Kaabi, 2010).

A cost-effective EOR method has high potential when both displacement and sweep efficiency are improved. The displacement efficiency can be improved by low salinity water flooding, while the sweep efficiency can be improved by nanogel and surfactant flooding. This dissertation will examine the effect of nanogel combined with surfactant followed by the use of low salinity water flooding; thus bypassing the limitations of each method when implemented individually. The objective of this study is to examine the performance of low salinity seawater flooding for enhanced oil recovery improved by polymeric nanogel coupled with surfactant through core flooding experiments in sandstone and carbonate reservoirs. The degree of seawater dilution, sequence of nanogel and surfactant injections, and concentration of nanogel are the main examined parameters. Also, the ability of the novel combination to improve the stability of oil-in-water Pickering emulsions will be elucidated.

1.2. POTENTIAL IMPACT AND CONTRIBUTIONS

The research focuses on a novel combination between newly developed nanosized particles, surfactants and low salinity water flooding in mature reservoirs as a potential EOR method. Understanding the recovery mechanisms and performance behind the proposed combination is crucial and beneficial when it comes to the ability to extract more amounts of oil economically. The potential and possible contributions from this research are summarized as follows:

- Summarize the recovery mechanisms of conventional nanoparticles, alone and coupled with surfactants, in EOR applications.
- Synthesize a polymeric nanogel with a uniform size distribution with one peak pointing to a predominant homogeneous droplet size.
- Evaluate the performance of polymeric nanogel coupled with surfactants in sandstone and carbonate reservoirs and combined with low salinity water flooding.
- Study the Pickering oil-in-water emulsion stability improvement by polymeric nanogel and surfactants.

1.3. STATEMENT OF WORK

1.3.1. Objectives. Enhanced oil recovery (EOR) techniques are receiving substantial attention worldwide due to the major decline in the conventional oil resources. However, lots of challenges and limitations such as high costs, low sweep efficiency, and possible formation damage hinder the improvement of the current EOR techniques. As nanotechnology being widely employed in different applications, there is a strong belief that it may be exploited to develop novel materials with enhanced performance to overcome the limitations of traditional EOR techniques. Furthermore, surfactants are added to nanoparticle solutions to enhance their stability. The interactions between surfactants and nanoparticles

can lead to a considerable change in the surface activity of surfactants. Multiple layers of surfactant-nanoparticle can be formed by the strong attraction between surfactant and nanoparticle molecules.

The main objective of this dissertation is to investigate the enhancement and improvement in enhanced oil recovery caused by a novel combination of polymeric nanogel and surfactants and explain the mechanisms behind it. The ability to understand the recovery mechanisms behind the combination will be very beneficial when it comes to the ability to extract more amounts of oil economically. To achieve the main objective, comprehensive evaluation of a polymeric nanogel combined with surfactants in terms of enhancing the oil recovery at different conditions will take place through core flooding experiments. The degree of adsorption density of nanogels on sandstone and carbonate rock surfaces will also be studied. Also, the effect of the coupled technique on improving the stability of Pickering emulsions will be elucidated. This study will contribute toward a better understanding of how the different factors of nanogel and surfactants affect the recovered oil from reservoirs. Figure 1.1 illustrates the main experimental tasks to achieve the objective of this dissertation.

1.3.2. Scope of Work. This research is mainly an experimental laboratory study to primarily investigate the performance of the proposed novel EOR method on improving oil recovery from sandstone and carbonate mature reservoirs. Core flooding experiments are intended to provide a thorough understanding of the combined technology and show the improved incremental oil recovery by this method. Additionally, different effects will be evaluated during core flooding experiments to provide a wider comprehension for better reservoir design and development.

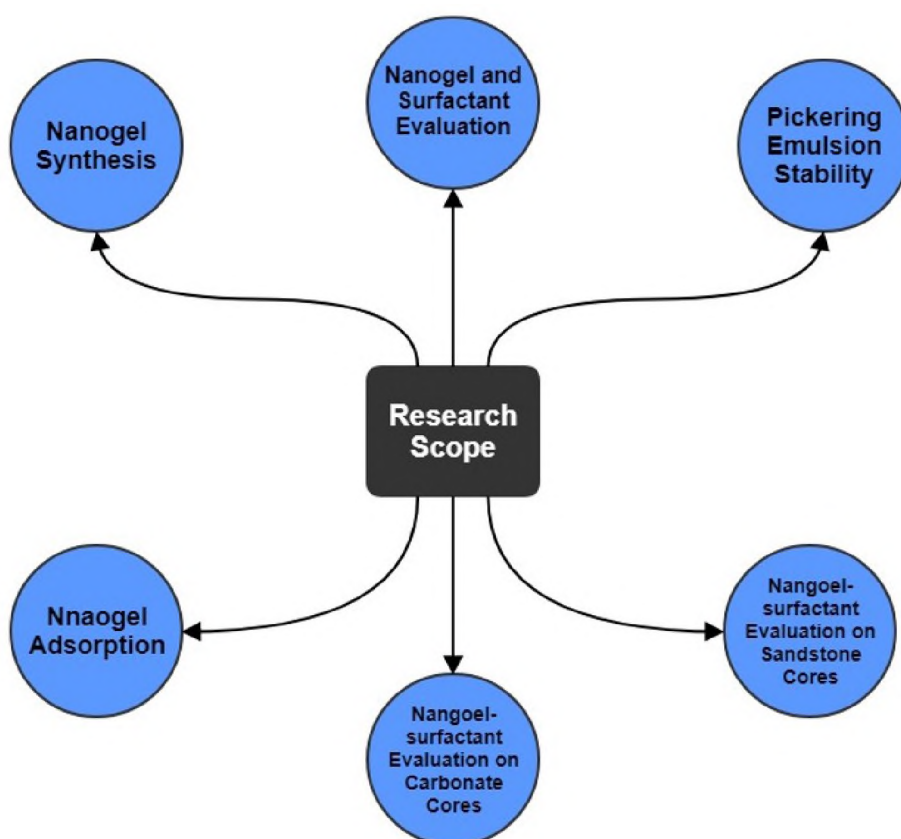


Figure 1.1. Research Scope.

PAPER

I. LITERATURE REVIEW: THE SYNERGISTIC EFFECTS OF NANOPARTICLE-SURFACTANT NANOFLUIDS IN EOR APPLICATIONS

Mustafa M. Almahfood, Author ^{a, b}

Baojun Bai, Co-Author ^a

^aDepartment of Geosciences & Petroleum Engineering

Missouri University of Science and Technology

Rolla, Missouri 65409

^b EXPEC Advanced Research Center, Saudi Aramco, Saudi Arabia

Email: mmantc@mst.edu

ABSTRACT

Enhanced oil recovery (EOR) techniques are receiving substantial attention worldwide due to the major decline in the available oil resources. However, lots of challenges and limitations such as high costs, low sweep efficiency, and possible formation damage hinder the improvement of these EOR techniques. In addition, nanoparticles have proven to be potential solutions or improvements to a number of challenges associated with the traditional EOR techniques. Furthermore, surfactants are added to nanoparticle solutions to enhance their stability. In general, surfactant-coated nanoparticles are functionalized nanoparticles that consist of a nanoscale part with their surface active groups to perform specific tasks such as adsorbing at the oil-water interface to modify some of their properties including wettability and interfacial tension (IFT). The relative concentration ratio

between surfactants and nanoparticles defines the properties of the modified surfactant-coated nanoparticles. If the concentration ratio between surfactants and nanoparticles is low, only a small portion of the nanoparticles would be coated with surfactants. Conversely, large concentration ratios mean that surfactants can form a double layer on the particle's surface. The interactions between surfactants and nanoparticles can lead to a considerable change in the surface activity of surfactants. Multiple layers of surfactant-nanoparticle can be formed by the strong attraction between surfactant and nanoparticle molecules. Generally, surfactants with higher concentrations, which are entitled with a higher adsorption into the surface, can greatly reduce the interfacial tension (IFT) and alter the wettability towards a water-wet condition. The aim of this paper is to conduct a review of the recent literature on nano-technology and determine the most reliable mechanisms associated with different particles. The paper mainly focuses on the development and usage of nanoparticles in combination with surfactants to improve and enhance oil recovery. Different tests and experimental studies are presented to better understand the recovery mechanisms of the combination. The first part of this paper focuses on the recovery mechanisms of different types of nanoparticles. Next, the recovery mechanisms of surfactant-nanoparticle solutions are presented along with different experimental studies. Finally, the possible limitations and challenges that face the combination of surfactants and nanoparticles in EOR applications are presented.

Keywords: Chemical EOR, Enhanced oil recovery, surfactants, polymer, nanoparticles, nanotechnology, nanofluid

1. INTRODUCTION

Due to the significant decline in production rates from existing reservoirs and the low frequency of new economic reservoirs, the importance of EOR technologies has risen in the last few decades. In addition, the injected fluids employed in EOR processes interact with reservoir rock and oil phase. Usually, these interactions result in lower interfacial

tensions, oil viscosity reduction, oil swelling, and wettability modification. Additionally, the target of EOR considerably varies for different types of reservoirs. Figure 1 illustrates the target of EOR for typical light oil reservoirs, heavy oil reservoirs, and tar sand (also known as oil sand) (Thomas, 2008).

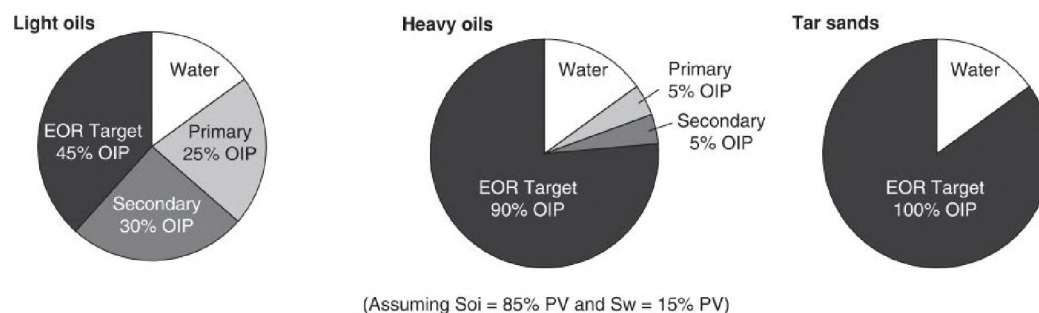


Figure 1. EOR target for different hydrocarbons.

Moreover, the traditional EOR methods (thermal, chemical, gas injection, and microbial methods) are facing dramatic challenges including early breakthrough from injection to production wells, resulting in leaving huge amounts of oil unrecovered (Ahmadi *et al.*, 2015). Additionally, the employment of chemical processes such as surfactant and polymer floodings is limited due to the high cost of chemicals, possible formation damage, and the loss of chemicals into the rocks. Although surfactant flooding has played an essential role in enhanced oil recovery processes over the years through reducing oil-water interfacial tension (IFT), altering the wettability of oil phase towards water wet state, and emulsifying crude oil (Green *et al.*, 1998; Johannessen and Spildo, 2013; Wu *et al.*, 2008b), its implementation is limited due to the unavoidable loss of chemicals to the rocks (Ahmadall *et al.*, 1993; Thomas, 2008). Yet, large quantities of polymers such as Lignosulfonate have been combined with surfactant flooding as an inexpensive preflush chemicals to reduce the loss of surfactants to the rocks (Ng *et al.*, 2003; Rana *et al.*, 2002; Touhami *et al.*, 2001). Furthermore, over the next few decades, the global energy demand is projected to rise about 60%. This challenging trend might only be met by a revolutionary enhancement

and improvement in energy science and technology. As a result, the oil and gas industry requires outstanding discoveries in underlying core science and engineering. Thus, the improvements in nanotechnologies open the door of moving beyond the current alternatives for energy supply by introducing technologies that are more efficient, reliable, and environmentally friendly. Generally, nanotechnology is characterized by the participation and collaboration of multiple disciplines, making the technology more precise than other technologies. Hence, nanoparticle injection alone and combined with other chemicals offers great opportunities to address the challenges caused by traditional EOR methods.

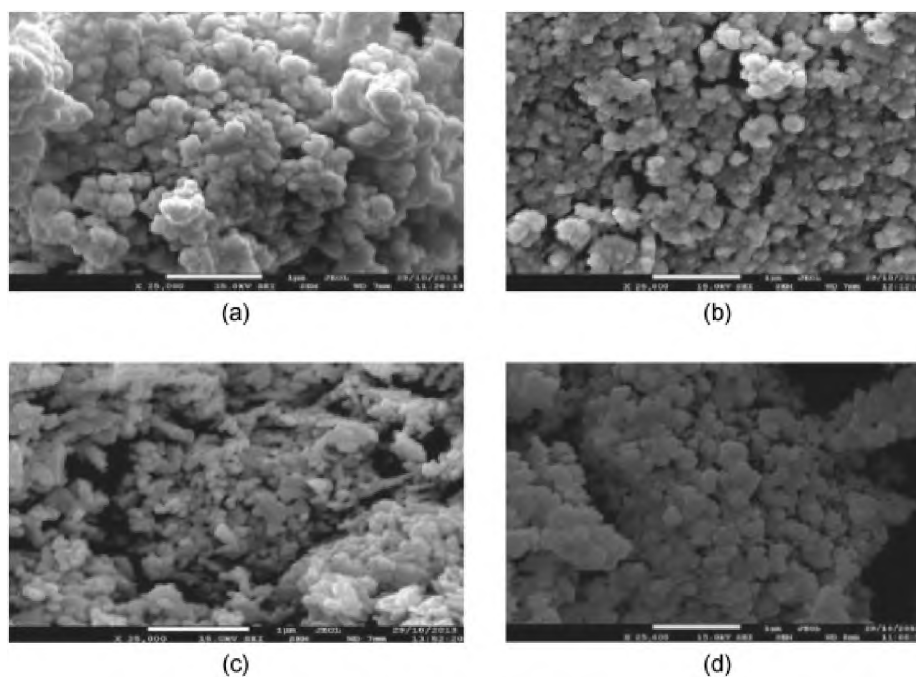


Figure 2. Microscopic images of (a) Titanium oxide, (b) aluminum oxide, (c) Nickel oxide, and (d) silicon oxide. Figure was obtained from Alomair *et al.* (2014).

Nanotechnology is the manipulation and integration of atoms and molecules to form materials, structures, and components at the nanoscale (Hornyak *et al.*, 2009). One nanometer equals 1 billionth of a meter (Figure 2). As implied by Figure 3, a water molecule equals about one-tenth of a nanometer, and a glucose molecule equals about 1 nanometer. In addition, as materials shrink in size to the nanoscale, their properties are different from

those found in bulk materials due to the huge surface area associated with nanoparticles (Figure 4). Therefore, they are more reactive when they are in contact with surrounding materials. In recent years, applications of nanotechnology in the oil and gas industry have been widely discussed. Lau *et al.* (2017) mentioned that in the last three years, the number of published papers discussing nanotechnology in the oil industry reached more than 1300.

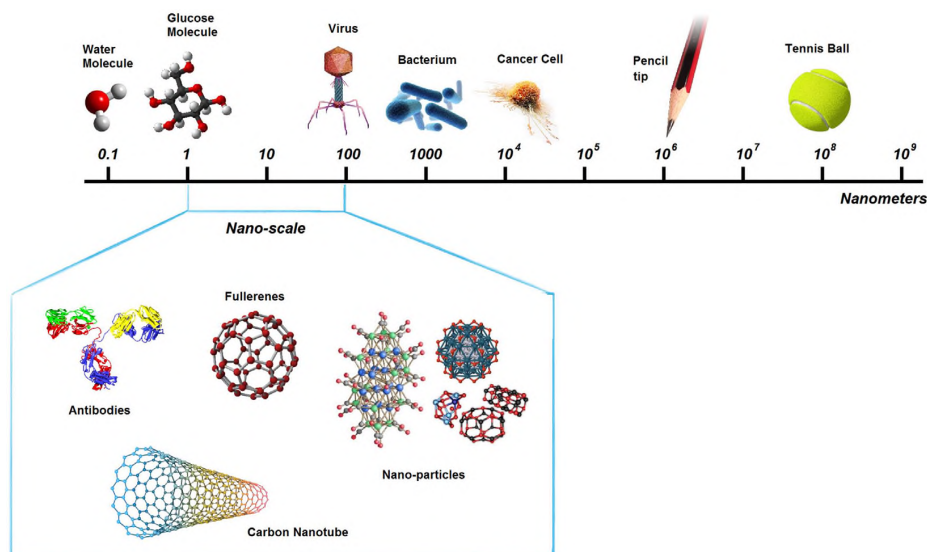


Figure 3. Nanoscale comparison. Figure was obtained from Lau *et al.* (2017).

Furthermore, a new fluid type, which is referred to as "smart fluids" is becoming increasingly available to the oil industry. Basically, these smart fluids are designed by adding nanoparticles to a specified fluid to improve some of its properties. Generally, the nanoparticles are suspended in the liquid phase in low concentrations where the liquid phase can be oil, water, or fluid mixtures. Preferably, the nanoparticles used in such a design are inorganic because they limit the accumulation and aggregation in the liquid environment.

Due to the above mentioned features of nanoparticles and surfactants, their potential of resolving and preventing some of the existing challenges that are facing the oil industry is high. Consequently, this paper provides an overview of nanoparticles employed to enhance

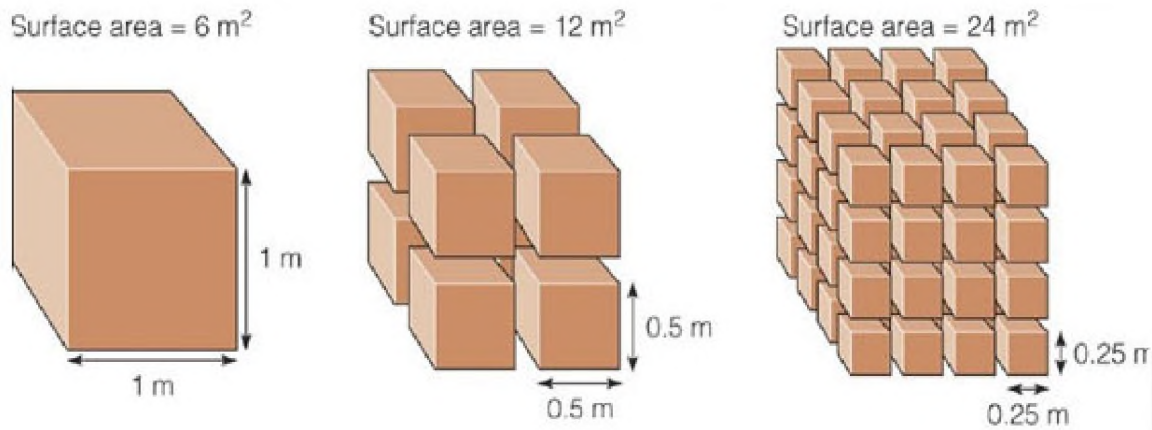


Figure 4. An illustration of the huge surface area of nanoparticles.

oil recovery. First, major recovery mechanisms of nanoparticles, alone and combined with surfactants, will be addressed. Then, a review of different studies will be presented. Later, the challenges that are facing this technology in EOR processes will be briefly discussed.

2. TYPES OF NANOPARTICLES

Due to their extremely small size and environmental friendliness, nanoparticles have been considered for EOR applications. In the context of EOR, nanoparticles could be subdivided into four main categories: (1) metal oxide, (2) magnetic, (3) silica, and (4) organic particles. Table 1 summarizes the different types with their associated possible mechanisms.

3. RECOVERY MECHANISMS OF NANOPARTICLE FLOODING

Understanding the recovery mechanisms of different nanoparticles is very crucial when determining the types to be employed in an EOR process. Although recent studies revealed some possible EOR mechanisms, they are not fully understood. In addition, applications of nanoparticles in EOR processes can be divided into three major types:

Table 1. Types of nanoparticles.

Category	Type	Possible EOR Mechanism	References	
Metal Oxide	Aluminum oxide (Al_2O_3)	IFT reduction Oil viscosity reduction	(Ogolo <i>et al.</i> , 2012) (Hendraningrat and Torsæter, 2015)	
	Copper oxide (CuO)	Heavy oil viscosity reduction	(Shah <i>et al.</i> , 2009)	
	Iron oxide (Fe_2O_3)	Viscosity reduction	(Wu <i>et al.</i> , 2008a) (Kothari <i>et al.</i> , 2010)	
	Nickel oxide (NiO_3)	Displacing fluid viscosity enhancement Oil viscosity reduction	(Ogolo <i>et al.</i> , 2012) (Nwidee <i>et al.</i> , 2017)	
	Magnesium oxide (MgO)	Weak recovery agent Causes permeability impairment	(Ogolo <i>et al.</i> , 2012) (Huang <i>et al.</i> , 2010)	
	Tin oxide (SnO_2)	Wettability modification	(Naje <i>et al.</i> , 2013) (Jiang <i>et al.</i> , 2005)	
	Titanium dioxide (TiO_2)	Wettability modification IFT reduction	(Ehtesabi <i>et al.</i> , 2014)	
	Zinc oxide (ZnO)	Causes permeability impairment	(Ogolo <i>et al.</i> , 2012) (Feng, 2012)	
	Zirconium oxide (ZrO_2)	Not common in EOR applications	(Ogolo <i>et al.</i> , 2012)	
Magnetic	Ferro nanofluids	IFT reduction	(Kothari <i>et al.</i> , 2010) (Huh <i>et al.</i> , 2014)	
	Cobalt Ferrite	Oil viscosity reduction	(Yahya <i>et al.</i> , 2012)	
Silica	SiO_2	Wettability modification IFT reduction	(Ogolo <i>et al.</i> , 2012) (Skauge <i>et al.</i> , 2010) (Tarek <i>et al.</i> , 2015b)	
	Alumina Coated	Wettability modification	(Singh <i>et al.</i> , 2016)	
	Hydrophobic oxide	Wettability modification	(Salyer, 1993)	
	Spherical fumed silica	Wettability modification	(Zhang <i>et al.</i> , 2010)	
	Nano composite	IFT reduction	(Nguyen <i>et al.</i> , 2012)	
	Polysilicon NP (HLP-LHP-NWP)	IFT reduction Wettability modification	(Roustaei <i>et al.</i> , 2012) (Shahrabadi <i>et al.</i> , 2012) (Hendraningrat <i>et al.</i> , 2013a)	
Organic	Carbon Nanoparticles	Wettability modification	(Yu <i>et al.</i> , 2010) (Kanj <i>et al.</i> , 2011)	
	Carbonate nanotubes(CNT)	Oil viscosity reduction	(Friedheim <i>et al.</i> , 2012)	
	Polymer	CDGs	Sweep improvement	(Diaz <i>et al.</i> , 2008) (Chang <i>et al.</i> , 2006)
		Polymer coated	Viscosity reduction Sweep improvement	(Schmidt and Malwitz, 2003)

(1) nanofluids, (2) nanoemulsions, and (3) nanocatalysts. Next, the possible recovery mechanisms associated with each nanoparticle application are presented. It should be noted that this paper is not intended to deeply investigate nanoemulsions and nanocatalysts.

3.1. NANOFUIDS

A nanofluid in oil and gas applications is defined as the base fluid that contains at least one additive with a particle size less than 100 nm (El-Diasty *et al.*, 2013). Generally, the base fluid can be oil, water, or gas. These nanofluids are utilized to enhance oil recovery. The major recovery mechanisms associated with nanofluids include disjoining pressure, IFT reduction, wettability modification, plugging pore channels, viscosity enhancement of injected fluids, and preventing asphaltene precipitation. Table 2 illustrates the available nanoparticle flooding experiments in the literature.

3.1.1. Disjoining Pressure. Nanoparticles in an aqueous dispersion tend to form a self-assembled structural array at the discontinuous phase such as oil, gas, or polymer. The particles in the three phase contact region prefer to arrange themselves into a wedge-like structure and begin to force themselves between the discontinuous phase and the solid surface (rocks) as illustrated by Figure 5. Particles that are present in the bulk fluid continuously push the particles in the confined region forward and impart a huge force known as the disjoining pressure force (Chengara *et al.*, 2004). The energies that drive this mechanism are Brownian motion and electrostatic repulsion between the particles. Furthermore, the magnitude of the disjoining pressure is greatly affected by the size of nanoparticles, temperature, and the salinity of the base fluid. Moreover, the force imparted by a single particle is extremely weak, but when large amounts of small particles are present, the force can be upwards of 50,000 pascals at the vertex, as mentioned by Mcelfresh *et al.* (2012a). Therefore, the disjoining pressure causes the system to lose its equilibrium. In order for the system to regain its equilibrium, some of its properties, such as IFT and wettability, would be modified and oil displacement would occur (Aveyard *et al.*, 2003).

Table 2. Summary of nanoparticle flooding experiments.

References	NP/ Base fluid	Oil Type	Oil Viscos- ity,cp	Core Type	Tested Parameters	Incremental Recovery,%
(El-Diasty <i>et al.</i> , 2015)	SiO_2 /Brine	Medium	NA	Sandstone	NP size, Concentration	4 to 34
(Ogolo <i>et al.</i> , 2012)	Metal oxide NPs / Brine, Ethanol, Water	Medium	53	Sandpacks	NP type, Base fluid	-40 to 30
(Mohebbifar <i>et al.</i> , 2015)	SiO_2 , TiO_2 /Brine	Heavy	200	Micro-model Shale	Concentration, Orientation, Length	7 to 50
(Tarek <i>et al.</i> , 2015b)	$Al_2O_3+Fe_2O_3$ + SiO_2 /Brine	Heavy	5	Sandstone	Concentration, Injection regime	8 to 20
(Salem <i>et al.</i> , 2015)	SiO_2 , Al_2O_3 /Brine	Light	75	Sandstone	NP Type, Concentration	SiO_2 :9 to 14 Al_2O_3 :-8 to -5
(Roustaei <i>et al.</i> , 2012)	Polysilicon/Brine	Light	11	Sandstone	NP type	28 to 32
(Tarek <i>et al.</i> , 2015a)	$SiO_2+Al_2O_3$ + Fe_2O_3 /Brine	Medium	5.12	Sandstone	Salinity, Injection regime	0.9 to 9.5
(Li <i>et al.</i> , 2013a)	SiO_2 /Brine	Light	5.1	Sandstone	Concentration, PV, Core permeability	2.9 to 14.3
(Li <i>et al.</i> , 2013b)	SiO_2 /Brine	Light	5.1	Sandstone	Concentration	4.26 to 9.49
(Kazemzadeh <i>et al.</i> , 2015)	Fe_3O_4 , SiO_2 , NiO /Brine	Heavy	NA	Micro-model	NP type, concentration	Fe_3O_4 :8.0 SiO_2 :18.0 NiO :12.0
(Ehtesabi <i>et al.</i> , 2014)	TiO_2 /Brine	Medium	41	Sandstone	Concentration	-7 to 31
(Li <i>et al.</i> , 2015)	SiO_2 /Brine	Light	15.3	Sandstone	Concentration	5 to 13
Roustaei <i>et al.</i> , 2015	SiO_2 /Brine	Light	11	Carbonate	Aging time	9 to 17
(Alomair <i>et al.</i> , 2014)	Al_2O_3 , NiO , SiO_2 , TiO_2 /Brine	Heavy	206	Sandstone	NP Type	Al_2O_3 :-0.3 to 6 SiO_2 :-4 to 6 $SiO_2+Al_2O_3$: -7 to 24
(Hendraningrat <i>et al.</i> , 2014)	SiO_2 , TiO_2 , Al_2O_3 /Brine	Light	5.1	Sandstone	NP type	1 to 7
(Ragab <i>et al.</i> , 2015)	SiO_2 /Brine	Light	75	Sandstone	NP size, Concentration	1 to 11
(Haroun <i>et al.</i> , 2012)	CuO , NiO , Fe_2O_3 /Brine	Medium	48	Carbonate	NP type	8 to 14

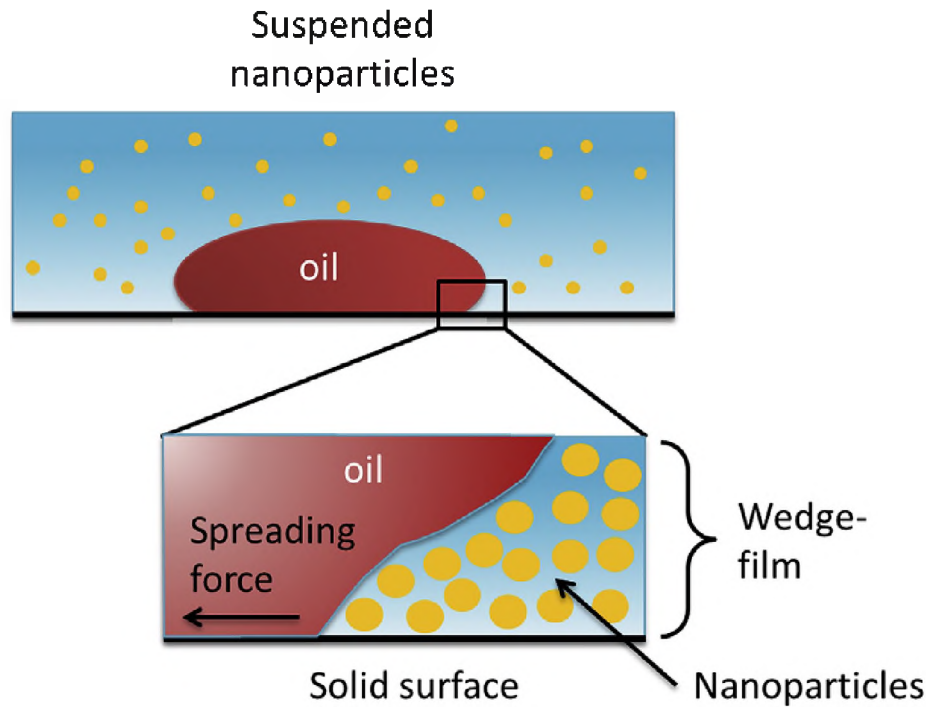


Figure 5. Nanofluid wedge-film structure. The figure was obtained from Lau *et al.* (2017).

3.1.2. IFT Reduction. Interfacial tension (IFT) is considered one of the main parameters measured to determine fluid distribution and movement in porous media. In addition, IFT is one of the major EOR mechanisms for nanofluid flooding. Thus, it is crucial to accurately measure the IFT between oil and injected fluids to evaluate their effectiveness on EOR applications. Furthermore, some types of nanoparticles are considered as potential agents for IFT reduction.

Moreover, the IFT between the injected fluid and the crude oil is usually measured in labs using the pendant drop method (Suleimanov *et al.*, 2011). A typical apparatus consists of: (1) an experimental cell, (2) light source, (3) a viewing system to visualize the drop (microscopic camera), and (4) a data acquisition system to accurately read the IFT value. Figure 6 illustrates a typical apparatus of this technique. During the experimental process,

an oil droplet is generated from the needle at the tested pressure and temperature. Then, the IFT is calculated from the shape of the oil droplet using a sophisticated camera and a computer software.

Li *et al.* (2013a) measured the IFT between crude oil and silicon dioxide SiO_2 nanoparticles using the pendant drop technique. Figure 7 illustrates the IFT measurements of crude oil and brine/nanoparticles at various concentrations. Initially, the IFT of the oil-brine system was $19 \frac{mN}{m}$. However, after introducing nanoparticles into the system, the IFT was reduced to $8 \frac{mN}{m}$. Additionally, the IFT values were greatly sensitive to nanoparticle concentrations. Similar IFT behavior was reported by Parvazdavani *et al.* (2014).

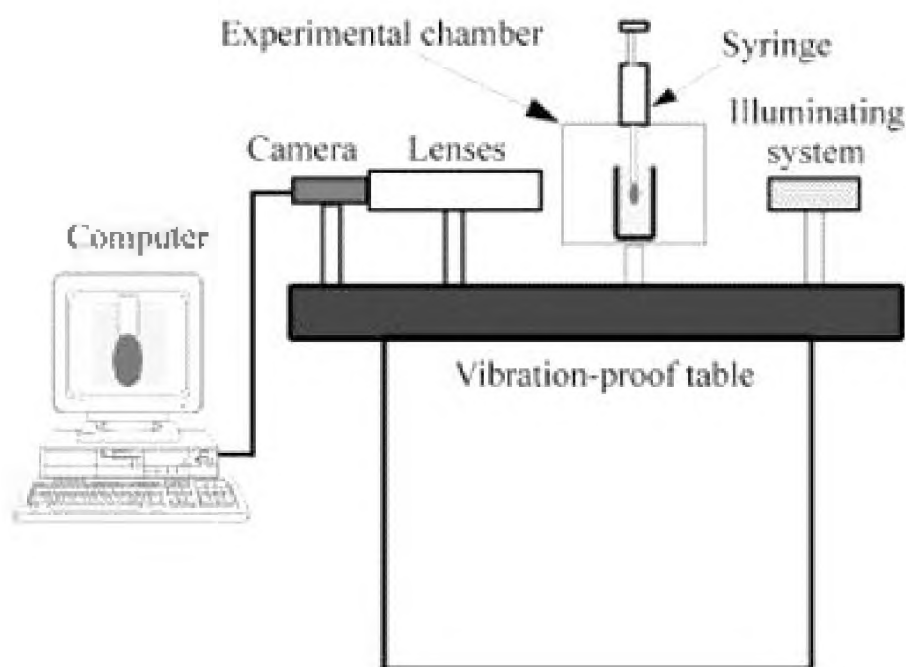


Figure 6. Typical Pendant Drop Apparatus. The figure was obtained from Arashiro and Demarquette (1999).

3.1.3. Wettability Modification. Wettability is defined as the tendency of one fluid to spread on or adhere to a solid surface in the presence of another immiscible fluid. Wettability is considered one of the key parameters in multi-phase flow and affects other reservoir parameters such as capillary pressure, relative permeability, and oil recovery efficiency

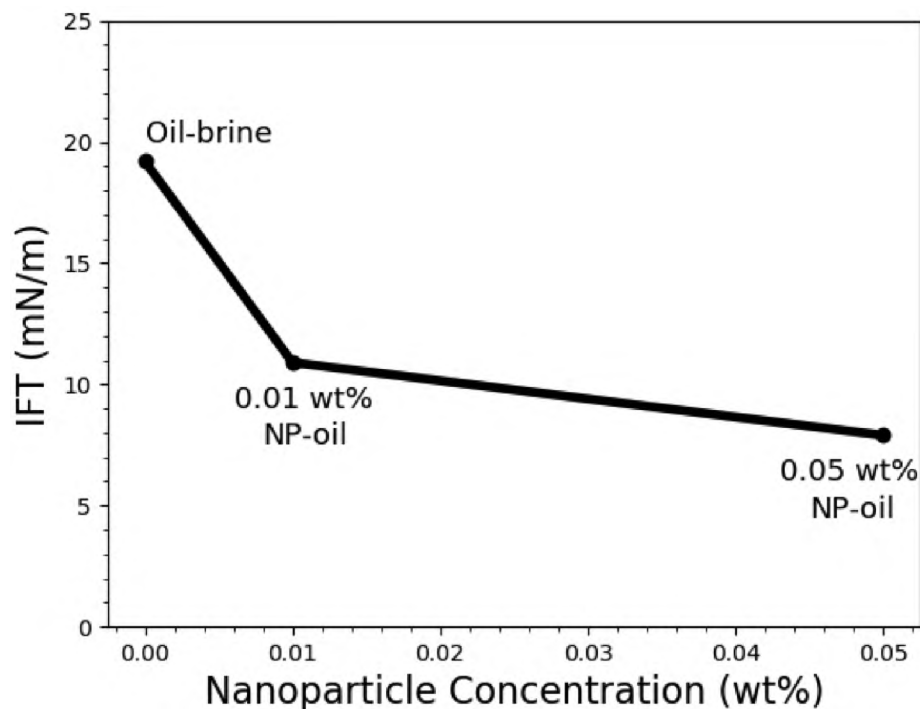


Figure 7. IFT measurement of oil-brine/nanofluid system at various nanoparticle concentrations. Data were obtained from Li *et al.* (2013a).

(Craig, 1971). Additionally, wettability governs the fluid flow, residual oil saturation, and distribution in rocks (Anderson *et al.*, 1986). Different qualitative and quantitative methods are available in the literature for wettability measurements (Anderson *et al.*, 1986). Qualitative methods include imbibition tests, microscopic visualization, and wettability evaluation using relative permeability curves (Craig, 1971), whereas quantitative methods include contact angle measurements and the Amott method (Amott *et al.*, 1959). However, contact angle measurements are the most common method to evaluate the wettability. In addition, rocks can be either water-wet, oil-wet, or intermediate-wet. Figure 8 illustrates the range of contact angles for each type.

In general, the highest portion of oil recovery is proportional to the tendency towards the most water wet state in the reservoir. Wettability alteration using chemical treatments is an ongoing and developing field of research that is motivated by academic and industrial

interests (Muller *et al.*, 2008). As a result, wettability alteration is an important technique to increase the oil recovery from oil-wet or intermediate-wet reservoirs.

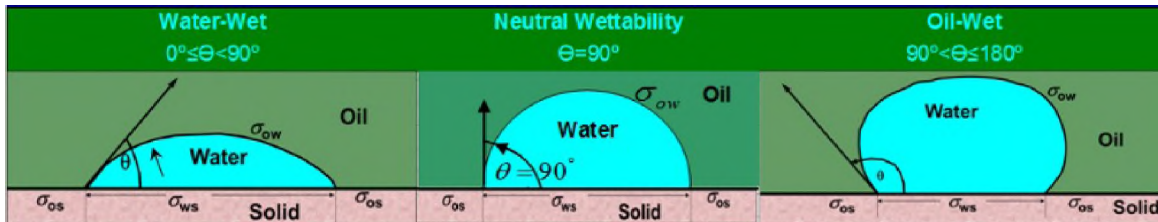


Figure 8. A schematic diagram of rock wettability systems. Figure was obtained from Ogunberu and Ayub (2005).

A number of experimental studies have been conducted to study the effect of different nanoparticles on wettability modification. Al-Anssari *et al.* (2016) indicated that SiO_2 nanoparticles induced wettability modification on oil-wet and intermediate-wet calcites, as shown in Figure 9. These results are consistent with the findings of Roustaei and Bagherzadeh (2015).

Furthermore, wettability modification caused by nanoparticles is affected by different factors, such as nanoparticle size, concentration (Figure 9), and base-fluid salinity. Hendraningrat *et al.* (2013b) indicated that the contact angle of the aqueous phase decreased as nanoparticle size decreased. Meanwhile, incremental oil recovery due to nanoparticles increased as the size of nanoparticles decreased. This is because the electrostatic repulsion force between nanoparticles becomes bigger when the amount of nanoparticles is large and the size is small.

3.1.4. Discussion of Nanofluid Recovery Mechanisms. The above mentioned recovery mechanisms of nanofluids are basically linked together during the recovery process. However, one or more mechanism might have a higher impact on the recovery. In general, the size, type and concentration of nanoparticles are the main criteria that lead to a different nanofluid recovery mechanism. In addition, it is well documented in the literature that increasing the nanoparticle size might result in a formation damage (pore plugging), which

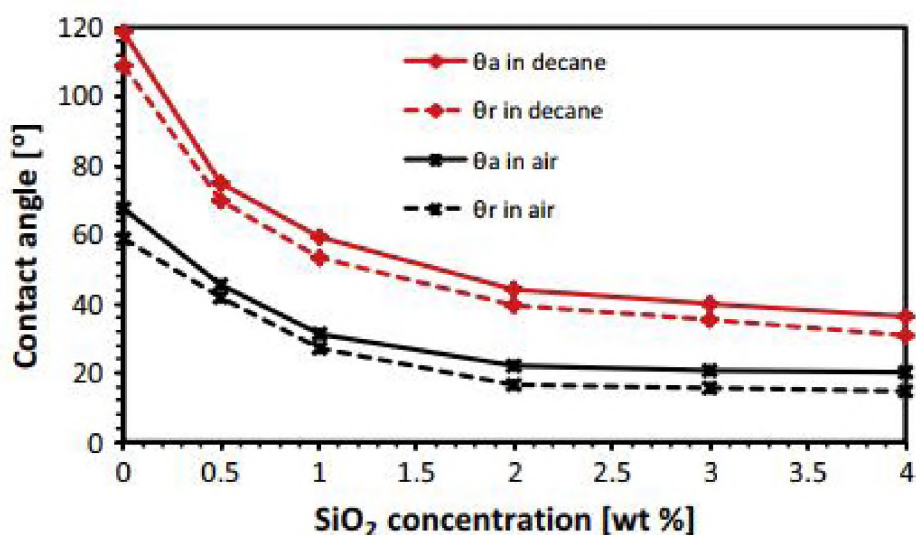


Figure 9. Contact angle measurements of SiO_2 nanoparticles in air and oil as a function of concentration. Figure was obtained from Al-Anssari *et al.* (2016).

ultimately reduces the oil recovery. On the other hand, the smaller size of nanoparticles can increase electrostatic repulsion between nanoparticles, which causes higher disjoining pressure. Yet, the extra small size of nanoparticles can cause pore bridging, which might reduce the oil recovery. Similarly, the higher concentration of nanoparticles will lead to lower IFT values and higher disjoining pressure. However, lower nanoparticle concentrations are more economic and can form more stable dispersion.

3.2. NANOEMULSION

Generally, "smart fluids" can be prepared by the applications of nanotechnology, and have become increasingly employed in the oil and gas industry (Amanullah *et al.*, 2009). Additionally, nanoemulsion is considered one of the "smart fluid" types, which are intended to recover more oil from reservoir rocks. Nanoemulsion is a kind of conventional emulsions, that is stabilized by nanoparticles, which demonstrates a great ability to overcome the challenges and drawbacks of conventional emulsions (Mandal *et al.*, 2012). Due to the small droplet size of nanoemulsions, which could be in the range of 50-500 nm, they have

attracted a great deal of attention. Although nanoemulsion and microemulsion droplets both fall in the same length range (< 100 nm), nanoemulsions are more kinetically controlled systems that could retain their morphology with the change in oil volume fraction (Binks and Lumsdon, 2000). As a result, nanoemulsions could be employed and remain stable in harsh conditions such as high temperature, pressure, and salinity.

Silicas SiO_2 are the most commonly used nanoparticles for emulsions. Mcelfresh *et al.* (2012b) have mentioned that the wettability of these nanoparticles can be modified by changing the amount of silanol groups on their surface. For instance, more stable oil-in-water emulsions can be formed by hydrophilic nanoparticles with a high percentage of silanol group ($> 90\%$), as illustrated in Figure 10. Conversely, when silica nanoparticles are coated with a small percentage of the silanol group ($< 10\%$) on their surface, water-in-oil emulsions will be formed. It should be noted that this paper is not intended to deeply investigate nanoemulsions.

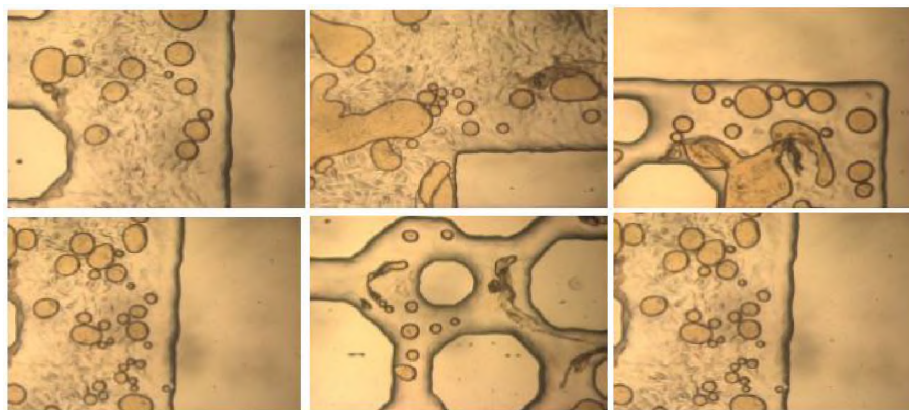


Figure 10. Nano-emulsions observed during nano-flooding process. Figure was obtained from Li *et al.* (2013b).

3.3. NANO-CATALYSTS

Nanocatalysts are defined as nano-sized particles used as catalysts during steam injection into heavy oil reservoirs (Hashemi *et al.*, 2014). Over conventional catalysts, nanocatalysts are considered to have larger surface area to volume ratios. In EOR applications, nanocatalysts are employed to decrease heavy oil viscosity (Shokrlu *et al.*, 2011). It should be noted that this paper is not intended to deeply investigate nanocatalysts.

4. COMBINATION OF NANOPARTICLES AND SURFACTANTS

Previous chapters introduced the mechanisms of surfactant and nanoparticle floodings. One might inquire what is going to happen if both nanoparticles and surfactants (and polymers) are combined together in EOR processes. Preferably, nanoparticles in enhanced oil applications are to be synthesized with other chemicals such as surfactants and polymers to simply combine all mechanisms, increase the stability of nanoparticles, and eliminate some of the drawbacks, such as the high cost of chemicals. In addition, utilizing nanoparticles in surfactant flooding processes can enhance their properties and therefore increase the influence of surfactant solutions on recovery processes. Moreover, surfactant-based nanoparticles are basically functionalized nanoparticles that consist of a nanoscale part with their surface active groups to perform specific tasks, such as adsorbing at the oil-water interface to alter and modify some of their properties including wettability and interfacial tension (IFT).

Moreover, when surfactants are combined with nanoparticles, surfactants act as a bridge between nanoparticles and the base-fluid (Yu *et al.*, 2012). The selection of the employed surfactants mainly depends on the properties of the nanoparticles and the solution. For instance, when there is a need to disperse metal oxide nanoparticles into a non polar-base-fluid (metal oxide nanoparticles are easily dispersed in polar fluids), the addition

of surfactants is required to enhance the stability of the nanoparticles. Additionally, the degree of nanoparticle stability is indicated by the zeta potential value. Generally, high zeta potential values indicate higher stability.

Furthermore, the relative concentration of surfactants and nanoparticles basically defines the properties of surfactant-coated nanoparticles. If the concentration ratio of surfactant to nanoparticle is relatively low, only a small fraction of the particle surface would be coated with surfactants. On the other hand, larger concentration ratios mean that the surfactant can form a double layer on the particle's surface, which leads to a hydrophilic nanoparticle surface (Engeset, 2012). Generally, surfactant-nanoparticle solutions (nanofluids) will generate stable foams and emulsions at concentration ratios that result in maximum nanoparticle flocculation (ShamsiJazeyi *et al.*, 2014; XU *et al.*, 2016). Moreover, Limage *et al.* (2010) stated that most flocculated nanoparticles correspond to hydrophobic particles, containing a mono-layer surfactant on the surface. However, surfactants with single chains are considered to be better for foam generation when mixed with nanoparticles since the double-chain surfactants might result in the formation of double layer adsorption on particles at concentrations lower than that of single-chain surfactants (Cui *et al.*, 2010). Figure 11 demonstrates a schematic representation of surfactant adsorption on a nanoparticle and generated emulsions stabilized by surfactant-coated nanoparticles.

Generally, the interaction between nanoparticles and surfactants is capable of causing a considerable change in the surface activity of the surfactant molecules. Basically, surfactants with higher surface activity (concentration) are entitled with a higher adsorption into the surface. As a result, they could significantly reduce the interfacial tension (IFT) and alter the wettability strongly towards a water-wet condition. Multiple layers of nanoparticle-surfactants could be formed by the strong attraction between nanoparticle and surfactant molecules. The formation of these layers can significantly affect and alter the wetting property of the oil phase (Karimi *et al.*, 2012).

Hydrophobic nanoparticles can affect the formation of bubbles from shear and compression stresses, which influences the rheology and stability of surfactant solutions composed of foams and emulsions. This is due to the formation of a rigid nanoparticle skin on the surface of the bubbles (Jiang *et al.*, 2016). Next, the main mechanisms associated with surfactant-nanoparticle solutions will be discussed.

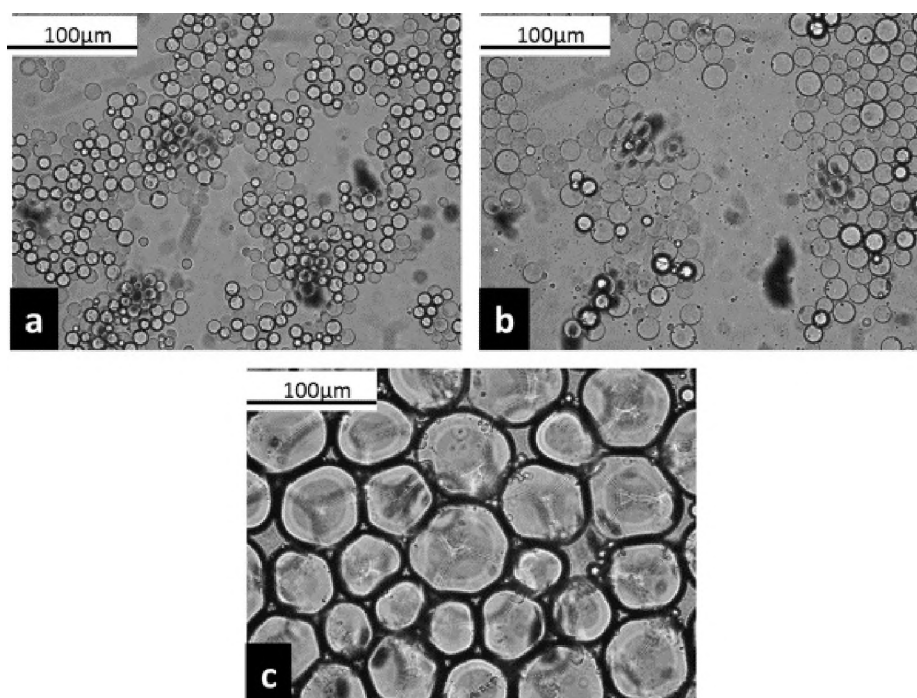


Figure 11. Optical micrographs of emulsions stabilized with 1% silica nanoparticles (NP)+0.05% CAPB at (a) pH 4; (b) pH 6; and (c) pH 8. Micrographs taken 1 day after emulsion formation. Figure was obtained from Worthen *et al.* (2013).

4.1. ROCK WETTABILITY MODIFICATION

As nanoparticles are evolving in the oil industry, multiple experimental studies have shown and proven that the combination of nanoparticles and surfactants is capable of altering the wetting property of a reservoir towards a water-wet state. Generally, the small size of nanoparticles enables them to pass through pore throats in typical reservoirs and access the residual oil where conventional EOR processes are not able to reach into.

Moreover, numerical, theoretical and experimental studies revealed that these nanofluids reduce oil adsorption on a rock surface by introducing a structural disjoining force (film tension) between the oil and rock surface by forming a wedge film structure on the rock surface (Figure 5); thereby releasing a great amount of the trapped oil (Wasan *et al.*, 2011; Wasan and Nikolov, 2003). This encouraged researchers to further experimentally investigate the effects of nanoparticle and surfactant combination on wettability alteration. Experimentally, wettability conditions are estimated before and after surface modification with different chemicals by measuring the oil phase contact angle in presence of displacing fluid.

The effect of surfactant-based nanofluids on reducing the surface forces have been widely investigated in the last several years (Espinoza *et al.*, 2010; Fletcher *et al.*, 2010; Zhang *et al.*, 2010). Table 3 summarizes the experimental studies that discuss the wettability modification of nanoparticle surfactant floodings.

Hunter *et al.* (2009) provided an explanation of the interfacial mechanisms and interaction behavior of hydrophobic silica nanoparticles and nonionic surfactant solutions. Their experimental study used pre-hydrophobized nanoparticles grafted with octyl coating, which yielded to moderately high contact angles that are not expected to be enhanced by surfactant adsorption. This allowed the analysis to be merely focused on the measurement of contact angle and interfacial tension. Their results revealed that at higher surfactant concentrations (above CMC), the contact angles are greatly reduced, leading to the removal of the particles from the surface of the bubble interface, as illustrated in Figure 12. Therefore, the foam stability approaches that of pure surfactant systems.

Surface modification of $CaCO_3$ nanoparticles and anionic surfactants (linear alkyl-benzene sulfonic acid (LABSA) and branched alkyl-benzene sulfonic acid (BABSA)) was investigated by contact angle measurements (Song *et al.*, 2014). The results showed that both surfactant solutions exhibited the same trend. Basically, the contact angle increases with increasing surfactant concentrations, reaches a maximum value, and after that decreases

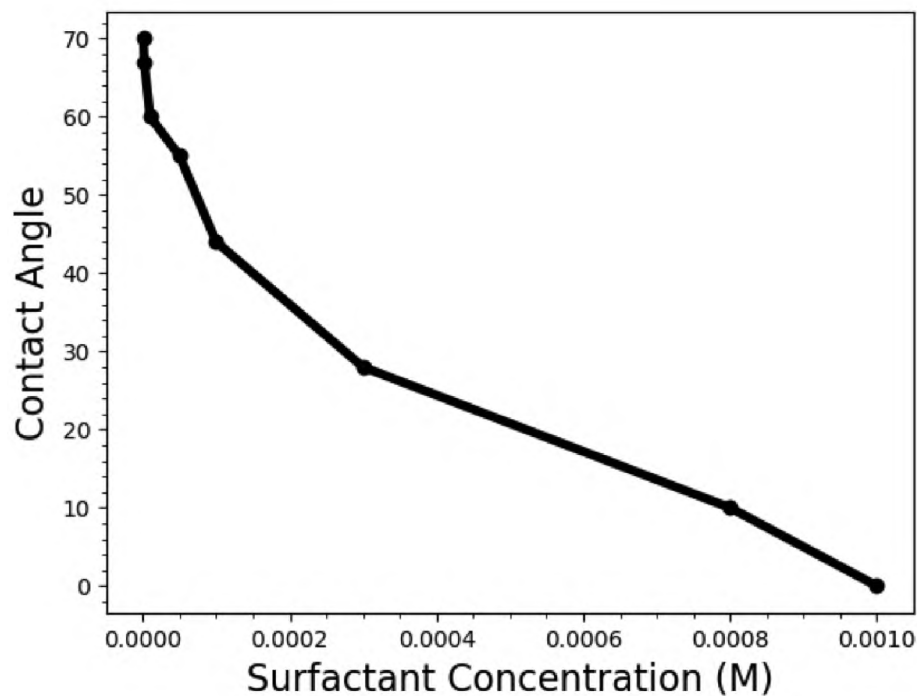


Figure 12. Contact angle measurement of non-ionic surfactant (TX-100) and silica nanoparticles. The data were obtained from Hunter *et al.* (2009).

at higher concentrations. Additionally, their analysis revealed that the initial increase in contact angle is caused by the formation of mono-layer of surfactant molecules on the surface, which causes the hydrophobic condition. However, after the increase in surfactant concentration above (CMC), bi-layer formation of surfactant molecules on the surface was observed. This resulted in reversing the surface back to a hydrophilic condition, and leading to the reduction in contact angle. Similarly, Sharma *et al.* (2016) have shown that solutions composed of hydrophilic silica nanoparticles, anionic surfactant (SDS), and polyacrylamide polymer were efficient in modifying wettability from intermediate wet to strongly water-wet conditions.

Nwidee *et al.* (2017) studied the behavior of surfactant-nanoparticle solutions on the wettability alteration of limestone samples. In order to achieve this goal, different approaches, including contact angle measurements and water imbibition tests, were adopted to evaluate the efficiency of the combined solution. In this experiment, two different

surfactants (cationic and nonionic) and metal nanoparticles (zirconium oxide (ZrO_2) and nickel oxide (NiO)) were evaluated as a function of surfactant type and concentration, nanoparticle-surfactant type and concentration, and imbibition. They have found that the contact angle depends on the nanoparticle-surfactant types and concentration. Moreover, the nanofluid system containing the non-ionic surfactant showed better compatibility with NiO than ZrO_2 . On the other hand, nanofluids composed of (ZrO_2 and cationic surfactant) and (NiO and cationic surfactant) always decreased the contact angle further than the non-ionic surfactant solutions. Their results are in agreement with the literature that the contact angle is affected by fluid-rock interactions (Bera *et al.*, 2012). Additionally, their results indicate that the presence of nanoparticles can enhance the surfactant performance and improve the stability of the formed emulsion. Therefore, the examined nanofluids are feasible for long-distance migration in the reservoir and have the potential of resolving wettability issues associated with limestone formations.

Karimi *et al.* (2012) have shown that the solutions composed of ZrO_2 nanoparticles and nonionic surfactants (NON-EO4 and LA2) are wettability modifiers in carbonate systems, and can be implemented for enhanced oil recovery applications. Their results revealed that this nanofluid is capable of altering the wettability from strongly oil-wet to strongly water-wet conditions. On the other hand, the wettability alteration caused by the combination of ZrO_2 nanoparticles and nonionic surfactants is a slow process that requires a period of at least two days.

Binks *et al.* (2008) reported a detailed experimental study that investigated the behavior of silica nanoparticles and pure cationic surfactants. The results revealed that an initially hydrophilic surface in the absence of surfactants exhibited a contact angle of 8° . Then, adsorption of surfactants to the air-water, solid-water, and most importantly, air-solid interfaces resulted in an increase in the contact angle to a maximum of 63° , followed by a significant decrease at higher concentrations. Therefore, silica particles went through a transition from hydrophilic to hydrophobic, and back to hydrophilic again.

Ahmadi *et al.* (2012) introduced a novel combination between different types of nanosilica and *Zyziphus Spina Christi*, a novel surfactant, in aqueous solutions for EOR applications. Their technique was implemented to assess the adsorption of the surfactant and nanosilica in the aqueous phase. The results revealed the ability of this surfactant to change the wettability of the surface due to the adsorption on the carbonate rock. Additionally, they conducted another set of experiments onto shale sandstone rock surfaces (Ahmadi and Shadizadeh, 2013). Their results showed that hydrophobic nanosilica was more effective than hydrophilic nanosilica to prevent adsorption losses into the shale sandstone.

The effectiveness of alumina-based nanofluids that are composed of Al_2O_3 nanoparticles and anionic PRNS surfactant in altering the wettability of sandstone cores was experimentally studied by Giraldo *et al.* (2013). The results revealed that the usefulness of the anionic PRNS surfactant as a surface modifier can be enhanced by the addition of oxide nanoparticles in low concentrations. Additionally, the contact angle values were initially measured as high as 142° and were reduced after the addition of nanofluids to almost 0° . This reveals that the wettability of the system was converted from strongly oil-wet to strongly water-wet.

In contrast, an experimental study of an aqueous solution of metal nanoparticles and anionic surfactants showed that wettability remained unchanged with nanofluid addition (Suleimanov *et al.*, 2011). However, core flooding tests have revealed that oil recovery has improved. As a result, the recovery mechanism of this experimental study cannot be explained using wettability alteration.

Although wettability alteration towards water wet condition is preferred to enhance oil production, altering the wettability towards oil-wet will lead to improving the relative amount of water phase, which can enhance injection rates for water injection wells. Generally, lipophobic and hydrophilic polysilicon (LHP) and naturally wet polysilicon (NWP) nanoparticles (with or without the combination of surfactants) are usually employed in

oil fields to enhance oil production rates. However, the adsorption of hydrophobic and lipophilic polysilicon (HLP) nanofluids leads to enhancing water injection rates, which is of great importance to low permeability reservoirs (Ju *et al.*, 2002).

4.2. OIL-WATER INTERFACIAL TENSION (IFT) REDUCTION

4.2.1. Silica Nanoparticles. Referring to a book published by the U.S. Bureau of Mines (Ampian and Virta, 1992), it is well documented that silicates (also known as silicon dioxide) are the most abundant compounds on earth, as they form over 90% of the earth's crust. As a result, this has made silicate compounds the most commonly used, environmentally friendly, and cost-effective nanoparticles.

The change in oil-water interfacial tension due to surfactant-based nanofluid treatments is still an open question. However, some studies are available that discuss the effectiveness of nanoparticles and surfactant combinations on the interfacial tension of oil-water systems. Table 4 summarizes the experimental studies that discuss the effect of nanoparticle-surfactant flooding on IFT.

Ravera *et al.* (2008) studied the liquid-air and liquid-liquid interfacial tension of nanosilica dispersions in the presence of a cationic surfactant. They have found that the addition of the silica nanoparticles decreased the surface and interfacial tension, as shown in Figure 13. In addition, they have assigned the interfacial tension behavior to the formation of a mixed layer that is composed of attached nanoparticles and surfactants in diluted particle concentrations, and to the adsorption of the particles above a specific concentration.

The effect of the combination of silica nanoparticles and ionic and nonionic surfactant systems on surface and interfacial tension was reported by Ma *et al.* (2008). They have shown that silica nanoparticles have a negligible effect on the surface and interfacial tension of nonionic surfactant systems, while increases the surface activity of the anionic surfactant solution, and accordingly decreases the interfacial and surface tension. On the other hand, the interfacial tension of oil-water interface in the presence of silica nanoparticles and

Table 3. Summary of wettability modification of nanoparticle-surfactant flooding experiments.

References	NP	Surfactant	Base Fluid	Oil Type	Core Type	Tested Parameters	Contact Angle (From - To)
(Suleimanov <i>et al.</i> , 2011)	Non-ferrous metal NP	(Anionic) Sulphanole	NA	Heavy	NA	Concentration	40° - 19°
(Hunter <i>et al.</i> , 2009)	Hydrophobic silica	Non-ionic (TX-100)	NA	NA	NA	Foam stability, Concentration	70° - 0°
(Karimi <i>et al.</i> , 2012)	ZrO ₂	Non-EO4 LA2 LA7 Tween-80 Span 20 Span 80 Span 85	Distilled water	Heavy	Carbonate	Concentration, Surfactant combinations	180° - 30°
(Binks <i>et al.</i> , 2008)	Silica	(Cationic) CTAB CDMAB	NA	NA	NA	PH, Foam stability, Concentration	35° - 63° - 8°
(Sharma <i>et al.</i> , 2016)	Hydrophilic silica	Anionic SDS	DI	Medium	Sandpack	Concentration, Temperature	Intermediate to strongly water wet
(Nwidee <i>et al.</i> , 2017)	ZrO ₂ NiO	TX-100 CTAB	DI	NA	Limestone	Concentration, Temperature	155° - 18°
(Song <i>et al.</i> , 2014)	CaCO ₃	Anionic LABSA, BABSA	NA	NA	NA	PH, Concentration	15° - 60°
(Ahmadi <i>et al.</i> , 2012)	Aerosil 200 Aerosil R816	(Non-ionic) Zyziphus Spina Christi	DI	NA	Carbonate	Concentration	Wettability change due to adsorption
(Giraldo <i>et al.</i> , 2013)	Al ₂ O ₃	(Anionic) PRNS	DI	Heavy	Sandstone	Concentration	142° - 0°
(Bera <i>et al.</i> , 2012)	Silica	(Non-ionic) Tergitol 15-S-5 Tergitol 15-S-7 Tergitol 15-S-9 Tergitol 15-S-12	Brine	Light	Quartz surface	Temperature, Salinity	85° - 50°

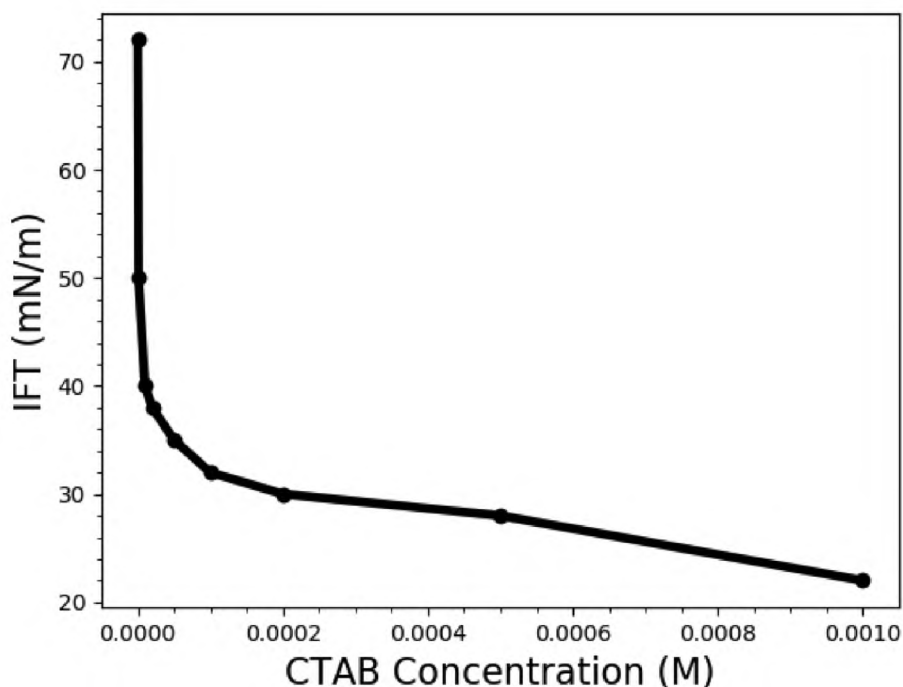


Figure 13. Interfacial tension of the oil-water system at different surfactant concentrations. The data were obtained from Ravera *et al.* (2008).

cationic surfactants (cetyltrimethyl ammonium bromide) was evaluated by Lan *et al.* (2007). Their analysis indicated that silica nanoparticles have a minimal impact on the interfacial tension of cationic surfactant solutions. This minimal nanoparticle effect is probably caused by the high degree of surfactant adsorption to the rock's surface. Furthermore, these results perfectly match the behavior of surfactant-polymer solutions reported by Bell *et al.* (2007). Similarly, Le *et al.* (2011) reported that SiO_2 nanoparticles blended with anionic surfactant solutions [XSA-1416D, SS16-47A, and IAMS-M2-P] resulted in ultra-low IFT values.

Understanding the interactions and synergy between hydrophobic silica nanoparticles and ionic surfactants might shed a light on the implications of such nanoparticles in enhanced oil recovery applications. The interactive behavior between hydrophobic silica nanoparticles combined with charged surfactants (CTAB, SDBS, and CPC) was investigated by Jiang *et al.* (2016). In this experiment, the concentration of silica nanoparticles was varied, while the surfactant concentration was fixed below CMC levels. However,

it was noticed that nanoparticles started to aggregate when the concentration was above 1%. Therefore, the synergy between silica nanoparticles and ionic surfactants was only tested when the nanoparticle concentration was below 1% (Figure 14). Furthermore, it was observed that both the surface tension and the magnitude of the zeta potential increased with the addition of nanoparticles to CTAB and CPC surfactants, suggesting that the silica nanoparticles were attracting surfactant molecules, as illustrated by Figure 15.

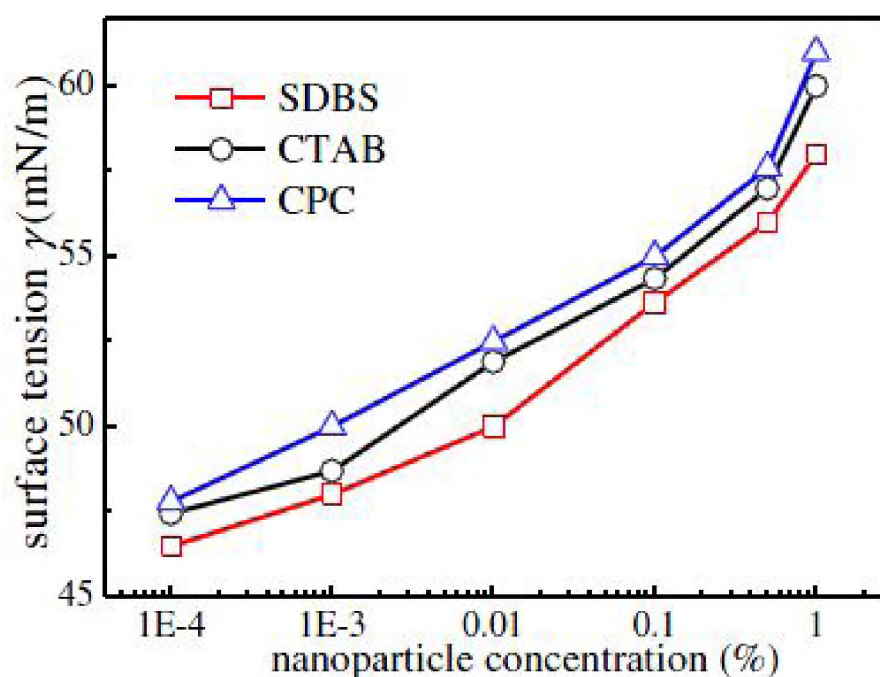


Figure 14. The change in interfacial tension due to the change in NP concentration. The plot was obtained from Jiang *et al.* (2016).

Qiu *et al.* (2010b) presented an experimental evaluation of the potential application of hydrophobic fumed silica nanoparticles (CAB-O-SIL TS-530) and a nonionic surfactant (Triton X-100) to recover heavy oil from the Alaska North Slope heavy oil reservoirs. Basically, this type of nanoparticles was employed to stabilize the emulsion with the surfactant. Also, it is capable of thickening the emulsion and providing an excellent resistance that reduces the adsorption by the rocks. In this experiment, rheology study on the emulsion has been performed by adding different amounts of nanoparticles. The results indicated that

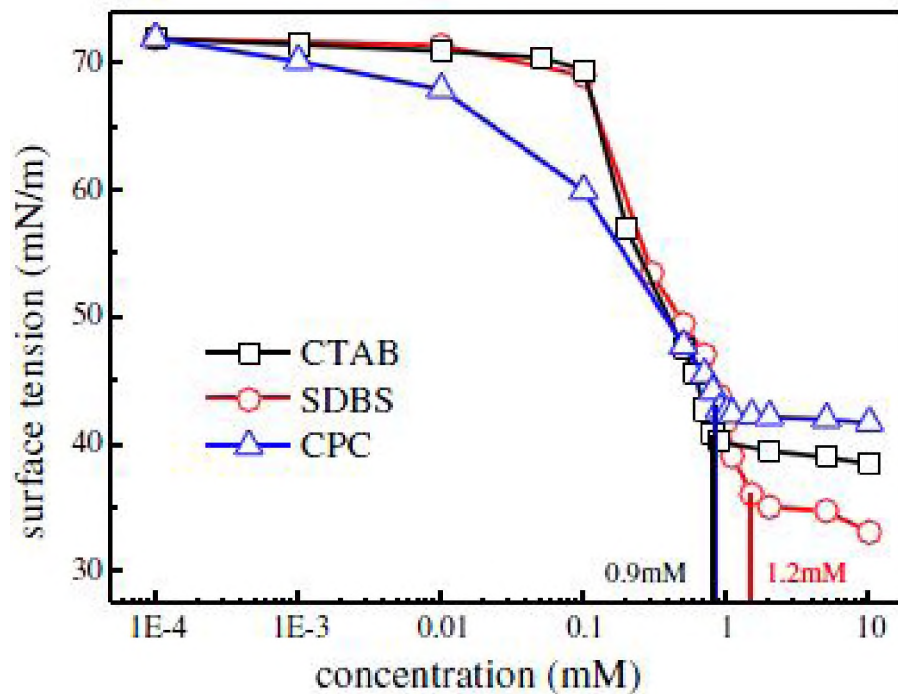


Figure 15. Interfacial tension changes with surfactant concentration. The plot was obtained from Jiang *et al.* (2016).

the employed nanofluids are capable of stabilizing the emulsion due to their huge surface area, which can provide low interfacial tension values with immiscible phases. Moreover, core flooding testing has shown that the emulsion flooding considerably increased the oil recovery factor after water flooding from 76% to 95% (Qiu *et al.*, 2010a). This improvement indicated that the emulsion blocked the water channels, increased the sweep efficiency, and mobilized the residual oil.

Although the addition of particles to surfactant systems does not always enhance the stability of emulsions as implied by Legrand *et al.* (2005), a stability and rheology study of oil-in-water emulsion containing a mixture of hydrophilic silica nanoparticles and non-ionic surfactant molecules was reported by Binks *et al.* (2007). The oil-water interfacial tension of the nanofluid mixture has dramatically decreased with increasing the concentration of surfactants from 31 to $1.7 \frac{\text{dyne}}{\text{cm}}$. The decrease in interfacial tension is predicted to further enhance the recovered oil. Furthermore, Sun *et al.* (2014) studied foam

stability by blending partially hydrophobic SiO_2 nanoparticles with an anionic surfactant (SDS). The results revealed that the reduction in interfacial tension values by a factor of 80% after the addition of nanofluid has led to foam stability, and as expected, their results indicated that foam stability decreased with an increase in the temperature.

Similarly, the effect of hydrophilic SiO_2 nanoparticles blended with an anionic surfactant (SDS) and a polymer (polyacrylamide, PAM) on wettability alteration and IFT reduction was reported by Sharma *et al.* (2016). Their results showed that ultra-low IFT values were obtained when these nanofluids were employed, compared to each solution alone.

In addition, Vatanparast *et al.* (2017) applied different experiments for the investigation of CTAB surfactant and hydrophilic silica nanoparticle solutions at low surfactant to nanoparticle ratios, in which only few surfactant molecules were adsorbed at the nanoparticles' surface. They have found that hydrophilic silica nanoparticles are not surface modifiers alone, and have minimal effects on the oil-water interfacial tension. However, in the presence of CTAB surfactant, nanoparticles turn into surface modifiers by adsorbing surfactant molecules and strongly affecting the interfacial tension values. Similarly, Bazazi *et al.* (2017) revealed that interfacial tension values between heavy oil and water reduced 75% after the addition of nonionic surfactant-based silica nanoparticle solutions.

Zargartalebi *et al.* (2015) conducted an extensive series of interfacial tension measurements on hydrophobic and hydrophilic silica nanoparticles dispersed in an anionic surfactant (SDS). It was observed that the adsorption amount of the employed surfactant was reduced when mixed with nanoparticles. The results of the interfacial tension measurements between surfactant-coated nanoparticle solution and oil revealed a strange behavior that started with a rapid decrease in low surfactant concentration, followed with an increase at higher concentrations.

Table 4. Summary of interfacial tension reduction of silica nanoparticle-surfactant flooding experiments.

References	NP	Surfactant	Base Fluid	Oil Type	Core Type	Tested Parameters	IFT mN/m (From-To)
(Lan <i>et al.</i> , 2007)	Silica Aerosil 200	CTAB	DI	NA	NA	Concentration, NP size	52 - 5
(Vatanparast <i>et al.</i> , 2017)	Hydrophilic silica	CTAB	Distilled water	Heptane	NA	Concentration	51 - 2
(Ravera <i>et al.</i> , 2008)	Colloidal silica	CTAB (cationic)	Water	Hexane	NA	Frequency, Concentration	72.5 - 21
(Le <i>et al.</i> , 2011)	SiO_2	(Anionic) XSA-1416D SS16-47A IAMS-M2-P	DI	Crude oil	Sandstone	Concentration, Surfactant type	24 - 0.2
(Jiang <i>et al.</i> , 2016)	Hydrophobic silica	CTAB SDBS CPC	Water	NA	NA	Concentration	73 - 32
(Zargartalebi <i>et al.</i> , 2015)	Hydrophilic fumed silica (A-300) Hydrophobic silica (R-816)	(Anionic) SDS	Distilled water	Medium	Sandpack	Concentration, Injection regime	20 - 2
(Qiu <i>et al.</i> , 2010b)	Hydrophobic fumed silica	(Non-ionic) Triton X-100	Brine	Heavy	Sandstone	Concentration	29 - 0.08
(Binks <i>et al.</i> , 2007)	hydrophilic silica	(Non-ionic) alkylpolyoxyethylene	Water	Medium	NA	Concentration	31 - 1.7
(Sharma <i>et al.</i> , 2016)	Hydrophilic silica	(Anionic) SDS	DI	Medium	Sandstone	NP size, Concentration, Adding polymer, Temperature	NA - 2
(Sun <i>et al.</i> , 2014)	Hydrophobic silica	(Anionic) SDS	Brine	Crude	Sandpack	Concentration, Temperature	22 - 6
(Ma <i>et al.</i> , 2008)	Colloidal silica	SDS Triton X-100	Water	Tri-chloroethylene	NA	Concentration	40 - 2
(Bazazi <i>et al.</i> , 2017)	SiO_2	(Non-ionic) Tween 20	DI	Heavy	Carbonate	Concentration, Dye effect	42 - 10

4.2.2. Metallic Oxide Nanoparticles. Although silicates are the most commonly examined nanoparticle type, some studies have reported the effect of metallic oxide nanoparticles. Generally, these nanoparticles are considered as hydrophilic materials. In addition, Table 5 summarizes the experimental studies that explore the effect of metallic nanoparticles and surfactants on IFT. Esmailzadeh *et al.* (2014) have reported the liquid-liquid and liquid-air interfacial tension of zirconium oxide nanoparticles in cationic, anionic, and nonionic surfactant solutions. They have shown that ZrO_2 nanoparticles adsorbed at the oil-water interface, resulting in a reduction in the interfacial tension value. In addition, the experiment revealed that ZrO_2 nanoparticles strongly interacted with all examined surfactants. It was also found that the tested nanoparticles have no effect on the interfacial tension when the concentrations of the surfactants are above the critical micelle concentration (CMC). Conversely, ZrO_2 nanoparticles have a lowering effect for all tested surfactants when the concentration is below CMC. It was also reported that the lowest interfacial tension value was observed when nanoparticles were mixed with the nonionic surfactant (LA7). Furthermore, an experimental study of an aqueous solution of anionic surfactants and metal nanoparticles was reported by Suleimanov *et al.* (2011). It was shown that the implication of the nanofluid permitted a 70% to 90% reduction of interfacial tension on the oil boundary, compared with each surfactant solution alone.

Additionally, wet foams generated from the nanofluids are thermodynamically unstable due to their large air-water interfacial area. Although surfactants could be used to reduce the interfacial area in wet foams, they can be easily desorbed from the air-water interface because their energy of attachment to the interface is comparable to thermal energy. As a result, surfactants alone are not capable of ultimately reducing the interfacial area in wet foams. Thus, particles have been introduced to wet foams to stabilize them by reducing the interfacial area between the air-water interface. Surfactant-coated nanoparticles have been proven to stabilize wet foam further than surfactants alone (Murray and Ettelaie, 2004). An experimental study of different metal nanoparticles [Al_2O_3 , ZrO_2 , $Ca_3(PO_4)_2$, and TiO_2]

and nonionic surfactant [Triton X-45] presented a novel method for the preparation of high volume surfactant-coated nanoparticles stabilized foams, which intended to overcome the bubble growth and drainage issues (Gonzenbach *et al.*, 2006). The stability of the generated foam was proven by the reduction in interfacial tensions.

Vashisth *et al.* (2010) have reported that the addition of surfactant displaces nanoparticles from the interface. They have also stated that a complete interfacial displacement and nanoparticle recovery can only be achieved when surfactant concentration is above the CMC. In addition, they indicated that the required energy to remove a trapped nanoparticle from the interface is at least equivalent to several thousand times more than the typical "Brownian thermal energy well". Since this energy is proportional to the oil-water interfacial tension (Binks, 2002), the addition of surfactant is capable of reducing the desorption energy by lowering the oil-water interfacial tension.

4.3. OIL VISCOSITY REDUCTION AND CONFORMANCE CONTROL

Modifying the viscosity of injection fluids to match that of the oil phase is a significant technique to obtain better conformance and mobility control capabilities. Different studies have shown that aqueous dispersion viscosity increases as the size of silica nanoparticles decreases (Lau *et al.*, 2017; Metin *et al.*, 2013, 2012, 2011a,b), as illustrated in Table 6. In addition, Rankin and Nguyen (2014) reported the concept of silica nanoparticle gels for conformance control in heterogeneous and fractured reservoirs. They showed that permeability reduction resulted from gelation could be achieved at low concentrations of silica nanoparticles.

As explained earlier, nanoparticles can be employed to stabilize emulsion and foam due to their surface activities, which lead to the enhancement of injection fluids. In addition, nanofluids composed of hydrophilic silica nanoparticles and cationic surfactants (CTAB) were experimentally found to stabilize emulsions and improve heavy oil recovery (Pei *et al.*, 2015). A possible explanation of this behavior is that the oil-in-water emulsions

stabilized by surfactant-coated silica nanoparticles might have exhibited significant shear thinning behavior with high viscosity at low shear rates, making them valid candidates for conformance control agents. Furthermore, Ogolo *et al.* (2012); Salem *et al.* (2015) revealed that aluminum oxide nanofluids dispersed in brine were able to reduce oil viscosity by breaking carbon-sulfur bonds, which eventually could be used for conformance and mobility control. Additionally, Sharma *et al.* (2015) conducted a series of experiments and concluded that the performance of conventional surfactant-polymer flooding tests was improved by an emulsion stabilized with nanoparticle-surfactant-polymer solution due to improved water viscosity and oil-water IFT.

Furthermore, polyacrylamide micro-gel nano spheres have been studied experimentally by Wang *et al.* (2010). These particles were dispersed in a mixture of emulsions in combination with *NaOH*, which was a key factor in reducing IFT by forming in situ surfactants. The results showed that oil recovery from a heavy oil reservoir increased by 20%. On the other hand, the utilization of this nanofluid in field applications is limited due to its extremely high cost (Negin *et al.*, 2016).

Likewise, viscosity reduction of heavy oil reservoirs by adding surfactant-based nanoparticle solutions has been reported by Srinivasan *et al.* (2014). The results from this experimental study revealed that the generated nanoemulsions composed of *CuO* nanoparticles and Triton X-100 surfactant were successful in reducing the viscosity of the heavy oil to lower values compared to the regular viscosity reducers, especially at higher shear rates, as illustrated by Figure 16. In addition, a significant reduction in interfacial tension values was also observed after the formation of the oil-in-water emulsion system.

Qiu *et al.* (2010b) indicate that the viscosity of the employed emulsion increased with increasing the amount of nanoparticles, and the emulsion tended to behave like a Newtonian fluid. This study also mentions that the employed nanofluids can improve the

mobility of the emulsion by thickening it. Ultimately, these surfactant-based nanofluids can reduce the surfactant adsorption by the porous media and indirectly limit its usage in the whole enhanced oil recovery process.

Pei *et al.* (2015) presented a study of silica nanoparticle-surfactant (CTAB-cationic) stabilized emulsion to enhance heavy oil recovery. They first conducted phase behavior and rheology tests to investigate the influence of nanoparticles on the stability and rheological properties of the emulsion system. Later, they conducted core flooding tests to investigate the displacement mechanisms for enhanced heavy oil recovery by nanofluids. The phase behavior results have revealed that the addition of nanoparticles cannot only enhance the stability of the emulsion, but also considerably increase the emulsion's viscosity. Additionally, the microscopic visualization study suggested that nanoparticles can thicken the emulsion to the desirable mobility, leading to great improvement in sweep efficiency. The heavy oil was emulsified into the water phase to form emulsions with the assist of ionic surfactants, which were the recovery mechanisms for enhanced oil recovery by silica nanoparticle-surfactant stabilized emulsion.

4.4. DISCUSSION OF SURFACTANTS-NANOPARTICLES RECOVERY MECHANISMS

The employment of different sizes, types, and concentrations of surfactants and nanoparticles leads to different recovery mechanisms. Thus it is crucial to define the goal and objective of a surfactant-nanoparticle solution upon selecting the size, type and concentration of surfactants and nanoparticles. In other words, the required recovery mechanisms could be achieved by selecting the appropriate surfactants and nanoparticles. Moreover, the selection of the employed surfactants mainly depends on the properties of the nanoparticles and the solution. For example, when metal oxide nanoparticles are dispersed into a non-polar base fluid (knowing that metal oxide nanoparticles are easily dispersed in polar fluids), it is required to add surfactants to enhance the stability of the

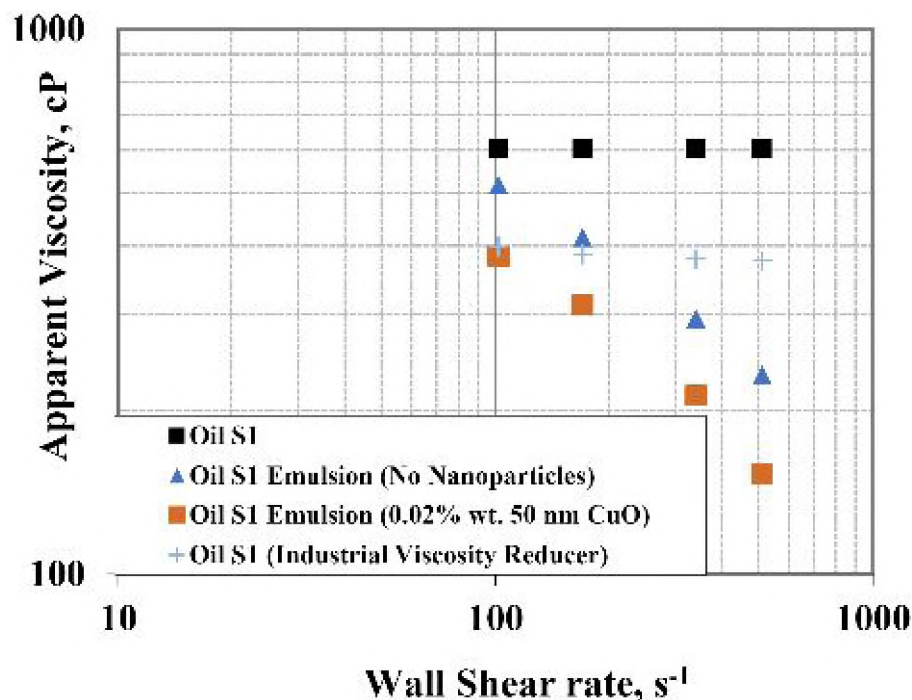


Figure 16. Heavy oil viscosity reduction using surfactant-based CuO nanofluid. The plot was obtained from Srinivasan *et al.* (2014).

nanoparticles. Furthermore, the relative concentration of surfactants and nanoparticles defines the properties of surfactant-coated nanoparticles. If the concentration ratio between surfactants and nanoparticle is relatively low, only a small portion of the nanoparticle surface would be coated with surfactants. However, larger concentration ratios can form a double layer of surfactants on the nanoparticles.

5. CHALLENGES AND LIMITATIONS

Although nanoparticles alone and combined with surfactants are laboratory-proved to be potential candidates in EOR processes, their utilization in field applications is very limited. Basically, several challenges have to be resolved before this technology is implemented in practical field applications. These challenges are as follows:

Table 5. Summary of interfacial tension reduction of metallic nanoparticle-surfactant flooding experiments

References	NP	Surfactant	Base Fluid	Oil Type	Tested Parameters	IFT mN/m (From - To)
(Esmailzadeh <i>et al.</i> , 2014)	ZrO_2	SDS CTAB LA7	Distilled water	Heptane	Concentration, NP size	51 - 5
(Suleimanov <i>et al.</i> , 2011)	Non-ferrous metal NP	(Anionic) Sulphanole	NA	Heavy	Concentration	18 - 1
(Gonzenbach <i>et al.</i> , 2006)	Al_2O_3 , ZrO_2 , $Ca_3(PO_4)_2$, TiO_2	(Non-ionic) Triton X-45	DI	NA	NP type, PH, Concentration	72 - 55
(Srinivasan <i>et al.</i> , 2014)	CuO	Triton X-100	Brine	Heavy	Concentration, Temperature	20 - 0.1

Table 6. Summary of viscosity reduction of nanoparticle-surfactant flooding experiments

References	NP	Surfactant	Base Fluid	Oil Type	Core Type	Tested Parameters	Viscosity, cp (From - To)
(Srinivasan <i>et al.</i> , 2014)	<i>CuO</i>	Triton X-100	Brine	Heavy	NA	Concentration, Temperature	600 - 150 at 70 F° 50 - 18 at 175 F°
(Sharma <i>et al.</i> , 2015)	Hydrophilic <i>SiO₂</i>	SDS	Brine	Light	Sandstone	NP size, Injection regime, Adding polymer	800 - 10 at 100 F° 800 - 7 at 200 F°
(Wang <i>et al.</i> , 2010)	Polyacrylamide microgel nano-spheres	SLPS	DI	Heavy	Sandpack	Concentration, Adding polymer	238 - 5 at 130 F°
(Pei <i>et al.</i> , 2015)	Hydrophilic <i>SiO₂</i>	CTAB	Distilled water	Heavy	NA	Concentration, Shear rate	350 - 2 at 130 F°

1. Technical challenges associated with nanoparticles: As mentioned earlier, nanoparticles tend to aggregate and block pore throats due to the strong interactions, especially under harsh conditions. As a result, it is very crucial to generate homogeneous suspensions of nanoparticles and utilize strong and economic surfactants to enhance their stability (Ehtesabi *et al.*, 2014).
2. The available experimental studies conducted using metallic oxide nanoparticles proved their ability as EOR agents. However, the number of these studies is very limited compared with studies conducted using silica nanoparticles. This is probably due to the availability of silicas over metallic oxides. Therefore, conducting experimental studies on different types of nanoparticles, including metallic, magnetic and inorganic, is important to test their ability to enhance oil production.
3. The lack of experiments using a mixture of nanoparticles and surfactants. This lack of experimental studies on nanofluid mixtures hinders their possible wide enhancement in EOR processes.
4. The number of core flooding experiments is limited. Conducting these experiments is significantly important to visualize the production enhancement at laboratory scale.

Therefore, it is crucial to conduct experimental studies that overcome the above mentioned challenges. In addition, building mathematical models for various surfactant-based nanoparticles might be helpful to better understand the recovery mechanisms. These models are intended to help in selecting the best and suitable nanofluid mechanisms for field applications and reduce the risk associated with it.

6. CONCLUSION

This paper presented a literature review of the synergy between surfactants and nanoparticles. Basically, the recovery mechanisms associated with this combination are mainly classified into three categories: (1) rock wettability modification towards water-wet, (2) ultra-low oil-water interfacial tension values, and (3) oil viscosity reduction and conformance control. These mechanisms are achieved by introducing a disjoining pressure between the oil phase and rock surface by creating a wedge-film structure on the rock surface. Moreover, the stability of nanoparticle solutions could be enhanced by the addition of surfactants, which is basically the main reason of adding surfactants to nanoparticles. This review has clearly shown that the recovery mechanisms of nanoparticle flooding are enhanced and improved by adding surfactants to the solution. The different recovery mechanisms could be achieved by the employment of different sizes, types, and concentrations of surfactants and nanoparticles. Throughout this review, the interactions between different types of surfactants and nanoparticles have been reviewed. In addition, the stabilization of nanoparticles is sensitive to surfactant-nanoparticle concentration ratios. At low concentration ratios of surfactant to nanoparticle, a mono-layer of surfactant is adsorbed on the particle's surface, resulting in hydrophobic surface. However, if a bi-layer of surfactant is adsorbed to nanoparticles, it might lead to higher stabilization due to electrostatic repulsion. Although field trials have not yet been conducted using this combination, lab studies have proven that different surfactant-based nanofluids are effective in recovering extra amounts of oil.

NOMENCLATURE

IFT Interfacial tension, mN/m.

PPM Parts per million.

SDS Sodium dodecyl sulfate.

PV Pore volume.

CMC Critical micelle concentration.

DI Deionized water.

REFERENCES

- Ahmadall, T., Gonzalez, M. V., Harwell, J. H., Scamehorn, J. F., *et al.*, 'Reducing surfactant adsorption in carbonate reservoirs,' *SPE reservoir engineering*, 1993, **8**(02), pp. 117–122.
- Ahmadi, M. A., Shadizadeh, S. R., and , 'Adsorption of novel nonionic surfactant and particles mixture in carbonates: enhanced oil recovery implication,' *Energy & Fuels*, 2012, **26**(8), pp. 4655–4663.
- Ahmadi, M. A. and Shadizadeh, S. R., 'Induced effect of adding nano silica on adsorption of a natural surfactant onto sandstone rock: experimental and theoretical study,' *Journal of Petroleum Science and Engineering*, 2013, **112**, pp. 239–247.
- Ahmadi, Y., Eshraghi, S. E., Bahrami, P., Hasanbeygi, M., Kazemzadeh, Y., and Vahedian, A., 'Comprehensive water–alternating–gas (wag) injection study to evaluate the most effective method based on heavy oil recovery and asphaltene precipitation tests,' *Journal of Petroleum Science and Engineering*, 2015, **133**, pp. 123–129.
- Al-Anssari, S., Barifcani, A., Wang, S., and Iglauer, S., 'Wettability alteration of oil-wet carbonate by silica nanofluid,' *Journal of colloid and interface science*, 2016, **461**, pp. 435–442.
- Alomair, O. A., Matar, K. M., Alsaeed, Y. H., *et al.*, 'Nanofluids application for heavy oil recovery,' in '*SPE Asia Pacific Oil & Gas Conference and Exhibition*,' Society of Petroleum Engineers, 2014 .

- Amanullah, M., Al-Tahini, A. M., *et al.*, 'Nano-technology-its significance in smart fluid development for oil and gas field application,' in 'SPE Saudi Arabia Section Technical Symposium,' Society of Petroleum Engineers, 2009 .
- Amott, E. *et al.*, 'Observations relating to the wettability of porous rock,' 1959.
- Ampian, S. G. and Virta, R. L., *Crystalline silica overview: Occurrence and analysis*, volume 9317, US Department of the Interior, Bureau of Mines, 1992.
- Anderson, W. G. *et al.*, 'Wettability literature survey-part 1: rock/oil/brine interactions and the effects of core handling on wettability,' *Journal of petroleum technology*, 1986, **38**(10), pp. 1–125.
- Arashiro, E. Y. and Demarquette, N. R., 'Use of the pendant drop method to measure interfacial tension between molten polymers,' *Materials Research*, 1999, **2**(1), pp. 23–32.
- Aveyard, R., Binks, B. P., and Clint, J. H., 'Emulsions stabilised solely by colloidal particles,' *Advances in Colloid and Interface Science*, 2003, **100**, pp. 503–546.
- Bazazi, P., Gates, I. D., Sanati Nezhad, A., Hejazi, S. H., *et al.*, 'Silica-based nanofluid heavy oil recovery a microfluidic approach,' in 'SPE Canada Heavy Oil Technical Conference,' Society of Petroleum Engineers, 2017 .
- Bell, C. G., Breward, C. J., Howell, P. D., Penfold, J., and Thomas, R. K., 'Macroscopic modeling of the surface tension of polymer- surfactant systems,' *Langmuir*, 2007, **23**(11), pp. 6042–6052.
- Bera, A., Ojha, K., Kumar, T., and Mandal, A., 'Mechanistic study of wettability alteration of quartz surface induced by nonionic surfactants and interaction between crude oil and quartz in the presence of sodium chloride salt,' *Energy & Fuels*, 2012, **26**(6), pp. 3634–3643.
- Binks, B. and Lumsdon, S., 'Influence of particle wettability on the type and stability of surfactant-free emulsions,' *Langmuir*, 2000, **16**(23), pp. 8622–8631.
- Binks, B. P., 'Particles as surfactants—similarities and differences,' *Current opinion in colloid & interface science*, 2002, **7**(1), pp. 21–41.
- Binks, B. P., Desforges, A., and Duff, D. G., 'Synergistic stabilization of emulsions by a mixture of surface-active nanoparticles and surfactant,' *Langmuir*, 2007, **23**(3), pp. 1098–1106.
- Binks, B. P., Kirkland, M., and Rodrigues, J. A., 'Origin of stabilisation of aqueous foams in nanoparticle–surfactant mixtures,' *Soft Matter*, 2008, **4**(12), pp. 2373–2382.
- Chang, H. L., Sui, X., Xiao, L., Guo, Z., Yao, Y., Yiao, Y., Chen, G., Song, K., Mack, J. C., *et al.*, 'Successful field pilot of in-depth colloidal dispersion gel (cdg) technology in daqing oilfield,' *SPE Reservoir Evaluation & Engineering*, 2006, **9**(06), pp. 664–673.

- Chengara, A., Nikolov, A. D., Wasan, D. T., Trokhymchuk, A., and Henderson, D., 'Spreading of nanofluids driven by the structural disjoining pressure gradient,' *Journal of colloid and interface science*, 2004, **280**(1), pp. 192–201.
- Craig, F. F., *The reservoir engineering aspects of waterflooding*, volume 3, HL Doherty Memorial Fund of AIME New York, 1971.
- Cui, Z.-G., Cui, Y.-Z., Cui, C.-F., Chen, Z., and Binks, B., 'Aqueous foams stabilized by in situ surface activation of CaCO_3 nanoparticles via adsorption of anionic surfactant,' *Langmuir*, 2010, **26**(15), pp. 12567–12574.
- Diaz, D., Somaruga, C., Norman, C., Romero, J. L., *et al.*, 'Colloidal dispersion gels improve oil recovery in a heterogeneous argentina waterflood,' in 'SPE Symposium on Improved Oil Recovery,' Society of Petroleum Engineers, 2008 .
- Ehtesabi, H., Ahadian, M., and Taghikhani, V., 'Investigation of diffusion and deposition of TiO_2 nanoparticles in sandstone rocks for eor application,' in '76th EAGE Conference and Exhibition 2014,' 2014 .
- El-Diasty, A. I., Ragab, A. M. S., *et al.*, 'Applications of nanotechnology in the oil & gas industry: Latest trends worldwide & future challenges in egypt,' in 'North Africa Technical Conference and Exhibition,' Society of Petroleum Engineers, 2013 .
- El-Diasty, A. I. *et al.*, 'The potential of nanoparticles to improve oil recovery in bahariya formation, egypt: An experimental study,' in 'SPE Asia Pacific Enhanced Oil Recovery Conference,' Society of Petroleum Engineers, 2015 .
- Engeset, B., *The Potential of Hydrophilic Silica Nanoparticles for EOR Purposes: A literature review and an experimental study*, Master's thesis, Institutt for petroleumsteknologi og anvendt geofysikk, 2012.
- Esmailzadeh, P., Hosseinpour, N., Bahramian, A., Fakhroueian, Z., and Arya, S., 'Effect of ZnO nanoparticles on the interfacial behavior of surfactant solutions at air–water and n-heptane–water interfaces,' *Fluid Phase Equilibria*, 2014, **361**, pp. 289–295.
- Espinoza, D. A., Caldelas, F. M., Johnston, K. P., Bryant, S. L., Huh, C., *et al.*, 'Nanoparticle-stabilized supercritical CO_2 foams for potential mobility control applications,' in 'SPE Improved Oil Recovery Symposium,' Society of Petroleum Engineers, 2010 .
- Feng, Z. C., *Handbook of zinc oxide and related materials: volume two, devices and nano-engineering*, volume 2, CRC press, 2012.
- Fletcher, A., Davis, J., *et al.*, 'How eor can be transformed by nanotechnology,' in 'SPE Improved Oil Recovery Symposium,' Society of Petroleum Engineers, 2010 .
- Friedheim, J. E., Young, S., De Stefano, G., Lee, J., Guo, Q., *et al.*, 'Nanotechnology for oilfield applications-hype or reality?' in 'SPE International Oilfield Nanotechnology Conference and Exhibition,' Society of Petroleum Engineers, 2012 .

- Giraldo, J., Benjumea, P., Lopera, S., Cortes, F. B., and Ruiz, M. A., 'Wettability alteration of sandstone cores by alumina-based nanofluids,' *Energy & Fuels*, 2013, **27**(7), pp. 3659–3665.
- Gonzenbach, U. T., Studart, A. R., Tervoort, E., and Gauckler, L. J., 'Stabilization of foams with inorganic colloidal particles,' *Langmuir*, 2006, **22**(26), pp. 10983–10988.
- Green, D. W., Willhite, G. P., *et al.*, *Enhanced oil recovery*, volume 6, Henry L. Doherty Memorial Fund of AIME, Society of Petroleum Engineers Richardson, TX, 1998.
- Haroun, M. R., Alhassan, S., Ansari, A. A., Al Kindy, N. A. M., Abou Sayed, N., Kareem, A., Ali, B., Sarma, H. K., *et al.*, 'Smart nano-eor process for abu Dhabi carbonate reservoirs,' in 'Abu Dhabi International Petroleum Conference and Exhibition,' Society of Petroleum Engineers, 2012 .
- Hashemi, R., Nassar, N. N., and Almao, P. P., 'Nanoparticle technology for heavy oil in-situ upgrading and recovery enhancement: Opportunities and challenges,' *Applied Energy*, 2014, **133**, pp. 374–387.
- Hendraningrat, L., Li, S., Torsaeter, O., *et al.*, 'Enhancing oil recovery of low-permeability berea sandstone through optimised nanofluids concentration,' in 'SPE Enhanced Oil Recovery Conference,' Society of Petroleum Engineers, 2013a .
- Hendraningrat, L., Li, S., Torsater, O., *et al.*, 'Effect of some parameters influencing enhanced oil recovery process using silica nanoparticles: An experimental investigation,' in 'SPE Reservoir Characterization and Simulation Conference and Exhibition,' Society of Petroleum Engineers, 2013b .
- Hendraningrat, L. and Torsæter, O., 'Metal oxide-based nanoparticles: revealing their potential to enhance oil recovery in different wettability systems,' *Applied Nanoscience*, 2015, **5**(2), pp. 181–199.
- Hendraningrat, L., Torsaeter, O., *et al.*, 'Unlocking the potential of metal oxides nanoparticles to enhance the oil recovery,' in 'Offshore Technology Conference-Asia,' Offshore Technology Conference, 2014 .
- Hornyak, G. L., Tibbals, H. F., Dutta, J., and Moore, J. J., *Introduction to Nanoscience and Nanotechnology*, CRC Press, Baton Rouge, 1 edition, 2009, ISBN 1420047795;9781420047790.
- Huang, T., Evans, B. A., Crews, J. B., Belcher, C. K., *et al.*, 'Field case study on formation fines control with nanoparticles in offshore applications,' in 'SPE Annual Technical Conference and Exhibition,' Society of Petroleum Engineers, 2010 .
- Huh, C., Nizamidin, N., Pope, G. A., Milner, T. E., and Bingqing, W., 'Hydrophobic paramagnetic nanoparticles as intelligent crude oil tracers,' 2014, uS Patent App. 14/765,426.

- Hunter, T. N., Wanless, E. J., Jameson, G. J., and Pugh, R. J., 'Non-ionic surfactant interactions with hydrophobic nanoparticles: Impact on foam stability,' *Colloids and Surfaces A: Physicochemical and Engineering Aspects*, 2009, **347**(1), pp. 81–89.
- Jiang, L., Li, S., Yu, W., Wang, J., Sun, Q., and Li, Z., 'Interfacial study on the interaction between hydrophobic nanoparticles and ionic surfactants,' *Colloids and Surfaces A: Physicochemical and Engineering Aspects*, 2016, **488**, pp. 20–27.
- Jiang, L., Sun, G., Zhou, Z., Sun, S., Wang, Q., Yan, S., Li, H., Tian, J., Guo, J., Zhou, B., *et al.*, 'Size-controllable synthesis of monodispersed SnO_2 nanoparticles and application in electrocatalysts,' *The Journal of Physical Chemistry B*, 2005, **109**(18), pp. 8774–8778.
- Johannessen, A. M. and Spildo, K., 'Enhanced oil recovery (eor) by combining surfactant with low salinity injection,' *Energy & Fuels*, 2013, **27**(10), pp. 5738–5749.
- Ju, B., Dai, S., Luan, Z., Zhu, T., Su, X., Qiu, X., *et al.*, 'A study of wettability and permeability change caused by adsorption of nanometer structured polysilicon on the surface of porous media,' in 'SPE Asia Pacific Oil and Gas Conference and Exhibition,' Society of Petroleum Engineers, 2002 .
- Kanj, M. Y., Rashid, M., Giannelis, E., *et al.*, 'Industry first field trial of reservoir nanoagents,' in 'SPE Middle East Oil and Gas Show and Conference,' Society of Petroleum Engineers, 2011 .
- Karimi, A., Fakhroueian, Z., Bahramian, A., Pour Khiabani, N., Darabad, J. B., Azin, R., and Arya, S., 'Wettability alteration in carbonates using zirconium oxide nanofluids: Eor implications,' *Energy & Fuels*, 2012, **26**(2), pp. 1028–1036.
- Kazemzadeh, Y., Eshraghi, S. E., Kazemi, K., Sourani, S., Mehrabi, M., and Ahmadi, Y., 'Behavior of asphaltene adsorption onto the metal oxide nanoparticle surface and its effect on heavy oil recovery,' *Industrial & Engineering Chemistry Research*, 2015, **54**(1), pp. 233–239.
- Kothari, N., Raina, B., Chandak, K. B., Iyer, V., Mahajan, H. P., *et al.*, 'Application of ferrofluids for enhanced surfactant flooding in ior,' in 'SPE EUROPEC/EAGE Annual Conference and Exhibition,' Society of Petroleum Engineers, 2010 .
- Lan, Q., Yang, F., Zhang, S., Liu, S., Xu, J., and Sun, D., 'Synergistic effect of silica nanoparticle and cetyltrimethyl ammonium bromide on the stabilization of o/w emulsions,' *Colloids and Surfaces A: Physicochemical and Engineering Aspects*, 2007, **302**(1), pp. 126–135.
- Lau, H. C., Yu, M., and Nguyen, Q. P., 'Nanotechnology for oilfield applications: Challenges and impact,' *Journal of Petroleum Science and Engineering*, 2017, **157**, pp. 1160–1169.

- Le, N. Y. T., Pham, D. K., Le, K. H., and Nguyen, P. T., 'Design and screening of synergistic blends of sio₂ nanoparticles and surfactants for enhanced oil recovery in high-temperature reservoirs,' *Advances in Natural Sciences: Nanoscience and Nanotechnology*, 2011, **2**(3), p. 035013.
- Legrand, J., Chamerois, M., Placin, F., Poirier, J., Bibette, J., and Leal-Calderon, F., 'Solid colloidal particles inducing coalescence in bitumen-in-water emulsions,' *Langmuir*, 2005, **21**(1), pp. 64–70.
- Li, S., Genys, M., Wang, K., Torsæter, O., *et al.*, 'Experimental study of wettability alteration during nanofluid enhanced oil recovery process and its effect on oil recovery,' in 'SPE Reservoir Characterisation and Simulation Conference and Exhibition,' Society of Petroleum Engineers, 2015 .
- Li, S., Hendraningrat, L., , and Torsæter, O., 'A coreflood investigation of nanofluid enhanced oil recovery,' *Journal of Petroleum Science and Engineering*, 2013a, **111**, pp. 128–138.
- Li, S., Hendraningrat, L., and Torsaeter, O., 'Improved oil recovery by hydrophilic silica nanoparticles suspension: 2 phase flow experimental studies,' in 'IPTC 2013: International Petroleum Technology Conference,' 2013b .
- Limage, S., Kragel, J., Schmitt, M., Dominici, C., Miller, R., and Antoni, M., 'Rheology and structure formation in diluted mixed particle- surfactant systems,' *Langmuir*, 2010, **26**(22), pp. 16754–16761.
- Ma, H., Luo, M., and Dai, L. L., 'Influences of surfactant and nanoparticle assembly on effective interfacial tensions,' *Physical Chemistry Chemical Physics*, 2008, **10**(16), pp. 2207–2213.
- Mandal, A., Bera, A., Ojha, K., Kumar, T., *et al.*, 'Characterization of surfactant stabilized nanoemulsion and its use in enhanced oil recovery,' in 'SPE International Oilfield Nanotechnology Conference and Exhibition,' Society of Petroleum Engineers, 2012 .
- Mcelfresh, P. M., Holcomb, D. L., Ector, D., *et al.*, 'Application of nanofluid technology to improve recovery in oil and gas wells,' in 'SPE International Oilfield Nanotechnology Conference and Exhibition,' Society of Petroleum Engineers, 2012a .
- Mcelfresh, P. M., Olguin, C., Ector, D., *et al.*, 'The application of nanoparticle dispersions to remove paraffin and polymer filter cake damage,' in 'SPE International Symposium and Exhibition on Formation Damage Control,' Society of Petroleum Engineers, 2012b .
- Metin, C., Bonnacaze, R., Nguyen, Q., *et al.*, 'The viscosity of silica nanoparticle dispersions in permeable media,' *SPE Reservoir Evaluation & Engineering*, 2013, **16**(03), pp. 327–332.

- Metin, C. O., Baran, J. R., and Nguyen, Q. P., 'Adsorption of surface functionalized silica nanoparticles onto mineral surfaces and decane/water interface,' *Journal of Nanoparticle Research*, 2012, **14**(11), p. 1246.
- Metin, C. O., Bonnecaze, R. T., and Nguyen, Q. P., 'Shear rheology of silica nanoparticle dispersions,' *Applied Rheology*, 2011a, **21**(1), p. 13146.
- Metin, C. O., Lake, L. W., Miranda, C. R., and Nguyen, Q. P., 'Stability of aqueous silica nanoparticle dispersions,' *Journal of Nanoparticle Research*, 2011b, **13**(2), pp. 839–850.
- Mohebbifar, M., Ghazanfari, M. H., and Vossoughi, M., 'Experimental investigation of nano-biomaterial applications for heavy oil recovery in shaly porous models: A pore-level study,' *Journal of Energy Resources Technology*, 2015, **137**(1), p. 014501.
- Muller, P., Sudre, G., and Theodoly, O., 'Wetting transition on hydrophobic surfaces covered by polyelectrolyte brushes,' *Langmuir*, 2008, **24**(17), pp. 9541–9550.
- Murray, B. S. and Ettelaie, R., 'Foam stability: proteins and nanoparticles,' *Current opinion in colloid & interface science*, 2004, **9**(5), pp. 314–320.
- Naje, A. N., Norry, A. S., and Suhail, A. M., 'Preparation and characterization of sno2 nanoparticles,' *International Journal of Innovative Research in Science, Engineering and Technology*, 2013, **2**(12).
- Negin, C., Ali, S., and Xie, Q., 'Application of nanotechnology for enhancing oil recovery—a review,' *Petroleum*, 2016, **2**(4), pp. 324–333.
- Ng, W., Rana, D., Neale, G., and Hornof, V., 'Physicochemical behavior of mixed surfactant systems: petroleum sulfonate and lignosulfonate,' *Journal of applied polymer science*, 2003, **88**(4), pp. 860–865.
- Nguyen, P.-T., Do, B.-P. H., Pham, D.-K., Nguyen, Q.-T., Dao, D.-Q. P., Nguyen, H.-A., *et al.*, 'Evaluation on the eor potential capacity of the synthesized composite silica-core/polymer-shell nanoparticles blended with surfactant systems for the hpht offshore reservoir conditions,' in 'SPE International Oilfield Nanotechnology Conference and Exhibition,' Society of Petroleum Engineers, 2012 .
- Nwideo, L. N., Lebedev, M., Barifcani, A., Sarmadivaleh, M., and Iglauer, S., 'Wettability alteration of oil-wet limestone using surfactant-nanoparticle formulation,' *Journal of Colloid and Interface Science*, 2017.
- Ogolo, N., Olafuyi, O., Onyekonwu, M., *et al.*, 'Enhanced oil recovery using nanoparticles,' in 'SPE Saudi Arabia section technical symposium and exhibition,' Society of Petroleum Engineers, 2012 .
- Ogunberu, A. L. and Ayub, M., 'The role of wettability in petroleum recovery,' *Petroleum science and technology*, 2005, **23**(2), pp. 169–188.

- Parvazdavani, M., Masihi, M., and Ghazanfari, M. H., 'Monitoring the influence of dispersed nano-particles on oil–water relative permeability hysteresis,' *Journal of Petroleum Science and Engineering*, 2014, **124**, pp. 222–231.
- Pei, H., Zhang, G., Ge, J., Zhang, J., Zhang, Q., Fu, L., *et al.*, 'Investigation of nanoparticle and surfactant stabilized emulsion to enhance oil recovery in waterflooded heavy oil reservoirs,' in 'SPE Canada Heavy Oil Technical Conference,' Society of Petroleum Engineers, 2015 .
- Qiu, F., Mamora, D. D., *et al.*, 'Experimental study of solvent-based emulsion injection to enhance heavy oil recovery in alaska north slope area,' in 'Canadian Unconventional Resources and International Petroleum Conference,' Society of Petroleum Engineers, 2010a .
- Qiu, F. *et al.*, 'The potential applications in heavy oil eor with the nanoparticle and surfactant stabilized solvent-based emulsion,' in 'Canadian unconventional resources and international petroleum conference,' Society of Petroleum Engineers, 2010b .
- Ragab, A. M. S., Hannora, A. E., *et al.*, 'An experimental investigation of silica nano particles for enhanced oil recovery applications,' in 'SPE North Africa Technical Conference and Exhibition,' Society of Petroleum Engineers, 2015 .
- Rana, D., Neale, G., and Hornof, V., 'Surface tension of mixed surfactant systems: ligno-sulfonate and sodium dodecyl sulfate,' *Colloid and Polymer Science*, 2002, **280**(8), pp. 775–778.
- Rankin, K. and Nguyen, Q., 'Conformance control through in-situ gelation of silica nanoparticles,' in 'Nanotech Conference & Expo,' 2014 pp. 15–18.
- Ravera, F., Ferrari, M., Liggieri, L., Loglio, G., Santini, E., and Zanobini, A., 'Liquid–liquid interfacial properties of mixed nanoparticle–surfactant systems,' *Colloids and Surfaces A: Physicochemical and Engineering Aspects*, 2008, **323**(1), pp. 99–108.
- Roustaei, A. and Bagherzadeh, H., 'Experimental investigation of SiO_2 nanoparticles on enhanced oil recovery of carbonate reservoirs,' *Journal of Petroleum Exploration and Production Technology*, 2015, **5**(1), pp. 27–33.
- Roustaei, A., Moghadasi, J., Bagherzadeh, H., Shahrabadi, A., *et al.*, 'An experimental investigation of polysilicon nanoparticles' recovery efficiencies through changes in interfacial tension and wettability alteration,' in 'SPE International Oilfield Nanotechnology Conference and Exhibition,' Society of Petroleum Engineers, 2012 .
- Salem, A. M., Ragab, Hannora, A. E., *et al.*, 'A comparative investigation of nano particle effects for improved oil recovery–experimental work,' in 'SPE Kuwait Oil and Gas Show and Conference,' Society of Petroleum Engineers, 2015 .
- Salyer, I. O., 'Dry powder mixes comprising phase change materials,' 1993, uS Patent 5,211,949.

- Schmidt, G. and Malwitz, M. M., 'Properties of polymer–nanoparticle composites,' *Current opinion in colloid & interface science*, 2003, **8**(1), pp. 103–108.
- Shah, R. D. *et al.*, 'Application of nanoparticle saturated injectant gases for eor of heavy oils,' in 'SPE annual technical conference and exhibition,' Society of Petroleum Engineers, 2009 .
- Shahrabadi, A., Bagherzadeh, H., Roostaie, A., Golghanddashti, H., *et al.*, 'Experimental investigation of hlp nanofluid potential to enhance oil recovery: A mechanistic approach,' in 'SPE International Oilfield Nanotechnology Conference and Exhibition,' Society of Petroleum Engineers, 2012 .
- ShamsiJazeyi, H., Miller, C. A., Wong, M. S., Tour, J. M., and Verduzco, R., 'Polymer-coated nanoparticles for enhanced oil recovery,' *Journal of Applied Polymer Science*, 2014, **131**(15).
- Sharma, T., Iglauer, S., and Sangwai, J. S., 'Silica nanofluids in an oilfield polymer polyacrylamide: Interfacial properties, wettability alteration, and applications for chemical enhanced oil recovery,' *Industrial & Engineering Chemistry Research*, 2016, **55**(48), pp. 12387–12397.
- Sharma, T., Kumar, G. S., and Sangwai, J. S., 'Comparative effectiveness of production performance of pickering emulsion stabilized by nanoparticle–surfactant–polymer over surfactant–polymer (sp) flooding for enhanced oil recovery for brownfield reservoir,' *Journal of Petroleum Science and Engineering*, 2015, **129**, pp. 221–232.
- Shokrlu, Y. H., Babadagli, T., *et al.*, 'Transportation and interaction of nano and micro size metal particles injected to improve thermal recovery of heavy-oil,' in 'SPE Annual Technical Conference and Exhibition,' Society of Petroleum Engineers, 2011 .
- Singh, R., Mohanty, K. K., *et al.*, 'Foams stabilized by in-situ surface-activated nanoparticles in bulk and porous media,' *SPE Journal*, 2016, **21**(01), pp. 121–130.
- Skauge, T., Spildo, K., Skauge, A., *et al.*, 'Nano-sized particles for eor,' in 'SPE improved oil recovery symposium,' Society of Petroleum Engineers, 2010 .
- Song, E., Kim, D., Kim, B. J., and Lim, J., 'Surface modification of caco 3 nanoparticles by alkylbenzene sulfonic acid surfactant,' *Colloids and Surfaces A: Physicochemical and Engineering Aspects*, 2014, **461**, pp. 1–10.
- Srinivasan, A., Shah, S. N., *et al.*, 'Surfactant-based fluids containing copper-oxide nanoparticles for heavy oil viscosity reduction,' in 'SPE Annual Technical Conference and Exhibition,' Society of Petroleum Engineers, 2014 .
- Suleimanov, B., Ismailov, F., and Veliyev, E., 'Nanofluid for enhanced oil recovery,' *Journal of Petroleum Science and Engineering*, 2011, **78**(2), pp. 431–437.

- Sun, Q., Li, Z., Li, S., Jiang, L., Wang, J., and Wang, P., 'Utilization of surfactant-stabilized foam for enhanced oil recovery by adding nanoparticles,' *Energy & Fuels*, 2014, **28**(4), pp. 2384–2394.
- Tarek, M., El-Banbi, A. H., *et al.*, 'Comprehensive investigation of effects of nano-fluid mixtures to enhance oil recovery,' in 'SPE North Africa Technical Conference and Exhibition,' Society of Petroleum Engineers, 2015a .
- Tarek, M. *et al.*, 'Investigating nano-fluid mixture effects to enhance oil recovery,' in 'SPE Annual Technical Conference and Exhibition,' Society of Petroleum Engineers, 2015b .
- Thomas, S., 'Enhanced oil recovery-an overview,' *Oil & Gas Science and Technology-Revue de l'IFP*, 2008, **63**(1), pp. 9–19.
- Touhami, Y., Rana, D., Neale, G., and Hornof, V., 'Study of polymer-surfactant interactions via surface tension measurements,' *Colloid and Polymer Science*, 2001, **279**(3), pp. 297–300.
- Vashisth, C., Whitby, C. P., Fornasiero, D., and Ralston, J., 'Interfacial displacement of nanoparticles by surfactant molecules in emulsions,' *Journal of colloid and interface science*, 2010, **349**(2), pp. 537–543.
- Vatanparast, H., Javadi, A., and Bahramian, A., 'Silica nanoparticles cationic surfactants interaction in water-oil system,' *Colloids and Surfaces A: Physicochemical and Engineering Aspects*, 2017, **521**, pp. 221–230.
- Wang, L., Zhang, G., Li, G., Zhang, J., Ding, B., *et al.*, 'Preparation of microgel nanospheres and their application in eor,' in 'International Oil and Gas Conference and Exhibition in China,' Society of Petroleum Engineers, 2010 .
- Wasan, D., Nikolov, A., and Kondiparty, K., 'The wetting and spreading of nanofluids on solids: Role of the structural disjoining pressure,' *Current Opinion in Colloid & Interface Science*, 2011, **16**(4), pp. 344–349.
- Wasan, D. T. and Nikolov, A. D., 'Spreading of nanofluids on solids,' *Nature*, 2003, **423**(6936), pp. 156–159.
- Worthen, A. J., Bryant, S. L., Huh, C., and Johnston, K. P., 'Carbon dioxide-in-water foams stabilized with nanoparticles and surfactant acting in synergy,' *AIChE Journal*, 2013, **59**(9), pp. 3490–3501.
- Wu, W., He, Q., and Jiang, C., 'Magnetic iron oxide nanoparticles: synthesis and surface functionalization strategies,' *Nanoscale research letters*, 2008a, **3**(11), p. 397.
- Wu, Y., Shuler, P. J., Blanco, M., Tang, Y., Goddard, W. A., *et al.*, 'An experimental study of wetting behavior and surfactant eor in carbonates with model compounds,' *SPE Journal*, 2008b, **13**(01), pp. 26–34.

- XU, K., Zhu, P., Tatiana, C., Huh, C., Balhoff, M., *et al.*, 'A microfluidic investigation of the synergistic effect of nanoparticles and surfactants in macro-emulsion based eor,' in 'SPE Improved Oil Recovery Conference,' Society of Petroleum Engineers, 2016 .
- Yahya, N., Kashif, M., Nasir, N., Niaz Akhtar, M., and Yusof, N. M., 'Cobalt ferrite nanoparticles: an innovative approach for enhanced oil recovery application,' in 'Journal of Nano Research,' volume 17, Trans Tech Publ, 2012 pp. 115–126.
- Yu, H., Hermann, S., Schulz, S. E., Gessner, T., Dong, Z., and Li, W. J., 'Optimizing sonication parameters for dispersion of single-walled carbon nanotubes,' Chemical Physics, 2012, **408**, pp. 11–16.
- Yu, J., Berlin, J. M., Lu, W., Zhang, L., Kan, A. T., Zhang, P., Walsh, E. E., Work, S., Chen, W., Tour, J., *et al.*, 'Transport study of nanoparticles for oilfield application,' in 'SPE International Conference on Oilfield Scale,' Society of Petroleum Engineers, 2010 .
- Zargartalebi, M., Kharrat, R., and Barati, N., 'Enhancement of surfactant flooding performance by the use of silica nanoparticles,' Fuel, 2015, **143**, pp. 21–27.
- Zhang, T., Davidson, D., Bryant, S. L., Huh, C., *et al.*, 'Nanoparticle-stabilized emulsions for applications in enhanced oil recovery,' in 'SPE improved oil recovery symposium,' Society of Petroleum Engineers, 2010 .

II. CHARACTERIZATION AND OIL RECOVERY ENHANCEMENT BY A POLYMERIC NANOGEL COMBINED WITH SURFACTANT FOR SANDSTONE RESERVOIRS

Mustafa M. Almahfood, Author ^{a, b}

Baojun Bai, Co-Author ^a

^aDepartment of Geosciences & Petroleum Engineering

Missouri University of Science and Technology

Rolla, Missouri 65409

^b EXPEC Advanced Research Center, Saudi Aramco, Saudi Arabia

Email: mmantc@mst.edu

ABSTRACT

The characterization and enhanced oil recovery mechanisms of a nanosized polymeric crosslinked gel are presented herein. A negatively charged nanogel was synthesized using a typical free radical suspension polymerization process by employing 2-acrylamido 2-methyl propane sulfonic acid monomer. The synthesized nanogel showed a narrow size distribution with one peak pointing to a predominant homogeneous droplet size. The charged nanogels were also able to adsorb at the oil-water interfaces to reduce interfacial tension and stabilize oil-in-water emulsions, which ultimately improved the recovered oil from hydrocarbon reservoirs. In addition, a fixed concentration of negatively charged surfactant (sodium dodecyl sulfate or SDS) was combined with different concentrations of the nanogel. The effect of the nanogels combined with surfactant on sandstone core plugs was examined by running a series of core flooding experiments using multiple flow patterns. The results suggest the ability of the nanogel, both alone and combined with SDS, to improve the oil recovery by a factor of 15% after initial seawater flooding.

Keywords: nanogel, polymeric nanogel, surfactant-based-nanogel, enhanced oil recovery

1. INTRODUCTION

Most oilfields around the world have already reached or will soon reach the phase where the oil production rate is approaching the decline period (Li *et al.*, 2013). Thus, one of the major challenges that faces the oil industry today is how to delay the abandonment of current fields by reducing excess water production and extracting more oil economically. EOR applications are generally implemented in oilfields to enhance oil recovery and reduce water production. Chemical based EOR methods (thermal and gas methods) can improve oil recovery through four major mechanisms: (1) interfacial tension reduction, (2) wettability modification towards a water-wet state, (3) conformance control improvement for better sweep efficiency, and (4) emulsifying crude oil (Binks *et al.*, 2007; Thomas, 2008). Gel treatments have been proven to be a cost-effective method for conformance control improvements (Bai *et al.*, 2013). Different particle gels have been proposed to enhance oil recovery and control excess water production such as preformed particle gels (PPG) (Bai *et al.*, 2007), micro-gels (Rousseau *et al.*, 2005), temperature-sensitive gels which are commonly known as bright water (Frampton *et al.*, 2004), and pH-sensitive gels (Al-Anazi *et al.*, 2002). Nanosized cross-linked polymeric particles known as nanogels are newly developed particles in EOR applications. They are defined as base fluids with nanosized particles that have an average particle size of less than 100 nm (Sun *et al.*, 2017). They are, also, known for their easy injection process due to their small size, which is much smaller than the diameter of the pore throats in oil reservoirs (Qiu *et al.*, 2010). They are able to mobilize residual oil, which enhances oil recovery by mainly reducing the interfacial tension (Lenchenkov *et al.*, 2016).

In contrast to conventional in-depth plugging agents such as preformed particle gels (PPG) and in-situ gels, nanogels are characterized by low viscosity (Bai *et al.*, 2013; Moraes *et al.*, 2011). Also, nanogels can reduce the interfacial tension by adsorbing at the oil-water

interface, which stabilizes oil-in-water emulsions, leading to improvement of the recovered oil from reservoirs (Geng *et al.*, 2018a). Suleimanov and Veliyev (2017) showed that the oil recovery from a sandstone reservoir has increased by 6% after nanogel flooding, compared to gel treatment without nanosized particles.

Multiple experimental studies have concluded that nanogels can adsorb and form a blockage in porous media, which reduces the relative permeability of water (Almohsin *et al.*, 2014). However, the surface charge of nanogels can eliminate to some degree aggregation of dispersed nanogels in water, which enhances their stability during transport in porous media. Surface charges also affect the arrangement and adsorption of nanogels at rock surfaces (Johnson and Lenhoff, 1996). In general, nanogels are attracted to rock surfaces with opposite charges. It is extremely crucial to understand the interactions between nanogels and rock surfaces to better explain the permeability reduction mechanisms and nanogel transportation in porous media. Since sandstone reservoirs are characterized by negatively charged surfaces (Nasralla *et al.*, 2013), transportation of charged nanogels in porous media and adsorption at the oil-water interface are greatly impacted.

Additionally, the employment of conventional chemical processes such as surfactant and polymer flooding were widely discussed in the literature. Surfactant flooding has played an essential role in enhanced oil recovery processes over the years due to its effectiveness in reducing oil-water interfacial tension, modifying the wettability of the oil phase towards a water-wet state and emulsifying crude oil (Green *et al.*, 1998; Johannessen and Spildo, 2013). Due to the above mentioned features of both nanogels and surfactants, combining nanogels and surfactants together in oil fields is predicted to enhance their potential by greatly reducing the interfacial tension that leads to recovery of higher amounts of oil. To the best of our knowledge after a comprehensive literature review about the combination of nanosized particles and surfactants in our previous work (Almahfood and Bai, 2018), no studies have been reported on the effect of polymeric cross-linked nanogels combined with surfactants in EOR applications.

In this work, a negatively charged nanogel was synthesized using a free radical suspension polymerization process. The effect of adding a negatively charged surfactant (SDS) to the synthesized nanogel was demonstrated by measuring the interfacial tension between the combined dispersion and light mineral oil. Additionally, the combined dispersion was evaluated by conducting a series of core flooding experiments using multiple injection schemes.

2. EXPERIMENT

2.1. MATERIALS

Na-AMPS nanogel was synthesized in our laboratory. Sodium dodecyl sulfate (SDS, > 99%, CMC = 2400 mg/l) was purchased from Sigma-Aldrich and used without further purification. Light mineral oil with a viscosity of 27.8 cp was employed in all experiments. Due to its availability, seawater with a concentration that simulates the concentration of seawater in Saudi Arabia was employed in all experiments unless otherwise mentioned. Table 1 lists the composition of the employed seawater with a salinity of 5.8‰.

Table 1. Typical seawater composition in Saudi Arabia.

Ion	Sodium	Calcium	Magnesium	Sulfate	Chloride	Bicarbonate	Total
TDS	18,300	650	2,110	4,290	32,200	120	57,670

2.2. NANOGEL SYNTHESIS

Na-AMPS nanogel was prepared by a typical suspension polymerization process. The preparation process could be summarized as follows: NaOH is added to a stirred solution of 15 grams of 2-Acrylamido 2-methyl propane sulfonic acid (AMPS) and 15 grams

of deionized water at room temperature until the pH reaches exactly 7.0. Then, 0.1 gram of N,N'-methylene bis(acrylamide) (MBAA) is added to the solution while stirring. The solution is then added to n-decane (40 ml) containing Span[®] 80 (21 g) and Tween[®] 60 (9 g) in a three-neck flask and bubbled with nitrogen while kept in a water bath at 40° C for 15 minutes. After that, 0.2 ml of ammonium persulfate is added to the flask as an initiator. Stirring in the water bath is continued for 2 hours at 40° C. Then, the emulsion is precipitated and washed with acetone and separated by centrifugation. The process of washing the emulsion with acetone is repeated several times to ensure that all surfactants and unreacted monomers are washed out. The final isolated product is dried in the oven at 65° C for 24 hours. Figure 1 shows samples of the dried and dispersed Na-AMPS nanogel.

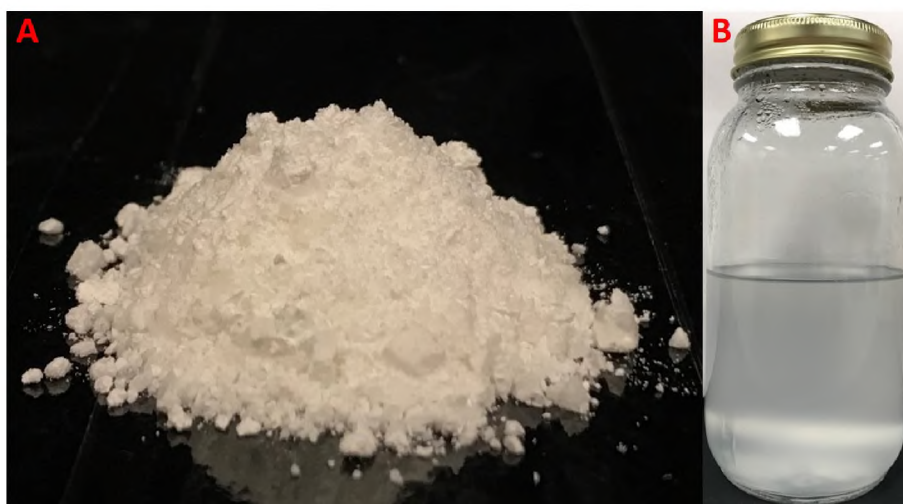


Figure 1. (A) Dried Na-AMPS nanogel. (B) Na-AMPS nanogel dispersed in seawater.

2.3. NANOGEL SIZE DISTRIBUTION AND ZETA POTENTIAL

A nanosizer (Nano ZS, Malvern Instruments, UK) equipped with helium-neon laser (633 nm) was employed to determine the size distribution and obtain the zeta potential values of nanogel dispersions, both alone and combined with SDS. Dynamic light scattering (DLS)

was used to measure the hydrodynamic radius of nanogel particles in the dispersing fluid. Furthermore, zeta potential values are essential for determining the charge nature of the particle surfaces. All measurements were taken at room temperature of 25° C and at a scattering angle of 90°. These measurements greatly help in studying the behavior of surfactant-nanogel systems and their molecular interactions.

2.4. RHEOLOGICAL PROPERTIES

Brookfield DV3T rheometer was employed to measure the rheological properties of the synthesized nanogel combined with SDS at 25° C.

2.5. INTERFACIAL TENSION MEASUREMENTS

Liquid–liquid interfacial tension between mineral oil and the aqueous nanogel dispersions and liquid–air surface tension between air and nanogel dispersions were measured using the pendant drop technique (ramè-hart advance goniometer 500-F1). The interfacial tension values were determined using the Young-Laplace equation. All measurements took place under ambient conditions with a typical temperature of 25° C.

2.6. POROUS MEDIA

Several Berea sandstone (water-wet) core plugs with a low-to-medium permeability ranging from 68.6 to 154 mD were employed in this study. The core plugs have a length of 5 inches and a diameter of 2 inches. The porosity, liquid permeability, and pore volumes of the cores were determined using conventional core analysis methods. Table 2 summarizes the petrophysical properties of each core plug.

Table 2. Petrophysical properties of core plugs.

Core ID	Length (cm)	Diameter (cm)	Porosity (%)	Pore Volume (cm ³)	Average Permeability (md)	Swi (%)	Soi (%)
A-1	12.65	5.08	19.5	50.4	134.3	40.4	59.6
A-2	12.63	5.08	19.9	51.4	154.8	36.8	63.2
A-3	12.59	5.08	19.2	50.4	134.7	40.5	59.5
A-4	12.62	5.08	17.3	44.7	68.6	37.4	62.6
A-5	12.67	5.08	18.4	47.5	74.2	40.1	59.9
A-6	12.61	5.08	18.9	48.8	93.6	39.5	60.5
A-7	12.57	5.08	19.7	50.9	122.9	39.7	60.3
A-8	12.64	5.08	18.3	47.1	75.9	38.4	61.6
A-9	12.50	5.08	18.6	48.0	84.3	39.5	60.5

2.7. CORE FLOODING EXPERIMENTS

Core plugs were mounted in a core holder that is designed for cores with 2 inches in diameter and up to 1 ft in length. A schematic of the core flooding apparatus is shown in Figure 2.

2.7.1. Experimental Procedure.

1. Core plugs are dried in an oven at 125 ° C for several weeks.
2. Core plugs are vacuumed for six hours and saturated with water used in the initial water flooding process.
3. Porosity and pore volumes are measured by weight difference and the density of the saturated brine at room temperature.

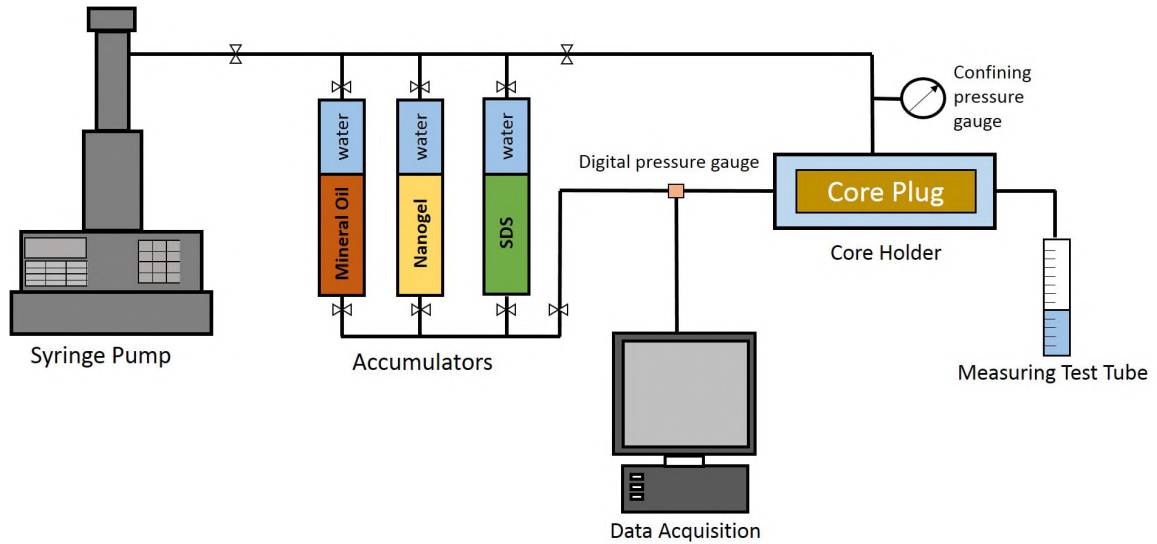


Figure 2. Schematic of the experimental setup.

4. Core plugs are placed into a Hassler type core holder and confined with a pressure of 850 psi using a Teledyne ISCO model 500D syringe pump.
5. Absolute permeability is determined by injecting water at different flow rates.
6. Irreducible water saturation is established by injecting oil to displace water.
7. Initial water flooding is conducted at a flow rate of $0.5 \frac{ml}{min}$ (which corresponds to a Darcy velocity of $1.16 \frac{ft}{day}$) until pressure stabilizes.
8. Different injection patterns of nanogel, surfactant, and post water flooding were conducted into the core plugs at a flow rate of $0.5 \frac{ml}{min}$. Only 1 PV of each Na-AMPS nanogel and SDS was injected for most cases, while 2 PVs were injected for the nanogel-SDS one-slug injection cases.
9. The effluent samples that flowed through the core plugs were collected using measuring test tubes. Oil recovery was calculated using the amount of extracted oil from original-oil-in-place. Additionally, a pressure transducer was installed at the inlet of

the core holder to monitor the injection pressure. All core flooding experiments were conducted at a temperature of 25° C to avoid the effects, if any, of nanogel thermal motion.

2.7.2. Injection Scheme. In this work, three sets of flooding schemes have been conducted after seawater flooding. In the first set, enhanced recovery over nanogel flooding and SDS have been studied using 1 PV for each separate injection (sequential). For the second set, 1 PV of Na-AMPS nanogel was injected after initial seawater flooding, and 1 PV of SDS was injected after the post seawater flooding (sequential). In the last set, 2 PVs of Na-AMPS nanogel and SDS as one-slug were injected after initial seawater flooding (one-slug). Table 3 summarizes the injection schedules for each employed core along with the studied parameter.

Table 3. Injection schedules for each core used in the experiments.

Core ID	Injection Mode	Purpose	Injection Schedules			
			1	2	3	4
A-1	-	Base case	SW	NG	SW	-
A-2	Sequential	NG-SDS sequence effect	SW	NG	SW	SDS
A-3	Sequential	NG-SDS sequence effect	SW	NG	SDS	SW
A-4	Sequential	NG concentration effect	SW	2*NG	SDS	SW
A-5	Sequential	NG concentration effect	SW	3*NG	SDS	SW
A-6	Sequential	NG concentration effect	SW	5*NG	SDS	SW
A-7	Sequential	NG concentration effect	SW	10*NG	SDS	SW
A-8	One-slug	Diluted nanogel effect	SW	0.5*(NG+SDS)	SW	DSW
A-9	One-slug	NG concentration effect	SW	NG+SDS	SW	-

3. RESULTS AND DISCUSSION

3.1. SIZE DISTRIBUTION OF NANOGEL

Table 4 illustrates the physiochemical properties of the synthesized Na-AMPS nanogel (0.1 wt%), including the surface ζ -potential, pH and polydispersity index (PDI) in seawater. The average hydrodynamic diameter of the nanogel in seawater is 222.5 nm, as shown in Figure 3. The size of nanogel is affected by the salinity of the displacing fluid. This was confirmed by measuring the size distribution of the nanogel in diluted seawater (0.58 wt%). It was observed that the diameter of the nanogel expanded in diluted seawater to 242.2 nm, as demonstrated in Figure 3. This figure also shows that both size distribution curves exhibited a mono model distribution, with one peak pointing to a predominant homogeneous droplet size. Nanogel dispersed in seawater showed good stability during a period of two weeks by well-maintaining the structural size within 220-225 nm, as shown in Figure 4. Furthermore, the magnitude of the zeta potential measurements shows an increasing trend with concentrated nanogels, as illustrated in Figure 5. It is possible that this increase in the magnitude is due to the increase in the total number of charged particles in the concentrated solutions or the charge increase per particle.

Table 4. Physiochemical properties of the synthesized nanogel with a concentration of 0.1 wt% dispersed in seawater.

Charge	Surface ζ-potential (mV)	Polydispersity index (PDI)	pH
Negative	- 21.5	0.215	7.0

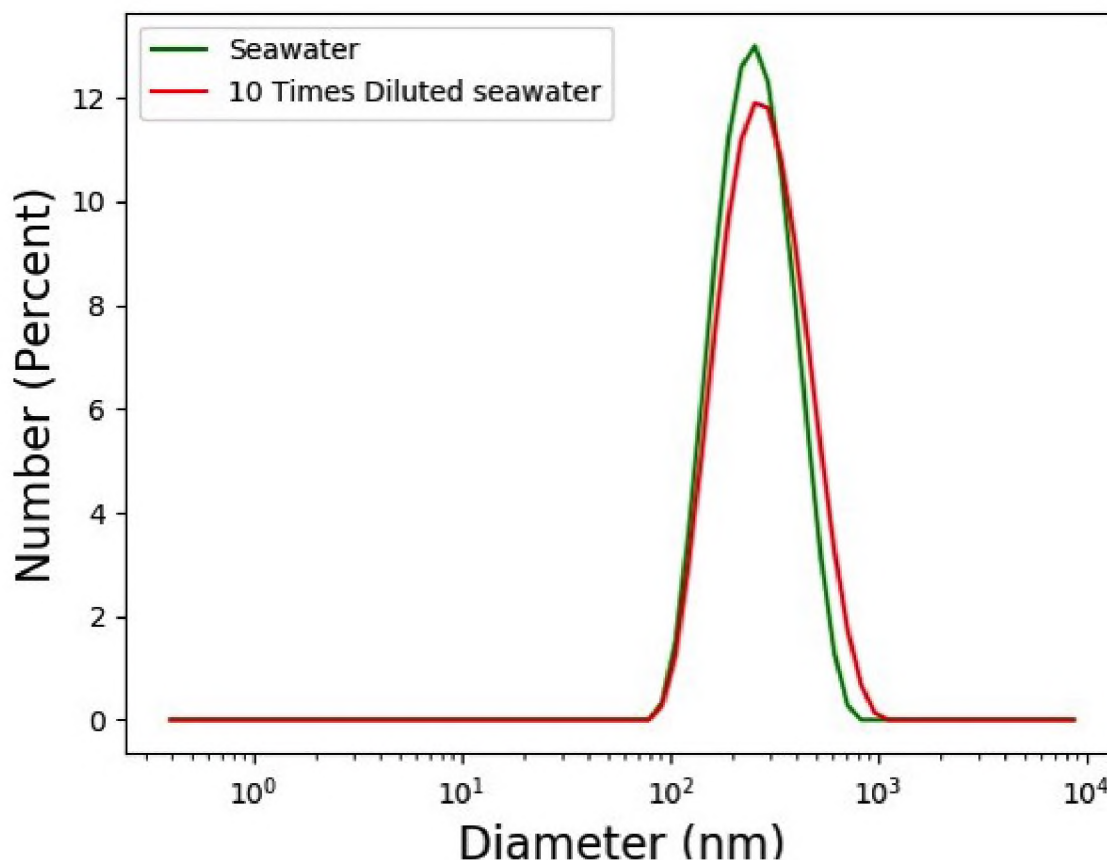


Figure 3. Hydrodynamic diameter distribution of Na-AMPS nanogel in seawater and diluted seawater measured at a concentration of 1 gram/liter and a temperature of 25° C.

3.2. RHEOLOGICAL PROPERTIES

As expected, the viscosity of nanogel dispersions (with and without the addition of SDS surfactant) was affected by the concentration of nanogels. As shown in Figure 6, the viscosity of nanogel dispersions was almost constant at low shear rates ($< 7 \text{ s}^{-1}$), which suggests a Newtonian behavior. However, the viscosity gradually increases at higher shear rates, which suggests a shear thickening behavior. The viscosity at low shear rates was Newtonian because the formation of the interparticle structure was hindered by the electrostatic repulsion. On the other hand, when the shear rate is above 120 s^{-1} , the attraction of nanogel dispersions was increased, which caused the viscosity to gradually rise. Moreover, as the shear rate increases, nanogel dispersions experience a sudden increase

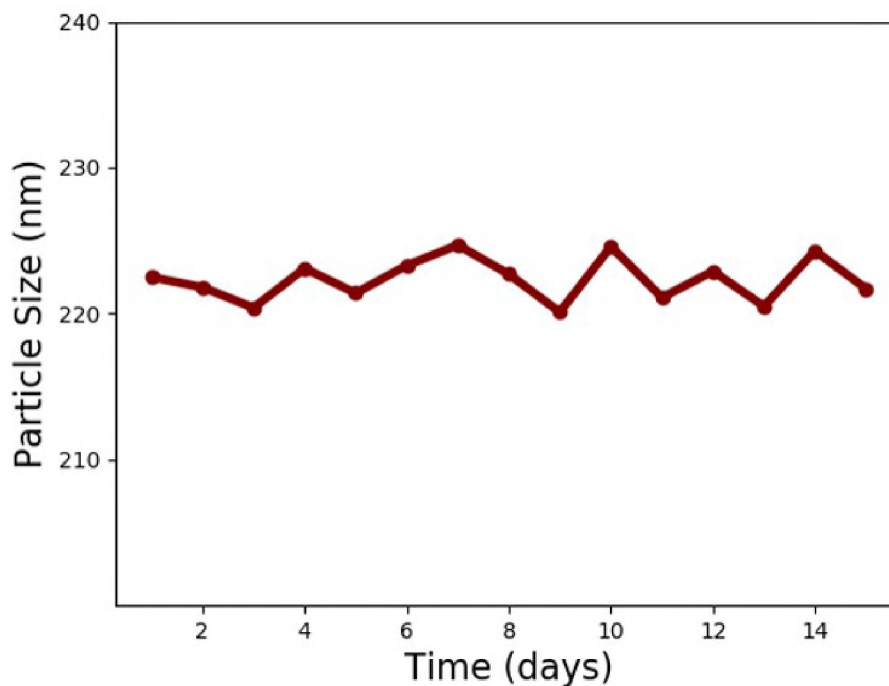


Figure 4. Nanogel stability evaluation in seawater for a two-week time period.

in viscosity measurements, which might be caused by the increased interaction among particles due to high rotational speed. Nevertheless, a higher concentration of nanogel dispersion (1.5 wt%) did not follow this trend. It was observed that higher concentration dispersions experienced a shear thinning behavior with increasing shear rate, as shown in Figure 6. This could be attributed to the change in the microstructure of nanogel dispersions at higher shear rates (Wagner and Brady, 2009).

Furthermore, the relative viscosity η_r is defined as the ratio of the viscosity of nanogel combined with SDS solution to the viscosity of the nanogel only solution at a constant shear rate. The relative viscosities η_r of nanogel dispersions combined with SDS at a constant shear rate of 120 s^{-1} at different concentrations are presented in Figure 7. It was found that the relative viscosity η_r is fitted by an exponential function of nanogel concentration. The change in slope indicates a change in polymer interaction in nanogel dispersions (Gupta *et al.*, 2005). When the concentration of nanogel dispersion is below 0.3 wt%, the nanogel is fully dispersed in the displacing fluid and the interactions between

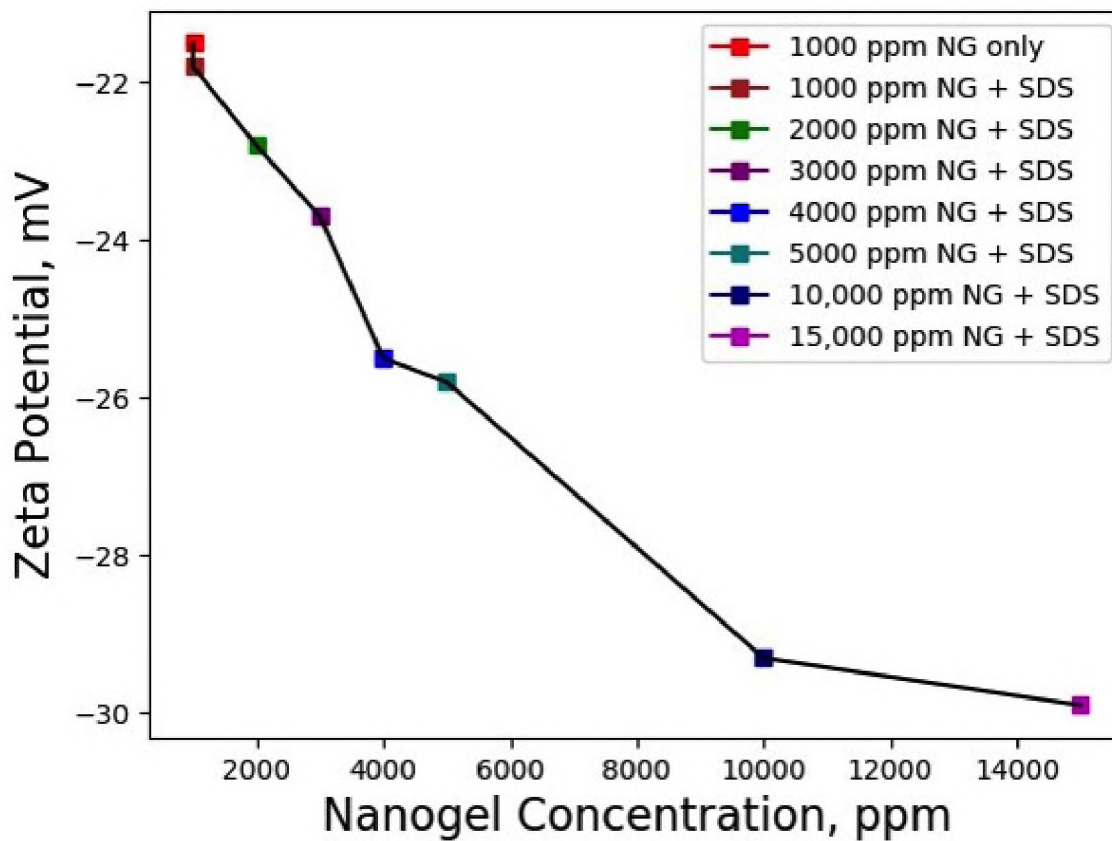


Figure 5. The change in zeta potential in the mixed nanogel-SDS solutions dispersed in seawater and measured at a temperature of 25° C. SDS concentration is kept constant at 1,000 ppm.

them fully dominate the flow behavior of nanogel dispersions. On the other hand, when the concentration of nanogel is above 0.4 wt%, the spacing between particles is greatly reduced and the interactions between neighboring particles are no longer minimal.

3.3. INTERFACIAL TENSION MEASUREMENTS

To understand the mechanism of nanogel flooding, IFT measurements were performed on nanogel–air and nanogel–mineral oil using the pendant drop method. Table 5 lists surface and interfacial tension measurements. It is evident from this table and Figures 8 and 9 that the addition of SDS surfactant to Na-AMPS nanogel dispersions considerably

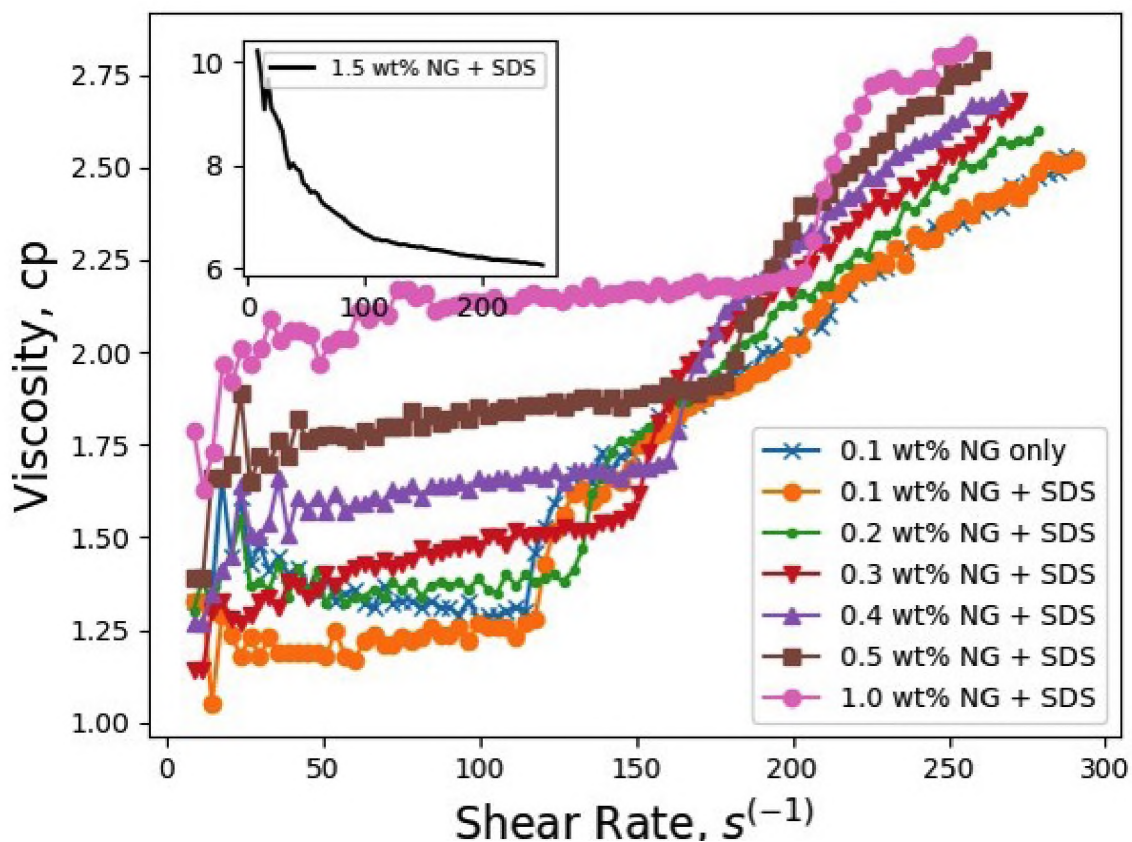


Figure 6. Viscosity of varying concentration of nanogel dispersions combined with SDS at different shear rates. SDS concentration is kept constant at 1,000 ppm.

reduces the interfacial tension between both nanogel–air and nanogel–oil phase. A number of research studies have shown that particles with appropriate surface charge stabilize emulsion droplets by the formation of a two-dimensional closed-packed structure on the oil-water interface (Binks *et al.*, 2003; Eskandar *et al.*, 2011). Furthermore, the high tendency of tested nanogel dispersions to adsorb at liquid–liquid interfaces is attributed to the effect of dissolved oil in the water phase.

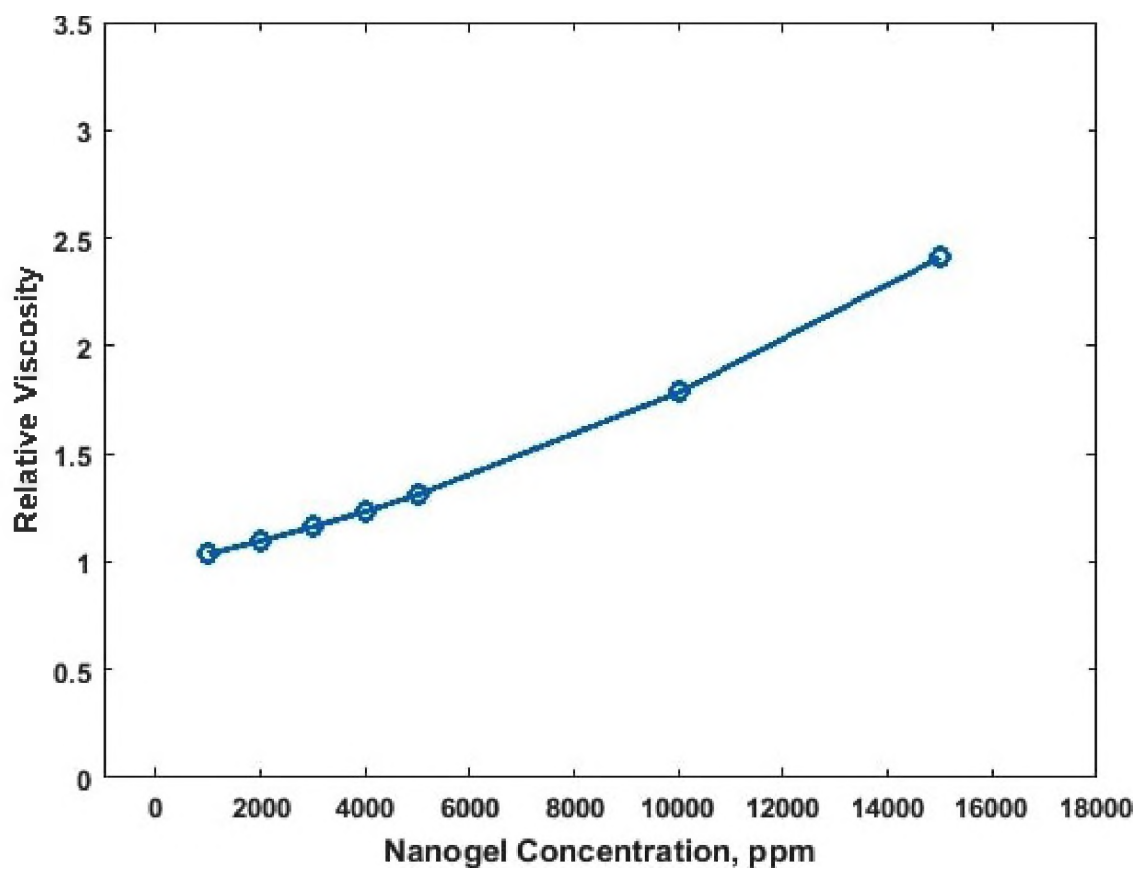


Figure 7. Relative viscosity η_r of different concentrations of nanogel dispersions combined with SDS in seawater at shear rate of 120 s^{-1} . SDS concentration is kept constant at 1,000 ppm.

Table 5. Surface and interfacial tension measurements of nanogel dispersions.

Fluid	Liquid–air	Liquid–liquid
	surface tension	interfacial tension
	$\frac{mN}{m}$	$\frac{mN}{m}$
0.1 wt% nanogel	45.88	26.52
0.1 wt% nanogel + 0.1 wt% SDS	17.54	23.39
0.2 wt% nanogel + 0.1 wt% SDS	16.85	15.80
0.4 wt% nanogel + 0.1 wt% SDS	12.57	8.22
0.5 wt% nanogel + 0.1 wt% SDS	10.27	6.91
1.0 wt% nanogel + 0.1 wt% SDS	2.51	NA

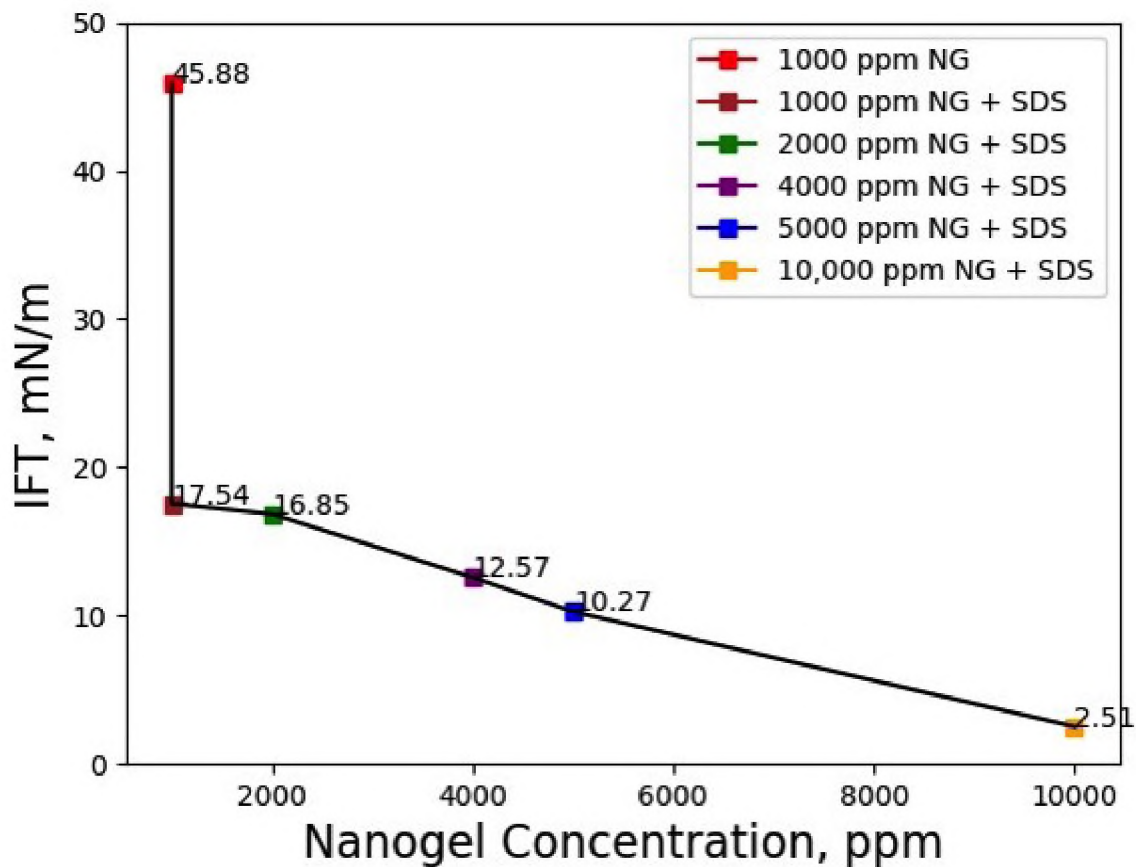


Figure 8. Surface tension between air and varying concentration of nanogel dispersions combined with SDS at a temperature of 25° C. SDS concentration is kept constant at 1,000 ppm.

Figure 9 shows the liquid–liquid interfacial tensions between oil phase and nanogel dispersions in the presence of both Na-AMPS nanogel and SDS. The figure demonstrates the effect of surfactant and particle concentrations on the interfacial tension measurements and indicates that in diluted surfactant and concentrated nanogels, the interfacial tension values are lower than that of the basic Na-AMPS solution (0.1 wt%). Thus, the addition of a small amount of SDS (1,000 ppm) to Na-AMPS nanogel solution greatly reduces the interfacial tension values. In other words, the particle adsorption energy reduces further to more negative values in the presence of SDS. It is worth mentioning that the addition of nanogel has no effect on the interfacial tension values when SDS concentration is equal or above the critical micelle concentration (CMC) (Jiang *et al.*, 2016). Our results of the effect

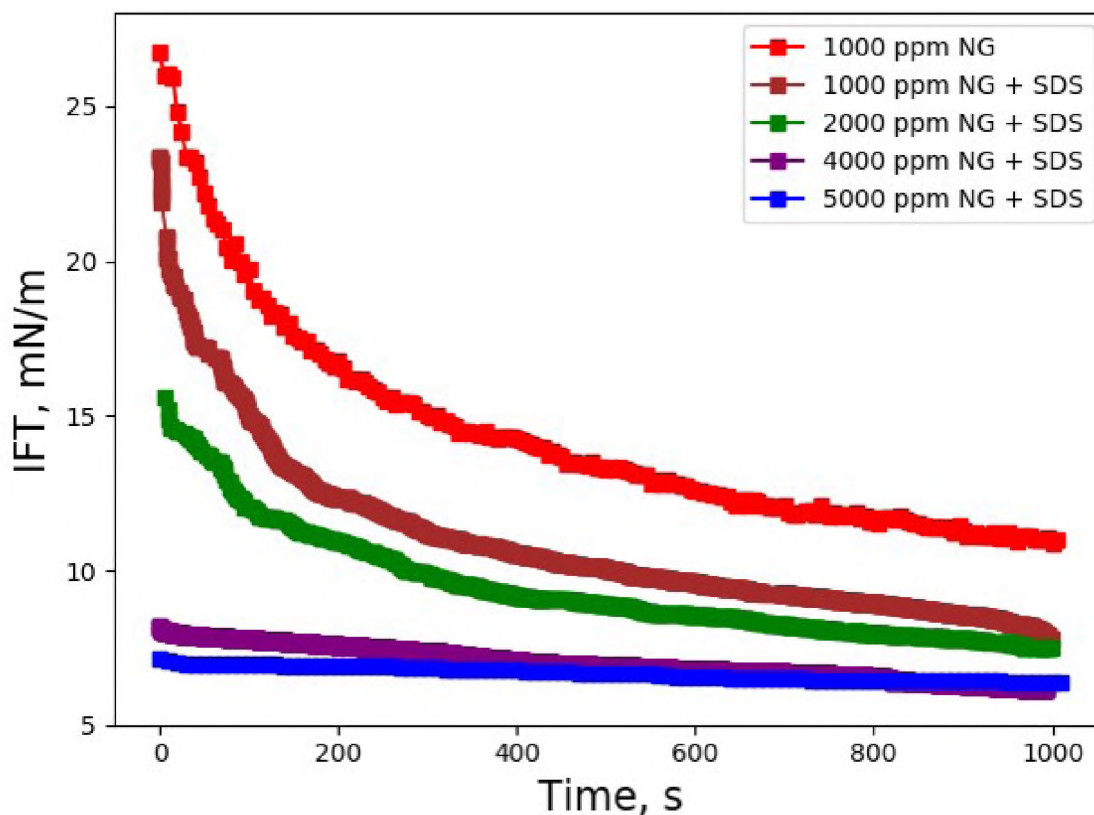


Figure 9. Dynamic interfacial tension between mineral oil and varying concentrations of nanogel dispersions combined with SDS. SDS concentration is kept constant at 1,000 ppm.

of SDS on interfacial tension values of nanogel dispersions are consistent with the findings of Geng *et al.* (2018b). Similar results were obtained for air–liquid surface tension values in the presence of Na-AMPS nanogel and SDS, as presented in Figure 8. The adsorption energy of particles to the liquid–air interface is lower than that of liquid–liquid interface. This explains the relatively higher surface tension values between nanogel dispersions and air. In addition, as Figures 9 and 10 illustrate, nanogel dispersions with a concentration below 0.2 wt% reached the equilibrium interfacial tension, where the adsorption rate of nanogel onto oil–water interface is equal to the desorption rate, in about 1,000 seconds. However, for nanogel dispersions with higher concentrations, the equilibrium state was reached much faster.

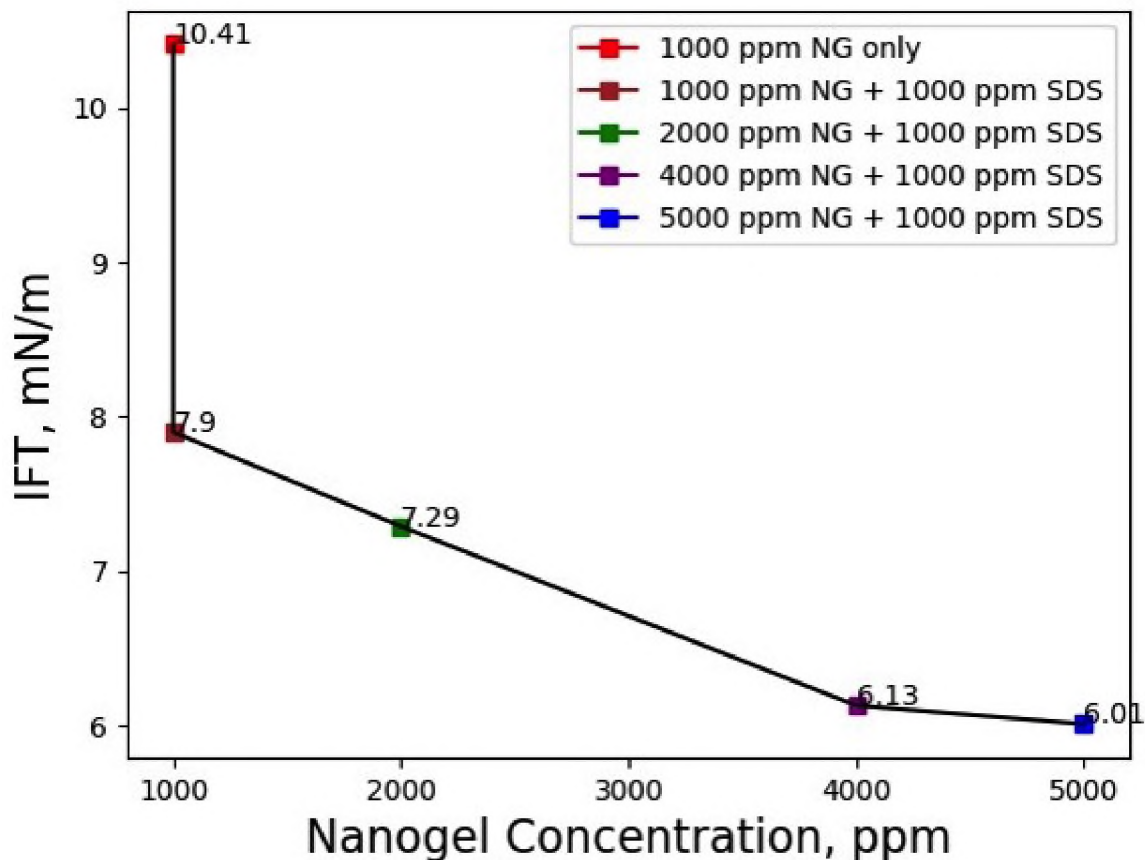


Figure 10. Equilibrium interfacial tension of nanogel dispersions combined with SDS. SDS concentration is kept constant at 1,000 ppm.

3.4. CONCENTRATION OF NANOGEL DISPERSIONS

A reference aqueous solution of Na-AMPS nanogel was prepared in a concentration of 0.1 wt%. Similarly, aqueous solutions with various concentrations of Na-AMPS nanogel (0.1, 0.2, 0.3, 0.4, 0.5, 1.0 wt%) and a fixed concentration of SDS were prepared. It was decided that SDS would be in a concentration below CMC (0.05 and 0.1 wt%) in all experiments, as concentrations above CMC have a slight effect (or even sometimes a negative effect) on enhancing oil recovery.

3.5. CONFIRMATION OF ENHANCED OIL RECOVERY BY CORE FLOODING

Series of core flooding experiments were conducted with water floods and injection of different concentrations of Na-AMPS nanogel and a fixed concentration of SDS surfactant (0.1 wt%) as one-slug injection and separate injections in Berea sandstone core plugs. Experimentally, it is confirmed that the oil recovery using Na-AMPS nanogel and SDS was higher than seawater flooding only. The incremental oil recovery by nanogel injection greatly increases with the concentration of the nanogel. The initial oil recovery by seawater flooding was 43.3%, compared to 48.6% with 0.1 wt% of Na-AMPS nanogel injection, and 55.7% with 0.1 wt% of Na-AMPS nanogel followed by 0.1 wt% SDS injection, as illustrated in Figure 11. Furthermore, the trend of injection pressure for both Na-AMPS nanogel and SDS was almost identical, as both stabilized toward the end of their segment injection especially in low nanogel concentrations, as shown in Figure 13. Resistance factor and residual resistance factor are two terms used to evaluate the injectivity process and plugging efficiency of gel treatments. Resistance factor (F_r) is defined as the ratio between water mobility (λ_w) and nanogel mobility (λ_{ng}). In other words, it is the ratio of pressure drop across the core caused by the injection of nanogel dispersion (ΔP_{ng}) to the pressure drop caused by the injection of brine (ΔP_w) at the same flow rate (equation 1). Residual resistance factor to water (F_{rrw}) is the ratio between water mobility before and after nanogel treatment (equation 2). As can be implied by Figure 15, nanogels are not recommended for use as strong plugging materials in sandstone reservoirs with permeability higher than 100 mD (plugging efficiency in this case was 40%). The figure also shows that the injectivity of nanogel was not much higher than that of seawater. In this case, F_r and F_{rrw} were 2.1 and 1.7, respectively.

$$F_r = \frac{\lambda_w}{\lambda_{ng}} = \frac{\Delta P_{ng}}{\Delta P_w} \quad (1)$$

$$F_{rrw} = \frac{(\lambda_w)_{Before}}{(\lambda_w)_{After}} = \frac{(\Delta P_w)_{After}}{(\Delta P_w)_{Before}} \quad (2)$$

A thorough investigation of the interfacial tension between different concentrations of nanogel dispersions and the oil phase can explain the enhancement in oil recovery. The equilibrium interfacial tension between 0.1 wt% nanogel and oil phase was measured to be $10.41 \frac{mN}{m}$. Upon adding 0.1 wt% SDS to the nanogel dispersion, the equilibrium interfacial tension value was reduced to $7.90 \frac{mN}{m}$, as shown in Figure 10. A similar trend was observed for higher concentrations of Na-AMPS nanogel with 0.1 wt% SDS, as illustrated in Table 5.

Additionally, the effect of injecting diluted seawater (0.58 wt%) was studied during core flooding experiments. As shown in Figure 14, it is observed that the injection pressure of the diluted seawater was higher than that of the concentrated seawater. This can be due to the fact that nanogels reacted to diluted seawater by further swelling and expanding in their diameter.

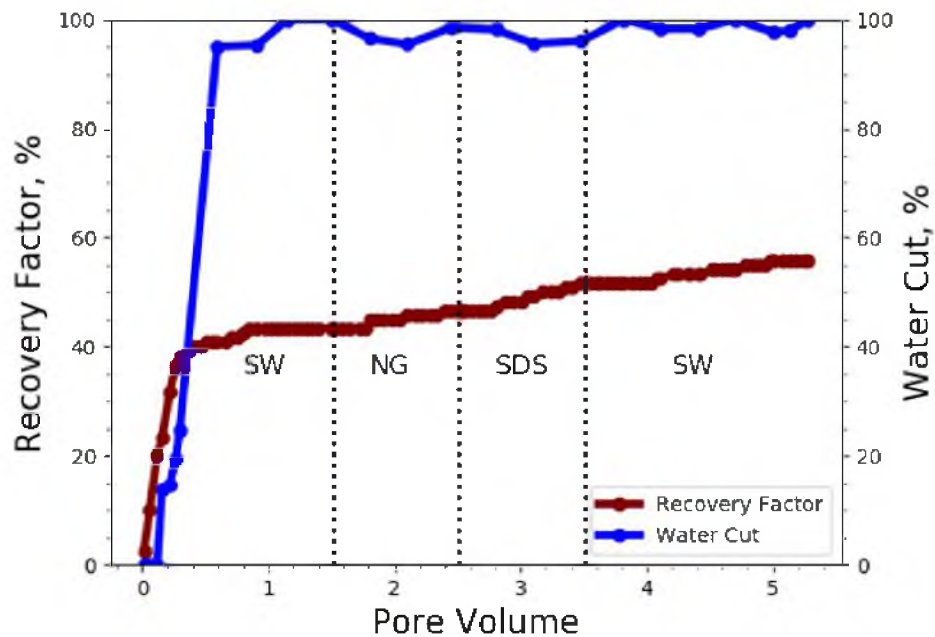


Figure 11. Oil recovery factor and water cut results of core A-3.

3.5.1. Injection Scheme. The recovered oil from core flooding tests varied with different injection schemes. Table 6 summarizes core flooding experiments when 1 PV of each Na-AMPS nanogel and SDS was injected and followed by extended seawater flooding.

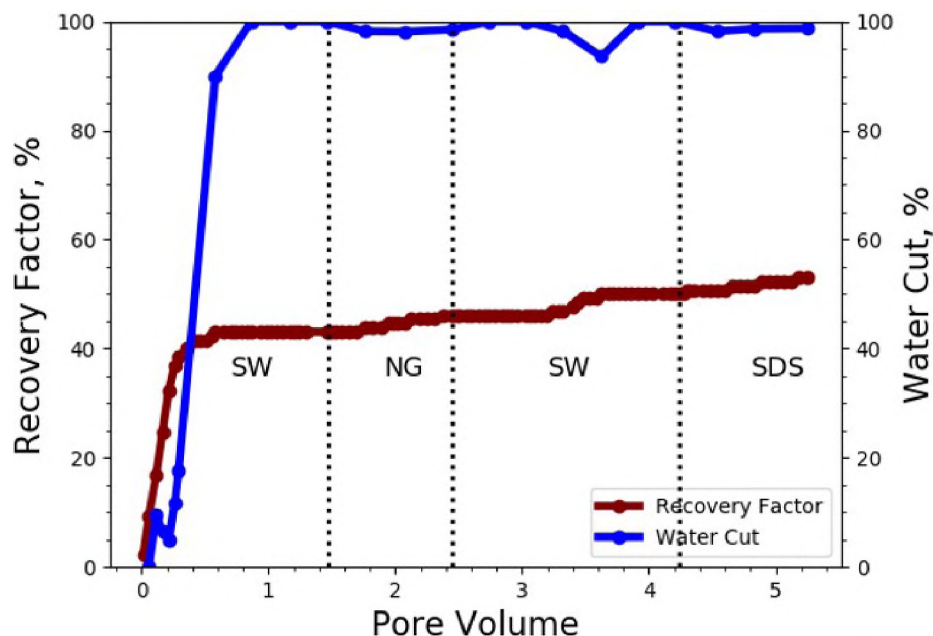


Figure 12. Oil recovery factor and water cut results of core A-2.

This injection scheme recovered higher amounts of oil compared to the other schemes. Figure 12 demonstrates that injecting Na-AMPS nanogel and SDS before the post seawater flooding resulted in higher oil recovery by a factor of 4% when compared to injecting SDS after post seawater flooding. Table 7 compares between separate and one-slug injection schemes and illustrates that separate injections of Na-AMPS nanogel and SDS recovered higher amounts of oil when compared to one-slug injection with the same concentration. Although one-slug injection is a common practice in field operations, lab-scale experiments showed that this injection scheme might not be the optimum.

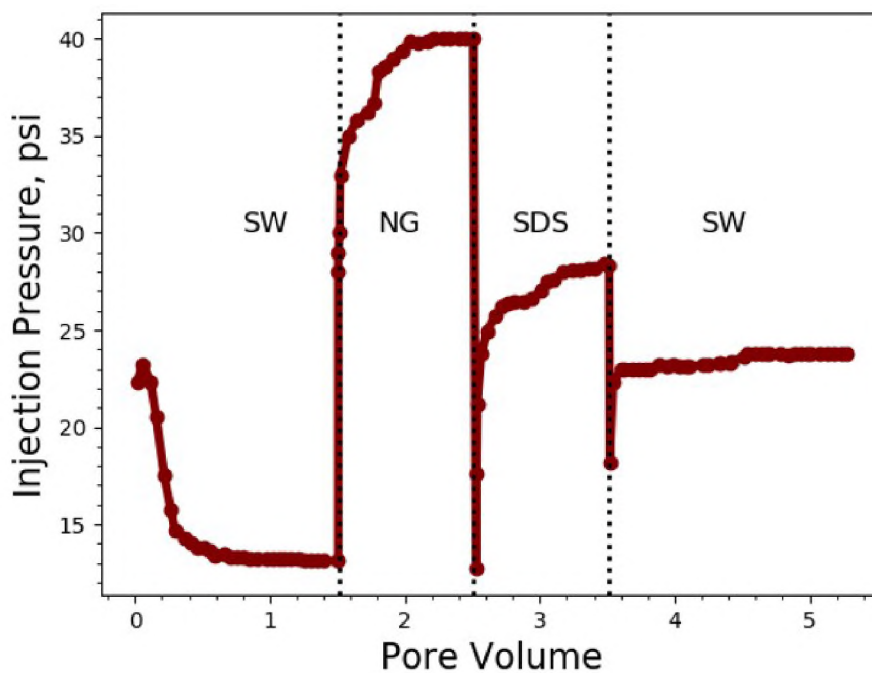


Figure 13. Injection pressure results of core A-3 using sequential injections of nanogel and SDS followed by seawater flooding.

Table 6. Summary of sequential injection core flooding experiments.

Core ID	Scenario	SW Flooding Recovery	Nanogel Recovery	SDS Recovery	Post Seawater Flooding Recovery	Total
A-1	NG	43.3	2.8	-	2.5	48.6
A-3	NG + SDS	43.2	3.0	5.3	4.2	55.7
A-4	2*NG + SDS	43.1	4.5	6.3	4.5	58.4
A-5	3*NG + SDS	43.4	6.1	6.1	3.5	59.1
A-6	5*NG + SDS	43.2	6.4	4.3	3.4	57.3
A-7	10*NG + SDS	43.1	8.1	4.1	2.4	57.7

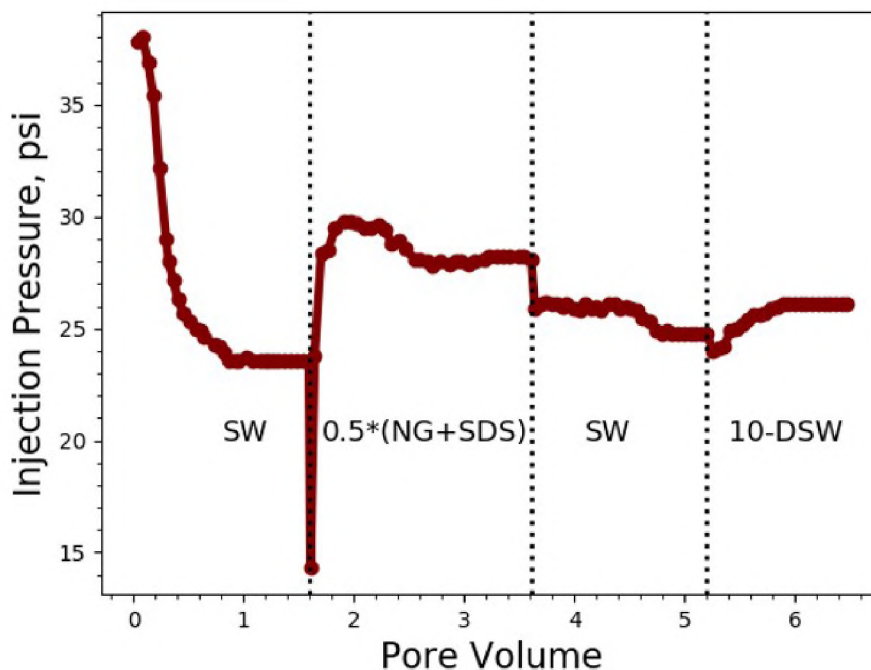


Figure 14. Injection pressure results of core A-8 using one-slug injection of nanogel-SDS (500 ppm each) followed by alternating seawater and 10-times diluted seawater injections.

Table 7. Comparison between sequential and one-slug injection schemes.

Core ID	Scenario	Mode	Seawater Flooding Recovery	Nanogel Recovery	SDS Recovery	Post Seawater Flooding Recovery	Total
A-2 ^a	0.1 wt% NG + 0.1 wt% SDS	Separate injections	43.1	3.1	3.1	3.8	53.1
A-3	0.1 wt% NG + 0.1 wt% SDS	Separate injections	43.2	3.0	5.3	4.2	55.7
A-8	0.05 wt% NG + 0.05 wt% SDS	One slug injection	43.1	4.3		3.5	50.9
A-9	0.1 wt% NG + 0.1 wt% SDS	One slug injection	43.3	4.5		2.5	50.3

^aInjection schedule of this core is NG → SW → SDS.

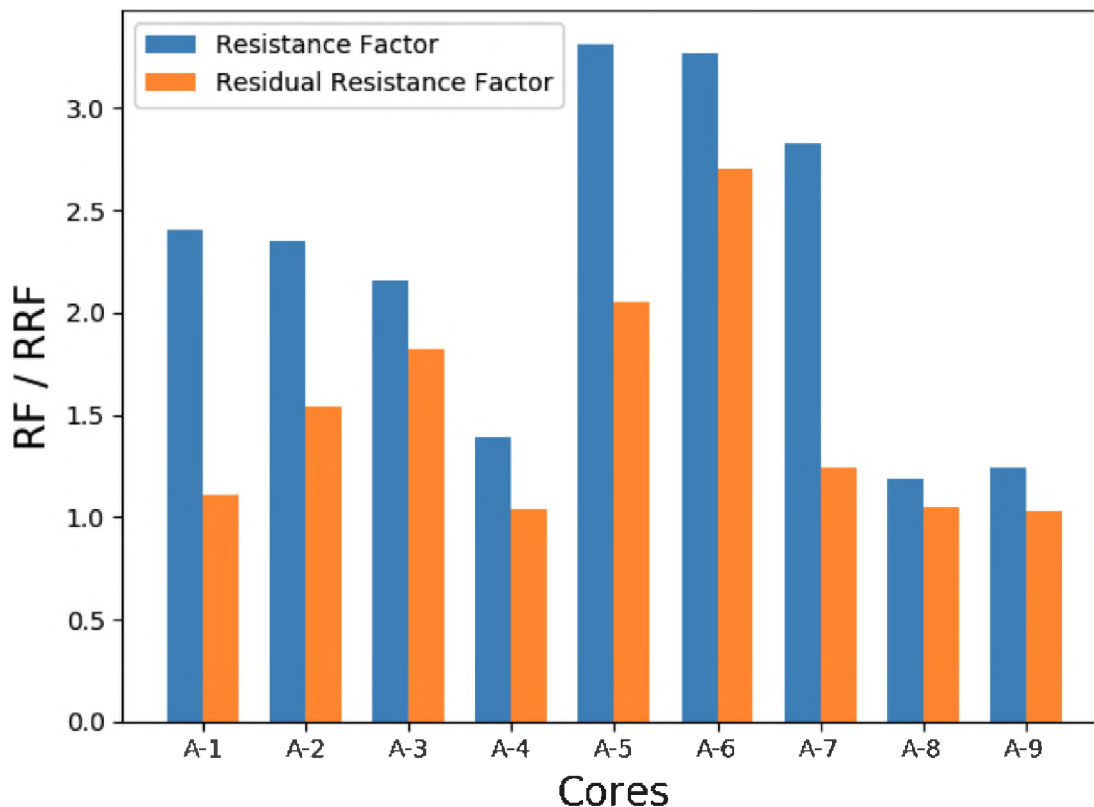


Figure 15. Resistance factor calculated at the end of NG/SDS injection and residual resistance factor calculated using stabilized pressure of last water slug of all employed cores.

4. CONCLUSION

The behavior and transportation of polymeric cross-linked nanogels are attracting more attention due to their stability in water with high salinity and ability to extract higher amounts of oil by adsorbing at the oil-water interface. In this work, negatively charged Na-AMPS nanogel and SDS surfactant were employed as potential feasible materials for enhanced oil recovery in sandstone reservoirs. The main results that could be obtained from this study are summarized as follows:

1. Na-AMPS nanogel can be dispersed in high salinity waters and still form a stable solution. This could be observed from the narrow size distribution with one peak pointing to a predominant homogeneous droplet size when dispersed in seawater.

2. Nanogel dispersion showed good long-term stability during a period of two weeks. The structural size of nanogel in seawater was well-maintained for this period with a hydrodynamic diameter within 220-225 nm.
3. The interfacial tension (IFT) reduced when low concentration of SDS was introduced to Na-AMPS nanogel dispersions. Lower IFT values were observed with increasing nanogel concentration from 0.1 to 1.0 wt%. This implies that IFT reduction might be a major EOR mechanism in nanogel-surfactant flooding.
4. Injection schemes of nanogel and surfactant played an essential role in the amount of recovered oil in sandstone core plugs. The results showed that sequential injections of nanogel and SDS after initial seawater flooding is the better scheme among the ones tested.
5. The results of core flooding experiments confirm that Na-AMPS nanogel combined with SDS could improve the oil recovery factor by 15% after initial seawater flooding by mainly interfacial tension reduction.

NOMENCLATURE

IFT Interfacial tension, mN/m.

NG Nanogel.

SW Seawater.

DSW Diluted seawater.

F_r Resistance factor.

F_{rrw} Residual resistance factor of water.

ppm Parts per million.

SDS Sodium dodecyl sulfate.

PV Pore volume.

CMC Critical micelle concentration.

AMPS 2-acrylamido 2-methyl propane sulfonic acid monomer.

TDS Total dissolved solids.

REFERENCES

- Al-Anazi, H. A., Sharma, M. M., *et al.*, ‘Use of a pH sensitive polymer for conformance control,’ in ‘International Symposium and Exhibition on Formation Damage Control,’ Society of Petroleum Engineers, 2002 .
- Almahfood, M. and Bai, B., ‘The synergistic effects of nanoparticle-surfactant nanofluids in eor applications,’ *Journal of Petroleum Science and Engineering*, 2018, **171**, pp. 196–210.
- Almohsin, A. M., Bai, B., Imqam, A. H., Wei, M., Kang, W., Delshad, M., Sepehrnoori, K., *et al.*, ‘Transport of nanogel through porous media and its resistance to water flow,’ in ‘SPE Improved Oil Recovery Symposium,’ Society of Petroleum Engineers, 2014 .
- Bai, B., Liu, Y., Coste, J.-P., Li, L., *et al.*, ‘Preformed particle gel for conformance control: transport mechanism through porous media,’ *SPE Reservoir Evaluation & Engineering*, 2007, **10**(02), pp. 176–184.
- Bai, B., Wei, M., Liu, Y., *et al.*, ‘Field and lab experience with a successful preformed particle gel conformance control technology,’ in ‘SPE Production and Operations Symposium,’ Society of Petroleum Engineers, 2013 .
- Binks, B. P., Clint, J. H., Dyab, A. K., Fletcher, P. D., Kirkland, M., and Whitby, C. P., ‘Ellipsometric study of monodisperse silica particles at an oil- water interface,’ *Langmuir*, 2003, **19**(21), pp. 8888–8893.
- Binks, B. P., Desforges, A., and Duff, D. G., ‘Synergistic stabilization of emulsions by a mixture of surface-active nanoparticles and surfactant,’ *Langmuir*, 2007, **23**(3), pp. 1098–1106.
- Eskandar, N. G., Simovic, S., and Prestidge, C. A., ‘Interactions of hydrophilic silica nanoparticles and classical surfactants at non-polar oil–water interface,’ *Journal of colloid and interface science*, 2011, **358**(1), pp. 217–225.

- Frampton, H., Morgan, J., Cheung, S., Munson, L., Chang, K., Williams, D., *et al.*, 'Development of a novel waterflood conformance control system,' in 'SPE/DOE Symposium on Improved Oil Recovery,' Society of Petroleum Engineers, 2004 .
- Geng, J., Han, P., Bai, B., *et al.*, 'Experimental study on charged nanogels for interfacial tension reduction and emulsion stabilization at various salinities and oil types,' in 'SPE Asia Pacific Oil and Gas Conference and Exhibition,' Society of Petroleum Engineers, 2018a .
- Geng, J., Pu, J., Wang, L., and Bai, B., 'Surface charge effect of nanogel on emulsification of oil in water for fossil energy recovery,' *Fuel*, 2018b, **223**, pp. 140–148.
- Green, D. W., Willhite, G. P., *et al.*, *Enhanced oil recovery*, volume 6, Henry L. Doherty Memorial Fund of AIME, Society of Petroleum Engineers Richardson, TX, 1998.
- Gupta, P., Elkins, C., Long, T. E., and Wilkes, G. L., 'Electrospinning of linear homopolymers of poly (methyl methacrylate): exploring relationships between fiber formation, viscosity, molecular weight and concentration in a good solvent,' *Polymer*, 2005, **46**(13), pp. 4799–4810.
- Jiang, L., Li, S., Yu, W., Wang, J., Sun, Q., and Li, Z., 'Interfacial study on the interaction between hydrophobic nanoparticles and ionic surfactants,' *Colloids and Surfaces A: Physicochemical and Engineering Aspects*, 2016, **488**, pp. 20–27.
- Johannessen, A. M. and Spildo, K., 'Enhanced oil recovery (eor) by combining surfactant with low salinity injection,' *Energy & Fuels*, 2013, **27**(10), pp. 5738–5749.
- Johnson, C. A. and Lenhoff, A. M., 'Adsorption of charged latex particles on mica studied by atomic force microscopy,' *Journal of colloid and interface science*, 1996, **179**(2), pp. 587–599.
- Lenchenkov, N. S., Slob, M., van Dalen, E., Glasbergen, G., van Kruijsdijk, C., *et al.*, 'Oil recovery from outcrop cores with polymeric nano-spheres,' in 'SPE Improved Oil Recovery Conference,' Society of Petroleum Engineers, 2016 .
- Li, S., Hendraningrat, L., , and Torsæter, O., 'A coreflood investigation of nanofluid enhanced oil recovery,' *Journal of Petroleum Science and Engineering*, 2013, **111**, pp. 128–138.
- Moraes, R. R., Garcia, J. W., Barros, M. D., Lewis, S. H., Pfeifer, C. S., Liu, J., and Stansbury, J. W., 'Control of polymerization shrinkage and stress in nanogel-modified monomer and composite materials,' *Dental Materials*, 2011, **27**(6), pp. 509–519.
- Nasralla, R. A., Bataweel, M. A., Nasr-El-Din, H. A., *et al.*, 'Investigation of wettability alteration and oil-recovery improvement by low-salinity water in sandstone rock,' *Journal of Canadian Petroleum Technology*, 2013, **52**(02), pp. 144–154.

- Qiu, F. *et al.*, 'The potential applications in heavy oil eor with the nanoparticle and surfactant stabilized solvent-based emulsion,' in 'Canadian unconventional resources and international petroleum conference,' Society of Petroleum Engineers, 2010 .
- Rousseau, D., Chauveteau, G., Renard, M., Tabary, R., Zaitoun, A., Mallo, P., Braun, O., Omari, A., *et al.*, 'Rheology and transport in porous media of new water shutoff/conformance control microgels,' in 'SPE international symposium on oilfield chemistry,' Society of Petroleum Engineers, 2005 .
- Suleimanov, B. A. and Veliyev, E. F., 'Novel polymeric nanogel as diversion agent for enhanced oil recovery,' *Petroleum Science and Technology*, 2017, **35**(4), pp. 319–326.
- Sun, X., Zhang, Y., Chen, G., and Gai, Z., 'Application of nanoparticles in enhanced oil recovery: a critical review of recent progress,' *Energies*, 2017, **10**(3), p. 345.
- Thomas, S., 'Enhanced oil recovery-an overview,' *Oil & Gas Science and Technology-Revue de l'IFP*, 2008, **63**(1), pp. 9–19.
- Wagner, N. J. and Brady, J. F., 'Shear thickening in colloidal dispersions,' *Physics Today*, 2009, **62**(10), pp. 27–32.

III. EXPERIMENTAL INVESTIGATION OF POLYMERIC NANOGEL COMBINED WITH SURFACTANT AND LOW SALINITY WATER FLOODING FOR SANDSTONE RESERVOIRS

Mustafa M. Almahfood, Author ^{a, b}

Baojun Bai, Co-Author ^a

^aDepartment of Geosciences & Petroleum Engineering

Missouri University of Science and Technology

Rolla, Missouri 65409

^b EXPEC Advanced Research Center, Saudi Aramco, Saudi Arabia

Email: mmantc@mst.edu

ABSTRACT

An experimental evaluation of polymeric nanogel combined with sodium dodecyl sulfate (SDS) surfactant and several salinities of water flooding as a potential enhanced oil recovery method for sandstone reservoirs is described herein. This paper investigates the impact of nanogel combined with SDS on improved oil recovery, and the effect of salinity of injected water on oil-brine-rock interactions. Also, it provides a laboratory investigation of the injectivity and plugging performance induced by nanogel flooding through sandstone cores. A newly developed polymeric crosslinkable nanogel is prepared using suspension polymerization process by employing 2-Acrylamido 2-methyl propane sulfonic acid. The produced nanogel displays good structural stability in different brine salinities with a narrow size distribution with one peak pointing to a predominant homogeneous droplet size. The core flooding results revealed that substantial oil recovery, up to 20%, beyond conventional water flooding can be obtained by nanogel combined with SDS injections and assisted with altering salinity of water injections. The resistance factor of nanogel in sandstone cores

slightly increased with nanogel concentration. The stabilized residual resistance factor for brine injections slightly increased with lower brine salinities from 1.11 to 1.17. The results also showed that SDS can reduce the adsorption density of nanogel from rock surfaces effectively.

Keywords: nanogel, polymeric nanogel, surfactant-based-nanogel, enhanced oil recovery, low salinity waterflooding

1. INTRODUCTION

The production rates from existing oil reservoirs are declining and the frequency of finding new explorations has become limited. Therefore, enhanced oil recovery techniques are receiving a great attention by research centers and oil companies (Ayatollahi *et al.*, 2012). The revolution of nano-technology is receiving a great interest in many fields including the oil and gas industry. Nanotechnology is defined as the manipulation and intergration of atoms and molecules to form materials, components and structures at the nano-scale (Almahfood and Bai, 2018). Nanoparticles have been investigated widely for their proposed applications in many fields including the oil industry. Nanosized cross-linked polymeric particles known as nanogels are newly developed particles in EOR applications. They are known for their easy injection process due to their small size, which is much smaller than the diameter of the pore throats in oil reservoirs (Qiu *et al.*, 2010). They are able to mobilize residual oil, which enhances oil recovery (Almahfood and Bai, 2020a,c; Lenchenkov *et al.*, 2016). A number of research studies have shown that nanosized particles can mobilize residual oil and enhance the oil recovery by mainly reducing the interfacial tension between oil-water phases and stabilizing oil-in-water emulsions formed in-situ. The interactions between nanogel-rock-brine in-situ can enhance the plugging performance induced by nanogel (Almahfood and Bai, 2020b). However, the surface charge of both nanogel and porous media can eliminate to a great extent the formation damage. In general, nanogels are attracted to rock surfaces with opposite charges. Understanding the

interactions between nanogels and rock surfaces is critically significant to better explain the transportation and plugging performance caused by nanogel flooding. Since sandstone rocks are characterized by negatively charged surfaces (Nasralla *et al.*, 2013), the transportation and injectivity of anionic nanogels are not greatly impacted. In other words, the formation damage caused by nanogel flooding in this reservoir rock is minimal.

Recently, the combination between nanosized particles and surfactants have attracted a great deal of attention by many researchers (Karimi *et al.*, 2012; Ma *et al.*, 2008; Mohajeri *et al.*, 2015; Wu *et al.*, 2017). Suleimanov *et al.* (2011) have shown that the usage of nanoparticles combined with anionic surfactant permitted a great reduction of surface tension. Moreover, it has been revealed that the usage of nanoparticles with an anionic surfactant has a major impact on increasing the ultimate oil recovery (Almahfood and Bai, 2020b). Almahfood and Bai (2020c) have studied the effect of nanosized particles combined with surfactants on sandstone reservoir rocks and reported that the combination has a strong capability for oil recovery enhancement.

The aim of this study is to examine the performance of nanosized particles when combined with two other promising technologies - surfactants and low salinity water flooding. The paper firstly presents the size distribution of the synthesized nanogel in several brine salinities. Afterwards, the paper provides a laboratory core flooding evaluation conducted using sandstone rock samples to investigate the impact of nanogel combined with surfactant and several brine salinities on oil recovery. Next, the paper provides adsorption and desorption study of nanogel in sandstone cores to evaluate nanogel-brine-rock interactions. Lastly, the degree of plugging performance induced by nanogel flooding is studied.

2. EXPERIMENT

2.1. MATERIALS

Na-AMPS nanogel was synthesized in our laboratory. 2-Acrylamido 2-methyl propane sulfonic acid monomer (99%), sodium dodecyl sulfate (SDS, > 99%, CMC = 2400 mg/l), Tween[®] 60 (CMC = 27 mg/l), N,N'-methylene bis(acrylamide) (MBAA, 99%), and sodium bicarbonate ($NaHCO_3$, $\geq 99.7\%$) were purchased from Sigma-Aldrich. Sorbitan monooleate (Span[®] 80), sodium hydroxide (NaOH, 97%), sodium chloride (NaCl, 99%), calcium chloride ($CaCl_2$, powder, 97%), magnesium chloride ($MgCl_2$, 99%), and n-Decane were purchased from Alfa Aesar. Ammonium persulfate ($\geq 98\%$), and sodium sulfate (Na_2SO_4 , $\geq 99\%$) were purchased from Acros Organics. All chemicals were of reagent grade and used as received without further purification.

2.2. NANOGEL SYNTHESIS

Na-AMPS nanogel was prepared by a typical suspension polymerization process. The preparation process could be summarized as follows: NaOH is added to a stirred solution of 15 grams of 2-Acrylamido 2-methyl propane sulfonic acid (AMPS) and 15 grams of deionized water at room temperature until the pH reaches exactly 7.0. Then, 0.1 gram of N,N'-methylene bis(acrylamide) (MBAA) is added to the solution while stirring. The solution is then added to n-decane (40 ml) containing Span[®] 80 (21 g) and Tween[®] 60 (9 g) in a three-neck flask and bubbled with nitrogen while kept in a water bath at 40° C for 15 minutes. After that, 0.2 ml of ammonium persulfate is added to the flask as an initiator. Stirring in the water bath is continued for 2 hours at 40° C. Then, the emulsion is precipitated and washed with acetone and separated by centrifugation. The process of washing the emulsion with acetone is repeated several times to ensure that all surfactants

and unreacted monomers are washed out. The final isolated product is dried in the oven at 65° C for 24 hours. Figure 1 shows samples of the dried and dispersed Na-AMPS nanogel.

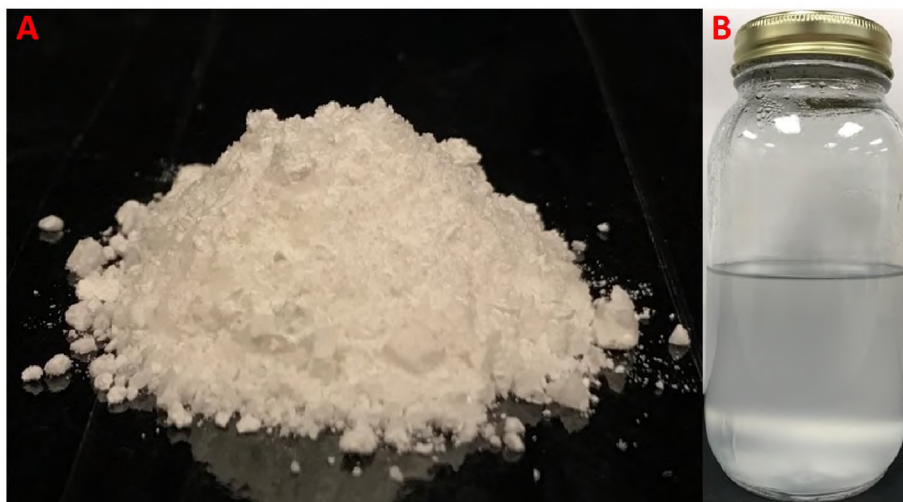


Figure 1. (A) Dried Na-AMPS nanogel. (B) Na-AMPS nanogel dispersed in seawater.

2.3. BRINE

Two different brines were used in this study, including seawater that simulates the salinity for seawater in Saudi Arabia, and a diluted version of seawater to simulate low salinity water flooding. All brines were prepared from deionized water and reagent grade chemicals on the basis of geochemical analysis of field water samples reported by Yousef *et al.* (2011). The employed seawater had a salinity of approximately 57,600 ppm by weight, while 10-times diluted seawater had a salinity of 5,760 ppm. Table 1 depicts the composition for each employed brine. The effect of salinity on physical properties of the prepared brine types was studied. The density and viscosity properties were measured at an average room temperature of 25° C. Table 2 lists the density and viscosity of the different brine types employed in the experiments.

2.4. CRUDE OIL

Light crude oil from a Saudi Arabian oil field with a viscosity of 11.5 cp at room temperature (density = 0.84 g/cc, API 36°) was employed in all experiments.

2.5. RHEOLOGICAL PROPERTIES

Brookfield DV3T rheometer was employed to measure the rheological properties of crude oil and several brine types with different salinities at 25° C.

2.6. SANDSTONE ROCK

Outcrop Berea sandstone cores were employed in all core flooding experiments. Core plugs with 2-inch in diameter and 5-inch in length were cut from a whole block. Table 3 summarizes the petrophysical properties of each core plug.

Table 1. Composition of all employed brine types with different salinities.

Ion	Seawater g/L	10 Times Diluted Seawater g/L
Sodium	18,300	1,830
Calcium	650	65
Magnesium	2,110	211
Sulfate	4,290	429
Chloride	32,200	3,220
Bicarbonate	120	12
TDS, ppm	57,670	5,767
Ionic Strength, mol/L	1.15	0.12

Table 2. Density and viscosity of different brine types at room temperature of 25° C.

Property	Seawater	10-Times Diluted Seawater
Density (g/cm^3)	1.040	1.001
Viscosity (cp)	1.012	0.901

2.7. EXPERIMENTAL SETUP AND PROCEDURE

Core plugs were mounted in a Hassler type core holder that is designed for cores with 2 inches in diameter and up to 1 ft in length. A schematic of the core flooding apparatus is shown in Figure 2. Experimental procedure is summarized below.

1. The core plugs are cleaned with distilled water.
2. The Core plugs are put in an oven to dry at 125 ° C for 3 days.
3. The cores are vacuumed for 24 hours and saturated with seawater with a salinity of 5.8 wt%.
4. Porosity and pore volumes are measured by the weight difference and the density of the saturated brine at room temperature.
5. Core plugs are placed into a Hassler type core holder and confined with a pressure of 850 psi using a Teledyne ISCO model 500D syringe pump.
6. Absolute permeability is determined by injecting water at different flow rates.
7. Crude oil is injected to simulate Irreducible water saturation (S_{wi}) and initial oil saturation (S_{oi}).
8. Two scenarios of initial water flooding using seawater and 10-times diluted seawater are conducted at a flow rate of $0.5 \frac{ml}{min}$ until no more oil is produced and pressure profile stabilizes.

9. Nanogel and SDS, dispersed in different brine salinities, are injected using different injection schemes and concentrations at a flow rate of $0.5 \frac{ml}{min}$.
10. Alternating seawater and 10-times diluted seawater are conducted as post water flooding. All brines are injected at a flow rate of $0.5 \frac{ml}{min}$.

The effluent samples that flowed through the core plugs were collected using measuring test tubes. Oil recovery was calculated using the amount of extracted oil from original-oil-in-place. A pressure transducer was installed at the inlet of the core holder to monitor the injection pressure. All core flooding experiments were conducted at an average room temperature of 25° C.

Table 3. Petrophysical properties of core plugs employed in core flooding experiments.

Core ID	Length (cm)	Diameter (cm)	Porosity (%)	Pore Volume (cm³)	Average Permeability (md)	Swi (%)	Soi (%)
B-1	12.682	5.08	19.04	49.02	59.75	45.48	54.52
B-2	12.499	5.08	18.01	46.37	50.43	45.03	54.97
B-3	12.560	5.08	18.66	48.04	57.12	44.90	55.10
B-4	12.631	5.08	18.62	47.94	61.33	44.79	55.21
B-5	12.614	5.08	18.56	47.79	33.52	47.18	52.82
B-6	12.703	5.08	17.70	45.59	37.23	46.77	53.23
B-7	12.603	5.08	18.01	46.37	48.73	43.45	56.55
B-8	12.605	5.08	17.86	45.98	48.43	44.03	55.97
B-9	12.677	5.08	18.27	47.06	56.57	44.27	55.73
B-10	12.631	5.08	18.08	46.57	60.82	44.21	55.79
B-11	12.781	5.08	17.82	45.88	38.79	47.65	52.35
B-12	12.563	5.08	18.36	46.75	91.48	–	–

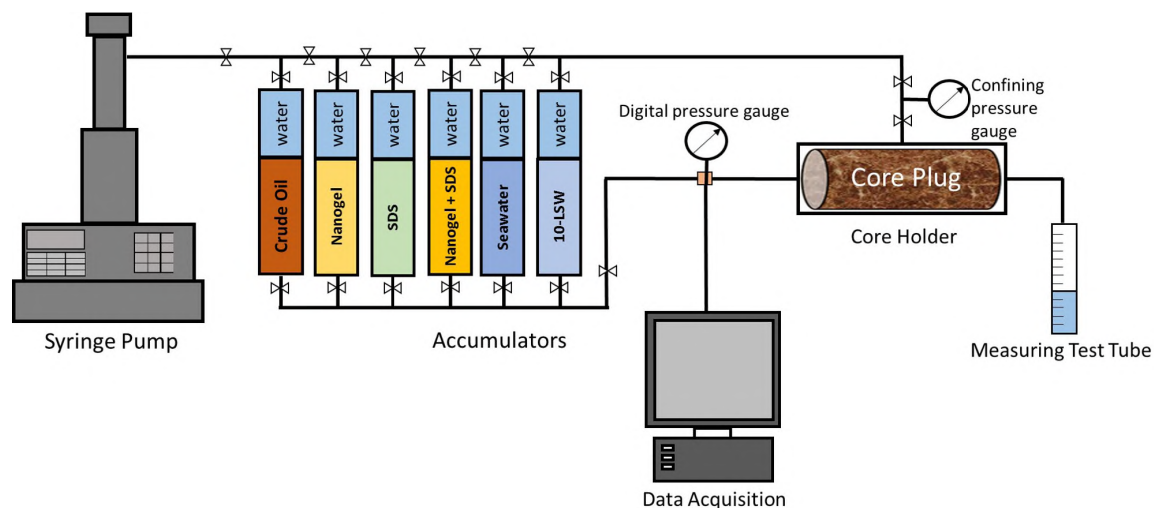


Figure 2. Schematic of the experimental setup.

2.8. NANOGEL SIZE DISTRIBUTION AND ZETA POTENTIAL

A nanosizer (Nano ZS, Malvern Instruments, UK) equipped with helium-neon laser (633 nm) was employed to determine the size distribution and obtain the zeta potential values of nanogel dispersions in different water types. Dynamic light scattering (DLS) was used to measure the hydrodynamic radius of nanogel particles in the dispersing fluid. All measurements were taken at room temperature of 25° C and at a scattering angle of 90°.

2.9. DYNAMIC ADSORPTION AND DESORPTION MEASUREMENTS

Berea sandstone cores saturated with seawater were used to perform dynamic adsorption measurements. A 1,000 ppm nanogel dispersion was injected through the cores. The concentration of nanogel dispersion was measured using Shimadzu UV-mini-1240 UV-vis spectrophotometer as a function of pore-volume injection with appropriate mixtures of seawater as a reference. The nanogel dispersion was diluted by seawater to a concentration that fell in the linear range of Lambert-Beer Law (equation 1), as shown by the calibration curve (Figure 3).

$$A = \varepsilon cL \quad (1)$$

Where A is the absorbance, ε is the molar absorption coefficient, c is the concentration of the dispersion, and L is the length of the light path. When the concentration of the nanogel in the effluent reached the original concentration, seawater was injected through the core to evaluate the desorption density. Petrophysical properties of the core plug (B-12) used to evaluate the adsorption density are listed in Table 3.

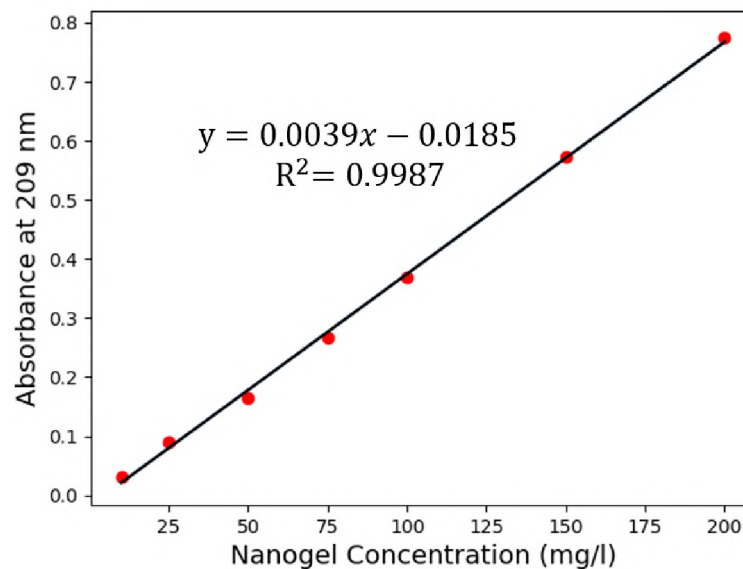


Figure 3. Calibration curve of nanogel standards at the peak wavelength of 209 nm.

2.10. INJECTIVITY AND PLUGGING PERFORMANCE OF NANOGEL IN SANDSTONE

Resistance factor and residual resistance factor are two terms used to evaluate the injectivity process and plugging efficiency of gel treatments. Resistance factor (F_r or RF) is defined as the ratio between water mobility (λ_w) and nanogel mobility (λ_{ng}). In other words, it is the ratio of pressure drop across the core caused by the injection of nanogel

dispersion (ΔP_{ng}) to the pressure drop caused by the brine injection (ΔP_w) at the same flow rate (equation 2). Residual resistance factor to water (F_{rrw} or RRF) is the ratio between water mobility before and after nanogel treatment (equation 3).

$$F_r = \frac{\lambda_w}{\lambda_{ng}} = \frac{\Delta P_{ng}}{\Delta P_w} \quad (2)$$

$$F_{rrw} = \frac{(\lambda_w)_{Before}}{(\lambda_w)_{After}} = \frac{(\Delta P_w)_{After}}{(\Delta P_w)_{Before}} \quad (3)$$

In this work, sandstone core plugs employed in core flooding experiments were used to evaluate the injectivity and plugging performance of nanogel. After simulating the core with initial oil saturation, seawater was injected until the injection pressure reached a stable state. Then, nanogel was injected for 1 PV to evaluate its injectivity for this injection volume. Lastly, several brine salinities were injected until pressure profile stabilizes to examine the plugging performance. Petrophysical properties of core plugs employed to evaluate the injectivity and plugging performance of nanogel are tabulated in Table 3.

3. RESULTS AND DISCUSSION

3.1. SIZE DISTRIBUTION OF NANOGEL

The characterization of the negatively charged nanogel such as surface ζ -potential, polydispersity index (PDI) and average particle size in two water types with different salinities are presented in Table 4. The results show the effect of water salinity on the particle size of nanogel. As shown in Figure 4, the average hydrodynamic diameter of nanogel in seawater is 222.5 nm. The particle size expands to 247 in 10-times diluted seawater. Figure 4 also illustrates that nanogel size distribution curves exhibited a mono-modal distribution, with one peak pointing to a predominant homogeneous droplet size. In addition,

nanogel dispersion showed good long-term stability during a period of two weeks by well-maintaining the structural particle size, as presented in Figure 5.

Table 4. Physiochemical properties of different nanogel dispersions in several water types.

Water Type	Surface ζ-potential (mV)	Polydispersity Index (PDI)	Average Particle Size (nm)
Seawater	- 30.8	0.215	222
10-DSW	- 39.4	0.273	247

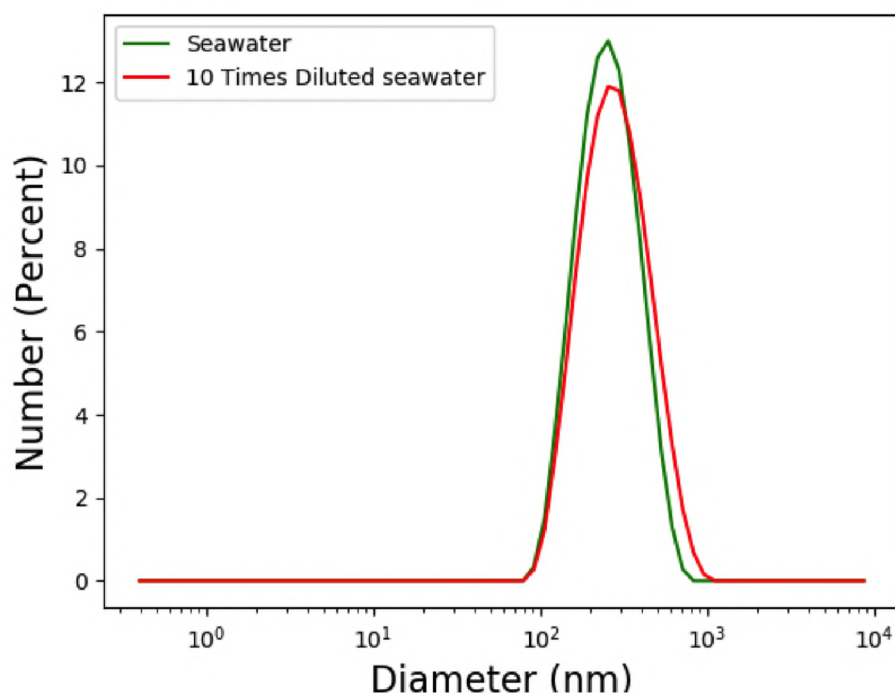


Figure 4. Particle size distribution of nanogel dispersed in several brine types at a concentration of 1 gram/liter and a temperature of 25° C.

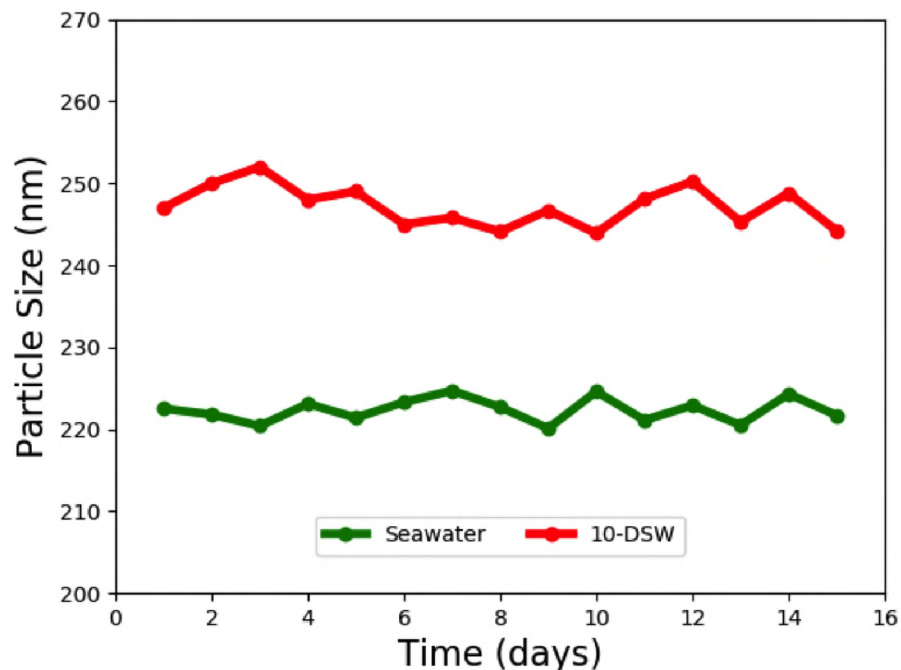


Figure 5. Nanogel stability evaluation in different water types for a two-week time period.

3.2. CONFIRMATION OF ENHANCED OIL RECOVERY BY CORE FLOODING

In core flooding experiments, seawater or diluted seawater were injected to simulate the initial water flooding. Next, separate and combined/one-slug injections of nanogel and SDS dispersions were injected. Then, two different salinity slugs of seawater were injected one after another starting with regular seawater and ending with 10-times diluted seawater in the first scenario. In the second scenario, two different salinity slugs of seawater were injected one after another starting with 10-times diluted seawater and ending with seawater. Table 5 summarizes the injection schedules and tested parameter for all core flooding experiments.

Table 5. Injection schedules for core plugs employed in core flooding experiments.

Core ID	Injection Mode	Purpose	Injection Schedules				
			1	2	3	4	5
B-1	Sequential	Sequence	SW	NG	SW	DSW ^a	SDS
B-2	Sequential	Sequence	SW	NG	SDS	SW	DSW
B-3	Sequential	LSW, Concentration	SW	2*NG	SDS	SW	DSW
B-4	Sequential	LSW, Concentration	SW	5*NG	SDS	SW	DSW
B-5	One-slug	LSW, Concentration	SW	0.5*(NG+SDS)	SW	DSW	-
B-6	One-slug	LSW, Concentration	SW	NG+SDS	SW	DSW	-
B-7	Sequential	SW, Concentration	DSW	NG	SDS	DSW	SW
B-8	Sequential	SW, Concentration	DSW	NG	SDS	DSW	SW
B-9	Sequential	SW, Concentration	DSW	5*NG	SDS	DSW	SW
B-10	One-slug	SW, Concentration	DSW	0.5*(NG+SDS)	DSW	SW	-
B-11	One-slug	SW, Concentration	DSW	NG+SDS	DSW	SW	-

^a10-times dilutes seawater

3.2.1. Validation of Nanogel and SDS Injection Sequence. Core plugs B-1 and B-2 were employed to evaluate the effect of nanogel and SDS sequence injection combined with low salinity water on enhancing the oil recovery. The cumulative oil recovery by regular seawater with salinity of 57,670 ppm was approximately 42.2%. This injection slug targets mobile oil in the core plug and represents the secondary oil recovery. The oil was recovered during the first 1.5 pore volumes of seawater injected. The injection of seawater was continued until there was no more oil produced and injection pressure reached a stable state to ensure that all mobile oil was recovered. This was followed by 1 injection-volume of nanogel (1,000 ppm). A substantial incremental of oil was produced equivalent to 4.59% beyond conventional seawater flooding. The injection of seawater as tertiary process was continued until no more oil was produced and injection pressure reached a stable state. With this injection slug, an incremental oil recovery of approximately 4.6% was obtained.

The injection of 10-times diluted seawater with a salinity of 5,767 ppm was followed until no more oil was produced and pressure stabilized. During this injection slug, no additional oil was produced. Lastly, the injection of 1 injection-volume of SDS (1,000 ppm) was followed. Surprisingly, no additional oil was recovered. Therefore, the total incremental oil recovery beyond initial seawater flooding was approximately 9.2% by nanogel and stepwise reduction of salinity of seawater followed by SDS, as illustrated in Figure 6.

Moreover, the most dominant effect in the injection pressure profile shown in Figure 7 is the pressure increase induced by nanogel injection. The injection pressure trend of water slugs following the nanogel injection showed an increasing behavior due to nanogel expansion phenomenon with lower salinity. The injection pressure profile of SDS injection promoted the ability of surfactant to reduce the adsorption density of nanogel in rock surfaces.

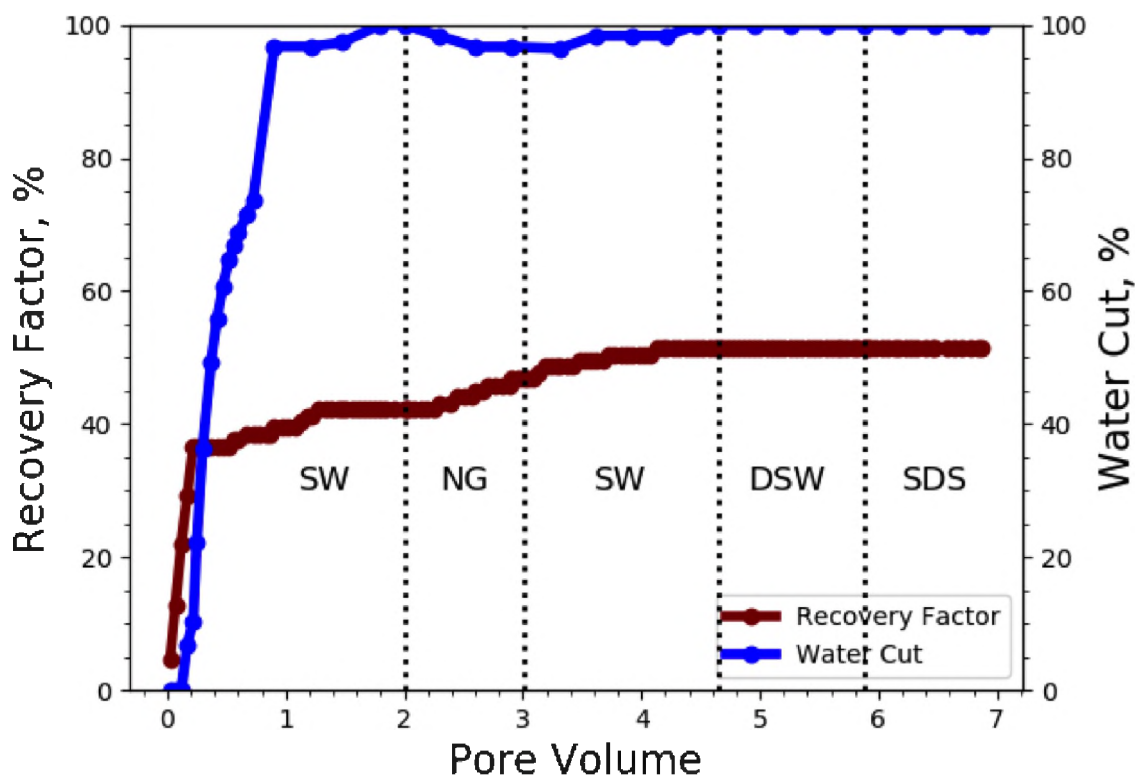


Figure 6. Oil recovery factor and water cut of Core B-1.

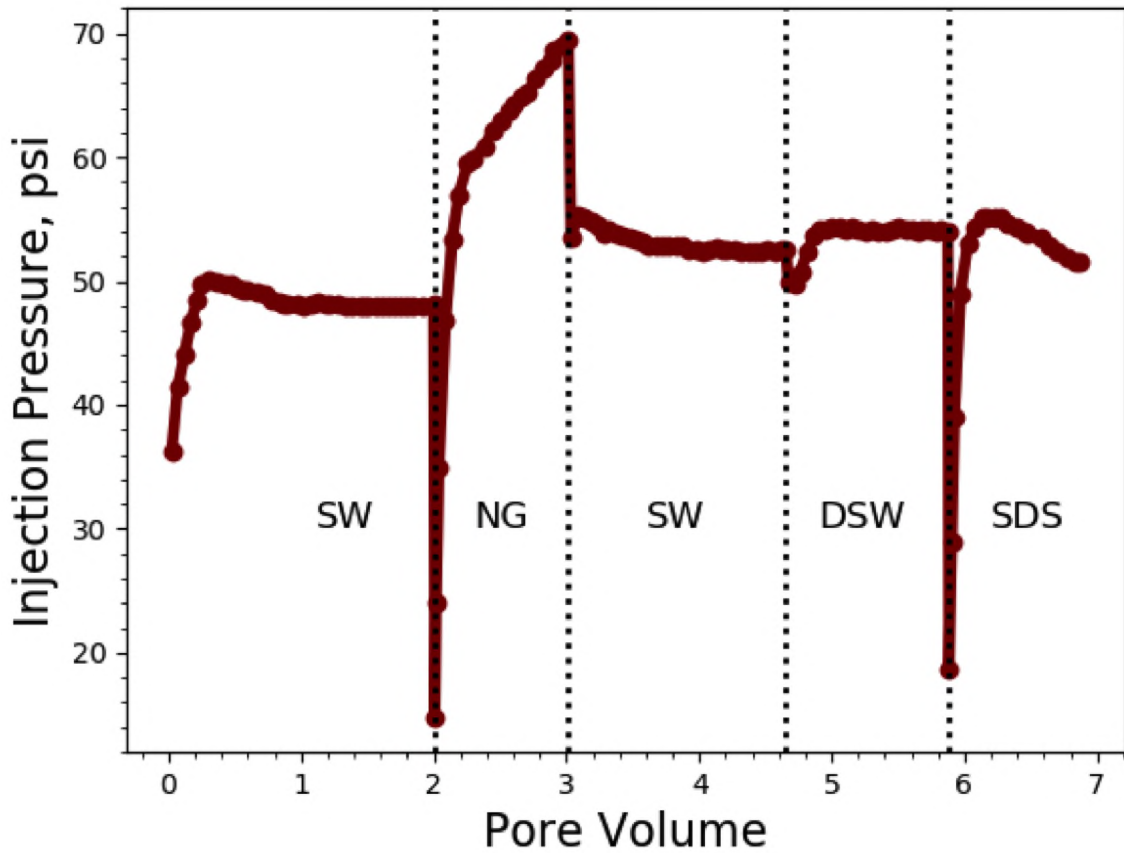


Figure 7. Injection pressure of Core B-1.

Another core flooding experiment was conducted to evaluate a different nanogel and SDS injection sequence (core B-2). The cumulative oil recovery by regular seawater was approximately 42.31% which represented the secondary oil recovery, as shown in Figure 8. This was followed by 1 injection-volume of nanogel (1,000 ppm). A substantial incremental oil was recovered equivalent to 4.8% beyond conventional seawater flooding. Next, 1 injection-volume of SDS (1,000 ppm) was followed, where an incremental oil recovery equivalent to 2.9% was obtained. This was followed by the injection of seawater until no more oil was produced and pressure reached a stable state. This injection slug recovered an incremental oil of 4.9%. The injection of 10-times diluted seawater was followed until no more oil was produced and pressure was stabilized. Even with this water slug, an incremental oil recovery equivalent to 1.93% was produced. As a result, the total incremental oil

recovery beyond initial seawater flooding was approximately 14.5% by sequence injection of nanogel and SDS followed by stepwise reduction of salinity of seawater. The injection pressure profile was consistent with the previous flooding experiment (core B-1), where a major pressure increase was observed by nanogel injection. The most dominant effect in injection pressure profile is the major decrease induced by SDS injection which represents the ability of SDS to reduce the adsorption density of nanogel in pore throats. Also, the water slugs following SDS injection showed a similar trend with the previous core flooding experiment (B-1) where an increase in pressure was observed with lower water salinity, as shown in Figure 9.

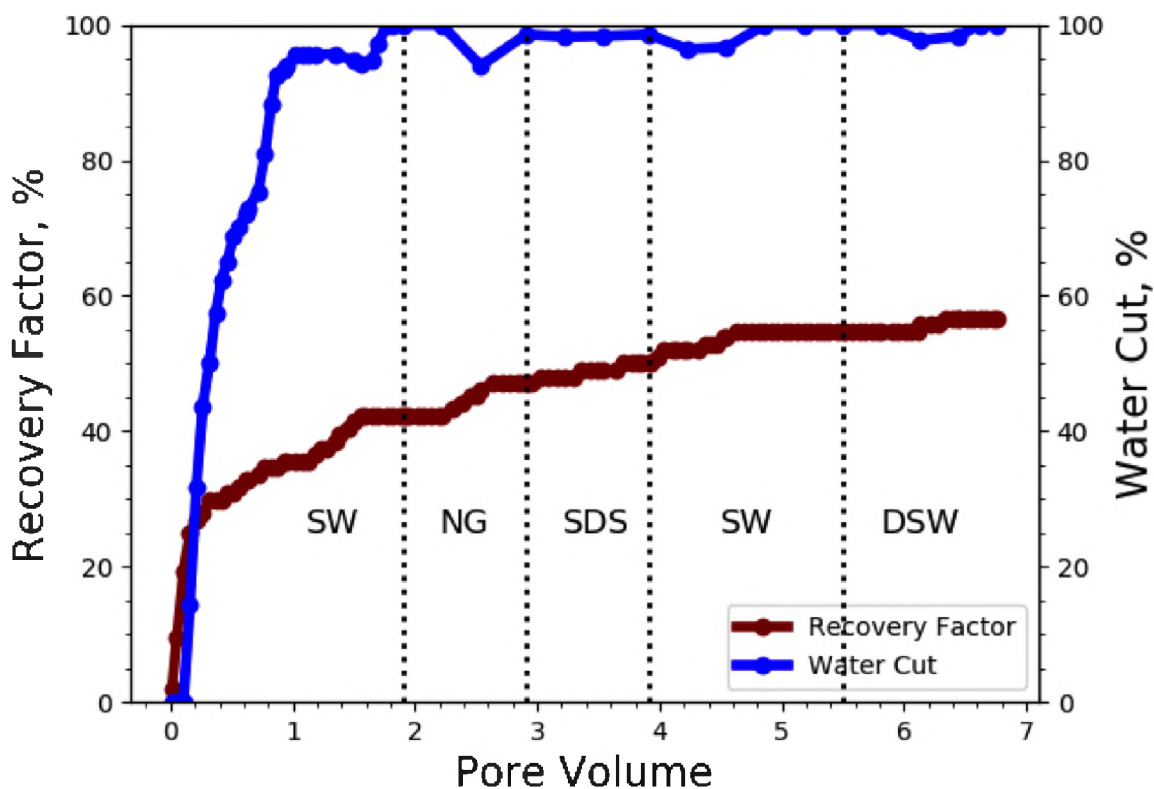


Figure 8. Oil recovery factor and water cut of Core B-2.

3.2.2. Effect of Nanogel Concentration. Another core flooding experiment was conducted to evaluate the effect of nanogel concentration combined with different diluted versions of seawater (core B-3). As shown in Figure 10, the cumulative oil recovery of

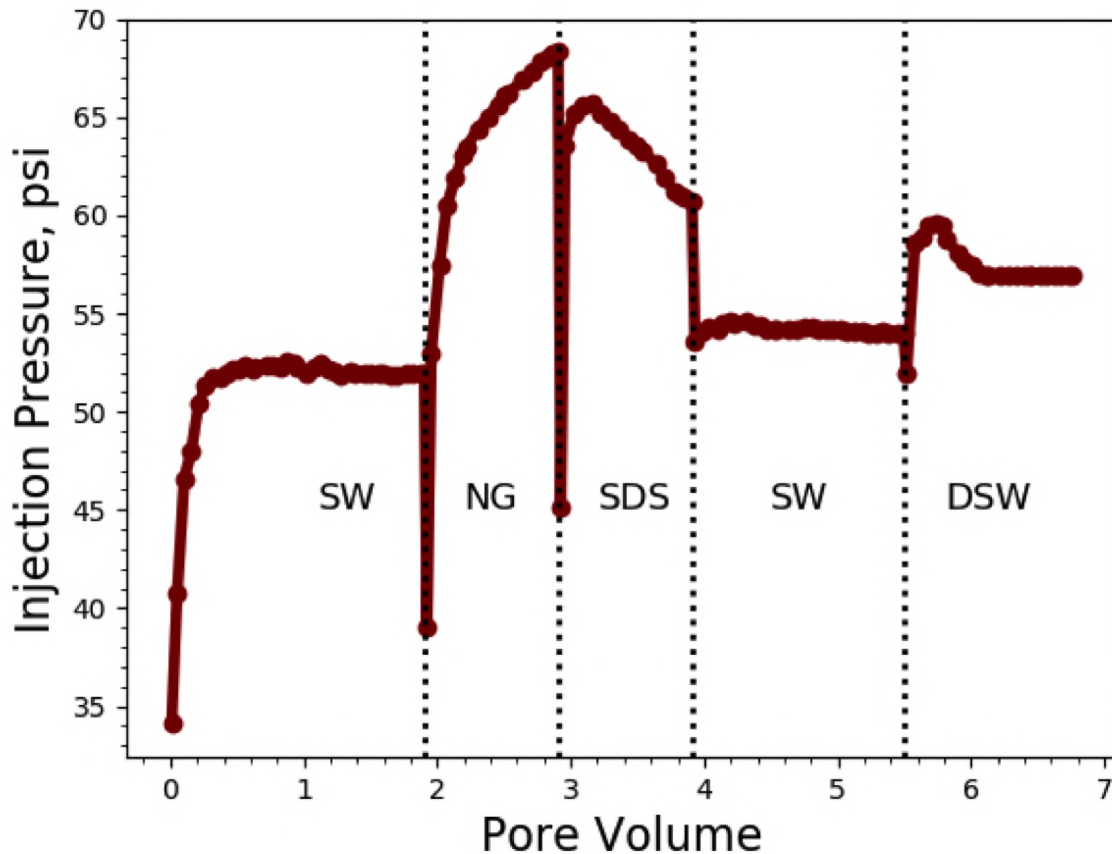


Figure 9. Injection pressure of Core B-2.

initial seawater slug was approximately 42.6% which represent the secondary recovery. This was followed by 1 injection-volume of nanogel (2,000 ppm). A substantial incremental of oil was produced equivalent to 6.48% beyond conventional seawater flooding. The injection of SDS (1,000 ppm) was followed, where a significant increment of oil equivalent to 5.55% was produced. The injection of seawater as tertiary process was continued until no more oil was produced and injection pressure reached a stable state. With this injection slug, an incremental oil recovery of approximately 3.7% was obtained. Then, 10-times diluted seawater was injected, and an incremental oil of approximately 1% was recovered. Therefore, the total incremental oil recovery beyond the conventional seawater flooding was approximately 16.65% by 2,000 ppm nanogel combined with SDS and stepwise reduction of salinity of seawater. Moreover, the most dominant effect in the injection pressure profile

shown in Figure 11 is the major pressure increase induced by nanogel injection. The injection pressure trend of water slugs following the nanogel injection showed an increasing behavior due to nanogel expansion phenomenon with lower salinity as illustrated earlier in Figure 4. Also, the ability of SDS to reduce the adsorption density of nanogel on rock surface was observed by the major pressure decline.

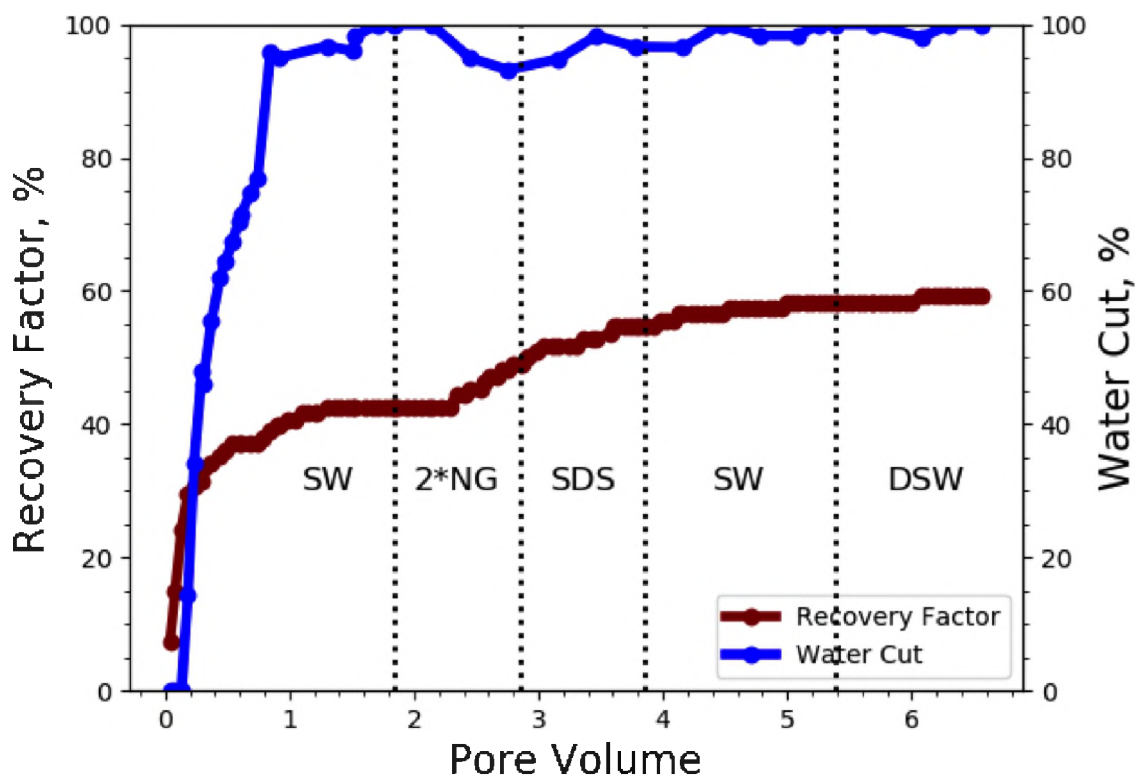


Figure 10. Oil recovery factor and water cut of Core B-3.

The effect of higher nanogel concentration combined with SDS and several salinities of seawater was evaluated using core B-4. As shown in Figure 12, the cumulative oil recovery by regular seawater was approximately 42.6%. This was followed by 1 injection-volume of nanogel (5,000 ppm) where a significant incremental oil of approximately 10.2% was obtained. This was followed by 1 injection-volume of SDS (1,000 ppm), where a substantial incremental oil equivalent to 8.3% was produced. Next, regular seawater was injected until no more oil was produced. An incremental oil recovery of approximately

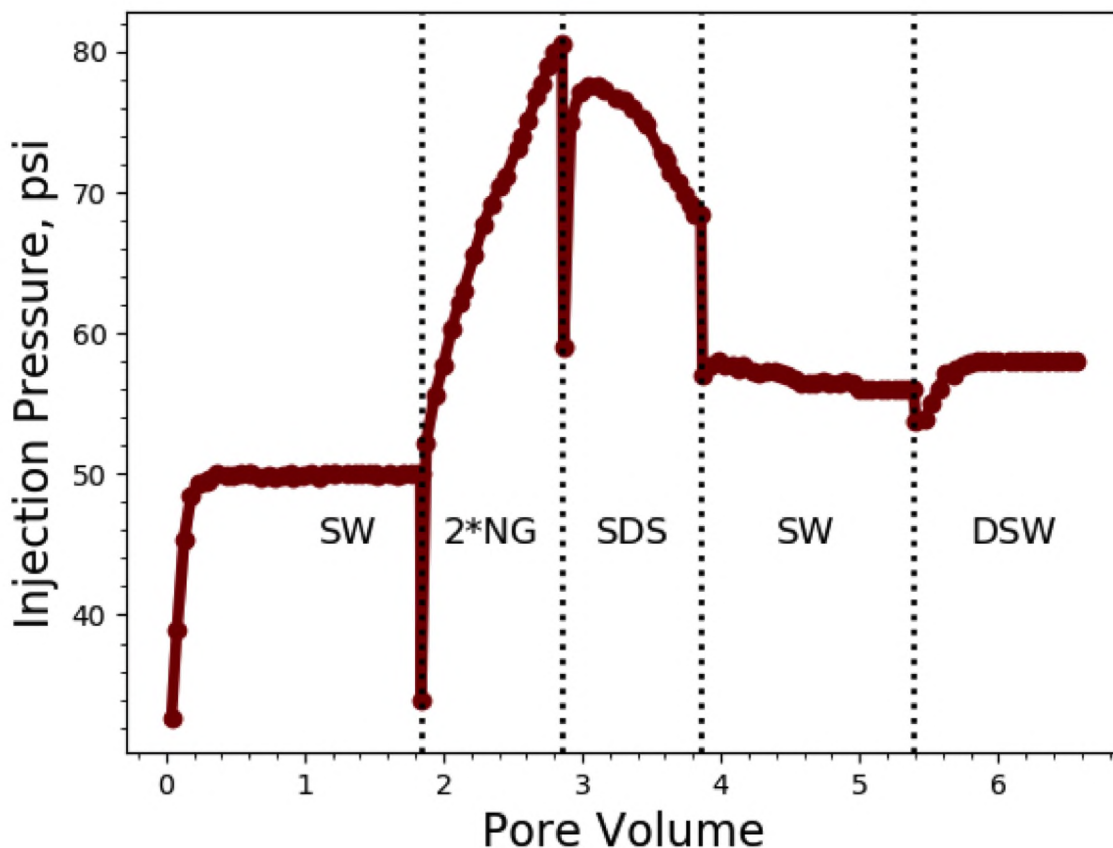


Figure 11. Injection pressure of Core B-3.

1.85% was recovered. The injection of 10-times diluted seawater was followed until no more oil was recovered. With this injection slug, no additional oil was produced. As a result, the total incremental oil recovery beyond the conventional seawater flooding was approximately 20.4% by 5,000 ppm nanogel combined with SDS and stepwise reduction of salinity of seawater. Additionally, the trend of injection pressure profile was consistent with the previous coreflood experiment (B-3), as shown in Figure 13. Here, the injection pressure of nanogel was higher due to the increase in its concentration. Also, the ability of SDS to reduce the adsorption of nanogel on rock surface was lower compared to the previous core flooding experiments (B-2 and B-3) with lower nanogel concentrations.

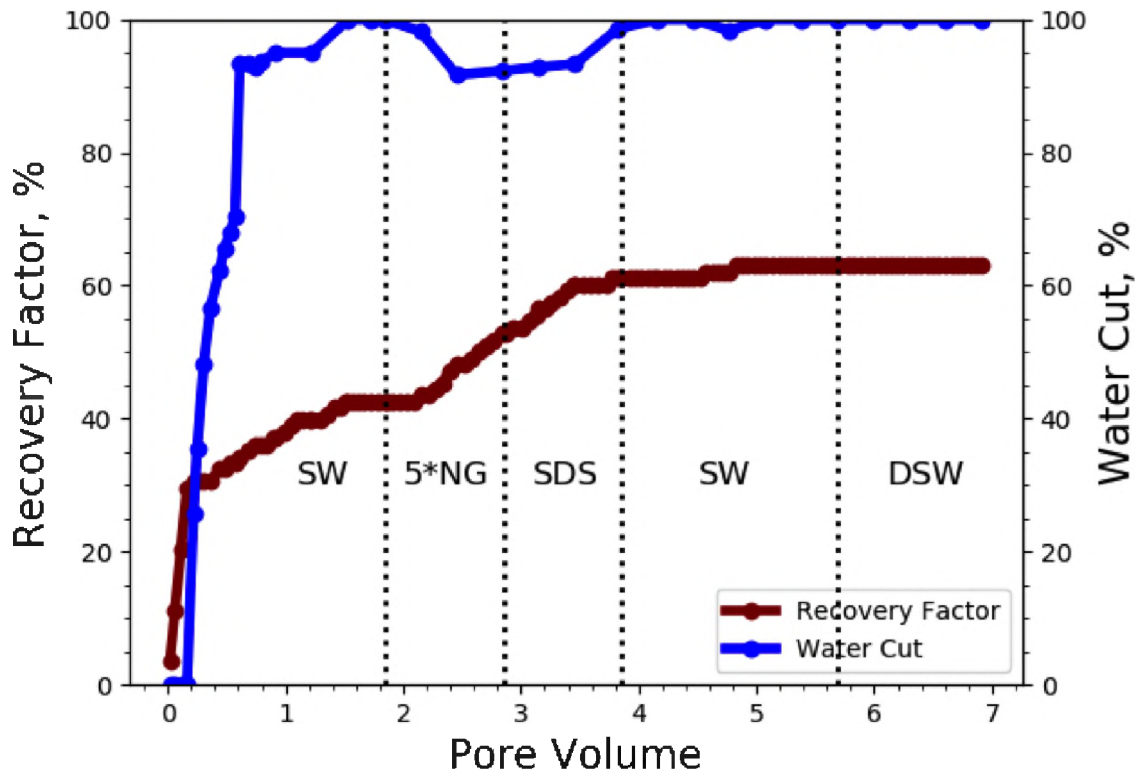


Figure 12. Oil recovery factor and water cut of Core B-4.

3.2.3. Evaluation of Nanogel and SDS One-Slug Injection Mode. Another core flooding experiment was conducted to study the potential of combining nanogel and SDS as one-slug injection and different diluted versions of seawater (B-5). As illustrated in Figure 14, the cumulative oil recovery by regular seawater slug was approximately 42.4%. This was followed by 2 injection-volumes of nanogel and SDS (500 ppm each) where an incremental oil recovery of 6.5% was recovered. Next, seawater was injected until no more oil was recovered and pressure stabilized. A significant incremental oil recovery of 4.35% was obtained. The injection of 10-times diluted seawater was followed where an additional oil of 1.1% was recovered. Therefore, the total incremental oil recovery, beyond conventional seawater flooding, was approximately 11.95% by one-slug injection of nanogel-SDS (500 ppm each) and diluted versions of seawater. Furthermore, the trend of injection pressure profile is illustrated in Figure 15. The most dominant effect in injection

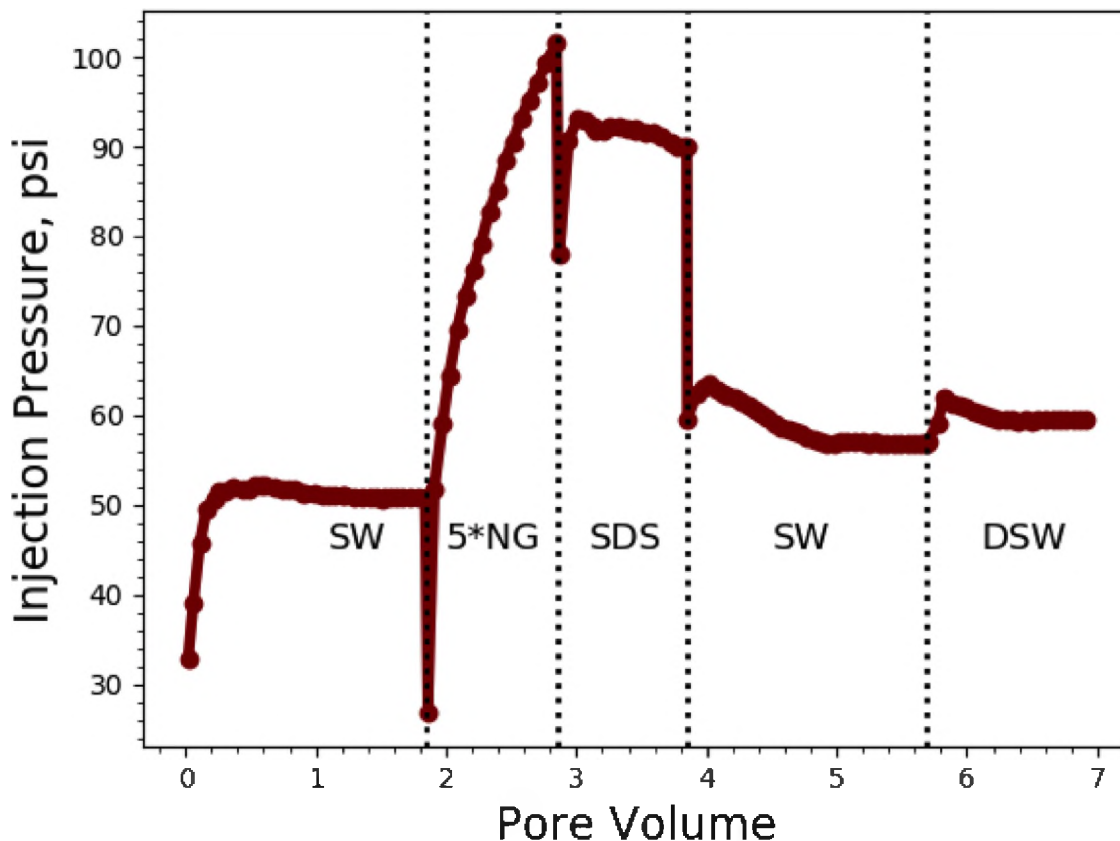


Figure 13. Injection pressure of Core B-4.

pressure profile is the stabilized pressure during nanogel-SDS injection which might be attributed to the low concentration. The water slugs following nanogel-SDS injection showed a similar trend to the previous core flooding experiment (B-3 and B-4) where an increase in pressure was observed with lower water salinity.

The effect of higher concentration of nanogel and SDS as one-slug combined with several salinities of seawater was studied using core B-6, as illustrated in Figure 16. The cumulative oil recovery by conventional seawater flooding was 42.53%. This was followed by 2 injection-volumes of nanogel-SDS as one-slug (1,000 ppm each) where a significant incremental oil of 6.9% was recovered. Next, seawater was injected until no more oil was produced and pressure stabilized. A significant incremental oil of 4.6% was recovered. The injection of 10-times diluted seawater was followed where an additional 1.15% of

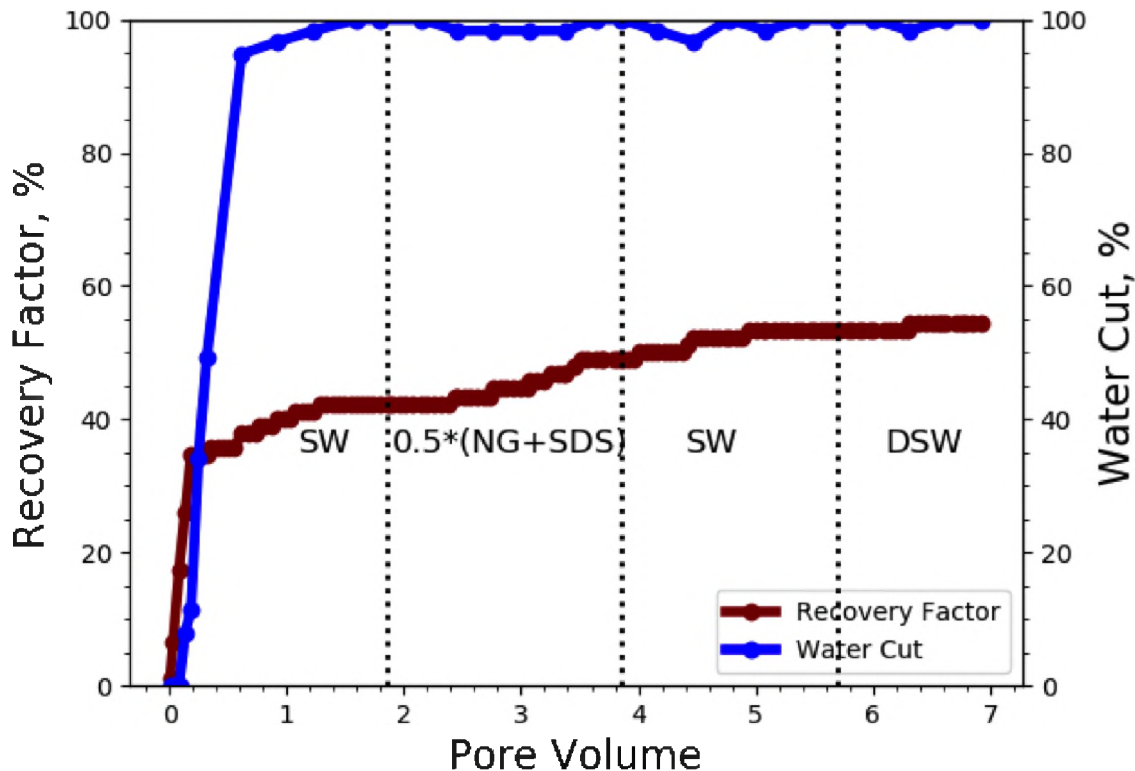


Figure 14. Oil recovery factor and water cut of Core B-5.

oil was produced. As a result, the total incremental oil recovery, beyond conventional seawater flooding, was approximately 12.65% by nanogel-SDS (1,000 ppm each) and various versions of seawater. In addition, the trend of injection pressure profile shown in Figure 17 is consistent with the previous flooding experiment (C-5) where the injection of nanogel-SDS showed lower increase (near stabilizing suggesting good injectivity). Also, the water slugs following SDS injection showed an increasing trend with lower salinity which is related to the size of nanogel when dispersed in lower salinities.

3.2.4. Effect of Diluted Seawater Salinity. The effect of dispersing nanogel in 10-times diluted seawater combined with stepwise increase in the salinity of the post waterflooding was evaluated using core B-7. As shown in Figure 18, the cumulative oil of 10-times diluted seawater as an initial waterflooding was approximately 46.73%. The injection of 1 injection-volume of nanogel (1,000 ppm dispersed in 10-times diluted

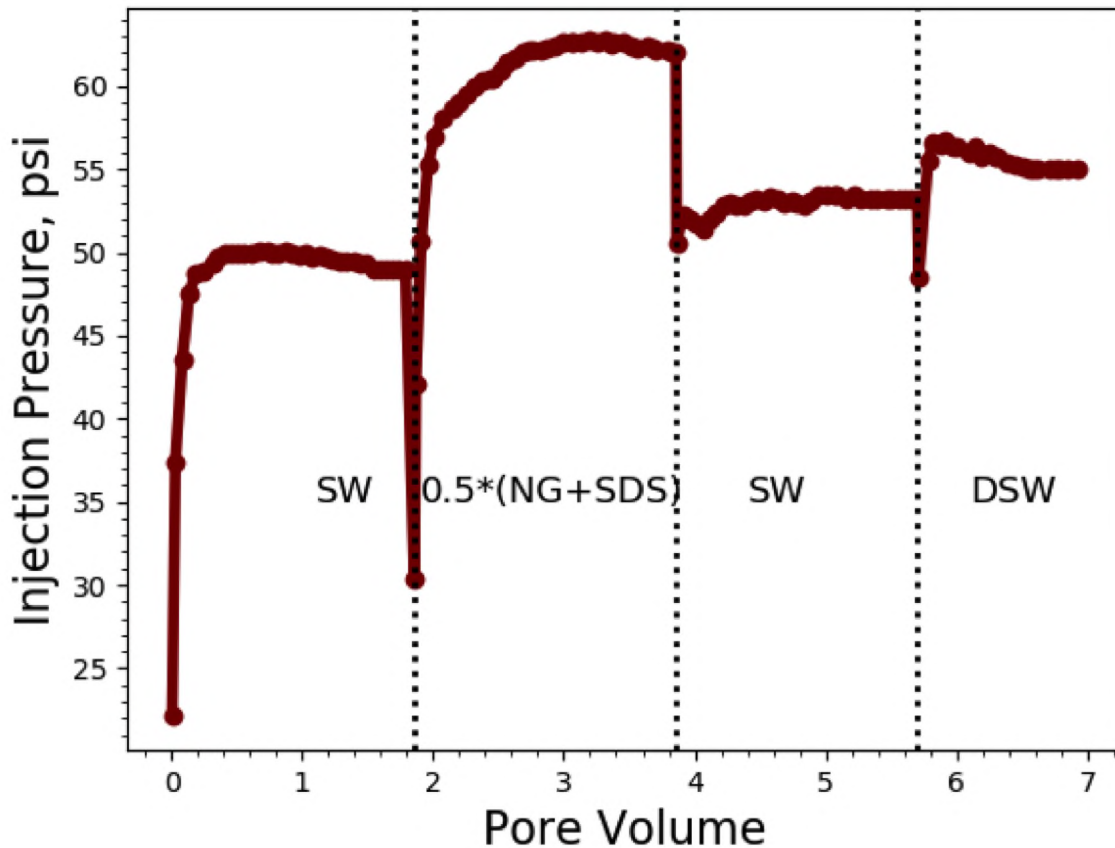


Figure 15. Injection pressure of Core B-5.

seawater) was followed where an incremental oil recovery of 1.0% was obtained. This was followed by an extended injection of 10-times diluted seawater until no more oil was recovered and pressure stabilized where an incremental oil equivalent to 1.2% was produced. Next, no additional oil production was observed with the extended injection of seawater. Finally, 1 injection-volume of SDS (1,000 ppm dispersed in 10-times diluted seawater) was followed, but no additional oil was produced. Therefore, the total incremental oil recovery, beyond conventional waterflooding, was approximately 2.2% by nanogel combined with stepwise increase in post waterflooding salinity and SDS injection. Moreover, the most dominant effect in injection pressure profile is the major pressure increase induced by nanogel injection, as illustrated in Figure 19. The injection pressure of the stepwise increase

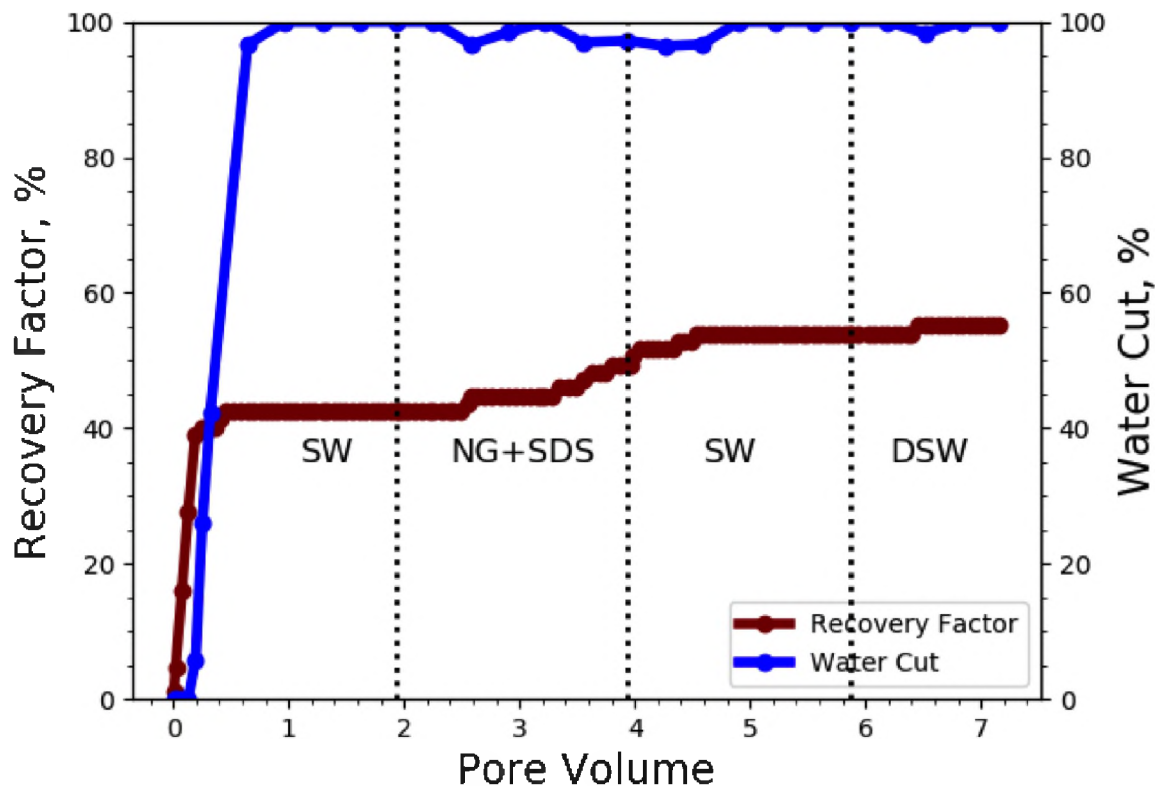


Figure 16. Oil recovery factor and water cut of Core B-6.

in the post waterflooding showed a decreasing trend with higher water salinity due to the shrinkage in nanogel size in higher brine salinity. In addition, the pressure profile of SDS injection revealed its ability to reduce the adsorption induced by nanogel injection.

Another core flooding experiment was conducted to evaluate the injection sequence effect of nanogel and SDS while dispersed in 10-times diluted seawater and combined with several salinities of seawater, as shown in Figure 20. The cumulative oil recovery by conventional 10-times diluted seawater was approximately 46.6%. 1 injection-volume of nanogel (1,000 ppm) was followed, and only 1.0% of incremental oil was recovered. Next, 1 injection-volume of SDS (1,000 ppm) was followed and an incremental oil of 2.1% was produced. This was followed by injecting 10-times diluted seawater until no more oil was recovered, and an additional incremental oil of approximately 6.6% was produced. Finally, seawater was injected where an incremental oil of 2.1% was obtained. Therefore, the total

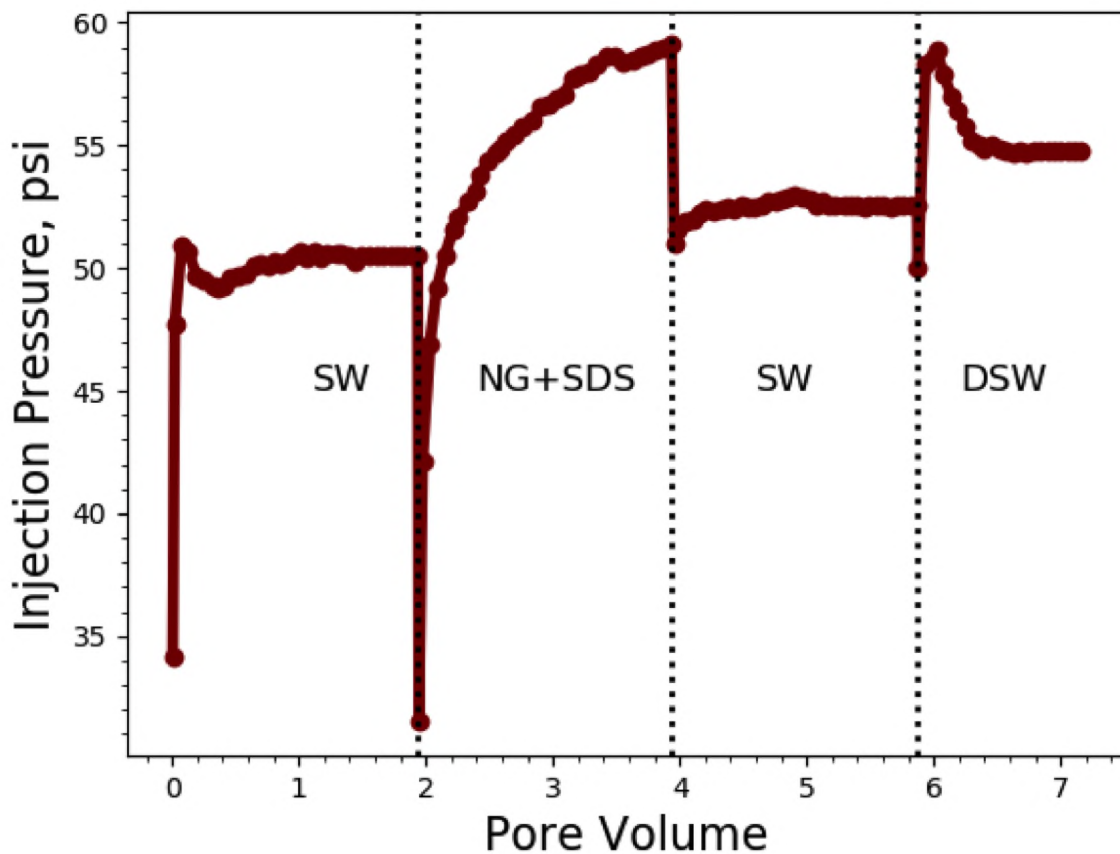


Figure 17. Injection pressure of Core B-6.

incremental oil beyond initial waterflooding is approximately 11.85% by nanogel combined with SDS and followed by several salinities of seawater. The injection pressure profile shown in Figure 21 is consistent with the previous core flooding experiment (B-6). Here, SDS injection (1,000 ppm) greatly reduced the adsorption caused by nanogel injection.

3.2.5. Effect of Nanogel Concentration Combined with Diluted Waterflooding.

The effect of higher nanogel concentration while dispersed in 10-times diluted seawater combined with SDS and several salinities of seawater was evaluated using core B-9. As shown in Figure 22, the cumulative oil recovery by regular 10-times diluted seawater was approximately 45.8%. This was followed by 1 injection-volume of nanogel (5,000 ppm) where a significant incremental oil of approximately 6.5% was obtained. This was followed by 1 injection-volume of SDS (1,000 ppm), where a substantial incremental oil equivalent

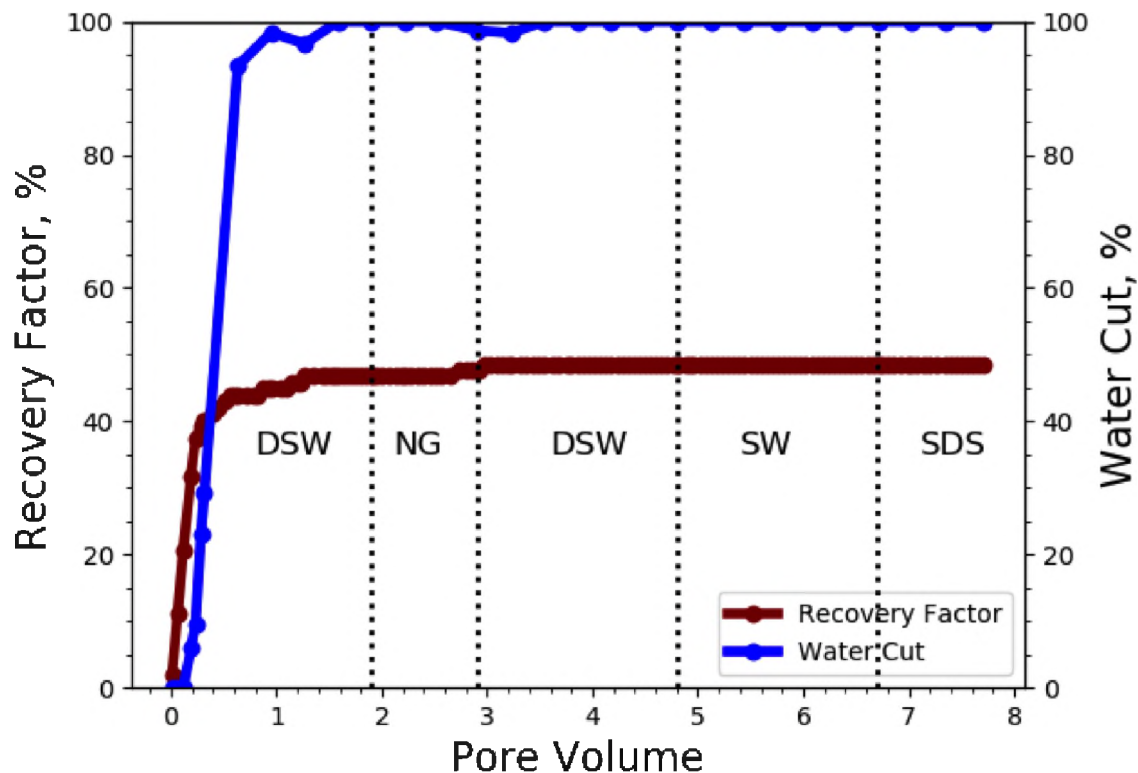


Figure 18. Oil recovery factor and water cut of Core B-7.

to 8.4% was produced. Next, 10-times diluted seawater was injected until no more oil was produced. An incremental oil recovery of approximately 2.8% was recovered. The injection of seawater was followed until no more oil was recovered. With this injection slug, no additional oil was produced. As a result, the total incremental oil recovery beyond the conventional waterflooding was approximately 17.7% by 5,000 ppm nanogel combined with SDS and stepwise increase in the salinity of seawater. Additionally, the trend of injection pressure profile was consistent with the previous coreflood experiments (B-7 and B-8), as shown in Figure 23. Here, the injection pressure of nanogel was higher due to the increase in its concentration. Also, the ability of SDS to reduce the adsorption of nanogel on rock surface was lower compared to the previous core flooding experiments with lower nanogel concentrations.

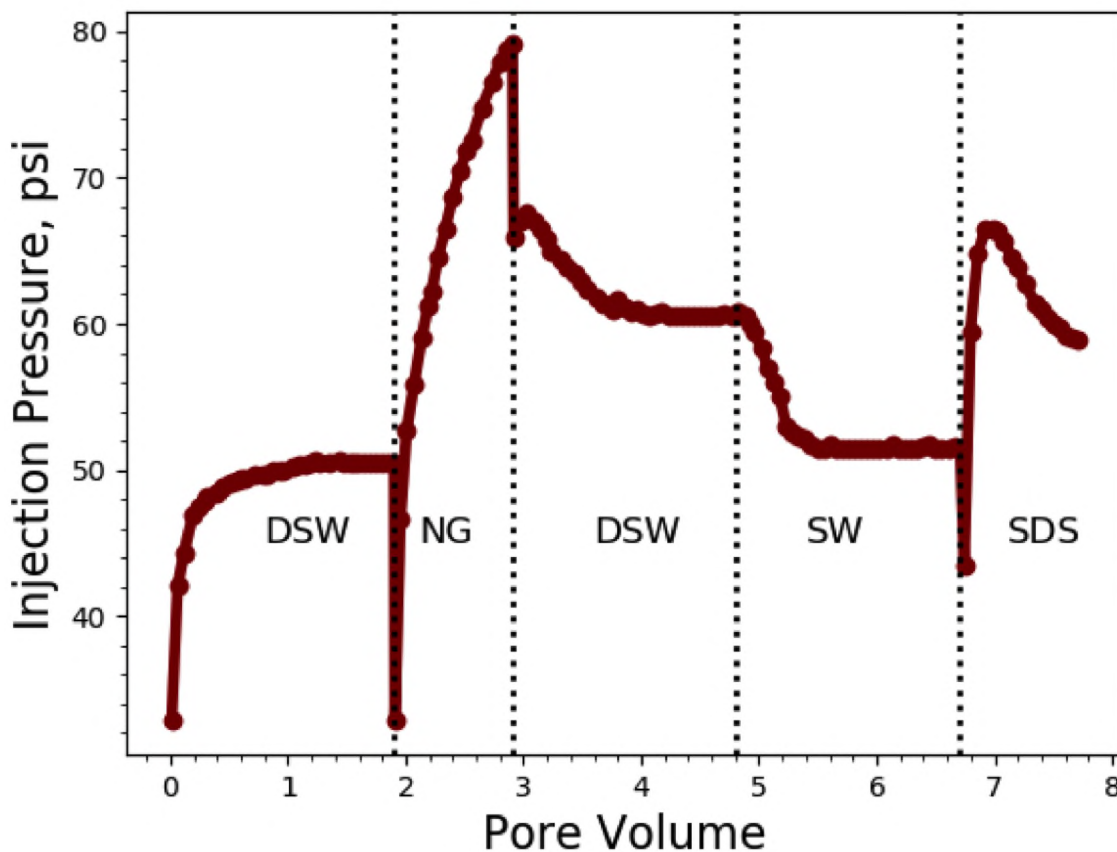


Figure 19. Injection pressure of Core B-7.

3.2.6. Evaluation of Nanogel and SDS One-Slug Injection Mode. The impact of injecting nanogel and SDS together as one-slug combined with several diluted versions of seawater was evaluated using core B-10. As illustrated in Figure 24, the cumulative oil recovery by 10-times diluted seawater as initial waterflooding was approximately 46.2%. The injection of 2 injection-volumes of nanogel coupled with SDS (500 ppm each dispersed in diluted seawater) as one-slug was followed. An incremental oil was produced, equivalent to 3.8%. This was followed by injecting 10-times diluted seawater where an additional oil of 5.7% was recovered. Lastly, seawater was injected, where no additional oil was recovered. The total incremental oil without conventional waterflooding was approximately

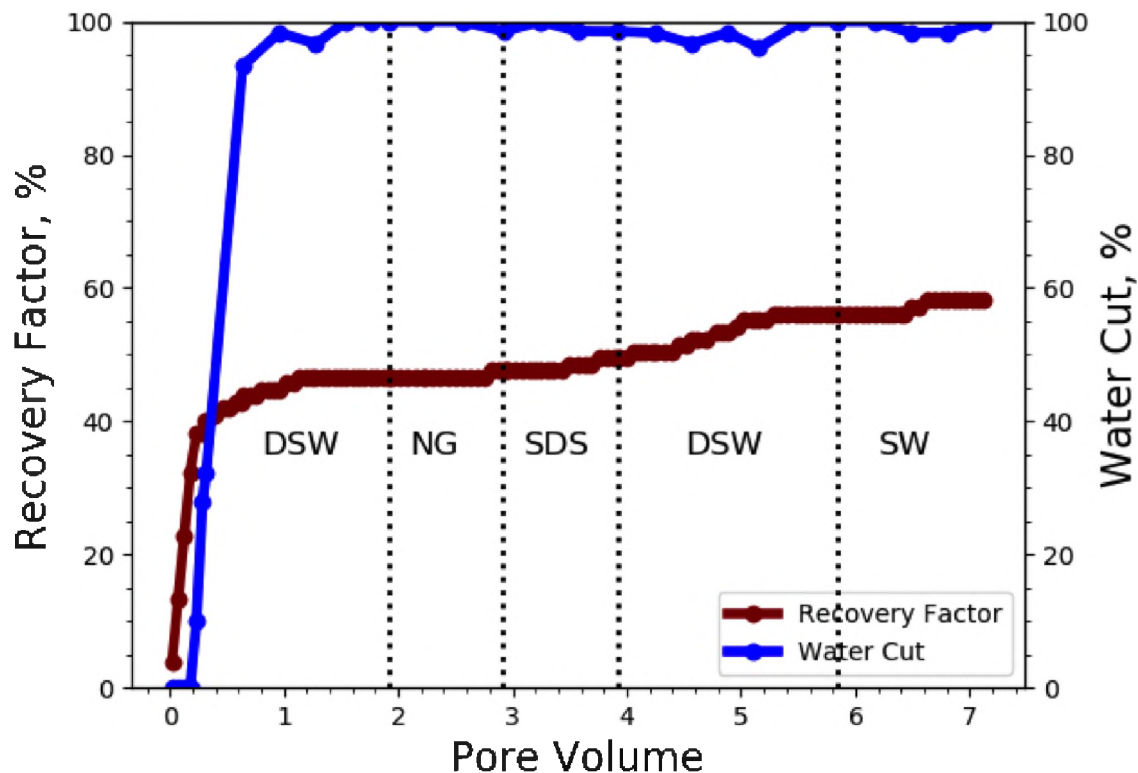


Figure 20. Oil recovery factor and water cut of Core B-8.

9.5%. The injection pressure profile showed a major increase induced by nanogel-SDS injection, as presented in Figure 25. The general pressure trend of the followed water slugs was consistent with previous core flooding experiments (B-8 and B-9).

Another core flooding experiment was conducted to study the impact of injecting higher concentration of nanogel and SDS as one-slug combined with several versions of seawater, as illustrated in Figure 26. The cumulative oil recovery by conventional waterflooding was 45.9%. The injection of nanogel and SDS (1,000 ppm each dispersed in 10-times diluted seawater) as one-slug was followed, and after 2 injection-volumes, a substantial incremental of oil was produced, equivalent to 5.1%. This was followed by injecting 10-times diluted seawater where a significant incremental oil of 6.1% was recovered. Finally, seawater was injected but no additional oil was recovered. The total incremental oil

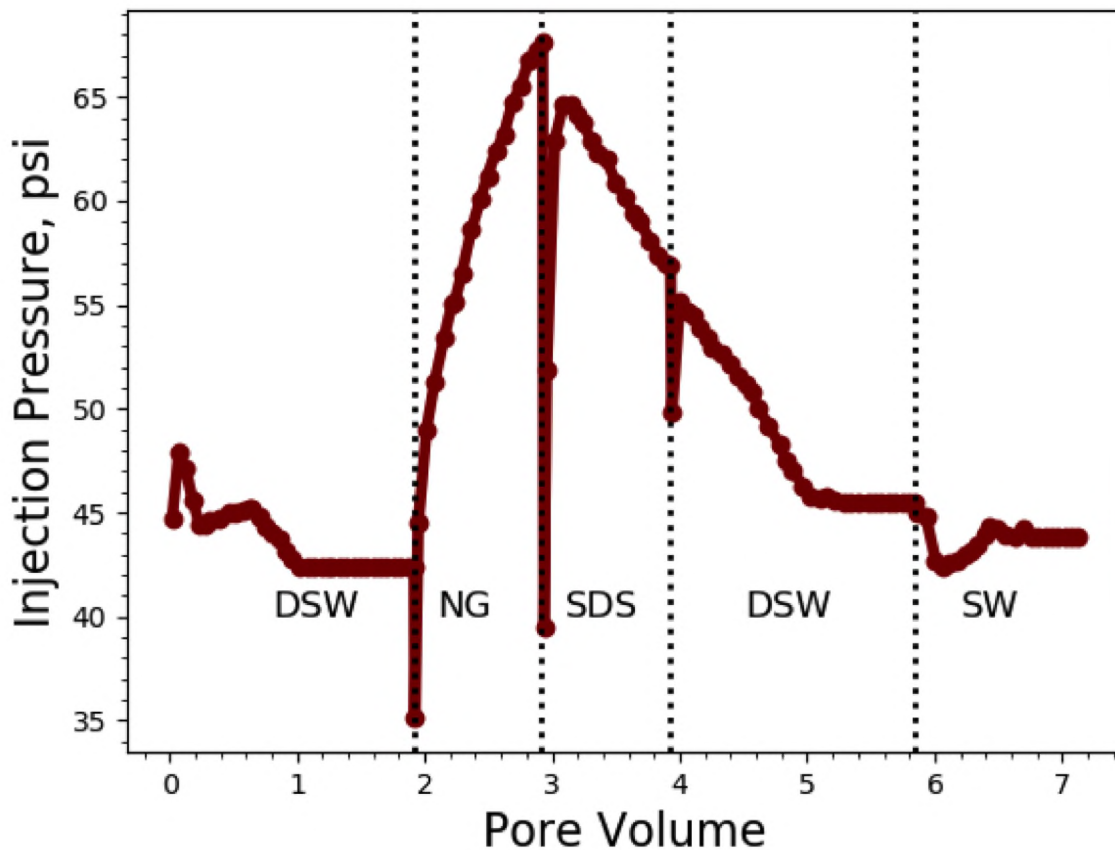


Figure 21. Injection pressure of Core B-8.

beyond the conventional waterflooding was approximately 11.2%. In addition, the trend of injection pressure profile is consistent with the previous experiments (B-8, B-9 and B-10), as shown in Figure 27.

3.3. DYNAMIC ADSORPTION AND DESORPTION MEASUREMENTS

In this work, nanogel dispersion with a concentration of $1,000 \frac{mg}{L}$ was injected in sandstone core plug until no more nanogel adsorbed on the pore throats. Then, seawater (TDS is 57,670 ppm) was injected through the core to desorb the nanogel from the rock surface. The injection pressure was continuously monitored throughout the experiment to study the plugging performance of nanogel. The injection pressure profile of nanogel

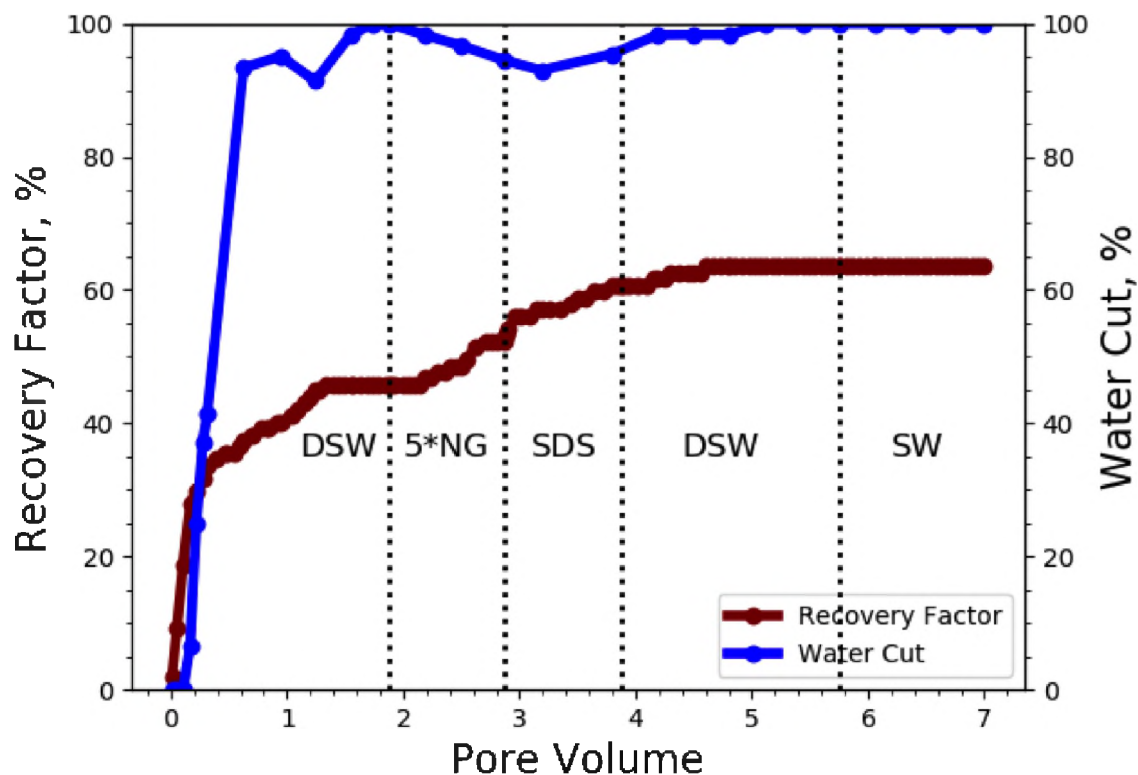


Figure 22. Oil recovery factor and water cut of Core B-9.

showed a continuous increasing trend until it reached around 10 psi, as shown in Figure 28. During the first injection-volume (1 PV), the injection pressure increased to 5 psi. Afterwards, the injection pressure increased with an average rate of 0.5 psi per injection-volume. Nanogel was not detected in the effluent until after 1 whole injection-volume. The concentration of nanogel in the effluent slightly increased to $150 \frac{mg}{L}$ at injection-volume of 1.75. Then, a sharp increase in the concentration of nanogel in the effluent was observed with an average concentration rate of $800 \frac{mg}{L}$ per PV until the injection volume reached 2.25 PV. Next, the average concentration rate of nanogel in the effluent reduced to $730 \frac{mg}{L}$ per PV until the injection volume reached 3 PV. Later, the concentration of nanogel in the effluent reached the concentration of the injected nanogel at 3.5 PV where no more nanogel was adsorbed at the pore throats which might suggest a piston-like displacement process of nanogel in porous media. The dynamic desorption behavior of nanogel was also

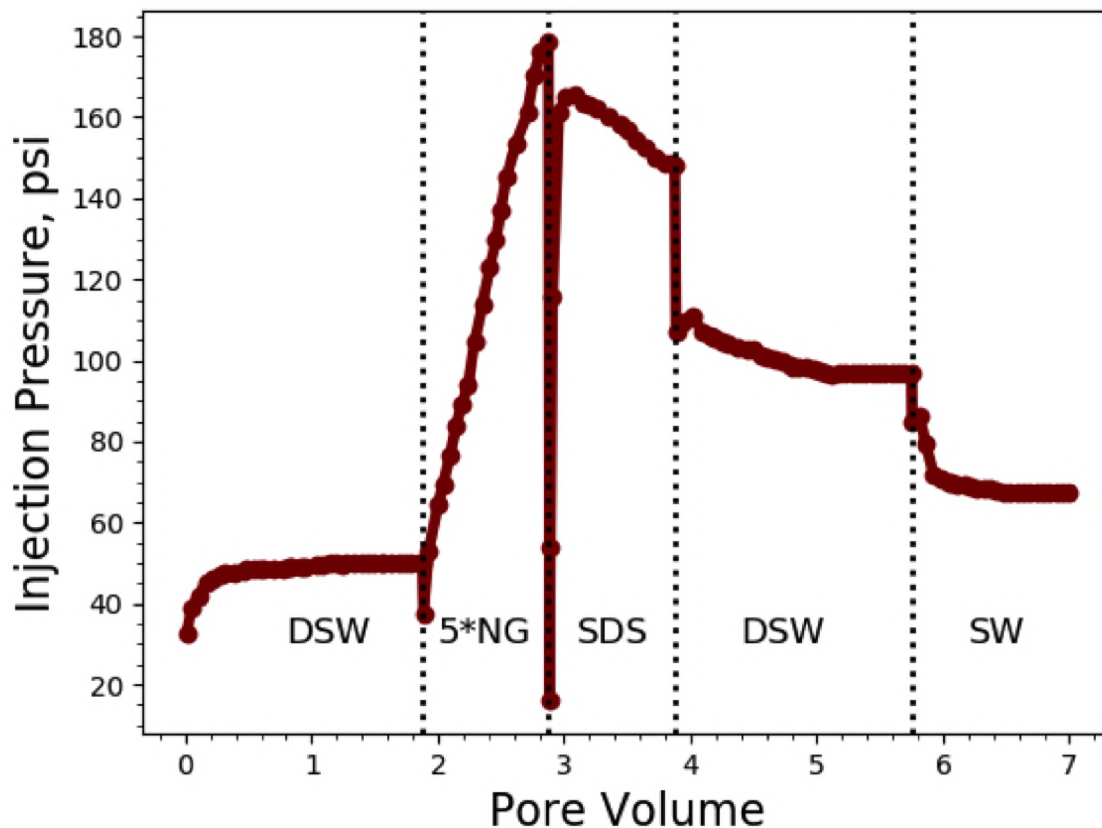


Figure 23. Injection pressure of Core B-9.

evaluated at room temperature, as presented in Figure 29. The injection pressure profile during the post seawater injection slightly fluctuated between 8 and 10 psi during the first injection-volume. Afterwards, the injection pressure remained almost stable at 8.5 psi. On the other hand, the concentration of nanogel in the effluent during the desorption process decreased slightly to $800 \frac{mg}{L}$ in the first 0.8 PV. Then, the concentration of nanogel in the effluent reduced in a power law relationship with injection volume. Different responding rates of injection pressure and nanogel concentration in the effluents were observed in both dynamic adsorption and desorption processes.

The narrow pore size distribution associated with sandstone cores resulted in detecting the nanogel in the effluent after more than 1 PV during the dynamic adsorption process. However, the equilibrium concentration of nanogel, where injected and efflu-

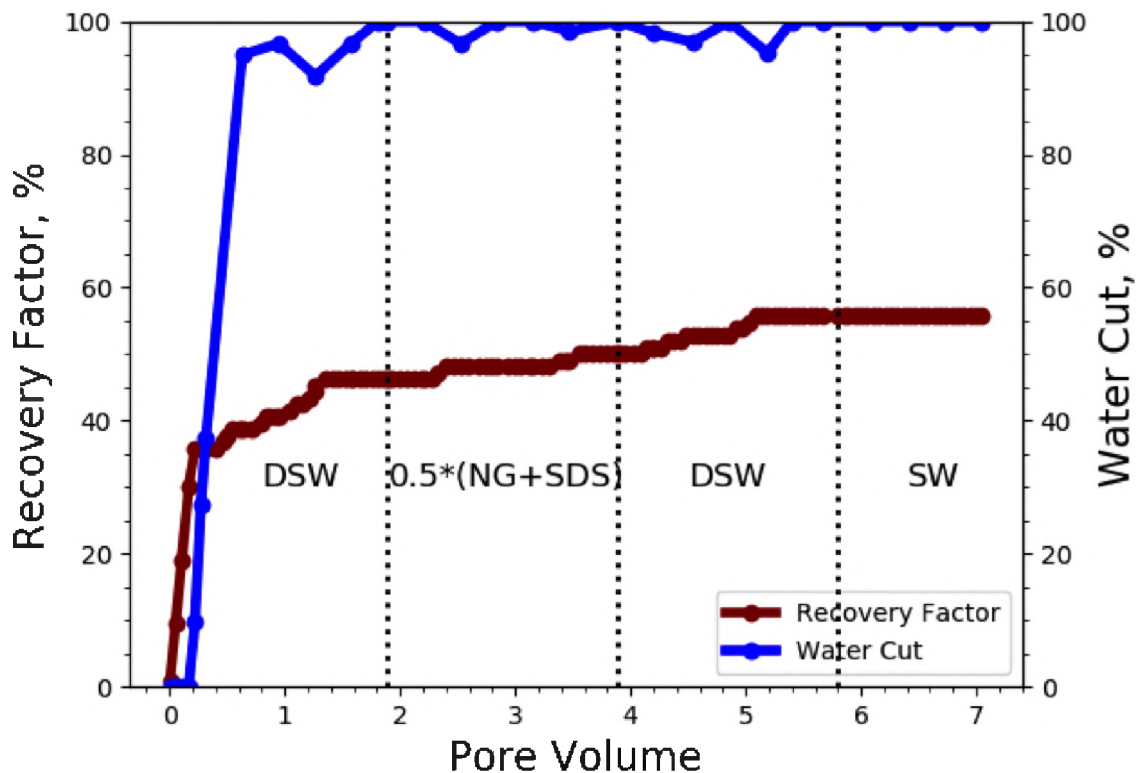


Figure 24. Oil recovery factor and water cut of Core B-10.

ent concentrations become equal, was not reached until after 3.5 injection volumes. The complex interactions between sandstone rock surface and nanogel dispersion caused this effluent nanogel concentration profile, where electrostatic repulsion accelerated the dynamic adsorption process to reach equilibrium state, whereas electrostatic attraction extended it. During the desorption process, however, the nanogel dispersion remained in rock surfaces and pore throats were flushed out by the displacing brine that resulted in the power-law trend of effluent nanogel concentration.

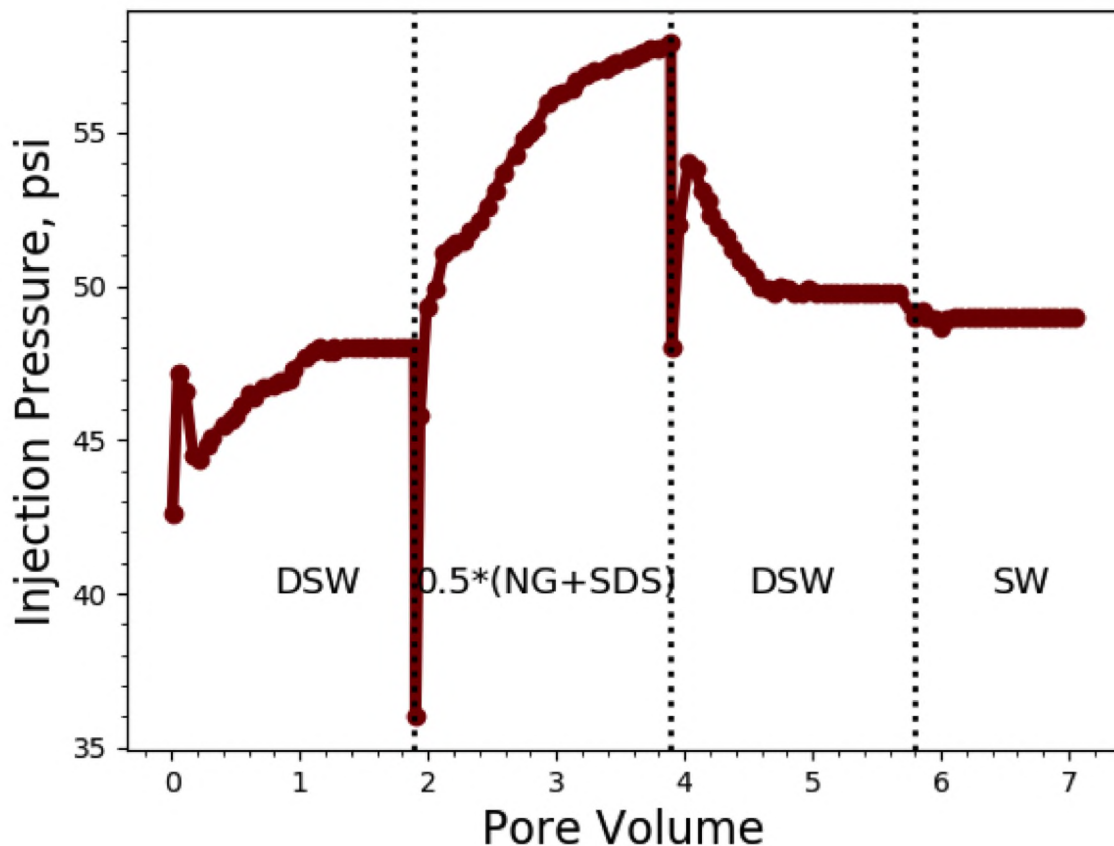


Figure 25. Injection pressure of Core B-10.

3.4. INJECTIVITY AND PLUGGING PERFORMANCE OF NANOGEL IN SANDSTONE

In order to assess the plugging performance caused by nanogel and SDS injections, the permeability reduction or residual resistance factor (F_{rr} or RRF) have to be evaluated using equation 3, while the injectivity evaluation of gel treatments is estimated using equation 2. Figure 30 summarizes the results of resistance factor and residual resistance factor of all cores used in core flooding experiments. Here, resistance factor was estimated at the end of NG or SDS volume injection, and residual resistance factor was calculated using the stabilized pressure of the final water slug. The resistance factor measurements were higher for core plugs with lower permeability and higher nanogel concentrations. However, the adsorption of nanogel in rock surfaces was limited due to the similar surface

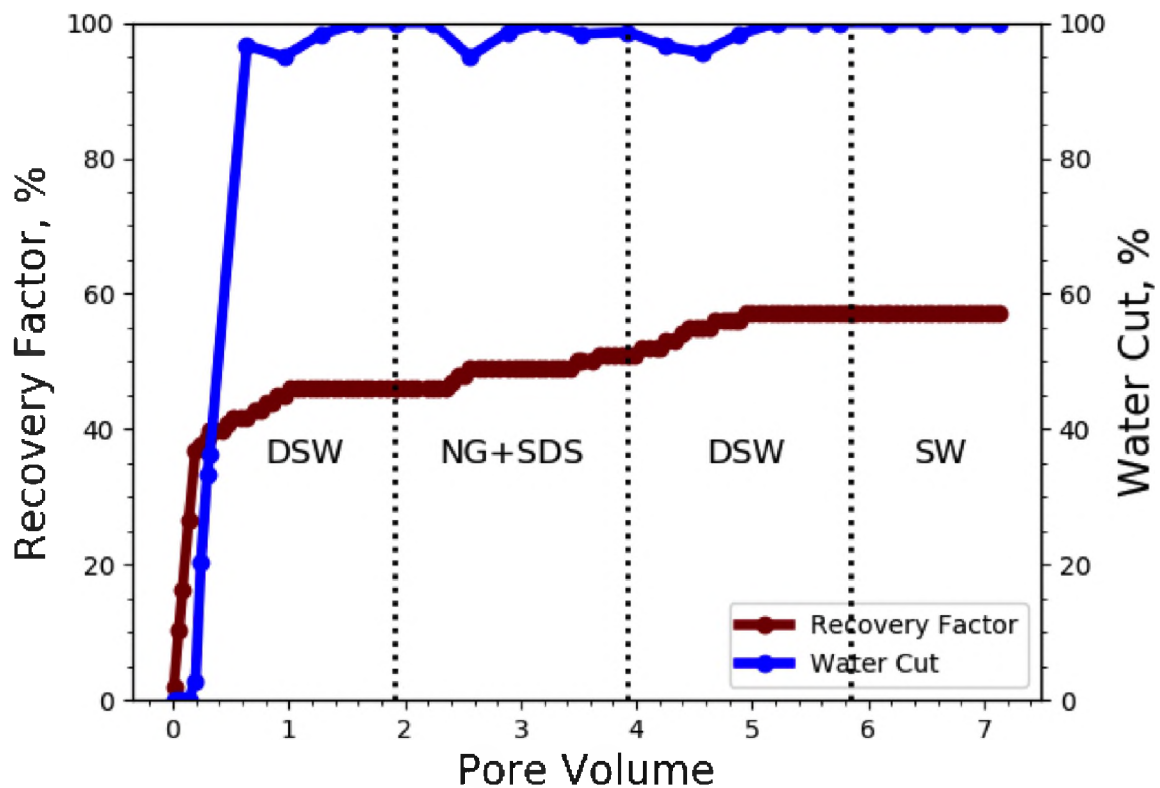


Figure 26. Oil recovery factor and water cut of Core B-11.

charges of nanogel and employed sandstone rock. Experimental results showed that residual resistance factor measurements in cores injected with only nanogel (no SDS) were higher when low salinity water slugs were applied. This is probably attributed to the fact that nanogel particles can expand in lower seawater salinities. Hence, SDS injections reduced the adsorption of nanogels in pore throats and caused lower blocking efficiency. In all, employed nanogel is not considered strong plugging materials in sandstone reservoirs and the formation damage induced by its injection is minimal.

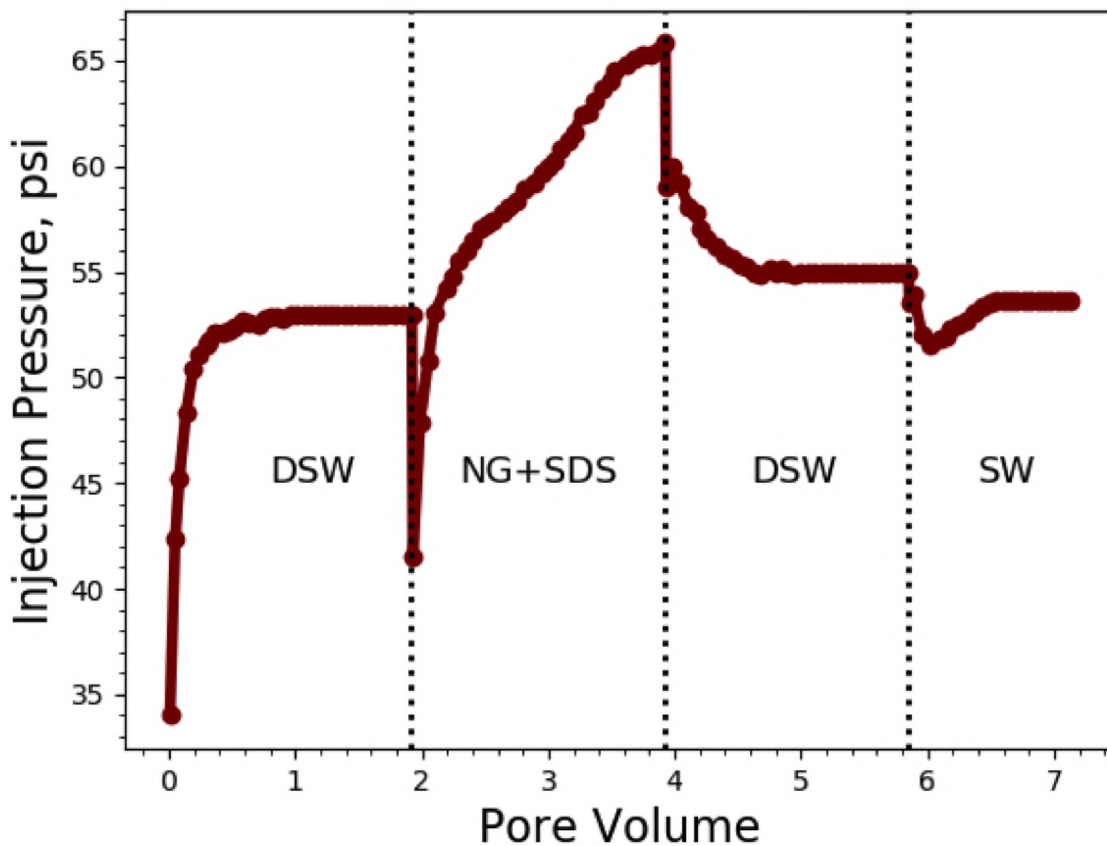


Figure 27. Injection pressure of Core B-11.

3.5. DISCUSSION

The most substantial observation that needs to be highlighted is the incremental oil recovery reported in this research work by nanogel and SDS injections combined with several salinities of seawater. In this work, two different sets of flooding experiments were conducted. In this first set, seawater with a salinity of 57,670 ppm was the main brine type where it had been used in initial waterflooding and dispersing nanogel and SDS. 10-times diluted seawater with a salinity of 5,767 ppm was the main brine type in the second set of experiments. The results of initial waterflooding revealed that lower brine salinity had greater potential to recover higher amounts of oil. In addition, higher concentrations of nanogel were able to recover more oil, especially when dispersed in seawater. Altering the

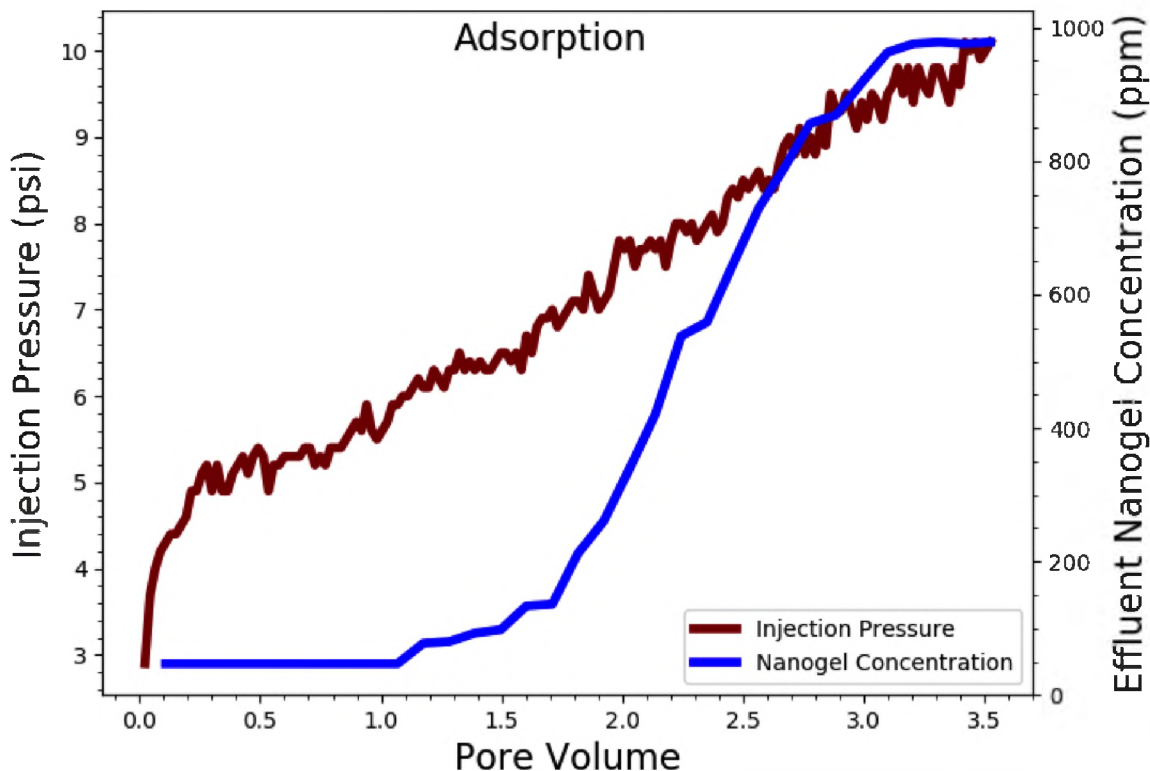


Figure 28. Effluent nanogel concentration and injection pressure as a function of injection volume of dynamic adsorption using Core B-12.

brine salinity in the post waterflooding has shown an impact on improved oil recovery. The results showed that about 2% of oil can be recovered by the alteration strategy in high permeability sandstone cores. The results also revealed that SDS injection had the ability to reduce the adsorption induced by nanogel injection. However, this reduction was lower when higher concentrations of nanogel were injected. Furthermore, the improved oil recovery by sequential injections of nanogel and SDS was almost doubled compared to one-slug injection mode. Combining nanogel and SDS with several brine salinities provided a significant increase in oil recovery up to 20% beyond conventional waterflooding.

The transportation of particles in porous media is a very complex process that is affected by the heterogeneity of porous media. The path of particles inside the porous media is governed by different factors such as particles' size and their surface properties, the structure of the porous media, the properties of the displacing fluid, and the interactions

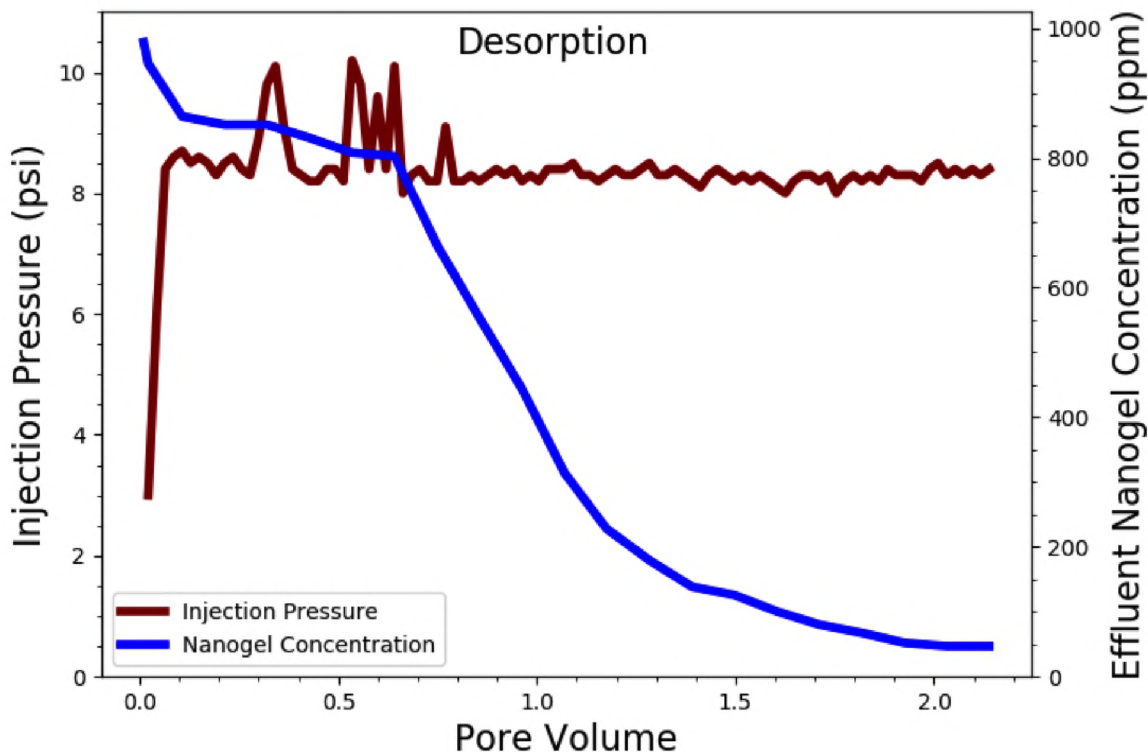


Figure 29. Effluent nanogel concentration and injection pressure as a function of injection volume of dynamic desorption using Core B-12.

between the particles and the porous media (Gao, 2007). The complex interactions between all these factors greatly govern the movement of particles, adsorption and desorption densities of particles in pore throats, and the permeability reduction induced by particles' movement (Gao, 2007). Additionally, the heterogeneity and complexity of porous media and particles might induce a log-jamming phenomenon in pore throats, which is generally affected by the size of particles and their concentration, pore size distribution, and flow rate (Bolandtaba *et al.*, 2009).

The results reported in this paper clearly indicate the potential of nanogel flooding when combined with two other promising technologies, surfactant and low salinity water flooding, in sandstone reservoirs. A substantial incremental oil recovery was obtained by higher concentrations of nanogels. Altering the salinity of the post water flooding segments

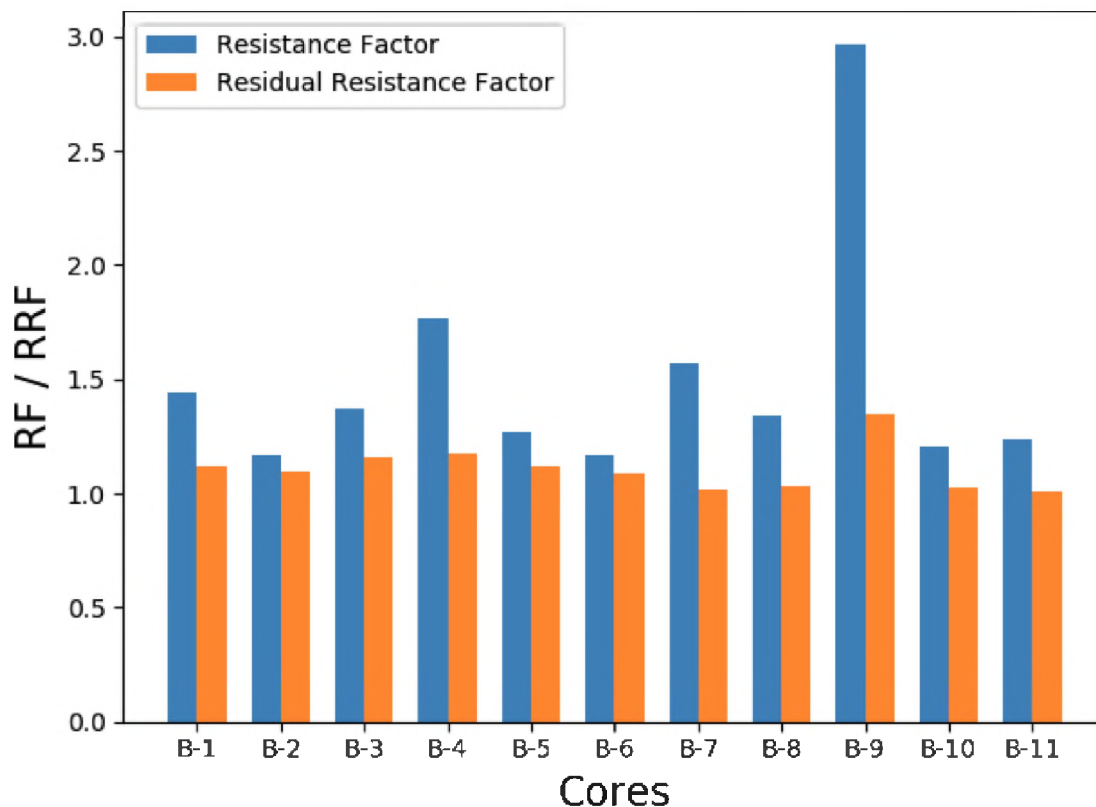


Figure 30. Resistance factor calculated at the end of NG/SDS injection and residual resistance factor calculated using stabilized pressure of last water slug of all cores used in core flooding experiments.

has also provided an additional oil recovery by mainly expanding the size of nanogel in pores, diverting the water to un-swept areas and releasing the carboxylic oil components from rock surface.

4. CONCLUSIONS

In this work, the performance of a newly developed particles known as nanogels combined with SDS and several salinities of seawater in sandstone reservoirs to improve oil recovery was reported as a potential EOR method. This was explained through well-tailored core flooding experiments using crude oil from one of Saudi reservoirs. The reported method consists of different injection practices of nanogel and SDS (sequential

and one-slug), and sequential injections of various salinities of seawater. The incremental oil recovery was approximately 10.2% with sequential nanogel injection, 8.3% with sequential SDS injection, 4.9% with regular seawater, and 1.9% with 10-times diluted seawater. The primary findings in this study are reported below.

- The results revealed that altering the salinity of seawater has a significant impact on the size of nanogel. Lower seawater salinities caused nanogel particles to expand and further swell.
- Nanogels showed good long-term stability when dispersed in brines with several salinities. The structural size of nanogels was well-maintained for a period of two weeks.
- Sequential injections of nanogel and SDS, one after another, has a higher potential to recover additional incremental oil compared to one-slug injection mode.
- The oil production of different seawater salinities after nanogel and SDS injections was triggered after about 1 pore volume of the new water type.
- The increase in injection pressure profile with different water slugs after nanogel and SDS injections is an indication of the ability of adsorbed nanogel to expand and swell in pores.
- The injection of SDS has a great ability to reduce the adsorption induced by nanogel injection.
- The adsorption measurement revealed that the injection pressure profile of nanogel was slightly increasing until it reached 10 psi which means that nanogel adsorption

was not significant. Nanogel was detected in the effluent after injection of more than 1 injection-volume due to the narrow pore size distribution.

- The residual resistance factor results suggest that nanogels are not considered strong plugging materials in sandstone reservoirs.

NOMENCLATURE

NG Nanogel.

SW Seawater.

DSW Diluted seawater.

F_r Resistance factor.

F_{rrw} Residual resistance factor of water.

ppm Parts per million.

SDS Sodium dodecyl sulfate.

PV Pore volume.

CMC Critical micelle concentration.

AMPS 2-acrylamido 2-methyl propane sulfonic acid monomer.

TDS Total dissolved solids.

REFERENCES

- Almahfood, M. and Bai, B., 'The synergistic effects of nanoparticle-surfactant nanofluids in eor applications,' Journal of Petroleum Science and Engineering, 2018, **171**, pp. 196–210.

- Almahfood, M. and Bai, B., 'Characterization and oil recovery enhancement by a polymeric nanogel combined with surfactant for sandstone reservoirs,' submitted to Journal of Petroleum Science, 2020a.
- Almahfood, M. and Bai, B., 'Experimental evaluation of polymeric nanogel combined with surfactant and low salinity water flooding for carbonate reservoirs,' Submitted to Journal of Petroleum Science and Engineering, 2020b.
- Almahfood, M. and Bai, B., 'Potential oil recovery enhancement by a polymeric nanogel combined with surfactant for sandstone reservoirs,' in 'OTC 2020,' Offshore Technology Conference, 2020c .
- Ayatollahi, S., Zerafat, M. M., *et al.*, 'Nanotechnology-assisted eor techniques: New solutions to old challenges,' in 'SPE international oilfield nanotechnology conference and exhibition,' Society of Petroleum Engineers, 2012 .
- Bolandtaba, S. F., Skauge, A., and Mackay, E., 'Pore scale modelling of linked polymer solution (lps)–a new eor process,' in 'IOR 2009-15th European Symposium on Improved Oil Recovery,' European Association of Geoscientists & Engineers, 2009 pp. cp–124.
- Gao, C., 'Factors affecting particle retention in porous media,' Emirates Journal for Engineering Research, 2007, **12**(3), pp. 1–7.
- Karimi, A., Fakhroueian, Z., Bahramian, A., Pour Khiabani, N., Darabad, J. B., Azin, R., and Arya, S., 'Wettability alteration in carbonates using zirconium oxide nanofluids: Eor implications,' Energy & Fuels, 2012, **26**(2), pp. 1028–1036.
- Lenchenkov, N. S., Slob, M., van Dalen, E., Glasbergen, G., van Kruijsdijk, C., *et al.*, 'Oil recovery from outcrop cores with polymeric nano-spheres,' in 'SPE Improved Oil Recovery Conference,' Society of Petroleum Engineers, 2016 .
- Ma, H., Luo, M., and Dai, L. L., 'Influences of surfactant and nanoparticle assembly on effective interfacial tensions,' Physical Chemistry Chemical Physics, 2008, **10**(16), pp. 2207–2213.
- Mohajeri, M., Hemmati, M., and Shekarabi, A. S., 'An experimental study on using a nanosurfactant in an eor process of heavy oil in a fractured micromodel,' Journal of petroleum Science and engineering, 2015, **126**, pp. 162–173.
- Nasralla, R. A., Bataweel, M. A., Nasr-El-Din, H. A., *et al.*, 'Investigation of wettability alteration and oil-recovery improvement by low-salinity water in sandstone rock,' Journal of Canadian Petroleum Technology, 2013, **52**(02), pp. 144–154.
- Qiu, F. *et al.*, 'The potential applications in heavy oil eor with the nanoparticle and surfactant stabilized solvent-based emulsion,' in 'Canadian unconventional resources and international petroleum conference,' Society of Petroleum Engineers, 2010 .

- Suleimanov, B., Ismailov, F., and Veliyev, E., 'Nanofluid for enhanced oil recovery,' *Journal of Petroleum Science and Engineering*, 2011, **78**(2), pp. 431–437.
- Wu, Y., Chen, W., Dai, C., Huang, Y., Li, H., Zhao, M., He, L., and Jiao, B., 'Reducing surfactant adsorption on rock by silica nanoparticles for enhanced oil recovery,' *Journal of Petroleum Science and Engineering*, 2017, **153**, pp. 283–287.
- Yousef, A. A., Al-Saleh, S. H., Al-Kaabi, A., Al-Jawfi, M. S., *et al.*, 'Laboratory investigation of the impact of injection-water salinity and ionic content on oil recovery from carbonate reservoirs,' *SPE Reservoir Evaluation & Engineering*, 2011, **14**(05), pp. 578–593.

IV. EXPERIMENTAL EVALUATION OF POLYMERIC NANOGEL COMBINED WITH SURFACTANT AND LOW SALINITY WATER FLOODING FOR CARBONATE RESERVOIRS

Mustafa M. Almahfood, Author ^{a, b}

Baojun Bai, Co-Author ^a

^aDepartment of Geosciences & Petroleum Engineering

Missouri University of Science and Technology

Rolla, Missouri 65409

^b EXPEC Advanced Research Center, Saudi Aramco, Saudi Arabia

Email: mmantc@mst.edu

ABSTRACT

A laboratory investigation of polymeric nanogel combined with sodium dodecyl sulfate (SDS) surfactant and several salinities of water flooding as a potential enhanced oil recovery method for carbonate reservoirs is described herein. This paper investigates the impact of nanogel combined with SDS on improved oil recovery, and the effect of salinity and modified ion content of injected water on oil-brine-rock interactions. Also, it provides a laboratory investigation of the injectivity and plugging performance induced by nanogel flooding through carbonate cores. A newly developed polymeric crosslinkable nanogel is prepared using suspension polymerization process by employing 2-Acrylamido 2-methyl propane sulfonic acid monomer. The resultant nanogel displays good structural stability in different brine salinities with a narrow size distribution of one peak pointing to a predominant homogeneous droplet size. The core flooding results revealed that substantial oil recovery, up to 27%, beyond conventional seawater flooding can be obtained by nanogel

combined with SDS injections and assisted with altering salinity and ionic content of water injections. The resistance factor of nanogel in carbonate cores significantly increased with injection volume. The stabilized residual resistance factor for brine injections increased with lower brine salinities from 5.62 to 7.05. The results also showed that SDS can reduce the adsorption density of nanogel from rock surfaces effectively.

Keywords: nanogel, polymeric nanogel, surfactant-based-nanogel, enhanced oil recovery, low salinity waterflooding, modified ionic composition

1. INTRODUCTION

A significant portion of oil reserves (approximately 60% of the world's proven oil reserves) is trapped in carbonate reservoirs (limestone, dolomite, and chalks), with a huge portion located in the Middle East; which comprise 75% of oil and 90% of gas reserves for this region (Akbar *et al.*, 2000). Carbonates are type of sedimentary rocks formed of minerals; predominantly calcite and dolomite (Akbar *et al.*, 2000). It is possible for carbonates to undergo dissolution and recrystallization by varying the temperature, pressure or pore fluid chemistry (Baker *et al.*, 1980). The minimal information with regards to the petrophysical properties of carbonate reservoirs including porosity, permeability and heterogeneity, is probably one of the major challenges that faces the oil industry today to manage such reservoirs and enhance their oil recovery factor (Bust *et al.*, 2011).

Nowadays, nanoparticles are widely employed to improve the overall performance of chemical and physical processes in many fields including the oil industry. Materials having a dimension of 1-100 nm are called "nanoparticles" (Das *et al.*, 2007). Previous studies proposed enhanced features of nanoparticles including their ability to modify the wetting behavior of reservoir rocks, the rheological properties of drilling fluids and their high surface to volume ratio (Almahfood and Bai, 2018; Ayatollahi *et al.*, 2012; Li *et al.*, 2016; Pourafshary *et al.*, 2009; Zhang *et al.*, 2010). Structural disjoining pressure is one of the main recovery mechanisms of nanoparticle-assisted flooding (Chengara *et al.*, 2004;

Wasan and Nikolov, 2003). This mechanism is explained as the energy existing between nanoparticles that leads to Brownian motion and electrostatic repulsion (Chengara *et al.*, 2004). The electrostatic repulsion and Brownian motion increase as nanoparticle size becomes smaller (Mcelfresh *et al.*, 2012). In order to regain the equilibrium of the system caused by disjoining pressure and electrostatic repulsion, some of the properties including IFT and wettability are modified which lead to extra oil recovery (Almahfood and Bai, 2018).

Nanosized cross-linked polymeric particles known as nanogels are newly developed particles in EOR applications. They are known for their easy injection process due to their small size (1-100 nm), which is much smaller than the diameter of the pore throats in oil reservoirs (Qiu *et al.*, 2010). They are also characterized by low viscosity, especially at low concentrations (Almahfood and Bai, 2020b; Moraes *et al.*, 2011). Also, nanogels can reduce the interfacial tension by adsorbing at the oil-water interface, which stabilizes oil-in-water emulsions, leading to improvement of the recovered oil from reservoirs (Almahfood *et al.*, 2020; Geng *et al.*, 2018). They are able to mobilize residual oil, which enhances oil recovery by mainly reducing the interfacial tension (Almahfood and Bai, 2020a,b; Lenchenkov *et al.*, 2016). In addition, surfactant flooding aims at reducing the interfacial tension between oil and water and mobilizing the residual oil (Green *et al.*, 1998; Johannessen and Spildo, 2013). Austad *et al.* (1997); Standnes and Austad (2000, 2003) have conducted a series of studies on oil recovery from carbonate cores and shown that surfactant solutions can enhance the oil recovery to 70% OOIP. Recently, the combination between nanosized particles and surfactants have attracted a great deal of attention by many researchers (Karimi *et al.*, 2012; Ma *et al.*, 2008; Mohajeri *et al.*, 2015; Wu *et al.*, 2017). Suleimanov *et al.* (2011) have shown that the usage of nanoparticles combined with anionic surfactant permitted a great reduction of surface tension. Moreover, it has been revealed that the usage of nanoparticles with an anionic surfactant has a major impact on increasing the ultimate oil recovery (Giraldo *et al.*,

2013). Karimi *et al.* (2012) have studied the effect of nanosized particles combined with several surfactants on carbonate reservoir rocks and reported that the combination has a strong capability for oil recovery enhancement.

During the secondary oil recovery mechanism, waterflooding is generally employed to support reservoir pressure above the bubble point pressure, improve the sweep efficiency, and displace additional oil (Lake, 1989; Thomas, 2008). During the early 1960s, Martin *et al.* (1959) and Reiter (1961) have shown that altering the brine composition or reducing the brine salinity below that of the initial formation water can lead to additional oil recovery from Berea sandstone reservoirs. These results did not attract additional investigation until the early 1990s when multiple researchers studied and evaluated the low salinity waterflooding as potential EOR method (Jadhunandan and Morrow, 1991; Jadhunandan *et al.*, 1995; Tang *et al.*, 1997; Tang and Morrow, 1999; Yildiz and Morrow, 1996). Since then there has been a continuous interest from oil companies and research centers in low salinity waterflooding for improved oil recovery (Ligthelm *et al.*, 2009; Mahani *et al.*, 2011; Nasralla *et al.*, 2016; Soraya *et al.*, 2009; Vledder *et al.*, 2010). Low salinity waterflooding, which is also known in the literature as smart waterflooding, designer waterflood, and ion tuned waterflood, injects brines with controlled ionic composition and concentration (Gupta *et al.*, 2011; Ligthelm *et al.*, 2009). The revised brine formulations destabilize the equilibrium of the initial oil-brine-rock system, which results in altering the wettability condition and improving the capillary pressure (Sheng, 2013). During low salinity waterflooding, no expensive chemicals are added, which makes this method cheap and environmentally friendly. Compared to conventional waterflooding, low salinity waterflooding can extract additional 10% of original oil in place (Kokal and Al-Kaabi, 2010). A number of studies in the literature shows that the wetting condition of carbonate reservoirs can be altered by increasing the concentration of the divalent anions such as SO_4^{2-} , decreasing the concentration of the divalent cations such as Ca^{2+} and Mg^{2+} , or decreasing the salinity of the employed brine, resulting in improved oil recovery by both spontaneous imbibition and forced displacement

(Austad *et al.*, 2011; Fathi *et al.*, 2011; RezaeiDoust *et al.*, 2009). Several recovery mechanisms have been suggested to explain low salinity waterflooding in carbonate reservoirs. The primary mechanisms are rock dissolution, fines migration, interfacial tension reduction, fluid-fluid interactions, ionic exchange and expansion of double layer (Afekare and Radonjic, 2017; Myint and Firoozabadi, 2015; Purswani *et al.*, 2017; Tetteh *et al.*, 2017; Tian and Wang, 2017; Yi *et al.*, 2012).

In general, a cost effective EOR method has high potential when both displacement and sweep efficiency are improved. The displacement efficiency can be improved by low salinity water and sulfate-enriched seawater flooding, while the sweep efficiency can be improved by nanogel and surfactant flooding. The aim of this study is to examine the performance of low salinity water (diluted seawater) and sulfate-enriched seawater flooding for enhanced oil recovery improved by polymeric nanogel coupled with surfactant. The paper firstly presents the size distribution of the synthesized nanogel in several brine salinities. Next, the paper provides a laboratory core flooding evaluation conducted using carbonate rock samples to investigate the impact of nanogel combined with surfactant and several brine salinities on oil recovery. Afterwards, the paper provides adsorption and desorption study of nanogel in carbonate cores to evaluate nanogel-brine-rock interactions. Lastly, the degree of plugging performance induced by nanogel flooding is studied.

2. EXPERIMENT

2.1. MATERIALS

Na-AMPS nanogel was synthesized in our laboratory. 2-Acrylamido 2-methyl propane sulfonic acid monomer (99%), sodium dodecyl sulfate (SDS, > 99%, CMC = 2400 mg/l), Tween[®] 60 (CMC = 27 mg/l), N,N'-methylene bis(acrylamide) (MBAA, 99%), and sodium bicarbonate ($NaHCO_3$, $\geq 99.7\%$) were purchased from Sigma-Aldrich. Sorbitan monooleate (Span[®] 80), sodium hydroxide (NaOH, 97%), sodium chloride (NaCl, 99%),

calcium chloride ($CaCl_2$, powder, 97%), magnesium chloride ($MgCl_2$, 99%), and n-Decane were purchased from Alfa Aesar. Ammonium persulfate ($\geq 98\%$), and sodium sulfate (Na_2SO_4 , $\geq 99\%$) were purchased from Acros Organics. All chemicals were of reagent grade and used as received without further purification.

2.2. NANOGEL SYNTHESIS

Na-AMPS nanogel was prepared by a typical suspension polymerization process. The preparation process could be summarized as follows: NaOH is added to a stirred solution of 15 grams of 2-Acrylamido 2-methyl propane sulfonic acid (AMPS) and 15 grams of deionized water at room temperature until the pH reaches exactly 7.0. Then, 0.1 gram of N,N'-methylene bis(acrylamide) (MBAA) is added to the solution while stirring. The solution is then added to n-decane (40 ml) containing Span[®] 80 (21 g) and Tween[®] 60 (9 g) in a three-neck flask and bubbled with nitrogen while kept in a water bath at 40° C for 15 minutes. After that, 0.2 ml of ammonium persulfate is added to the flask as an initiator. Stirring in the water bath is continued for 2 hours at 40° C. Then, the emulsion is precipitated and washed with acetone and separated by centrifugation. The process of washing the emulsion with acetone is repeated several times to ensure that all surfactants and unreacted monomers are washed out. The final isolated product is dried in the oven at 65° C for 24 hours. Figure 1 shows samples of the dried and dispersed Na-AMPS nanogel.

2.3. BRINE

Different brines were used in this study, including formation water and seawater that simulate the salinity in Saudi Arabia, and different diluted versions of seawater. Additionally, two versions of sulfate-enriched seawater (approximately 62,000 and 66,000 ppm) were also employed. All brines were prepared from deionized water and reagent grade chemicals on the basis of a geochemical analysis of field water samples reported by Yousef

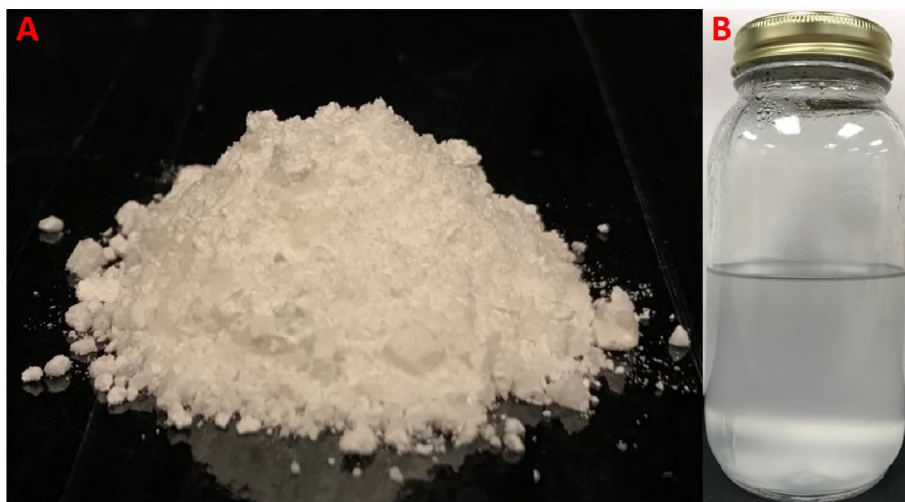


Figure 1. (A) Dried Na-AMPS nanogel. (B) Na-AMPS nanogel dispersed in seawater.

et al. (2011). The employed seawater had a salinity of approximately 57,600 ppm by weight, while formation water had a salinity of 213,000 ppm. Other dilute versions of seawater were prepared by mixing seawater with different volumes of deionized water, including 10-times diluted (approximately 6000 ppm), and 100-times diluted (approximately 600 ppm). Table 1 depicts the composition for each employed brine. The effect of salinity on physical properties of the prepared brine types was studied. The density and viscosity properties were measured at an average room temperature of 25° C. Table 2 lists the density and viscosity of the different brine types employed in the experiments.

2.4. CRUDE OIL

Light crude oil from a Saudi Arabian oil field with a viscosity of 11.5 cp at room temperature (density = 0.84 g/cc, API 36°) was employed in all experiments.

2.5. CARBONATE ROCK

Outcrop Indiana Limestone cores were employed in all core flooding experiments. Core plugs with 2-inch in diameter and 4-inch in length were cut from a whole block. Calcium carbonate is the primarily composition of the cores. Tables 3 and 4 summarize the petrophysical properties of each core plug.

Table 1. Composition of all employed brine types with different salinities.

Ion	Formation and Seawater Compositions ^a		Modified Seawater		Low Salinity Water	
	Formation Water g/L	Seawater g/L	2*SO ₄ ²⁻ g/L	3*SO ₄ ²⁻ g/L	10 Times	100 Times
					Diluted Seawater g/L	Diluted Seawater g/L
Sodium	59,491	18,300	18,300	18,300	1,830	183
Calcium	19,040	650	650	650	65	6.5
Magnesium	2,439	2,110	2,110	2,110	211	21.1
Sulfate	350	4,290	8,580	12,870	429	42.9
Chloride	132,060	32,200	32,200	32,200	3,220	322
Bicarbonate	354	120	120	120	12	1.2
TDS, ppm	213,734	57,670	61,960	66,250	5,767	576.7
Ionic Strength, mol/L	4.31	1.15	1.24	1.33	0.12	0.012

^aYousef *et al.* (2011)

Table 2. Density and viscosity of different brine types at room temperature of 25° C.

Property	Formation Water	Seawater	10-Times Diluted Seawater	100-Times Diluted Seawater	2*SO₄²⁻	3*SO₄²⁻
Density (g/cm³)	1.137	1.040	1.001	0.997	1.043	1.047
Viscosity (cp)	1.331	1.012	0.901	0.893	1.023	1.034

2.6. NANOGEL SIZE DISTRIBUTION AND ZETA POTENTIAL

A nanosizer (Nano ZS, Malvern Instruments, UK) equipped with helium-neon laser (633 nm) was employed to determine the size distribution and obtain the zeta potential values of nanogel dispersions in different water types. Dynamic light scattering (DLS) was used to measure the hydrodynamic radius of nanogel particles in the dispersing fluid. All measurements were taken at an average room temperature of 25° C and at a scattering angle of 90°.

2.7. RHEOLOGICAL PROPERTIES

Brookfield DV3T rheometer was employed to measure the rheological properties of several brine types with different salinities at 25° C.

2.8. CORE FLOODING EXPERIMENTAL SETUP AND PROCEDURE

Core plugs were mounted in a Hassler type core holder that is designed for cores with 2 inches in diameter and up to 1 ft in length. A schematic of the core flooding apparatus is shown in Figure 2. Experimental procedure is summarized below.

1. The core plugs are cleaned with distilled water.

2. The Core plugs are placed in an oven to dry at 125 ° C for 3 days.
3. The cores are vacuumed for 24 hours and saturated with formation water.
4. Porosity and pore volumes are measured by the weight difference and the density of the saturated brine at room temperature.
5. Core plugs are placed into a Hassler type core holder and confined with a pressure of 1500 psi using a Teledyne ISCO model 500D syringe pump.
6. Absolute permeability is determined by injecting water at different flow rates.
7. Crude oil is injected to simulate irreducible water saturation (S_{wi}) and initial oil saturation (S_{oi}).
8. Seawater flooding is conducted as initial waterflooding process at a flow rate of 0.5 $\frac{ml}{min}$ until no more oil is produced and pressure profile stabilizes.
9. Nanogel and SDS, dispersed in seawater, are injected using different injection schemes and concentrations at a flow rate of 0.5 $\frac{ml}{min}$.
10. Two scenarios of post waterflooding are conducted. Seawater and diluted versions of seawater are injected in the first scenario. For the second scenario, seawater and sulfate-enriched versions of seawater are injected. All brines are injected at a flow rate of 0.5 $\frac{ml}{min}$.

The effluent samples that flowed through the core plugs were collected using measuring test tubes. Oil recovery was calculated using the amount of extracted oil from original-oil-in-place. A pressure transducer was installed at the inlet of the core holder to monitor the injection pressure. All core flooding experiments were conducted at an average room temperature of 25° C.

Table 3. Petrophysical properties of core plugs employed in core flooding experiments.

Core ID	Length (cm)	Diameter (cm)	Porosity (%)	Pore Volume (cm ³)	Average Permeability (md)	Swi (%)	Soi (%)
C-1	10.048	5.08	15.56	31.71	3.46	32.05	67.95
C-2	10.168	5.08	15.57	32.08	5.69	31.40	68.60
C-3	10.033	5.08	15.61	31.75	4.58	32.52	67.48
C-4	10.211	5.08	15.90	32.92	8.78	30.57	69.43
C-5	10.046	5.08	16.07	32.74	7.45	28.87	71.13
C-6	10.046	5.08	15.78	32.14	3.43	32.44	67.56
C-7	10.094	5.08	15.39	31.48	1.96	35.67	64.33
C-8	10.155	5.08	15.65	32.20	3.05	35.56	64.44
C-9	10.008	5.08	15.58	31.61	2.57	29.89	70.11
C-10	9.693	5.08	15.69	30.83	2.94	29.99	70.01

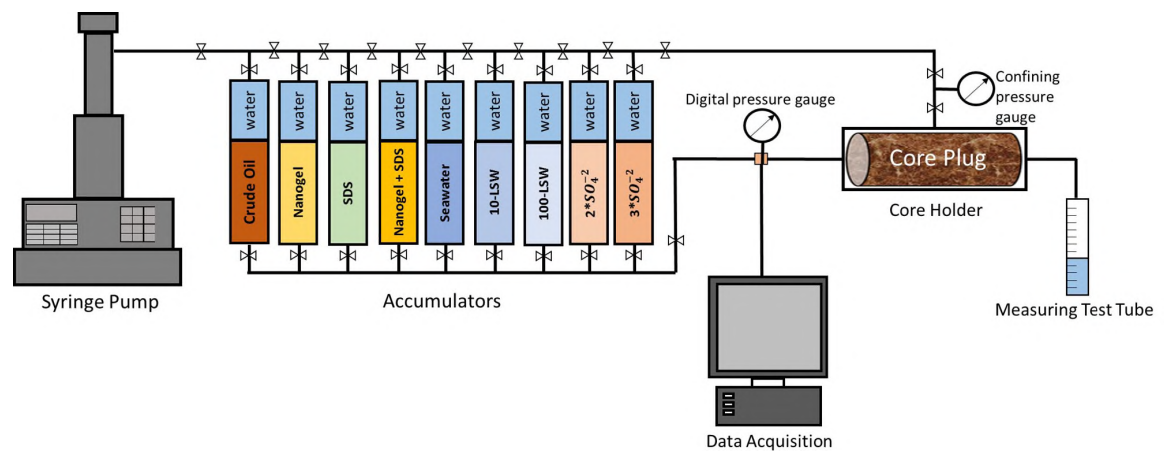


Figure 2. Schematic of the experimental setup.

2.9. NANOGEL DYNAMIC ADSORPTION AND DESORPTION MEASUREMENTS

A carbonate core (C-11) saturated with formation water was used to perform dynamic adsorption measurements. A $1,000 \frac{\text{mg}}{\text{L}}$ nanogel dispersion was injected through the core. The concentration of nanogel dispersion was measured using Shimadzu UV-mini-1240 UV-vis spectrophotometer as a function of pore-volume injection with appropriate mixtures of formation water as a reference. The nanogel dispersion was diluted by formation water to a concentration that fell in the linear range of Lambert-Beer Law (equation 1), as shown by the calibration curve (Figure 3).

$$A = \varepsilon cL \quad (1)$$

Where A is the absorbance, ε is the molar absorption coefficient, c is the concentration of the dispersion, and L is the length of the light path. When the concentration of the nanogel in the effluent reached the original concentration, formation water was injected through the core to evaluate the desorption density. Petrophysical properties of the core plug used to evaluate the adsorption and desorption densities are listed in Table 4.

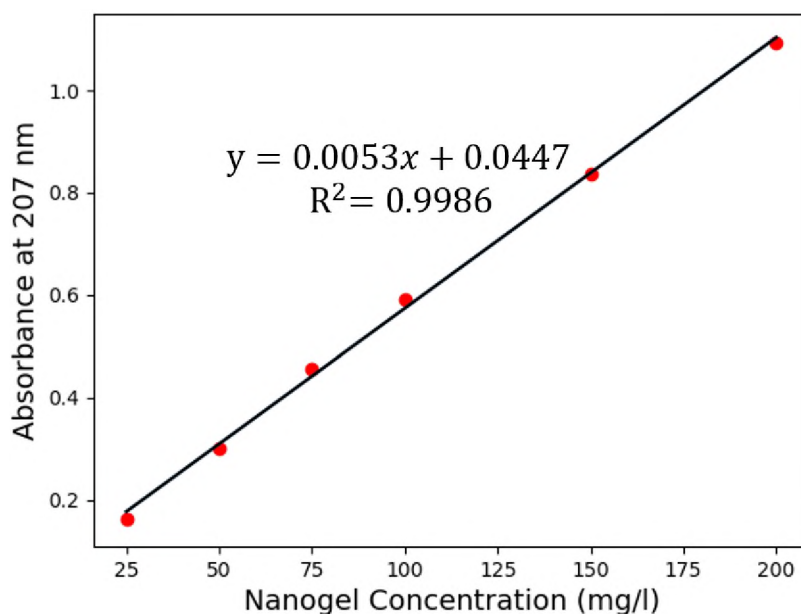


Figure 3. Calibration curve of nanogel standards at the peak wavelength of 207 nm.

Table 4. Petrophysical properties of core plugs employed for dynamic adsorption-desorption measurements and injectivity evaluation.

Core ID	Purpose	Length (cm)	Diameter (cm)	Porosity (%)	Pore Volume (cm ³)	Average Permeability (md)
C-11	Adsorption-desorption	9.924	5.08	15.44	31.05	5.19
C-12	Plugging performance	10.036	5.08	15.65	31.82	7.95

2.10. INJECTIVITY AND PLUGGING PERFORMANCE OF NANOGEL ON CARBONATE CORES

Resistance factor and residual resistance factor are two terms used to evaluate the injectivity and plugging efficiency of gel treatments. Resistance factor (F_r or RF) is calculated as the ratio between water mobility (λ_w) and nanogel mobility (λ_{ng}). In other words, it is the ratio of pressure drop across the core caused by the injection of nanogel dispersion (ΔP_{ng}) to the pressure drop caused by the brine injection (ΔP_w) at the same flow rate (equation 2). Residual resistance factor to water (F_{rrw} or RRF) is the ratio between water mobility before and after nanogel treatment (equation 3).

$$F_r = \frac{\lambda_w}{\lambda_{ng}} = \frac{\Delta P_{ng}}{\Delta P_w} \quad (2)$$

$$F_{rrw} = \frac{(\lambda_w)_{Before}}{(\lambda_w)_{After}} = \frac{(\Delta P_w)_{After}}{(\Delta P_w)_{Before}} \quad (3)$$

In this work, resistance factor, calculated at the end of nanogel or SDS injection volume, and stabilized brine residual resistance factor for cores employed in core flooding experiments (Table 3) are calculated. For further investigation, C-12 core plug initially saturated with formation water was employed to evaluate the injectivity and plugging per-

formance of extended nanogel flooding. After simulating the core with initial oil saturation, seawater was injected until the injection pressure reached a stable state. Then, nanogel was injected for several injection-volumes to evaluate its injectivity. Lastly, seawater was injected again until pressure profile stabilizes to examine the plugging performance.

3. RESULTS AND DISCUSSION

3.1. SIZE DISTRIBUTION OF NANOGEL

The characterization and physiochemical properties of the negatively charged nanogel such as surface ζ -potential, polydispersity index (PDI) and average particle size in several water types with different salinities are presented in Table 5. The results show the effect of water salinity on the particle size of nanogel. As shown in Figure 4, the average hydrodynamic diameter of nanogel in seawater is 222.5 nm. The particle size expands to 247 and 335 in 10-times diluted and 100-times diluted seawater, respectively. In addition, nanogel particle size responded to seawater with higher sulfate ratios by expanding and further swelling. The hydrodynamic diameters were 255 and 295 nm in 2-times and 3-times sulfate-enriched seawater, respectively. Figure 4 also illustrates that nanogel size distribution curves exhibited a mono-modal distribution, with one peak pointing to a predominant homogeneous droplet size. To assess the long-term stability of the nanogel in different brine salinities, particle size distribution was measured as a function of time for a period of 15 days. Nanogel dispersions showed good long-term stability during the period of two weeks by well-maintaining the structural particle size, as presented in Figure 5.

Table 5. Physiochemical properties of different nanogel dispersions in several water types.

Water Type	Surface ζ -potential	Polydispersity	Average Particle
	(mV)	Index (PDI)	Size (nm)
Seawater	- 30.8	0.215	222
10-DSW	- 39.4	0.273	247
100-DSW	- 56.4	0.443	335
2* SO_4^{2-}	- 17.6	0.287	255
3* SO_4^{2-}	- 18.5	0.342	295

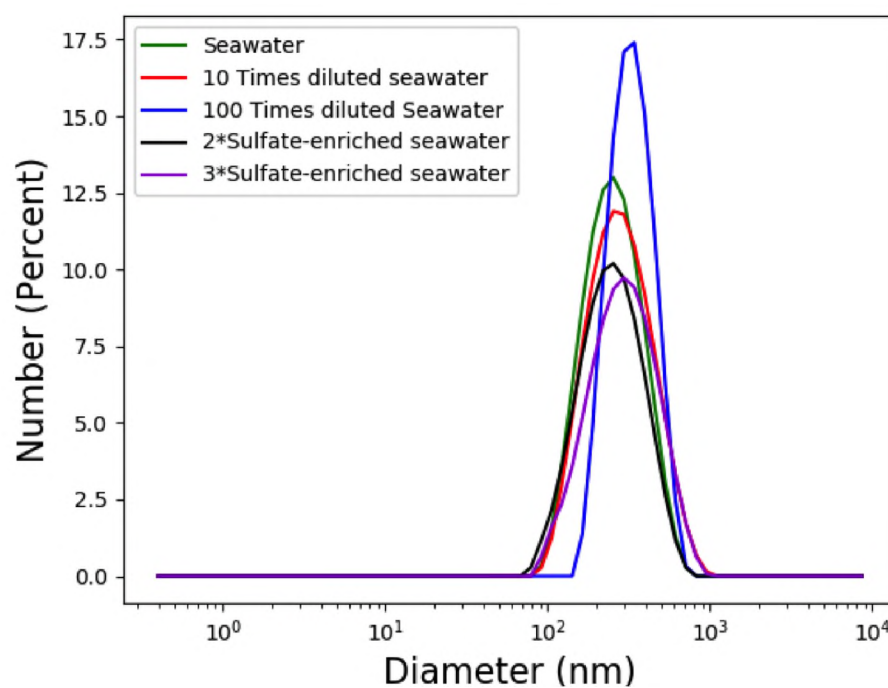


Figure 4. Particle size distribution of nanogel dispersed in several brine types at a concentration of 1 gram/liter and a temperature of 25° C.

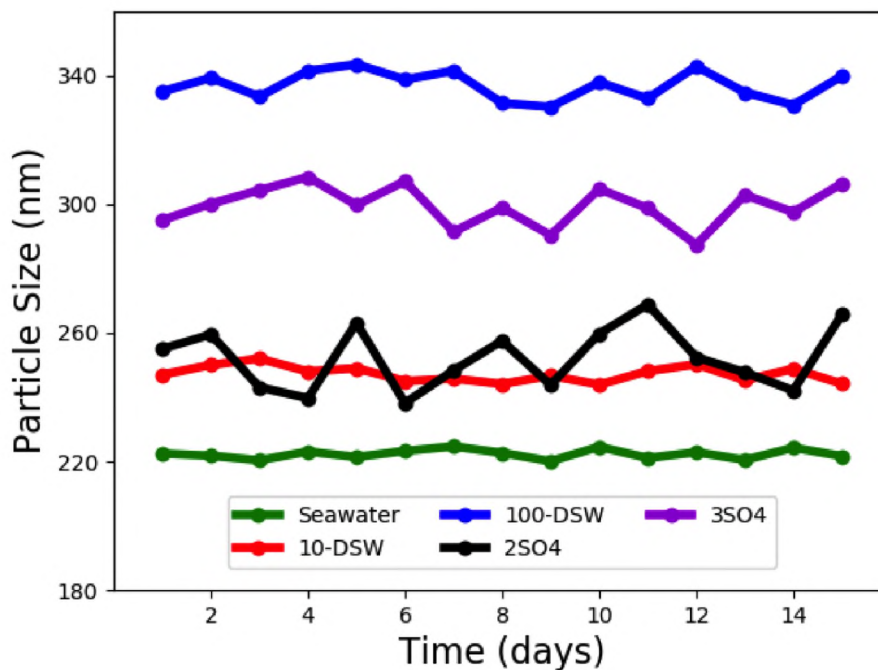


Figure 5. Nanogel stability evaluation in different water types for a two-week time period.

3.2. CONFIRMATION OF ENHANCED OIL RECOVERY BY CORE FLOODING

In core flooding experiments, seawater was injected to simulate the initial water flooding in all experiments. Next, separate and combined/one-slug injections of nanogel and SDS dispersions were injected. Then, three different salinity slugs of seawater were injected one after another in the first scenario, starting with regular seawater and ending with 100-times diluted seawater. In the second scenario, three different salinity slugs of seawater and sulfate-enriched seawater were injected one after another, starting with seawater and ending with 3-times sulfate-enriched seawater. Table 6 summarizes the injection schedules and tested parameters for all core flooding experiments.

Table 6. Injection schedules for core plugs employed in core flooding experiments.

Core ID	Injection Mode	Purpose	Injection Schedules					
			1	2	3	4	5	6
C-1	Base case	LSW	SW	10-DSW	100-DSW	-	-	-
C-2	Base case	SO_4^{2-}	SW	$2*SO_4^{2-}$	$3*SO_4^{2-}$	-	-	-
C-3	Sequential	LSW, NG	SW	NG	SW	10-DSW	100-DSW	-
C-4	Sequential	SO_4^{2-} , NG	SW	NG	SW	$2*SO_4^{2-}$	$3*SO_4^{2-}$	-
C-5	Sequential	LSW, SDS	SW	NG	SDS	SW	10-DSW	100-DSW
C-6	Sequential	SO_4^{2-} , SDS	SW	NG	SDS	SW	$2*SO_4^{2-}$	$3*SO_4^{2-}$
C-7	Sequential	LSW, Concentration	SW	$2*NG$	$2*SDS$	SW	10-DSW	100-DSW
C-8	Sequential	SO_4^{2-} , Concentration	SW	$2*NG$	$2*SDS$	SW	$2*SO_4^{2-}$	$3*SO_4^{2-}$
C-9	One-slug	LSW	SW	NG+SDS	SW	10-DSW	100-DSW	-
C-10	One-slug	SO_4^{2-}	SW	NG+SDS	SW	$2*SO_4^{2-}$	$3*SO_4^{2-}$	-

3.2.1. Base Cases. Core plugs C-1 and C-2 were employed to evaluate the effect of low salinity water and sulfate-enriched seawater on enhancing the oil recovery. The cumulative oil recovery by regular seawater with salinity of 57,670 ppm was approximately 54.55%. This injection slug targets mobile oil in the core plug and represents the secondary oil recovery. The oil was recovered during the first 1.5 pore volumes of seawater injected. The injection of seawater was continued until there was no more oil produced and injection pressure reached a stable state to ensure that all mobile oil was recovered. The injection of 10-times diluted seawater with a salinity of 5,767 ppm was followed (Core C-1) until no more oil was produced and pressure stabilized. A substantial increment of oil was recovered, equivalent to 4.55% beyond conventional seawater flooding. This was followed by injecting 100-times diluted seawater with a salinity of 576.7 ppm. Even with this diluted seawater slug, an incremental oil recovery of 3.03% was obtained, as illustrated in Figure 6. Therefore, the total incremental oil recovery beyond conventional seawater flooding was

approximately 7.5%. In addition, the injection of low salinity seawater slugs caused a slight decrease in injection pressure, as shown in Figure 7. The slight pressure reduction might be caused by the reduction of residual oil saturation due to low salinity water flooding.

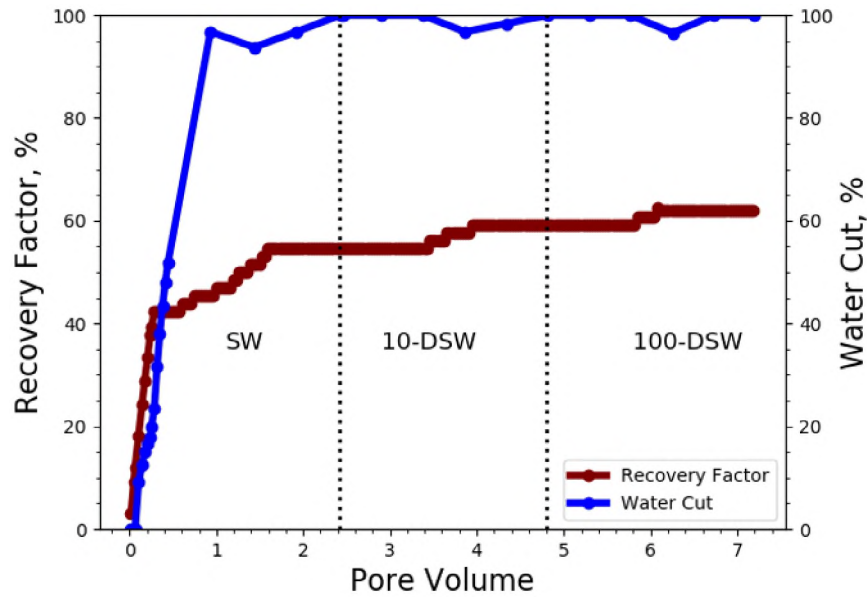


Figure 6. Oil recovery factor and water cut of core C-1.

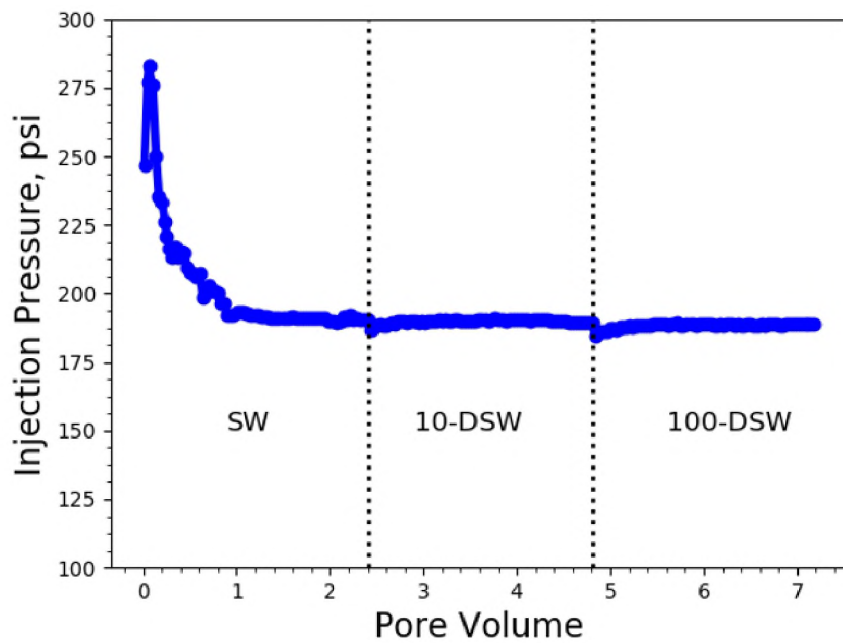


Figure 7. Injection pressure profile of core C-1.

Another core flooding experiment was conducted to evaluate the effect of sulfate-enriched seawater (core C-2). The cumulative oil recovery by regular seawater was approximately 53.23% which represent the secondary oil recovery. The injection of 2-times sulfate-enriched seawater with a salinity of approximately 61,900 ppm was followed until no more oil was recovered and pressure reached a stable state. The incremental oil recovery was equivalent to 3.23% beyond conventional seawater flooding. This was followed by the injection of 3-times sulfate-enriched seawater with a salinity of approximately 66,000 ppm. This injection slug recovered an incremental oil of 1.61%. As a result, the total incremental oil recovery beyond conventional seawater flooding was approximately 4.84%, as shown in Figure 8. The trend of injection pressure was consistent with low salinity seawater flooding experiment (core C-1), where a slight decrease was observed as the sulfate enrichment factor increased, as illustrated in Figure 9.

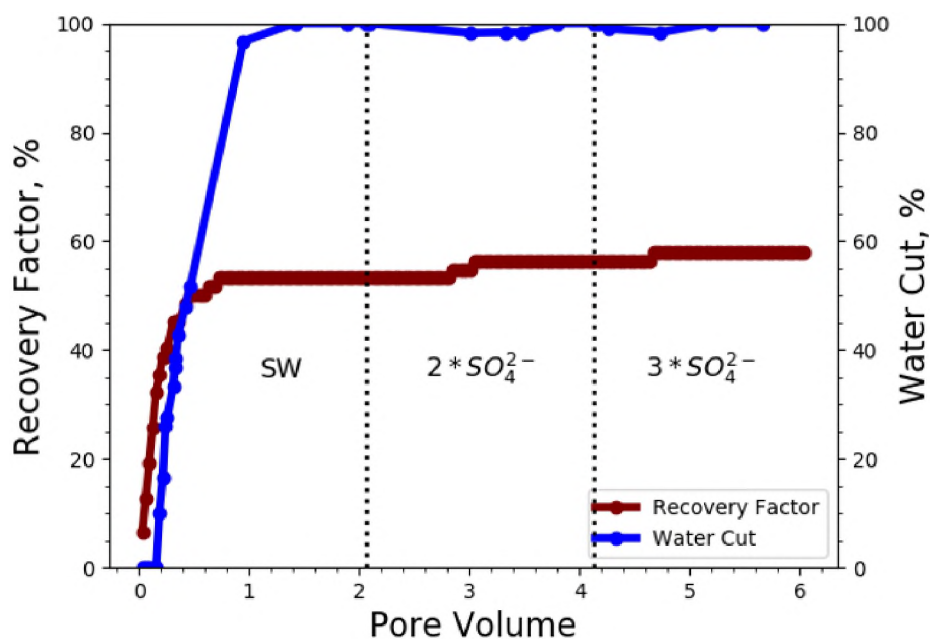


Figure 8. Oil recovery factor and water cut of core C-2.

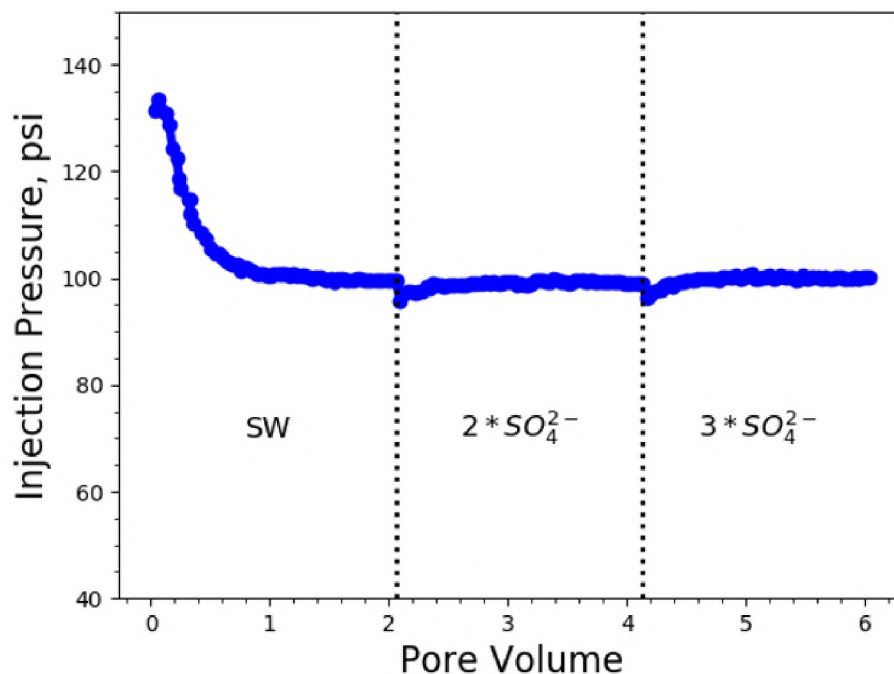


Figure 9. Injection pressure profile of Core C-2.

3.2.2. Validation of Nanogel Potential. Another core flooding experiment was conducted to validate the potential of the nanogel coupled with different diluted versions of seawater (C-3). As shown in Figure 10, the cumulative oil recovery of initial seawater slug was approximately 53.7% which represent the secondary recovery. This was followed by 1 injection-volume of nanogel (1,000 ppm). A substantial incremental of oil was produced equivalent to 5.56% beyond conventional seawater flooding. The injection of seawater as tertiary process was continued until no more oil was produced and injection pressure reached a stable state. With this injection slug, an incremental oil recovery of approximately 3.7% was obtained. Next, 10-times diluted seawater was injected, but no additional oil was recovered. Then, 100-times diluted seawater was injected, and an incremental oil of approximately 1.85% was recovered. Therefore, the total incremental oil recovery beyond the conventional seawater flooding was approximately 11.11% by nanogel coupled with stepwise reduction of salinity of seawater. Moreover, the most dominant effect in the injection pressure profile shown in Figure 11 is the major pressure increase induced by

nanogel injection due to its adsorption on rock surfaces. The injection pressure trend of water slugs following the nanogel injection shows an increasing behavior due to nanogel expansion phenomenon with lower salinity as illustrated earlier in Figure 4.

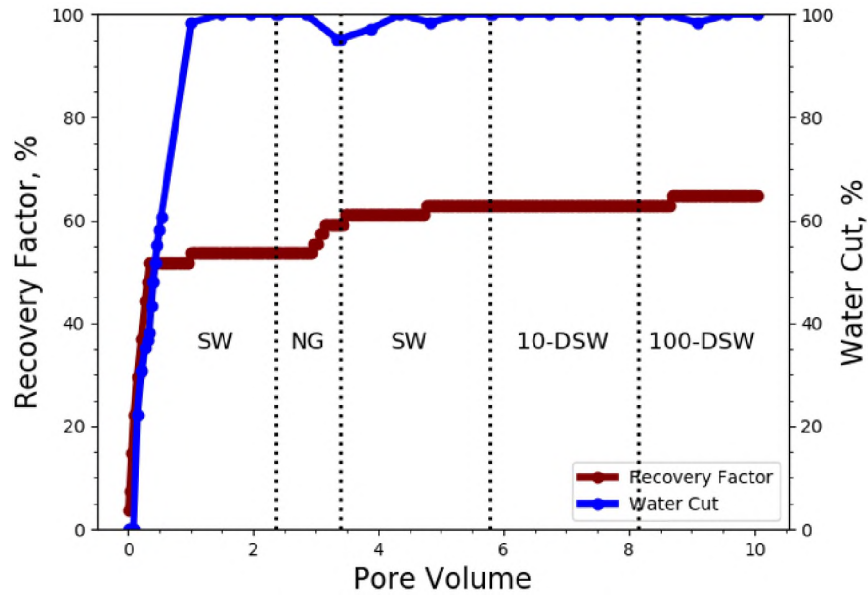


Figure 10. Oil recovery factor and water cut of Core C-3.

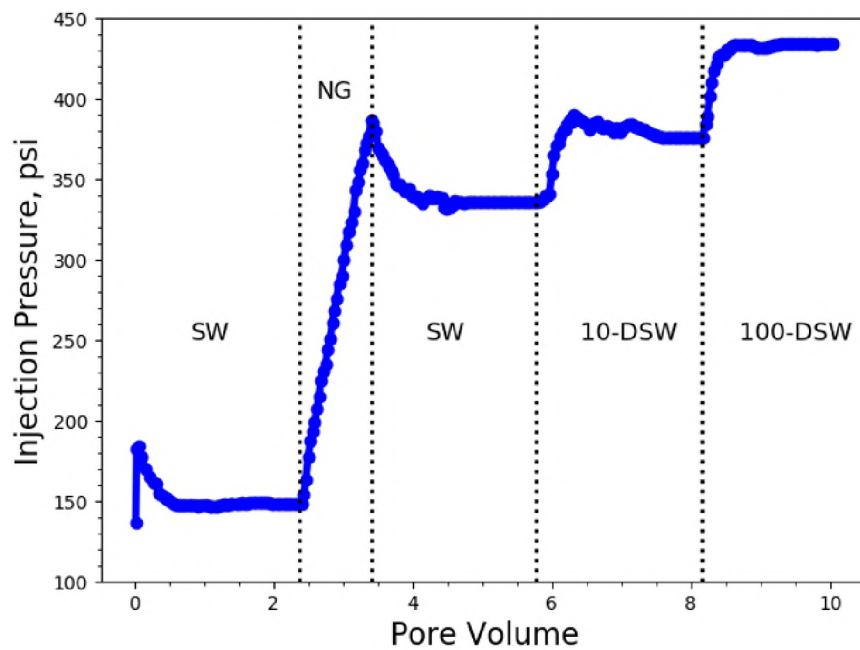


Figure 11. Injection pressure profile of Core C-3.

The effect of nanogel coupled with sulfate-enriched seawater was evaluated using core C-4. As shown in Figure 12, the cumulative oil recovery by regular seawater was approximately 55%. This was followed by 1 injection-volume of nanogel (1,000 ppm) where a significant incremental oil of approximately 5% was obtained. Next, regular seawater was injected until no more oil was produced. An incremental oil recovery of approximately 3.33% was recovered. The injection of 2-times sulfate-enriched seawater was followed until no more oil was recovered. An incremental oil of approximately 1.67% was produced. This was followed by injecting 3-times sulfate-enriched seawater which recovered an additional 1.70% oil. As a result, the total incremental oil recovery beyond the conventional seawater flooding was approximately 11.67% by nanogel and sulfate-enriched versions of seawater. Additionally, the trend of injection pressure profile was consistent with the previous coreflood experiment (C-3), as shown in Figure 13. However, the water slugs following nanogel injection showed lower increase which might be attributed to lower nanogel size when dispersed in sulfate-enriched seawater.

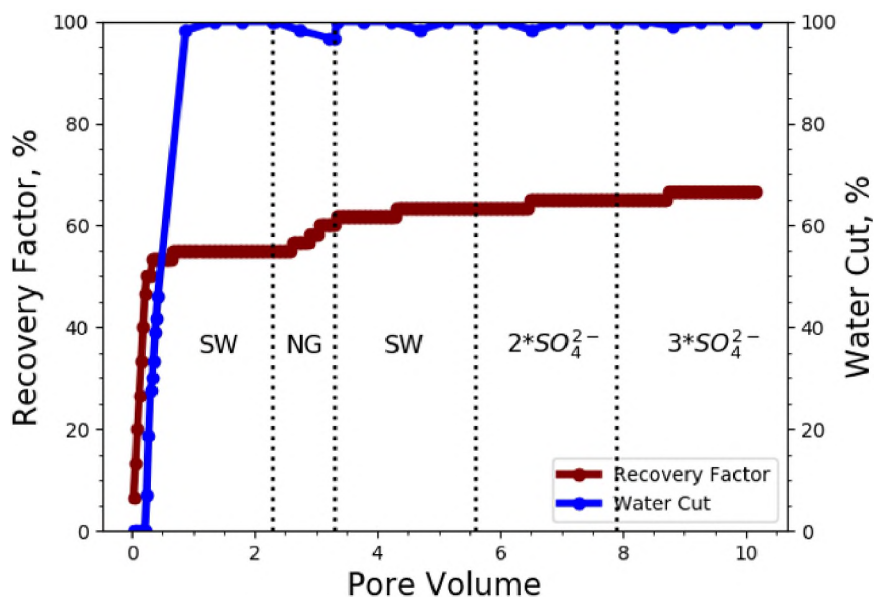


Figure 12. Oil recovery factor and water cut of Core C-4.

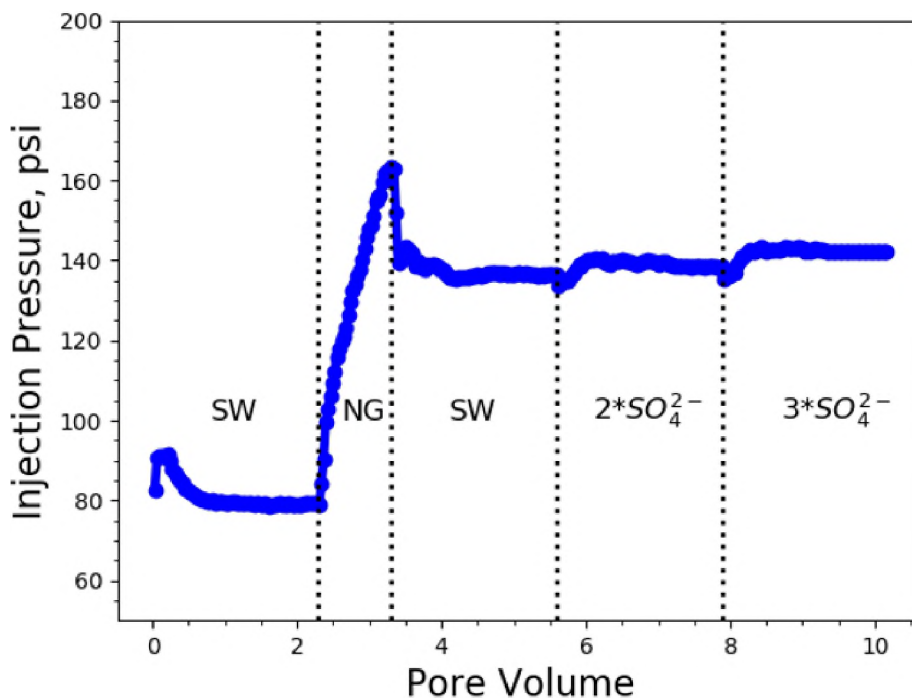


Figure 13. Injection pressure profile of Core C-4.

3.2.3. Validation of Nanogel Coupled with SDS Potential. Another core flooding experiment was conducted to study the potential of combining nanogel, SDS and different diluted versions of seawater (C-5). As illustrated in Figure 14, the cumulative oil recovery by regular seawater slug was approximately 56.25%. This was followed by 1 injection-volume of nanogel (1,000 ppm) where an incremental oil recovery of 4.69% was recovered. The injection of 1 injection-volume of SDS (1,000 ppm) was followed. A substantial incremental oil recovery equivalent to 9.38% beyond conventional seawater flooding was produced. Next, seawater was injected until no more oil was recovered and pressure stabilized. A significant incremental oil recovery of 7.81% was obtained. The injection of 10-times diluted seawater was followed where an additional oil of 3.13% was recovered. Next, 100-times diluted seawater was injected. A small increase in oil recovery of approximately 1.56% was observed. Therefore, the total incremental oil recovery, beyond conventional seawater flooding, was approximately 26.57% by nanogel, SDS and diluted versions of seawater. Furthermore, the trend of injection pressure profile is illustrated in Figure 15. The most

dominant effect in injection pressure profile is the major decrease induced by SDS injection which represents the ability of SDS to reduce the adsorption of nanogel in pore throats. Also, the water slugs following SDS injection showed a similar trend to the previous core flooding experiment (core C-3) where an increase in pressure was observed with lower water salinity.

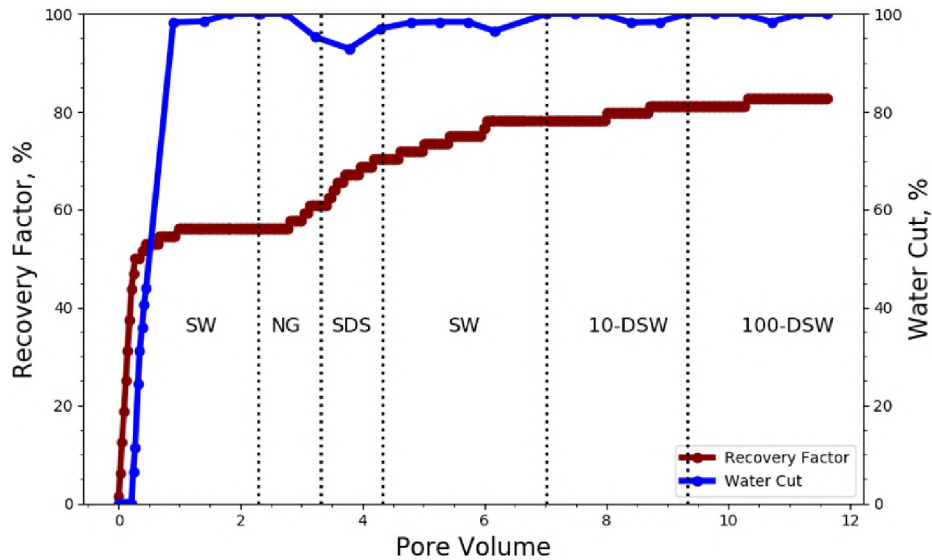


Figure 14. Oil recovery factor and water cut of Core C-5.

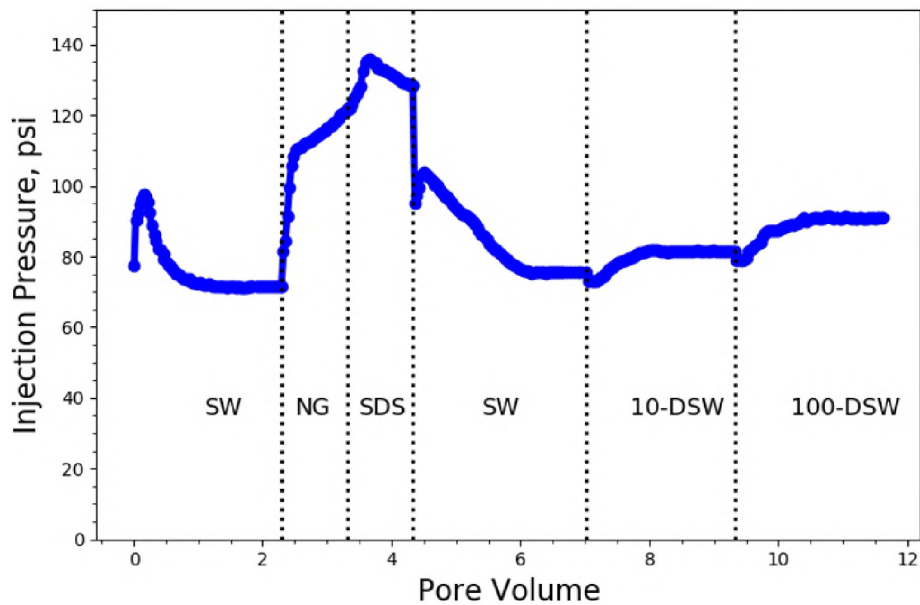


Figure 15. Injection pressure profile of Core C-5.

The effect of nanogel combined with SDS and sulfate-enriched seawater was studied using core C-6, as illustrated in Figure 16. The cumulative oil recovery by conventional seawater flooding was 58.11%. This was followed by 1 injection-volume of nanogel (1,000 ppm) where a significant incremental oil of 6.76% was recovered. The injection of 1 injection-volume of SDS (1,000 ppm) was followed where an incremental oil of approximately 6.80% was produced. Next, seawater was injected until no more oil was produced and pressure stabilized. A significant incremental oil of 5.41% was recovered. The injection of 2-times sulfate-enriched seawater was followed where an additional 4.05% of oil was observed. This was followed by injecting 3-times sulfate-enriched seawater where an incremental oil of approximately 4.1% was produced. As a result, the total incremental oil recovery, beyond conventional seawater flooding, was approximately 27.13% by nanogel, SDS and various versions of sulfate-enriched seawater. In addition, the trend of injection pressure profile shown in Figure 17 is consistent with the previous flooding experiment (core C-5) where the injection of SDS reduced the adsorption of nanogel. Also, the water slugs following SDS injection showed an increasing trend with sulfate enrichment factor which is related to the size of nanogel when dispersed in sulfate-enriched seawater.

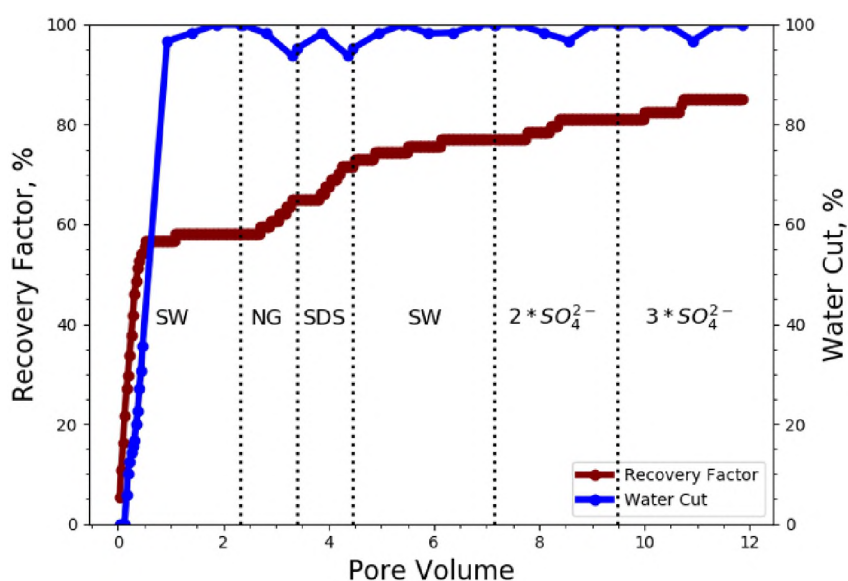


Figure 16. Oil recovery factor and water cut of Core C-6.

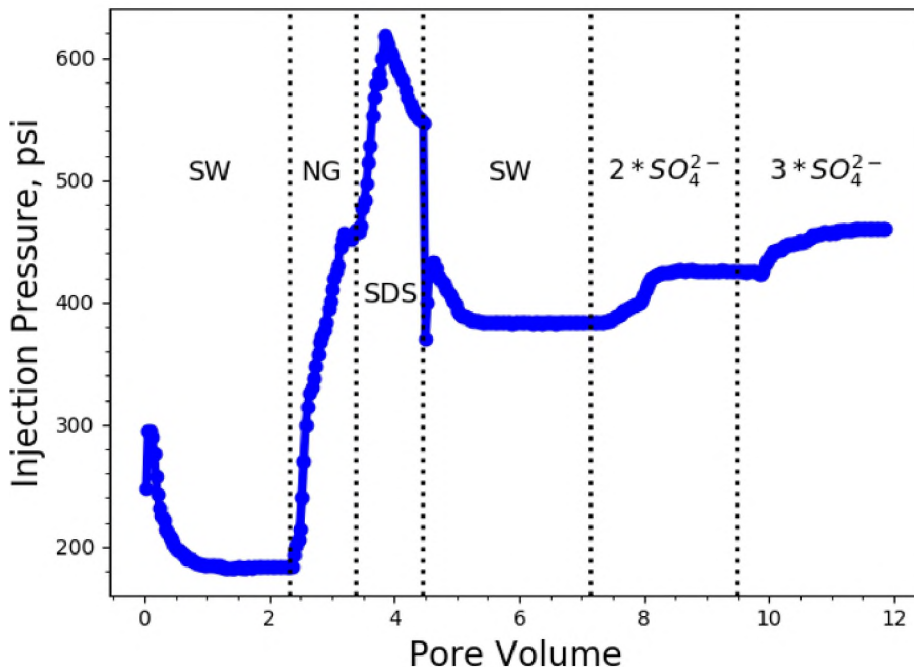


Figure 17. Injection pressure profile of Core C-6.

3.2.4. Effect of Nanogel and SDS Concentration. The effect of increasing the concentration of nanogel and SDS combined with low salinity water flooding was evaluated using core C-7. As shown in Figure 18, the cumulative oil of conventional seawater was approximately 53.1%. The injection of 1 injection-volume of nanogel (2,000 ppm) was followed where an incremental oil recovery of 4.94% was obtained. This was followed by injecting 1 injection-volume of SDS (2,000 ppm) where a substantial incremental oil equivalent to 6.17% was produced. Then, the injection of seawater was continued until no more oil was produced, and after injecting more than 2 injection-volumes, an incremental oil of 4.9% was recovered. This was followed by injecting 10-times diluted seawater where an additional oil of 3.7% was obtained. A small incremental oil, approximately 1.23%, was recovered when 100-times diluted seawater was injected. The total incremental oil, beyond the conventional seawater flooding, was approximately 21%. Moreover, the trend of injection pressure profile is consistent with previous experiments, as illustrated in Figure 19. However, nanogel adsorption reduction by SDS injection was lower than previous flooding

experiment (core C-5). Additionally, the pressure trend of water slugs following the SDS injection indicates the ability of nanogel to expand in lower salinities.

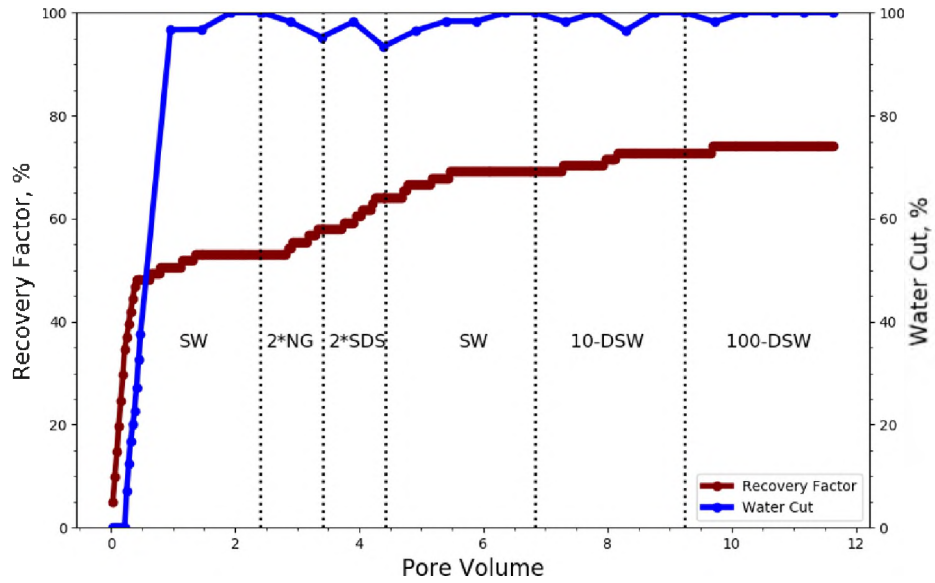


Figure 18. Oil recovery factor and water cut of Core C-7.

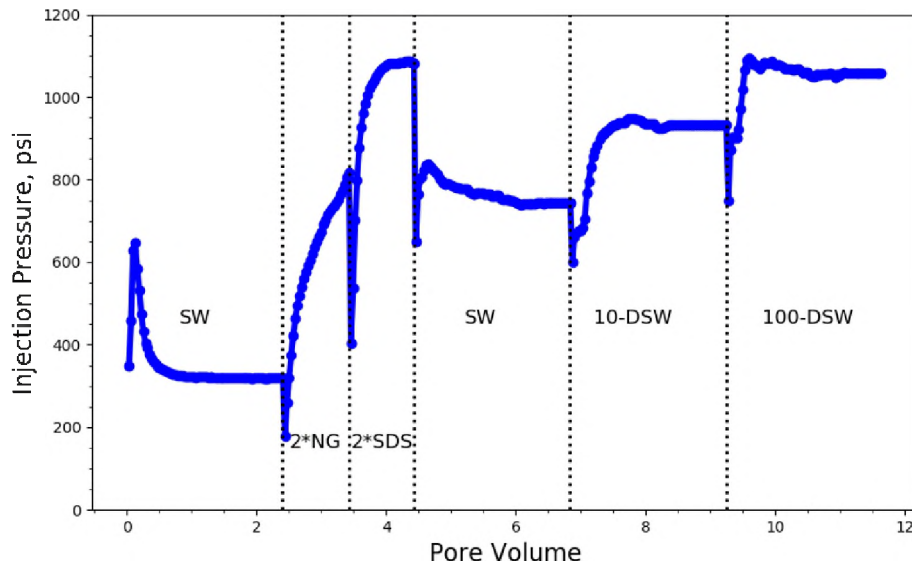


Figure 19. Injection pressure profile of Core C-7.

Another core flooding experiment was conducted to evaluate the effect of increasing the concentration of nanogel and SDS combined with several versions of sulfate-enriched seawater, as shown in Figure 20. The cumulative oil recovery by conventional seawater was approximately 57.8%. The injection of 1 injection-volume of nanogel (2,000 ppm) was followed, and a significant incremental oil of 6% was recovered. Next, 1 injection-volume of SDS (2,000 ppm) was followed and a substantial incremental oil was produced, equivalent to 7.23%. This was followed by injecting seawater until no more oil was recovered, and an additional incremental oil of approximately 6% was produced. Next, 2-times sulfate-enriched seawater was injected where an incremental oil of 3.61% was obtained. A small increase in oil recovery of approximately 1.2% was produced by injecting 3-times sulfate-enriched seawater. Therefore, the total incremental oil beyond initial seawater flooding was approximately 24% by concentrated nanogel and SDS combined with several versions of sulfate-enriched seawater. The injection pressure profile shown in Figure 21 is consistent with the previous core flooding experiment (core C-6). Here, SDS injection (2,000 ppm) slightly reduced the adsorption caused by nanogel injection.

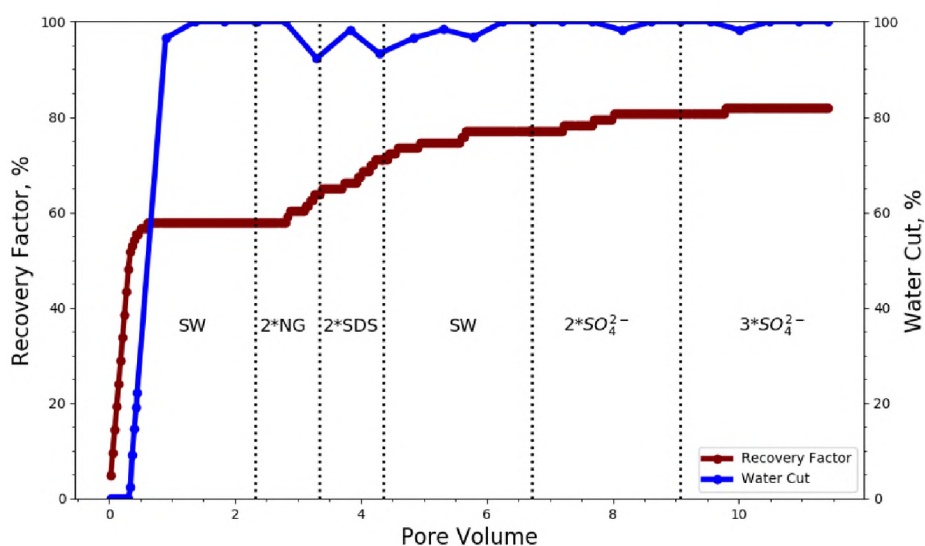


Figure 20. Oil recovery factor and water cut of Core C-8.

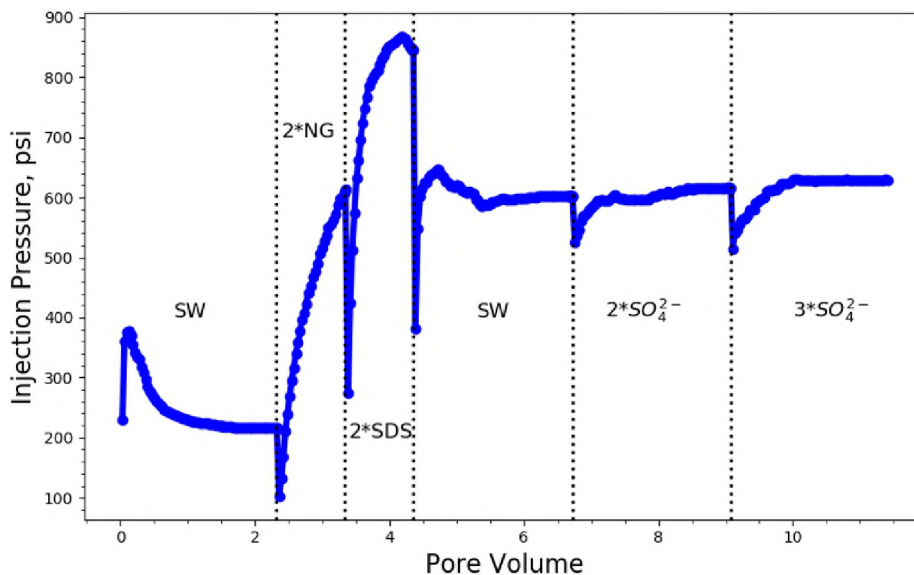


Figure 21. Injection pressure profile of Core C-8.

3.2.5. Evaluation of Nanogel and SDS One-Slug Injection Mode. The impact of injecting nanogel and SDS together as one-slug combined with several diluted versions of seawater was evaluated using core C-9. As illustrated in Figure 22, the cumulative oil recovery by seawater flooding was approximately 54%. The injection of 2 injection-volumes of nanogel coupled with SDS (1,000 ppm each) as one-slug was followed. A substantial incremental oil was produced, equivalent to 9.21%. This was followed by injecting seawater where an additional oil of 5.26% was recovered. Next, 10-times diluted seawater was injected, and an incremental oil of 2.6% was obtained. A small additional oil equivalent to 1.3% was recovered by 100-times diluted seawater. The total incremental oil without conventional seawater flooding was approximately 18.42%. The trend of injection pressure profile shows a major increase induced by nanogel-SDS injection, as presented in Figure 23. The general pressure trend of the followed water slugs is consistent with previous core flooding experiments (cores C-5 and C-7).

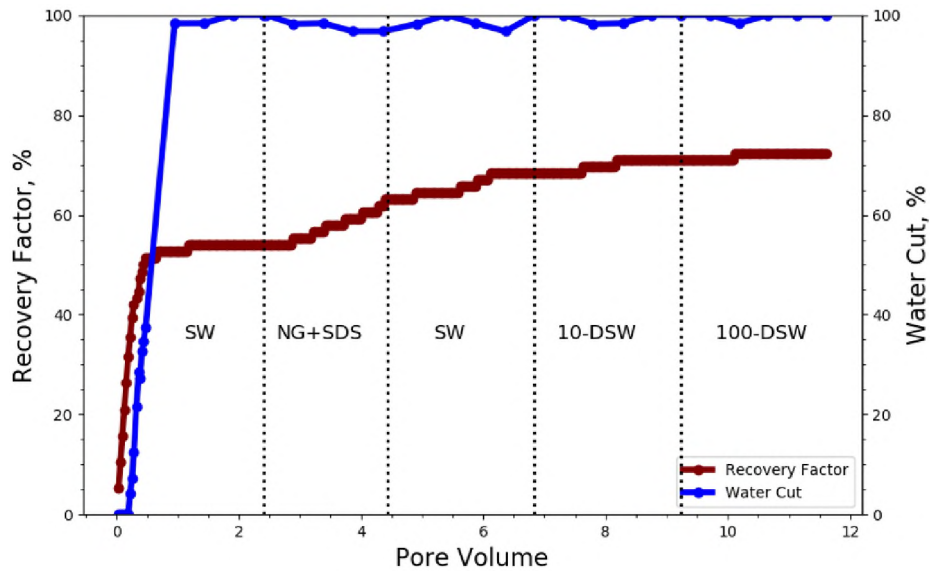


Figure 22. Oil recovery factor and water cut of Core C-9.

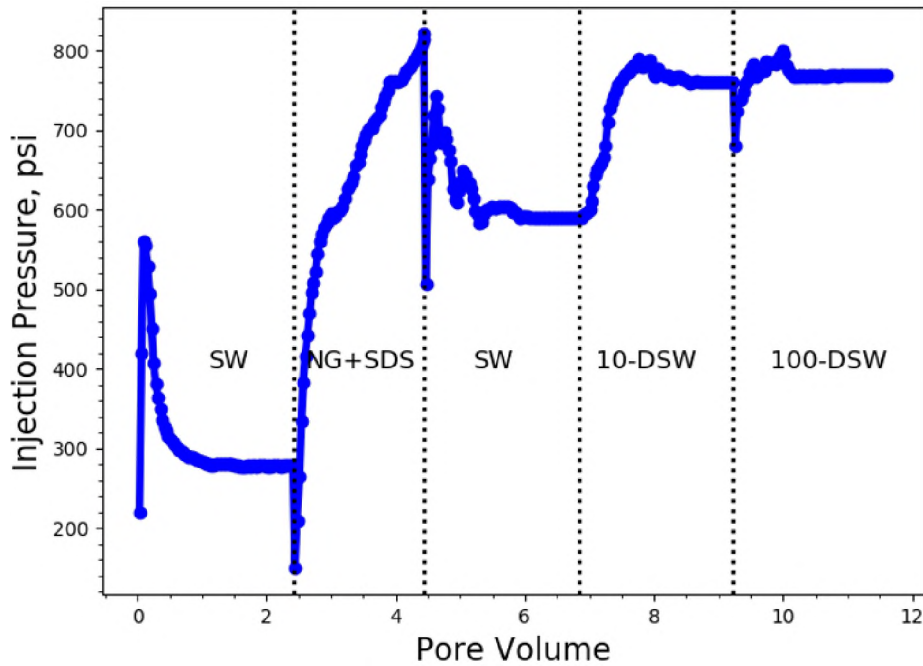


Figure 23. Injection pressure profile of Core C-9.

Another core flooding experiment was conducted to study the impact of injecting nanogel and SDS as one-slug combined with several versions of sulfate-enriched seawater, as illustrated in Figure 24. The cumulative oil recovery by conventional seawater was 52.7%. The injection of nanogel and SDS (1,000 ppm each) as one-slug was followed,

and after 2 injection-volumes, a substantial incremental of oil was produced, equivalent to 9.45%. This was followed by injecting seawater where an additional oil of 4.1% was recovered. Next, 2-times sulfate-enriched seawater was injected and produced an additional incremental oil of 2.7%. A small incremental oil equivalent to 1.35% was obtained when 3-times sulfate-enriched seawater was injected. The total incremental oil beyond the conventional seawater flooding was approximately 17.55%. In addition, the trend of injection pressure profile is consistent with the previous experiments (cores C-4, C-6 and C-8), as shown in Figure 25.

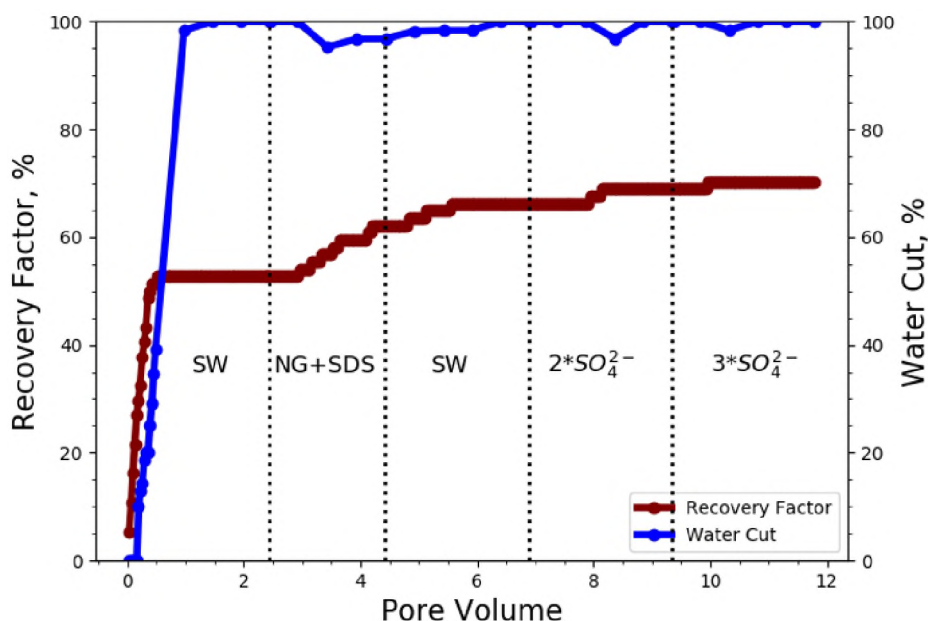


Figure 24. Oil recovery factor and water cut of Core C-10.

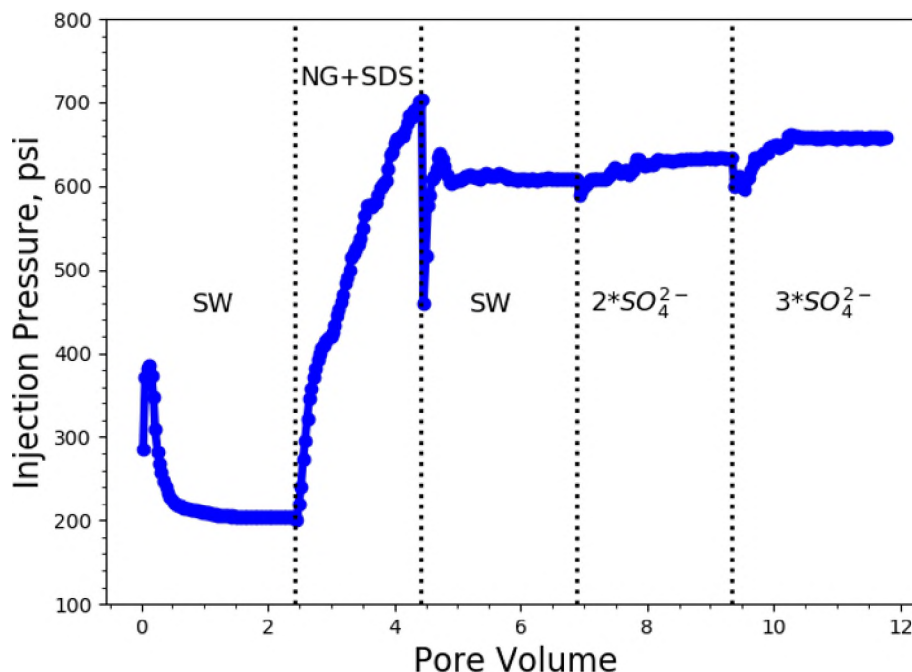


Figure 25. Injection pressure profile of Core C-10.

3.3. DYNAMIC ADSORPTION AND DESORPTION MEASUREMENTS

In this work, nanogel dispersion with a concentration of $1000 \frac{mg}{L}$ was injected through the carbonate core until no more nanogel adsorbed on the pore throat surface. After that, formation water (TDS is 213,734 ppm) was injected through the core to desorb the nanogel from the rock surface. The injection pressure was monitored throughout the experiment to evaluate the plugging behavior of the nanogel. The injection pressure of nanogel continuously increased to 456 psi with an average rate of 56 psi per injection volume, as shown in Figure 26. Nanogel was not detected in the effluent until 0.48 PV. The concentration of nanogel in the effluent increased suddenly to $244 \frac{mg}{L}$ at injection-volume of 0.75. Afterwards, a slight increase in the concentration of nanogel in the effluent was observed with an average concentration rate of $0.24 \frac{mg}{L}$ per PV until the injection volume reached 4.2 PV. Then, a dramatic increase in the concentration of nanogel in effluents was detected during the next 0.8 PV with an average concentration rate of $377 \frac{mg}{L}$ per PV. Later, the concentration of nanogel in the effluent increased dramatically and reached

the concentration of injected dispersion at 8.15 PV which might suggest a piston-like displacement phenomenon of nanogel adsorption in core plugs. The continuous increase in injection pressure might be related to deposited nanogel that reduce the flowing path inside the porous media, thus increasing the possibility of aggregation and pore throat bridging (Gao, 2007). The dynamic desorption behavior of the nanogel was also evaluated at room temperature, as illustrated in Figure 27. The injection pressure during post-brine injection slightly reduced during the first pore volume injection. After that, the injection pressure remained almost stable at 425 psi. On the other hand, the concentration of nanogel in the effluent during desorption process decreased in a power law relationship with injection volume. Different responding rates of injection pressure and nanogel concentration in the effluents were observed in both dynamic adsorption and desorption processes.

The wide pore size distribution associated with carbonate cores resulted in detecting the nanogel in the effluent in less than 1 PV during the dynamic adsorption process. However, the equilibrium concentration of nanogel, where injected and effluent concentrations become equal, was not reached until after 8.15 injection volumes. The complex interactions between carbonate rock surface and nanogel dispersion caused this effluent nanogel concentration profile, where electrostatic repulsion accelerated the dynamic adsorption process to reach equilibrium state, whereas electrostatic attraction extended it. During the desorption process, however, the nanogel dispersion remained in rock surfaces and pore throats were flushed out by the displacing brine that resulted in the power-law trend of effluent nanogel concentration.

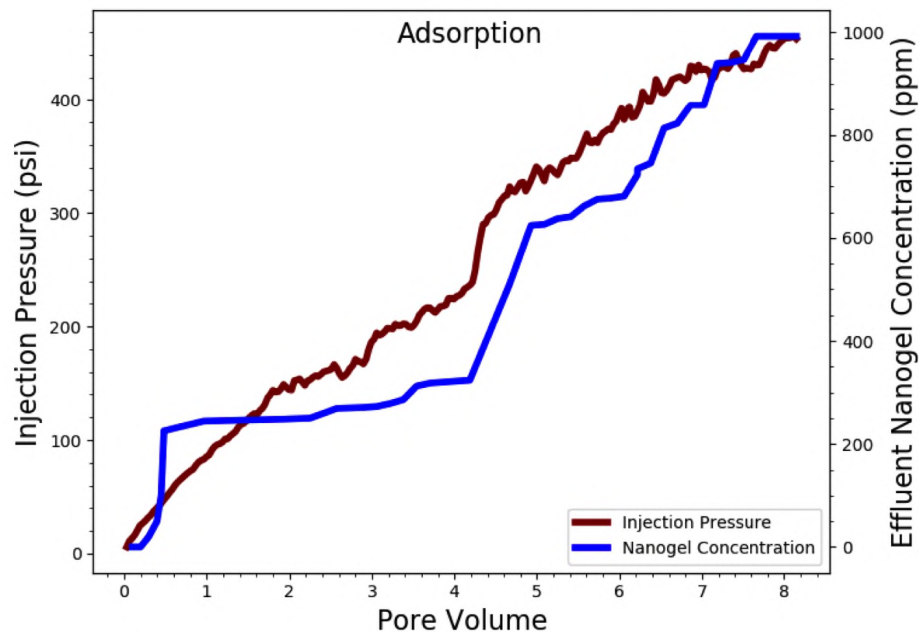


Figure 26. Effluent nanogel concentration and injection pressure profile as a function of injection volume of dynamic adsorption using Core C-11.

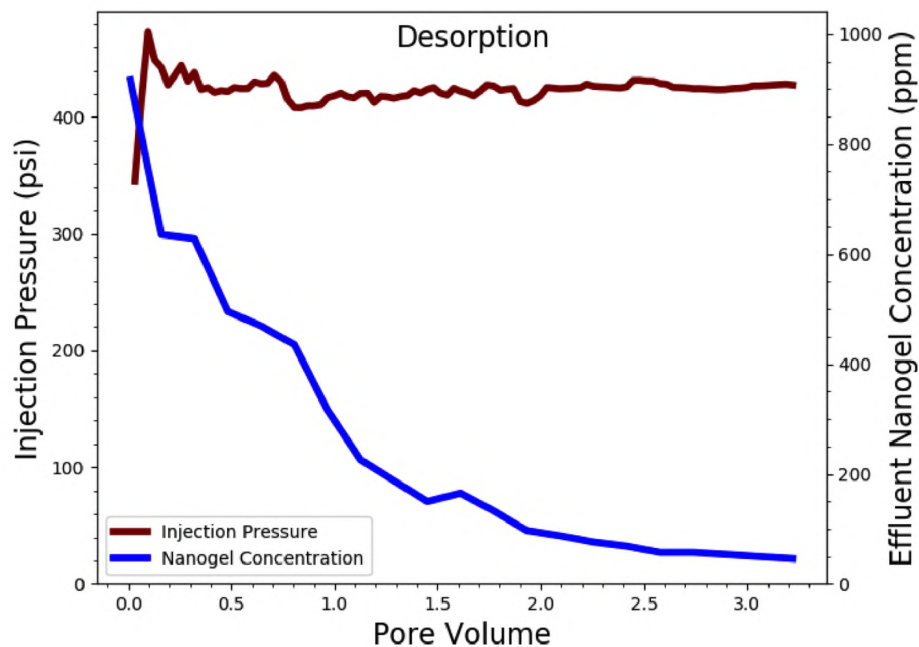


Figure 27. Effluent nanogel concentration and injection pressure profile as a function of injection volume of dynamic desorption using Core C-11.

3.4. INJECTIVITY AND PLUGGING PERFORMANCE OF NANOGEL

In order to assess the blocking performance induced by nanogel and SDS injections, the permeability reduction or residual resistance factor (RRF or RRF) have to be evaluated using equation 3, while the injectivity evaluation of gel treatments is estimated using equation 2. Figure 28 summarizes the calculated results of resistance factor and residual resistance factor of all cores used in core flooding experiments. Here, resistance factor was estimated at the end of NG or SDS volume injection, and residual resistance factor was calculated using the stabilized pressure of the final water slug. The resistance factor measurements were higher for core plugs with lower permeability. Experimental results showed that residual resistance factor measurements in cores injected with only nanogel (no SDS) were higher when low salinity water slugs were applied. This is probably attributed to the fact that nanogel particles can expand in lower seawater salinities, compared to sulfate-enriched seawater. Hence, SDS injections reduced the adsorption density of nanogels in pore throats and caused lower blocking efficiency.

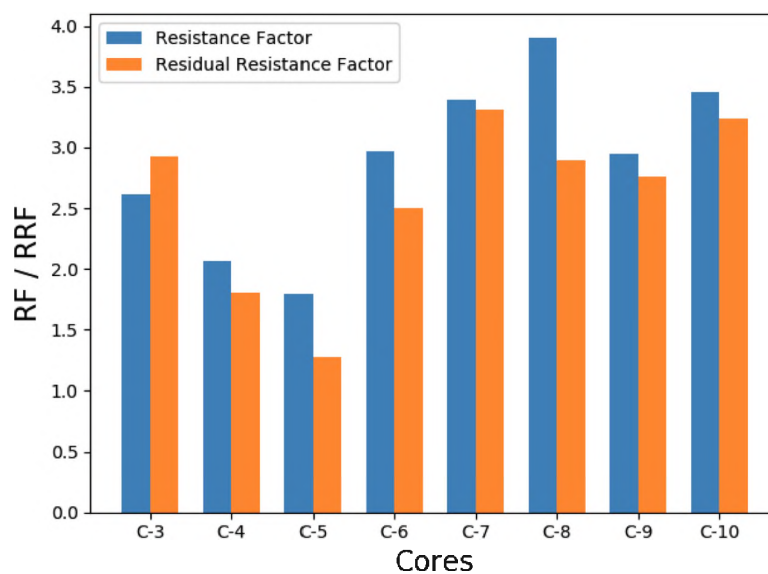


Figure 28. Resistance factor calculated at the end of NG/SDS injection and residual resistance factor calculated using stabilized pressure of last water slug of all cores used in core flooding experiments.

To further investigate the injectivity and plugging performance caused by nanogel in carbonate reservoirs another core plug, saturated with oil, was employed through an extended nanogel and water slug injections. As illustrated in Figure 29, nanogel injection pressure kept increasing and never stabilized, reaching an injection pressure of approximately 900 psi. This illustrates that nanogel continued adsorbing on rock surfaces due to the formation of complex clusters induced by rock-brine-nanogel interactions. The estimated RF after injecting more than 11 injection-volumes of nanogel was 11.37. In order to ascertain that the plugging of nanogel will remain-in after the post-flush water flooding, the stabilized pressures of extended water slugs were used to calculate RRF. The residual resistance factor was found to be increasing with lower seawater salinity due to the expansion of nanogel particle size. Here, RRF were calculated as 5.62, 5.92, and 7.05 for seawater, 10-timed diluted, and 100-times diluted seawater, respectively. These results show the ability of nanogel to form a solid-like structures in rock surfaces and maintain their characteristics in several salinities.

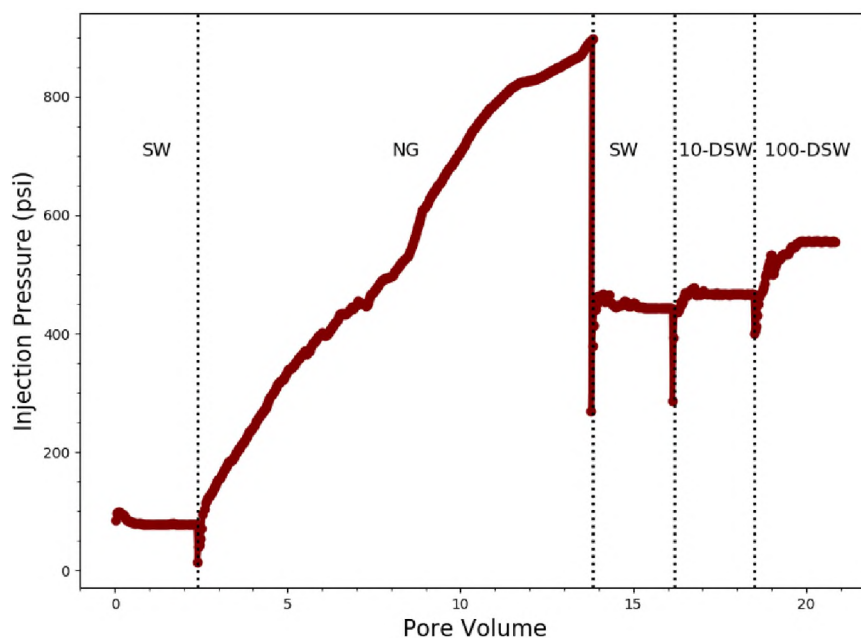


Figure 29. Pressure profile of core C-12 used to evaluate the injectivity and plugging performance caused by nanogel.

3.5. DISCUSSION

The most substantial observation that needs to be highlighted is the incremental oil recovery reported in this research work by nanogel and SDS injections combined with several salinities of seawater. In general, varying the salinity of seawater after nanogel and SDS injections provided a significant increase in oil recovery up to 27% beyond conventional seawater flooding. The results indicate that lowering the salinity and modifying the ionic composition of seawater have a significant influence on nanogel-water slugs-rock interactions. As a result, it can be concluded that lowering the salinity of seawater has a major impact on both the size of nanogel and nanogel-rock interactions. In addition, the reactivity of sulfate ions SO_4^{2-} in seawater proved to have the ability to improve oil recovery by changing surface charges and releasing the adsorbed carboxylic oil components from the rock (Zhang and Austad, 2006; Zhang *et al.*, 2007).

The movement of particles in porous media is a very complex process due to the heterogeneity of porous media and the forces controlling solid movement in porous media. The path of the particles through the porous media is governed by many factors such as the size of the particles and their surface properties, the morphology of the medium, the properties of the displacing fluid, and the complex interaction between the particles and the medium (Gao, 2007). All these factors acting together affect the transportation, adsorption and desorption of particles and the resulting plugging of the porous media (Gao, 2007). In addition, the complexity of the porous media and particles might cause a log-jamming phenomenon at the entrance of pore throats which is affected by particle size and concentration, pore size distribution and flow rate (Bolandtaba *et al.*, 2009).

The results reported here clearly indicate the potential of nanogel combined with SDS and several salinities of seawater in carbonate reservoirs. A significant increase in nanogel size with 100-times diluted seawater was observed (Figure 4) where a substantial incremental of oil was recovered. Modifying the composition of seawater with higher

content of SO_4^{2-} ion has also provided a major additional oil recovery by expanding the size of nanogel in pores, altering the water to un-swept zones and by releasing the carboxylic oil components from rock surface.

4. CONCLUSION

In this work, the performance of a newly developed particles known as nanogels combined with SDS and several salinities of seawater in carbonate reservoirs to improve oil recovery was reported as a potential EOR method. This was explained through well-tailored core flooding experiments using crude oil from one of Saudi reservoirs. The reported method consists of different injection practices of nanogel and SDS (sequential and one-slug), and sequential injections of various salinities of seawater. The incremental oil recovery was approximately 6.75% with sequential nanogel injection, 9.40% with sequential SDS injection, 7.80% with regular seawater, 3.70% with 10-times diluted seawater, 1.30% with 100-times diluted seawater, 4.05% with 2-times sulfate-enriched seawater, and 4.05% with 3-times sulfate-enriched seawater. The primary findings in this study are reported below.

- The results revealed that altering the salinity of seawater has a significant impact on the size of nanogel. Lower seawater salinities caused nanogel particles to expand and further swell which increased the plugging performance. It was also observed that SDS injection did not affect the size of nanogel.
- Sequential injections of several salinity versions of seawater, one after another, has a substantial potential to obtain additional incremental oil recovery.
- The tertiary oil production of the different seawater salinities after nanogel and SDS injections was triggered after about 1 pore volume of the new water type.

- The results show that sequential injections of nanogel and SDS have greater potential to produce higher oil quantities, compared to one-slug injection scheme.
- The increase in injection pressure profile with different water slugs after nanogel and SDS injections is an indication of the ability of adsorbed nanogel to expand and swell in pore throats.
- The adsorption test reveals that the injectivity and plugging performance of nanogel greatly depends on the injection volume. The results also show that lower brine salinities have higher plugging performance.

NOMENCLATURE

IFT Interfacial tension, mN/m.

CMC Critical micelle concentration.

F_r Resistance factor.

F_{rrw} Residual resistance factor of water.

ppm Parts per million.

NG Nanogel.

SDS Sodium dodecyl sulfate.

SW Seawater.

10-DSW 10-times diluted seawater.

100-DSW 100-times diluted seawater.

2 * SO_4 2-times sulfate-enriched seawater.

3 * SO_4 3-times sulfate-enriched seawater.

PV Pore volume.

REFERENCES

- Afekare, D. A. and Radonjic, M., 'From mineral surfaces and coreflood experiments to reservoir implementations: Comprehensive review of low-salinity water flooding (lswf),' *Energy & fuels*, 2017, **31**(12), pp. 13043–13062.
- Akbar, M., Vissapragada, B., Alghamdi, A. H., Allen, D., Herron, M., Carnegie, A., Dutta, D., Olesen, J.-R., Chourasiya, R., Logan, D., *et al.*, 'A snapshot of carbonate reservoir evaluation,' *Oilfield Review*, 2000, **12**(4), pp. 20–21.
- Almahfood, M. and Bai, B., 'The synergistic effects of nanoparticle-surfactant nanofluids in eor applications,' *Journal of Petroleum Science and Engineering*, 2018, **171**, pp. 196–210.
- Almahfood, M. and Bai, B., 'Characterization and oil recovery enhancement by a polymeric nanogel combined with surfactant for sandstone reservoirs,' submitted to *Journal of Petroleum Science*, 2020a.
- Almahfood, M. and Bai, B., 'Potential oil recovery enhancement by a polymeric nanogel combined with surfactant for sandstone reservoirs,' in 'OTC 2020,' *Offshore Technology Conference*, 2020b .
- Almahfood, M., Bai, B., Zhang, Y., and Neogi, P., 'Stability of oil-in-water pickering emulsion in the presence of polymeric nanogels and surfactants,' Submitted to *Nature Nanotechnology*, 2020.
- Austad, T., Milner, J., *et al.*, 'Spontaneous imbibition of water into low permeable chalk at different wettabilities using surfactants,' in 'International Symposium on Oilfield Chemistry,' *Society of Petroleum Engineers*, 1997 .
- Austad, T., Shariatpanahi, S., Strand, S., Black, C., and Webb, K., 'Conditions for a low-salinity enhanced oil recovery (eor) effect in carbonate oil reservoirs,' *Energy & fuels*, 2011, **26**(1), pp. 569–575.
- Ayatollahi, S., Zerafat, M. M., *et al.*, 'Nanotechnology-assisted eor techniques: New solutions to old challenges,' in 'SPE international oilfield nanotechnology conference and exhibition,' *Society of Petroleum Engineers*, 2012 .
- Baker, P., Kastner, M., Byerlee, J., and Lockner, D., 'Pressure solution and hydrothermal recrystallization of carbonate sediments—An experimental study,' *Marine Geology*, 1980, **38**(1-3), pp. 185–203.

- Bolandtaba, S. F., Skauge, A., and Mackay, E., 'Pore scale modelling of linked polymer solution (Ips)—a new eor process,' in 'IOR 2009-15th European Symposium on Improved Oil Recovery,' European Association of Geoscientists & Engineers, 2009 pp. cp-124.
- Bust, V. K., Oletu, J. U., Worthington, P. F., *et al.*, 'The challenges for carbonate petrophysics in petroleum resource estimation,' SPE Reservoir Evaluation & Engineering, 2011, **14**(01), pp. 25–34.
- Chengara, A., Nikolov, A. D., Wasan, D. T., Trokhymchuk, A., and Henderson, D., 'Spreading of nanofluids driven by the structural disjoining pressure gradient,' Journal of colloid and interface science, 2004, **280**(1), pp. 192–201.
- Das, S. K., Choi, S. U., Yu, W., and Pradeep, T., *Nanofluids: science and technology*, John Wiley & Sons, 2007.
- Fathi, S. J., Austad, T., and Strand, S., 'Water-based enhanced oil recovery (eor) by smart water: Optimal ionic composition for eor in carbonates,' Energy & fuels, 2011, **25**(11), pp. 5173–5179.
- Gao, C., 'Factors affecting particle retention in porous media,' Emirates Journal for Engineering Research, 2007, **12**(3), pp. 1–7.
- Geng, J., Han, P., Bai, B., *et al.*, 'Experimental study on charged nanogels for interfacial tension reduction and emulsion stabilization at various salinities and oil types,' in 'SPE Asia Pacific Oil and Gas Conference and Exhibition,' Society of Petroleum Engineers, 2018 .
- Giraldo, J., Benjumea, P., Lopera, S., Cortes, F. B., and Ruiz, M. A., 'Wettability alteration of sandstone cores by alumina-based nanofluids,' Energy & Fuels, 2013, **27**(7), pp. 3659–3665.
- Green, D. W., Willhite, G. P., *et al.*, *Enhanced oil recovery*, volume 6, Henry L. Doherty Memorial Fund of AIME, Society of Petroleum Engineers Richardson, TX, 1998.
- Gupta, R., Smith, G. G., Hu, L., Willingham, T., Lo Cascio, M., Shyeh, J. J., Harris, C. R., *et al.*, 'Enhanced waterflood for carbonate reservoirs-impact of injection water composition,' in 'SPE Middle East oil and gas show and conference,' Society of Petroleum Engineers, 2011 .
- Jadhunandan, P. and Morrow, N., 'Spontaneous imbibition of water by crude oil/brine/rock systems,' In Situ;(United States), 1991, **15**(4).
- Jadhunandan, P., Morrow, N. R., *et al.*, 'Effect of wettability on waterflood recovery for crude-oil/brine/rock systems,' SPE reservoir engineering, 1995, **10**(01), pp. 40–46.
- Johannessen, A. M. and Spildo, K., 'Enhanced oil recovery (eor) by combining surfactant with low salinity injection,' Energy & Fuels, 2013, **27**(10), pp. 5738–5749.

- Karimi, A., Fakhroueian, Z., Bahramian, A., Pour Khiabani, N., Darabad, J. B., Azin, R., and Arya, S., 'Wettability alteration in carbonates using zirconium oxide nanofluids: Eor implications,' *Energy & Fuels*, 2012, **26**(2), pp. 1028–1036.
- Kokal, S. and Al-Kaabi, A., 'Enhanced oil recovery: challenges & opportunities,' World Petroleum Council: Official Publication, 2010, **64**.
- Lake, L. W., 'Enhanced oil recovery,' 1989.
- Lenchenkov, N. S., Slob, M., van Dalen, E., Glasbergen, G., van Kruijsdijk, C., *et al.*, 'Oil recovery from outcrop cores with polymeric nano-spheres,' in 'SPE Improved Oil Recovery Conference,' Society of Petroleum Engineers, 2016 .
- Li, R., Jiang, P., Gao, C., Huang, F., Xu, R., and Chen, X., 'Experimental investigation of silica-based nanofluid enhanced oil recovery: the effect of wettability alteration,' *Energy & Fuels*, 2016, **31**(1), pp. 188–197.
- Ligthelm, D. J., Gronsveld, J., Hofman, J., Brussee, N., Marcelis, F., van der Linde, H., *et al.*, 'Novel waterflooding strategy by manipulation of injection brine composition.' in 'EUROPEC/EAGE conference and exhibition,' Society of Petroleum Engineers, 2009 .
- Ma, H., Luo, M., and Dai, L. L., 'Influences of surfactant and nanoparticle assembly on effective interfacial tensions,' *Physical Chemistry Chemical Physics*, 2008, **10**(16), pp. 2207–2213.
- Mahani, H., Sorop, T., Ligthelm, D. J., Brooks, D., Vledder, P., Mozahem, F., Ali, Y., *et al.*, 'Analysis of field responses to low-salinity waterflooding in secondary and tertiary mode in syria,' in 'SPE Europec/EAGE Annual Conference and Exhibition,' Society of Petroleum Engineers, 2011 .
- Martin, J. C. *et al.*, 'The effects of clay on the displacement of heavy oil by water,' in 'Venezuelan annual meeting,' Society of Petroleum Engineers, 1959 .
- Mcelfresh, P. M., Holcomb, D. L., Ector, D., *et al.*, 'Application of nanofluid technology to improve recovery in oil and gas wells,' in 'SPE International Oilfield Nanotechnology Conference and Exhibition,' Society of Petroleum Engineers, 2012 .
- Mohajeri, M., Hemmati, M., and Shekarabi, A. S., 'An experimental study on using a nanosurfactant in an eor process of heavy oil in a fractured micromodel,' *Journal of petroleum Science and engineering*, 2015, **126**, pp. 162–173.
- Moraes, R. R., Garcia, J. W., Barros, M. D., Lewis, S. H., Pfeifer, C. S., Liu, J., and Stansbury, J. W., 'Control of polymerization shrinkage and stress in nanogel-modified monomer and composite materials,' *Dental Materials*, 2011, **27**(6), pp. 509–519.
- Myint, P. C. and Firoozabadi, A., 'Thin liquid films in improved oil recovery from low-salinity brine,' *Current Opinion in Colloid & Interface Science*, 2015, **20**(2), pp. 105–114.

- Nasralla, R. A., Sergienko, E., Masalmeh, S. K., van der Linde, H. A., Brussee, N. J., Mahani, H., Suijkerbuijk, B. M., Al-Qarshubi, I. S., *et al.*, 'Potential of low-salinity waterflood to improve oil recovery in carbonates: Demonstrating the effect by qualitative coreflood,' *SPE Journal*, 2016, **21**(05), pp. 1–643.
- Pourafshary, P., Azimpour, S., Motamedi, P., Samet, M., Taheri, S., Bargozin, H., Hendi, S., *et al.*, 'Priority assessment of investment in development of nanotechnology in upstream petroleum industry,' in 'SPE Saudi Arabia section technical symposium,' Society of Petroleum Engineers, 2009 .
- Purswani, P., Tawfik, M. S., and Karpyn, Z. T., 'Factors and mechanisms governing wettability alteration by chemically tuned waterflooding: A review,' *Energy & Fuels*, 2017, **31**(8), pp. 7734–7745.
- Qiu, F. *et al.*, 'The potential applications in heavy oil eor with the nanoparticle and surfactant stabilized solvent-based emulsion,' in 'Canadian unconventional resources and international petroleum conference,' Society of Petroleum Engineers, 2010 .
- Reiter, P. K., *A water-sensitive sandstone flood using low salinity water*, Ph.D. thesis, University of Oklahoma, 1961.
- RezaeiDoust, A., Puntervold, T., Strand, S., and Austad, T., 'Smart water as wettability modifier in carbonate and sandstone: A discussion of similarities/differences in the chemical mechanisms,' *Energy & fuels*, 2009, **23**(9), pp. 4479–4485.
- Sheng, J., *Enhanced oil recovery field case studies*, Gulf Professional Publishing, 2013.
- Soraya, B., Malick, C., Philippe, C., Bertin, H. J., Hamon, G., *et al.*, 'Oil recovery by low-salinity brine injection: laboratory results on outcrop and reservoir cores,' in 'SPE Annual Technical Conference and Exhibition,' Society of Petroleum Engineers, 2009 .
- Standnes, D. C. and Austad, T., 'Wettability alteration in chalk: 1. preparation of core material and oil properties,' *Journal of Petroleum Science and Engineering*, 2000, **28**(3), pp. 111–121.
- Standnes, D. C. and Austad, T., 'Wettability alteration in carbonates: Interaction between cationic surfactant and carboxylates as a key factor in wettability alteration from oil-wet to water-wet conditions,' *Colloids and Surfaces A: Physicochemical and Engineering Aspects*, 2003, **216**(1-3), pp. 243–259.
- Suleimanov, B., Ismailov, F., and Veliyev, E., 'Nanofluid for enhanced oil recovery,' *Journal of Petroleum Science and Engineering*, 2011, **78**(2), pp. 431–437.
- Tang, G., Morrow, N. R., *et al.*, 'Salinity, temperature, oil composition, and oil recovery by waterflooding,' *SPE Reservoir Engineering*, 1997, **12**(04), pp. 269–276.

- Tang, G.-Q. and Morrow, N. R., 'Influence of brine composition and fines migration on crude oil/brine/rock interactions and oil recovery,' *Journal of Petroleum Science and Engineering*, 1999, **24**(2-4), pp. 99–111.
- Tetteh, J. T., Rankey, E., Barati, R., *et al.*, 'Low salinity waterflooding effect: Crude oil/brine interactions as a recovery mechanism in carbonate rocks,' in 'OTC Brasil,' Offshore Technology Conference, 2017 .
- Thomas, S., 'Enhanced oil recovery-an overview,' *Oil & Gas Science and Technology-Revue de l'IFP*, 2008, **63**(1), pp. 9–19.
- Tian, H. and Wang, M., 'Electrokinetic mechanism of wettability alternation at oil-water-rock interface,' *Surface Science Reports*, 2017, **72**(6), pp. 369–391.
- Vledder, P., Gonzalez, I. E., Carrera Fonseca, J. C., Wells, T., Ligthelm, D. J., *et al.*, 'Low salinity water flooding: proof of wettability alteration on a field wide scale,' in 'SPE Improved Oil Recovery Symposium,' Society of Petroleum Engineers, 2010 .
- Wasan, D. T. and Nikolov, A. D., 'Spreading of nanofluids on solids,' *Nature*, 2003, **423**(6936), pp. 156–159.
- Wu, Y., Chen, W., Dai, C., Huang, Y., Li, H., Zhao, M., He, L., and Jiao, B., 'Reducing surfactant adsorption on rock by silica nanoparticles for enhanced oil recovery,' *Journal of Petroleum Science and Engineering*, 2017, **153**, pp. 283–287.
- Yi, Z., Sarma, H. K., *et al.*, 'Improving waterflood recovery efficiency in carbonate reservoirs through salinity variations and ionic exchanges: A promising low-cost" smart-waterflood" approach,' in 'Abu Dhabi International Petroleum Conference and Exhibition,' Society of Petroleum Engineers, 2012 .
- Yildiz, H. O. and Morrow, N. R., 'Effect of brine composition on recovery of moutray crude oil by waterflooding,' *Journal of Petroleum science and Engineering*, 1996, **14**(3-4), pp. 159–168.
- Yousef, A. A., Al-Saleh, S. H., Al-Kaabi, A., Al-Jawfi, M. S., *et al.*, 'Laboratory investigation of the impact of injection-water salinity and ionic content on oil recovery from carbonate reservoirs,' *SPE Reservoir Evaluation & Engineering*, 2011, **14**(05), pp. 578–593.
- Zhang, P. and Austad, T., 'Wettability and oil recovery from carbonates: Effects of temperature and potential determining ions,' *Colloids and Surfaces A: Physicochemical and Engineering Aspects*, 2006, **279**(1-3), pp. 179–187.
- Zhang, P., Tweheyo, M. T., and Austad, T., 'Wettability alteration and improved oil recovery by spontaneous imbibition of seawater into chalk: Impact of the potential determining ions Ca^{2+} , Mg^{2+} , and SO_4^{2-} ,' *Colloids and Surfaces A: Physicochemical and Engineering Aspects*, 2007, **301**(1-3), pp. 199–208.

Zhang, T., Davidson, D., Bryant, S. L., Huh, C., *et al.*, 'Nanoparticle-stabilized emulsions for applications in enhanced oil recovery,' in 'SPE improved oil recovery symposium,' Society of Petroleum Engineers, 2010 .

V. STABILITY OF OIL-IN-WATER PICKERING EMULSION IN THE PRESENCE OF POLYMERIC NANOGELS AND SURFACTANTS

Mustafa M. Almahfood^{a, b}, Baojun Bai^a, Yandong Zhang^a, Parthasakha Neogi^c

^aDepartment of Geosciences & Petroleum Engineering

Missouri University of Science and Technology

Rolla, Missouri 65409

^b EXPEC Advanced Research Center, Saudi Aramco, Saudi Arabia

^c Department of Chemical and Biochemical Engineering

Missouri University of Science and Technology

Rolla, Missouri 65409

Email: mmantc@mst.edu

ABSTRACT

The stability against coalescence and flocculation of oil-in-water Pickering emulsions in the presence of both nanogels and surfactants is investigated. In particular, the effect of combining polymeric nanogel with multiple surfactant types in different brine salinities, pH and sonication times on the stability of O/W emulsions is studied. A newly developed polymeric crosslinkable nanogel is prepared using suspension polymerization process by employing 2-Acrylamido 2-methyl propane sulfonic acid monomer. The resultant nanogel displays good structural stability in different brine salinities with a narrow size distribution with one peak pointing to a predominant homogeneous droplet size. Three types of surfactants, Tween[®] 60, CTAB and SDS, with different surface charges were selected for their ability to produce O/W emulsions. The stability of oil-in-water Pickering emulsions is studied by visualizing the shape and measuring the size of emulsified oil droplets as

observed by confocal fluorescence microscopy. The behavior of emulsions stabilized by nanogel and surfactant was found to be dependent on the type of surfactant as emulsions stabilized by anionic nanogel combined with cationic surfactant produced less stable oil droplets that suffered from flocculation. Surprisingly, longer sonication periods were not sufficient enough to produce a stable nanogel-CTAB emulsion. In addition, lower brine salinities greatly influenced the stability of O/W emulsions, especially when nanogel was combined with anionic surfactant. Here, strong acidic conditions lowered the stability of the emulsion systems. The results presented here promote the ability of nanogel combined with anionic surfactant to improve the stability of Pickering emulsions.

Keywords: nanogel, polymeric nanogel, Pickering emulsion, surfactant-based-nanogel, confocal microscopy

1. INTRODUCTION

Oil-in-water emulsions stabilized by surfactants (and colloidal particles) have been extensively studied in the past years for several applications. These types of emulsions have been also employed in the oil and gas industry, however, with limited improvement due to their poor stability and large oil droplet size, providing difficulty in penetration into the oil reservoirs. Lately, the research interest on oil-in-water emulsions stabilized by solid particles, generally known as Pickering emulsions, has greatly increased due to their long-term stability against coalescence, flocculation and sedimentation (Midmore, 1998). These particles are capable of stabilizing oil droplets by forming adsorbed layers and providing better resistance than emulsions stabilized by conventional surfactants. Pickering emulsions can be used as conformance control agents due to their higher viscosity compared to displacing water (Griffith *et al.*, 2016). Silica is the most employed nano material to form Pickering emulsions due to its availability (Pyun *et al.*, 2003). In general, nano-silica enhances oil recovery by reducing the interfacial tension between oil and water phases and forming relatively stable Pickering emulsions (Aveyard *et al.*, 2003; Guzman *et al.*, 2014; He

et al., 2013). Regardless of these features of silicas, their implementation in the oil industry is limited due to their lack of forming long-term stable Pickering emulsion without surface modification with grafted polymer chains (Achilleos and Vamvakaki, 2010). Nevertheless, the surface modification is time-consuming which makes it economically unfeasible.

Furthermore, it is well established by multiple studies that the interaction and combination between nanoparticles and surfactants can either stabilize or de-stabilize oil-in-water emulsions (Johansson *et al.*, 1995). The long term stability is generally a function of surfactant type, composition, and emulsifier concentration (Pichot *et al.*, 2010). Almohsin *et al.* (2018) have reported that emulsions stabilized by nanosilica and non-ionic surfactant could not form a stable emulsified oil droplets. As a result, more research is still needed to improve the properties of different nano-size particles. Hence, Pickering emulsions stabilized by conventional nanoparticles and surfactants are not stable for the long-term as coalescence takes place within few hours (Delmas *et al.*, 2011). Therefore, the use of chemically-proven nano materials along with surfactants seems to be promising to ultimately create long-term stable emulsions.

Microgels and nanogels have been used for many years for multiple applications including pharmaceuticals, medicine and cosmetics (Kabanov and Vinogradov, 2009; Sharma and Sarangdevot, 2012). Their application to stabilize oil-in-water emulsions has been reported by Binks *et al.* (2006) and Ngai *et al.* (2006). In addition, it was observed by few researchers that oil-in-water emulsion stabilized by surfactants and nanoparticles with controlled pH and water concentration can provide significant improvements to emulsion stability by controlling the wettability and degree of flocculation (Binks and Whitby, 2005). Nanosized cross-linked polymeric particles known as nanogels are newly developed deformable particles in EOR applications. They are known for their easy injection process due to their small size (1-100 nm), which is much smaller than the diameter of the pore

throats in oil reservoirs. To the best of our knowledge, there is no reported research on the effect of combining polymeric nanogels and surfactants on the stability of Pickering emulsion in EOR applications.

In this work, polymeric nanogel, synthesized using a typical free radical suspension polymerization process, was combined with three types of surfactants with different surface charges (Tween[®] 60, CTAB and SDS). Pickering emulsions stabilized solely by either surfactants or nanogels were compared to emulsions stabilized by the combination of surfactants and nanogels under various conditions including brine salinity, pH, and ultrasound homogenizing time. The stability of oil-in-water Pickering emulsions was studied by measuring the size and shape of emulsified oil droplets as observed by confocal fluorescence microscopy.

2. EXPERIMENT

2.1. MATERIALS

Na-AMPS nanogel was synthesized in our laboratory. 2-Acrylamido 2-methyl propane sulfonic acid monomer (99%), sodium dodecyl sulfate (SDS, > 99%, CMC = 2400 mg/l), Tween[®] 60 (CMC = 27 mg/l), N,N'-methylene bis(acrylamide) (MBAA, 99%), and sodium bicarbonate ($NaHCO_3$, $\geq 99.7\%$) were purchased from Sigma-Aldrich. Sorbitan monooleate (Span[®] 80), sodium hydroxide (NaOH, 97%), sodium chloride (NaCl, 99%), calcium chloride ($CaCl_2$, powder, 97%), magnesium chloride ($MgCl_2$, 99%), and n-Decane were purchased from Alfa Aesar. Ammonium persulfate ($\geq 98\%$), and sodium sulfate (Na_2SO_4 , $\geq 99\%$) were purchased from Acros Organics. Cetyltrimethyl ammonium bromide (CTAB, $\geq 98\%$, CMC = 4000 mg/l) was purchased from CalBioChem. All chemicals were of reagent grade and used as received without further purification.

2.2. NANOGEL SYNTHESIS

Na-AMPS Nanogels were prepared using a free-radical suspension polymerization process by employing 2-acrylamido 2-methyl propane sulfonic acid monomer. The synthesis process is summarized as follows: sodium hydroxide was used to neutralize the monomer solution to a pH of exactly 7.0. Then, 0.1 gram of N,N'-methylene bis(acrylamide) (MBAA) was added to the solution as a cross-linker. The solution is then added to a three-neck flask containing n-decane, Span[®] 80, and Tween[®]. Initiator was then added to the solution and bubbled with nitrogen in a water bath at 40° C. After 2 hours of stirring, emulsified nanogel was produced. Further washing and drying at 65° C for 24 hours were required to produce powdered Na-AMPS nanogel. Figure 1 shows samples of the employed nanogels.

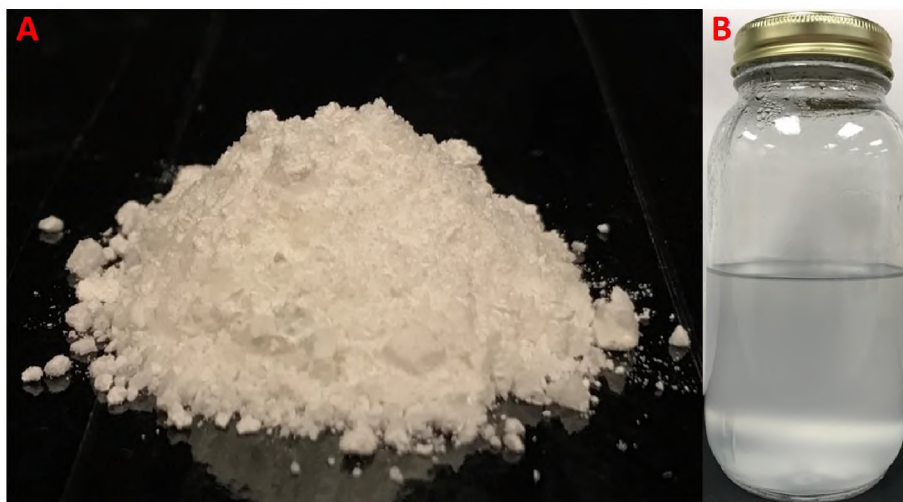


Figure 1. (A) Dried Na-AMPS nanogel. (B) Na-AMPS nanogel dispersed in seawater.

2.3. SURFACTANTS

Surface active agents or surfactants are chemical compounds that are adsorbed on the interface between two fluids. Critical micelle concentration (CMC) is defined as the surfactant concentration above which micelles will start to form, as illustrated in Figure 2. CMC is significant for determining the stabilization of surfactant-based emulsions (Samanta *et al.*,

2011). Three types of hydrophilic surfactants with different surface charges were employed in this study. Sodium dodecyl sulfate (SDS) was purchased from Stepan[®] with a purity > 99%. Cetyltrimethyl ammonium bromide (CTAB) was purchased from Calbiochem with a purity of $\geq 98\%$. Tween[®] 60 was purchased from Sigma Aldrich. All surfactants were used as received without further purification. Table 1 depicts the properties of the employed surfactants.

Table 1. Properties of surfactants.

Surfactant	Type	CMC, mg/L	Molecular weight, g/mol	Supplier
CTAB	Cationic	4000	364.45	CalBioChem
Tween [®] 60	Non-ionic	27	1,311.70	Sigma Aldrich
SDS	Anionic	2400	288.38	Stepan [®]

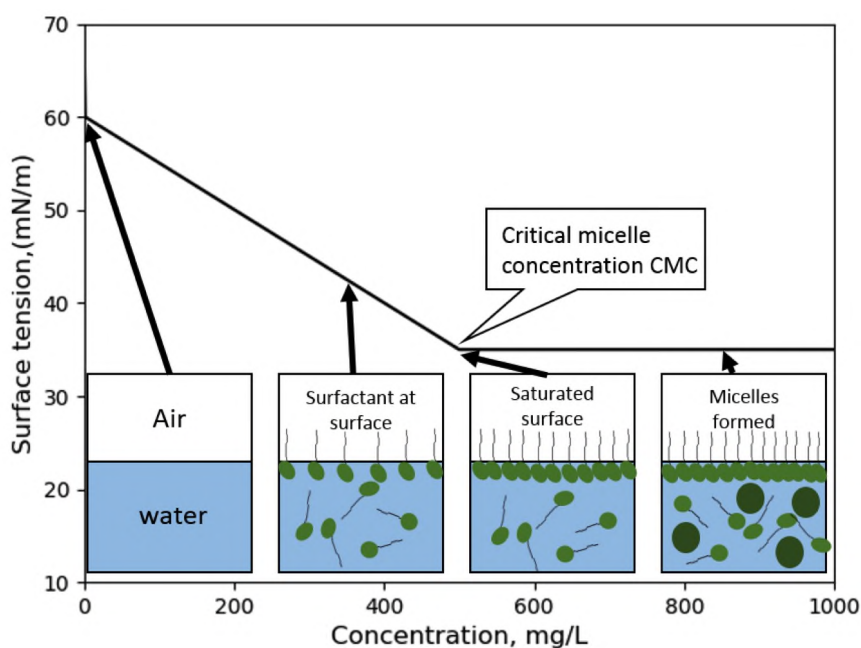


Figure 2. Surface tension of a surfactant solution with increasing concentration leading to forming micelles.

2.4. BRINE PROPERTIES

Different brines were used in this study, including seawater, that simulates the salinity of seawater in Saudi Arabia, and diluted versions of seawater. All brines were prepared from deionized water and reagent grade chemicals on the basis of geochemical analysis of field water samples reported by Yousef *et al.* (2011). The employed seawater had a salinity of approximately 57,600 ppm by weight. Other diluted versions of seawater were prepared by mixing seawater with different volumes of deionized water, including 10-times diluted (approximately 6000 ppm) and 100-times diluted (approximately 600 ppm). Table 2 lists the composition of the employed brines. The effect of salinity on physical properties of the prepared water types was studied. The density and viscosity properties were measured at an average room temperature of 25 °C and listed in Table 3.

Table 2. Composition of all employed brine types with different salinities.

Ion	Seawater g/L	10 Times Diluted Seawater g/L	100 Times Diluted Seawater g/L
Sodium	18,300	1,830	183
Calcium	650	65	6.5
Magnesium	2,110	211	21.1
Sulfate	4,290	429	42.9
Chloride	32,200	3,220	322
Bicarbonate	120	12	1.2
TDS, ppm	57,670	5,767	576.7
Ionic Strength, mol/L	1.15	0.12	0.012

Table 3. Density and viscosity of different brine types at room temperature of 25° C.

Property	Seawater	10 Times Diluted Seawater	100 Times Diluted Seawater
Density (g/cm^3)	1.040	1.001	0.997
Viscosity (cp)	1.012	0.901	0.893

2.5. CRUDE OIL

Light crude oil from a Saudi Arabian oil field with a viscosity of 11.5 cp at room temperature (density = 0.84 g/cc, API 36°) was employed in all experiments.

2.6. VISCOSITY MEASUREMENTS

Brookfield DV3T rheometer was employed to measure the rheological properties of crude oil and several brine types with different salinities. All viscosity measurements were obtained at a room temperature of 25° C.

2.7. PREPARATION OF PICKERING EMULSION SYSTEMS

Oil-in-water emulsions are considered stable if two phase separation did not occur. The separation of an emulsion into bulk oil and water phases is generally governed by four different mechanisms which are Brownian flocculation, creaming, sedimentation flocculation and disproportionation as illustrated schematically in Figure 3. The creaming process is not an actual breaking, but separation of emulsion into two emulsions, one of which is richer in disperse phase than the other (Becher, 1983). Flocculation process is defined as the aggregation of droplets to give 3-D clusters without coalescence occurring. It could be subdivided into 2 categories: caused by sedimentation aggregation and Brownian aggregation of droplets (Goddard and Vincent, 1984). On the other hand, Disproportionation

process is a rare process related to the diffusion of disperse molecules from smaller to larger droplets through the continuous phase (Van Boekel and Walstra, 1981).

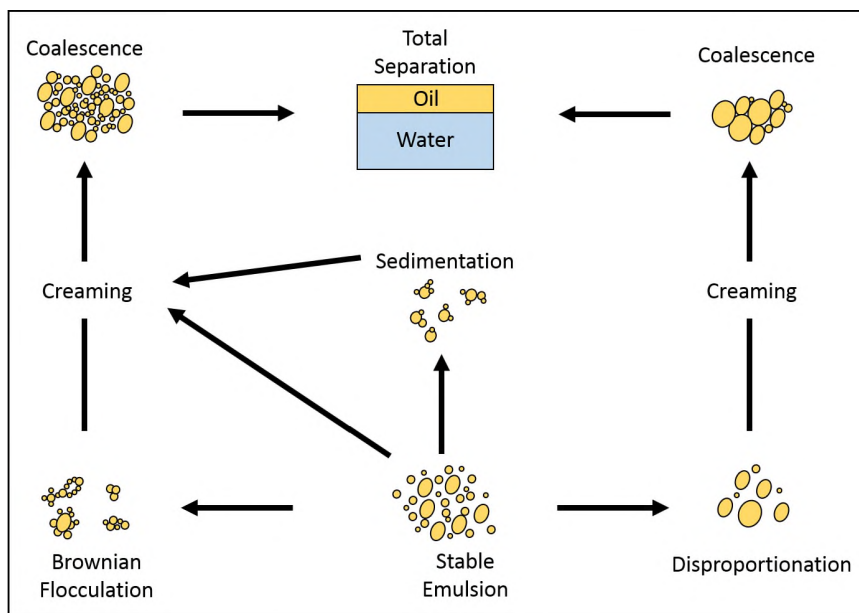


Figure 3. Processes of Emulsion Breakage.

In this work, three types of emulsion systems were investigated for their stability. The first two systems were stabilized solely by either nanogel or surfactants. The third emulsion system was stabilized by the combination of polymeric nanogel and surfactants. In general, CMC value of a surfactant solution is determined using surface tension measurements by pendant drop technique (Rame-hart advance goniometer 500-F1). CMC is defined as the minimum concentration at which the surface tension measurements are becoming almost constant, as shown in Figure 2. Surfactants are better to be employed at a concentration below CMC, as micelles will be formed above this concentration. The CMC of the employed surfactants are listed in Table 1. All surfactants in this study were employed with a concentration of 1000 mg/L to generate emulsions. Although CMC value of Tween[®] 60 is 27 mg/L, a 1000 mg/L concentration was used in this study for consistency with other surfactants. Furthermore, nanogels with a concentration of 1000 mg/L were used for the preparation of all oil-in-water emulsion systems stabilized by nanogel-surfactant systems.

Simple oil-in-water emulsions were prepared by mixing crude oil with the water phase that contains surfactants and nanogels in several brine salinities. Nanogel-surfactant dispersions were mixed with crude oil at a water-oil ratio of 9:1. All mixtures had a total volume of 10 mL and were emulsified using an ultrasonic homogenizer (VC-1500, Sonics & Materials Inc.) with a CV-294 probe at 160 W for 120 seconds (unless otherwise noted). The size and shape of emulsified oil droplets of different emulsion systems were measured and pictured using confocal fluorescence microscopy.

2.8. CHARACTERIZATION OF NANOGEL AND SURFACTANTS

The hydrodynamic diameter and surface ζ potential of the synthesized nanogel were measured at different salt concentrations ranging from 0.58 wt% to 5.8 wt% using glass cuvette and capillary cell (Nano ZS, Malvern Instruments, UK). The instrument is equipped with helium-neon laser (633 nm). All measurements were taken at a room temperature of 25° C and at a scattering angle of 90°.

2.9. PICKERING EMULSION CHARACTERIZATION

In order to study the emulsion stability caused by nanogel and several surfactants, confocal fluorescence microscopy (Nikon Eclipse Ti2) was employed to visualize the shape and size of oil drops. The average diameter of the emulsified oil drops was calculated from the microscopic images using ImageJ.

2.9.1. Methodology. In general, nanogels and/or surfactants in an aqueous dispersion tend to form a self-assembled structural array at the discontinuous oil-water phases. These particles prefer to arrange themselves into a wedge-like structure and begin to force themselves at the interface. Particles that are present in the bulk fluid continuously push

the particles in the confined region forward and impart a huge force known as the disjoining pressure force. The energies that drive this mechanism are Brownian motion and electrostatic repulsion between the particles.

Figure 4 illustrates how nanogels and surfactants might be attached to the oil droplet. Basically, the hydrophobic end of surfactants will be attached to oil molecules. Since nanogels are partially hydrophobic, they will basically fill the spaces between surfactants and oil molecules which leads, at best scenarios, to enhancing the stability of the Pickering emulsion. The 3-D confocal images show an oil drop stabilized by nanogel and surfactant. They both clearly illustrate that the combination of nanogel and surfactant will form clusters at the oil-water interface. The 3-D image on the right shows an emulsified oil droplet in green color, and nanogel-surfactant solution, in white color, at the interface. To better visualize the nanogel-surfactant clusters, oil droplet is not shown in the 3-D image on left. Here, the white color represents the solid-like clusters created by the synergy between nanogel and surfactant.

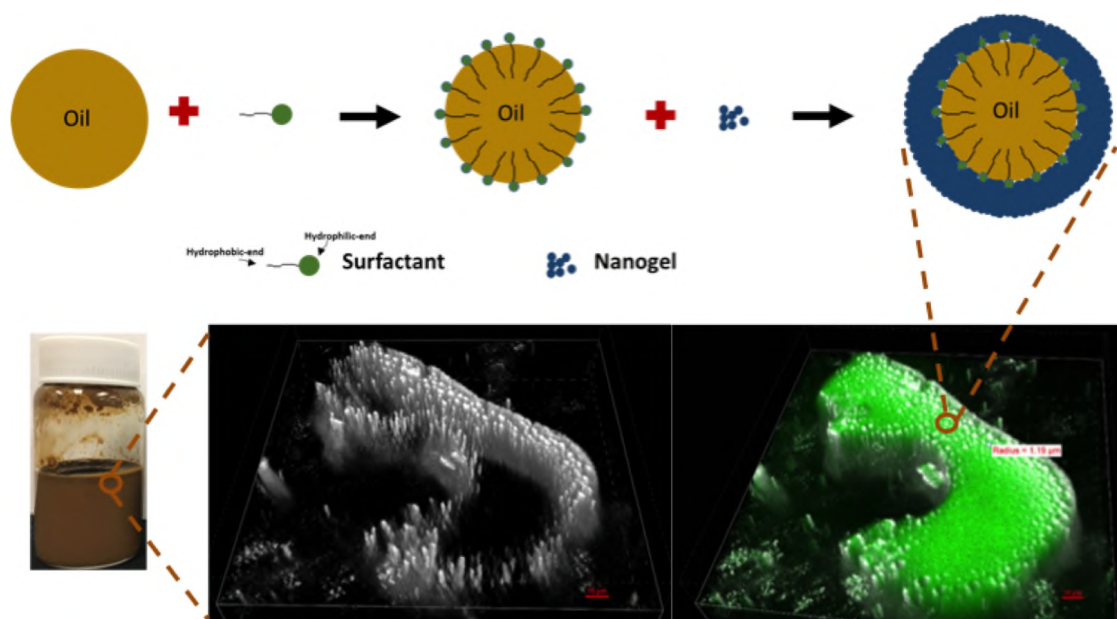


Figure 4. An illustration of emulsified oil droplet stabilized by nanogel and surfactant. 3-D confocal images show oil droplets in green and nanogel-surfactant clusters in white.

3. RESULTS AND DISCUSSION

The characterization and stability of nanogel-surfactant stabilized oil-in-water emulsion systems are discussed and compared with emulsion systems stabilized solely by surfactants or nanogels. The studies on particle size (DLS), surface ζ potential and confocal microscopic images are provided to give further insights into the investigation.

3.1. CHARACTERIZATION OF NANOGEL AND SURFACTANTS

The employed nanogels are crosslinked and deformable polymeric particles with a dried particle size of 50-100 nm that are able to swell several times in brine. Table 4 illustrates the physiochemical properties of the nanogel (1 gram/liter), including the surface ζ potential, pH and polydispersity index (PDI) in different brines. The average hydrodynamic diameter of the nanogel in seawater is 222.5 nm, as shown in Figure 5. The particle size expands to 247 and 335 in 10-times diluted and 100-times diluted seawater, respectively. The good stability of the synthesized nanogel in the displacing fluid is suggested by the narrow size distribution with one peak pointing to a predominant droplet size.

Table 4. Physiochemical properties of the employed nanogel dispersed in different brines.

Brine	Hydrodynamic diameter (nm)	Zeta potential (mv)	pH
Seawater	222.1	-30.8	7.0
10 DSW ^a	247.2	-39.4	7.0
100 DSW ^b	335.8	-56.2	7.0

^a10-times diluted seawater

^b100-times diluted seawater

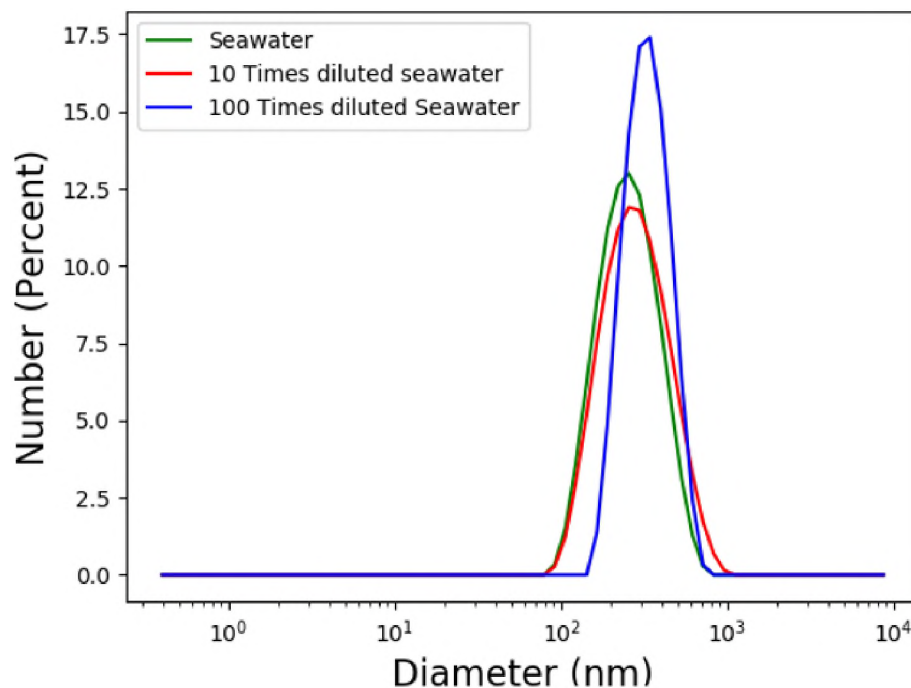


Figure 5. Particle size distribution of nanogel dispersed in several brine types at a concentration of 1 gram/liter and a temperature of 25° C.

Furthermore, the surface ζ -potential measurements, which reflect the stability of the dispersions, were highly related to brine concentrations. The ζ potential of nanogel solely dispersions showed an increase from -56.2 to -30.8 mV with brine concentration. Similar trend was observed for nanogel combined with anionic surfactant (SDS) as ζ potential increased from -48.6 to -21.7 mV. However, the ζ potential of nanogel combined with cationic surfactant (CTAB) slightly decreased from -6.6 to -7.4 mV, as shown in Figure 6, whereas the nanogels combined with neutral charged surfactant (Tween[®] 60) were hardly affected by brine concentration and stayed at \sim -9 mV as the brine concentration increased from 580 to 58,000 ppm.

The high ζ potential values reflect the stability of nanogel dispersions where the electrostatic repulsion exceeds the net attraction force between droplets which resists and minimizes aggregation and flocculation. The increase in ionic strength at high brine

concentrations reduced the ζ potential of nanogels alone and combined with anionic and neutral charged surfactants. However, the ionic strength was not high enough to reduce the ζ potential of nanogels combined with cationic surfactant.

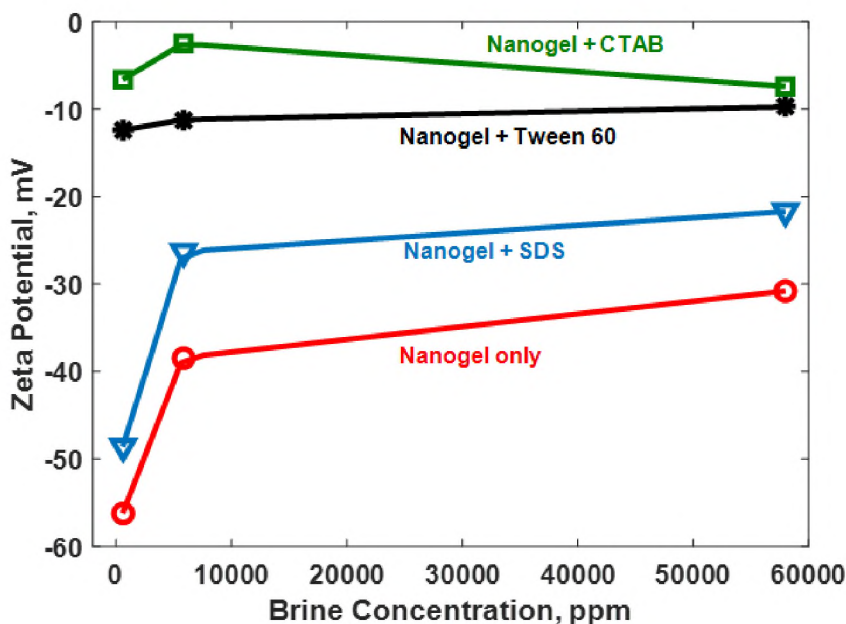


Figure 6. ζ potential of cationic, anionic, and neutral surfactants combined with anionic nanogel at various brine salinities.

3.2. PICKERING EMULSION CHARACTERIZATION

In this study, oil-in-water Pickering emulsions were stabilized by: (1) solely nanogel solutions in several brine salinities, (2) solely surfactants in several salinities, and (3) combination of nanogel and surfactants under various conditions including brine salinity, pH, and homogenizing time.

Figure 7 shows confocal microscopy images of Pickering emulsions stabilized by 0.1 wt.% nanogel dispersed in different brine salinities. It indicates that oil-in-water emulsions can be formed in both high and low brine salinities. However, smaller emulsified oil droplets were formed in higher brine salinity due to its smaller particle size (Figure 5). The shape of the emulsified oil droplets in both nanogel salinities was round which indicated that nanogels

were able to assemble themselves at the interface between oil and water phases. Figures 8, 9 and 10 show the confocal microscopy images of surfactants with different surface charges dispersed in several brine salinities. Tween[®] 60 can form emulsions with a mixture of small and big emulsified oil droplets. It was also observed that emulsions stabilized by Tween[®] 60 started to flocculate within few hours which might be due to the tested concentration which was much larger than the CMC, as illustrated in Figure 8. However, the shape of the emulsified oil droplets was very uniform indicating that Tween[®] 60 distributed evenly at the oil-water interface.

Figure 9 shows the confocal microscopy images of emulsions stabilized by CTAB in several brine salinities. It was observed that larger oil droplets were surrounded by very small ones which indicated that flocculation was faster in lower brine salinity. However, smaller emulsified oil droplets that flocculated within hours were observed in higher brine salinity.

Figure 10 illustrates the confocal images of emulsions stabilized by SDS in different brine salinities. It was observed that larger emulsified oil droplets were generated in high brine salinity which indicated that coalescence and flocculation were fast. However, oil-in-water emulsions stabilized by SDS in lower brine salinity generated smaller oil droplets that were stable against coalescence and flocculation for days.

These results indicate that the creaming process of the Pickering emulsions stabilized solely by nanogel, Tween[®] 60, CTAB, or SDS was greatly affected by the salinity of the displacing fluid.

3.3. EFFECT OF BRINE SALINITY ON NANOGEL-SURFACTANT PICKERING EMULSION

Reservoir salinity is a key factor that greatly influences the physiochemical properties of nanogels, and eventually the stability of the Pickering emulsions. In this work, the effect of brine salinity on the stability of several nanogel-surfactant Pickering emulsions was

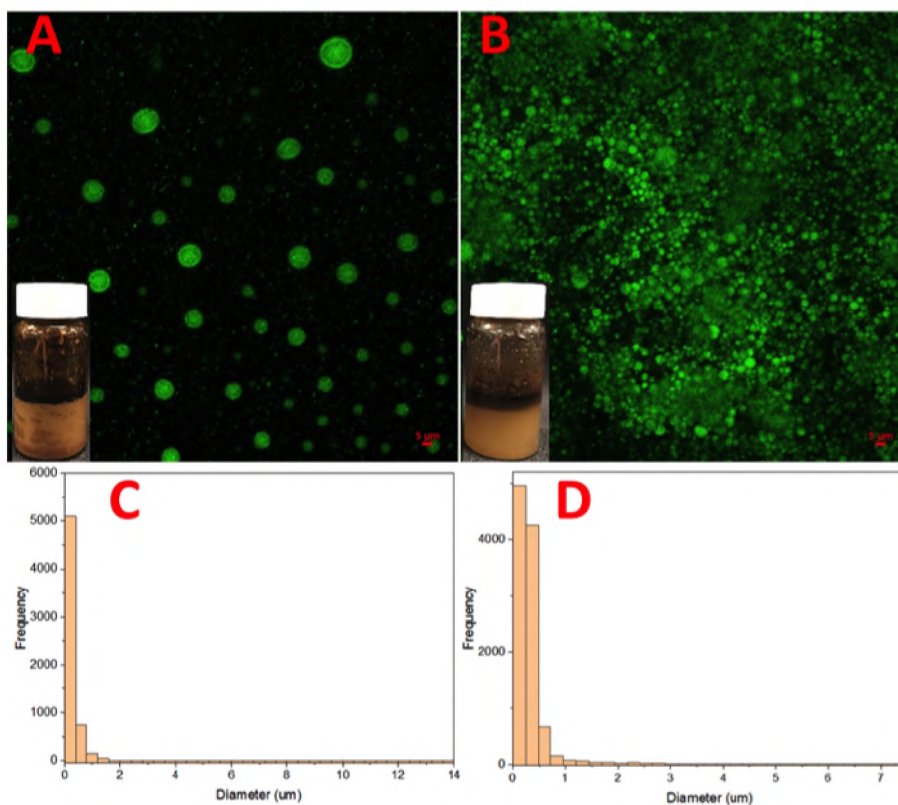


Figure 7. Confocal microscopy images of emulsions stabilized by 0.1 wt.% nanogel dispersed in (A) 100-times diluted seawater, and (B) seawater. Emulsified oil drops are shown in green color. Scale bars are 5 μm . Particle size distribution of emulsified oil droplets stabilized by nanogel in (C) 100-times diluted seawater, and (D) seawater.

evaluated. Figures 11 and 12 show the confocal images of emulsions stabilized by nanogel combined with Tween[®] 60 in several brine salinities. At neutral pH conditions, lower brine salinity generated relatively larger oil droplets with elongated shape indicating that smaller oil drops flocculated to form larger ones. However, higher brine salinity generated smaller oil droplets with uniform round shape, as illustrated in Figure 12.

Figure 13 illustrates the confocal images of emulsions stabilized by nanogel combined with CTAB while dispersed in 100-times diluted seawater. At neutral pH condition, emulsified oil droplets flocculated to form larger oil bulks. Similar phenomenon was ob-

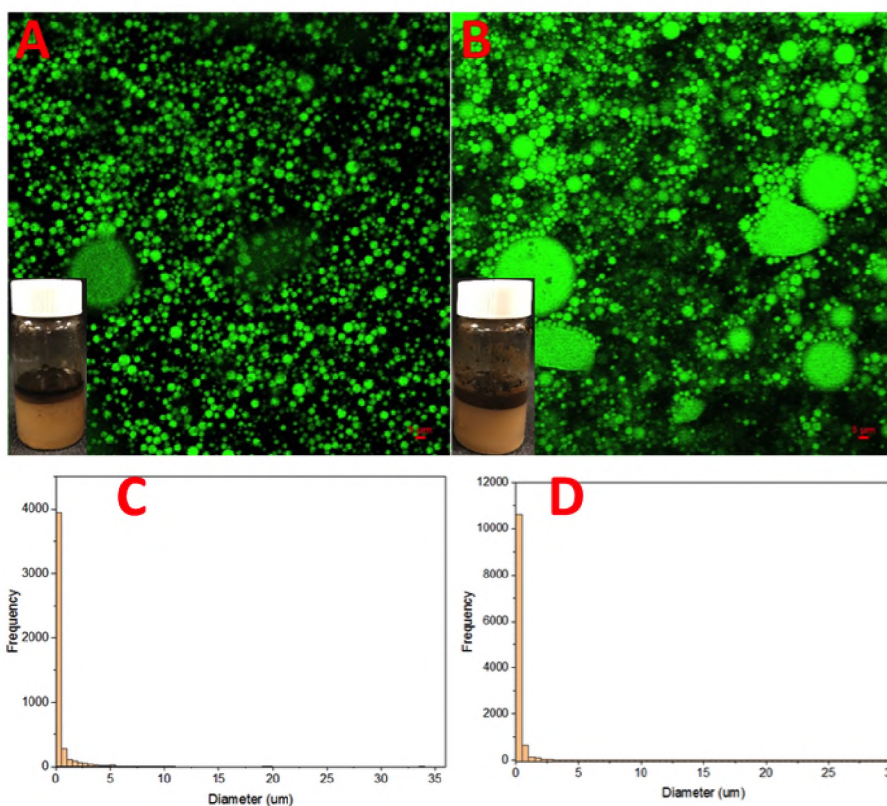


Figure 8. Confocal microscopy images of emulsions stabilized by 0.1 wt.% Tween[®] 60 dispersed in (A) 100-times diluted seawater, and (B) seawater. Emulsified oil drops are shown in green color. Scale bars are 5 μm . Particle size distribution of emulsified oil droplets stabilized by Tween[®] 60 in (C) 100-times diluted seawater, and (D) seawater.

served when nanogel and CTAB were dispersed in seawater, as shown in Figure 14. This indicates that the synergy between anionic nanogel and cationic surfactant destabilizes Pickering emulsions.

Figure 15 displays confocal images of emulsions stabilized by nanogel and SDS while dispersed in 100-times diluted seawater. It shows, at neutral pH condition, that smaller emulsified oil droplets were generated with uniform round shape indicating that nanogel-SDS particles were distributed evenly at the interface. On the other hand, larger emulsified oil droplets were generated in seawater, as shown in Figure 16, indicating that higher brine salinity destabilized the Pickering emulsion.

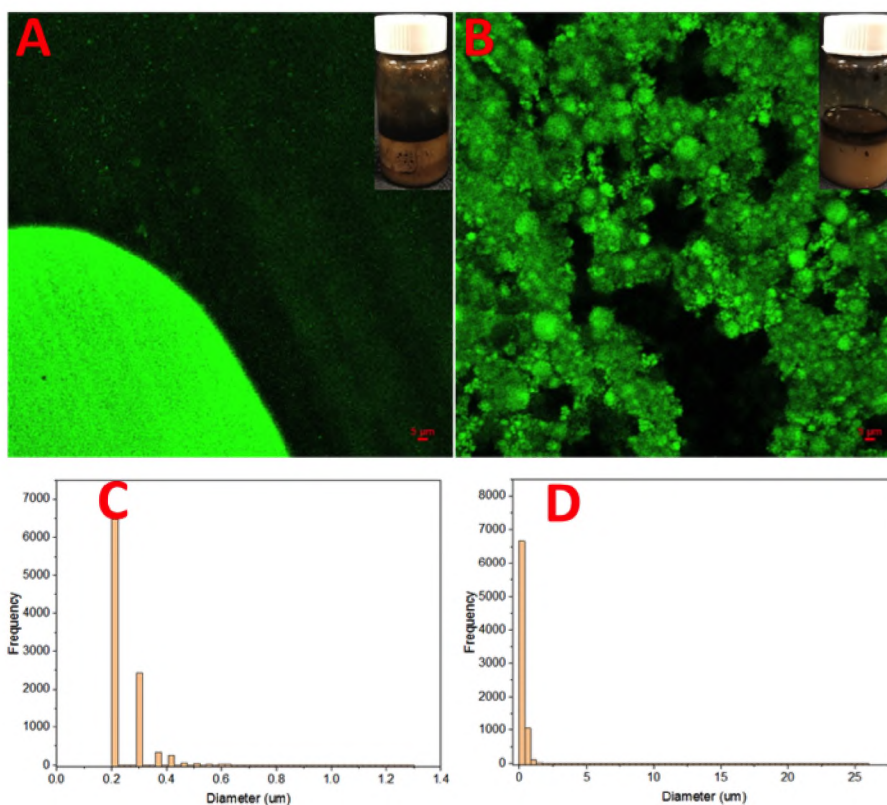


Figure 9. Confocal microscopy images of emulsions stabilized by 0.1 wt.% CTAB dispersed in (A) 100-times diluted seawater, and (B) seawater. Emulsified oil drops are shown in green color. Scale bars are 5 μm . Particle size distribution of emulsified oil droplets stabilized by CTAB in (C) 100-times diluted seawater, and (D) seawater.

3.4. EFFECT OF PH ON NANOGEL-SURFACTANT PICKERING EMULSION

The behavior of the Pickering emulsions stabilized by nanogel combined with several surfactants while dispersed in different brine salinities was examined under several pH. The pH of the Pickering emulsions in the experiment was adjusted by the addition of minimal concentrated hydrochloric acid (HCl) or Sodium hydroxide (NaOH) to brine solution, ranging from 1.0 to 13.0.

It was observed that the emulsion stability in nanogel-Tween[®] 60 systems dispersed in 100-times diluted seawater significantly reduced under pH 13.0 while the creaming process of the emulsion phase dramatically delayed in basic conditions than the in acidic

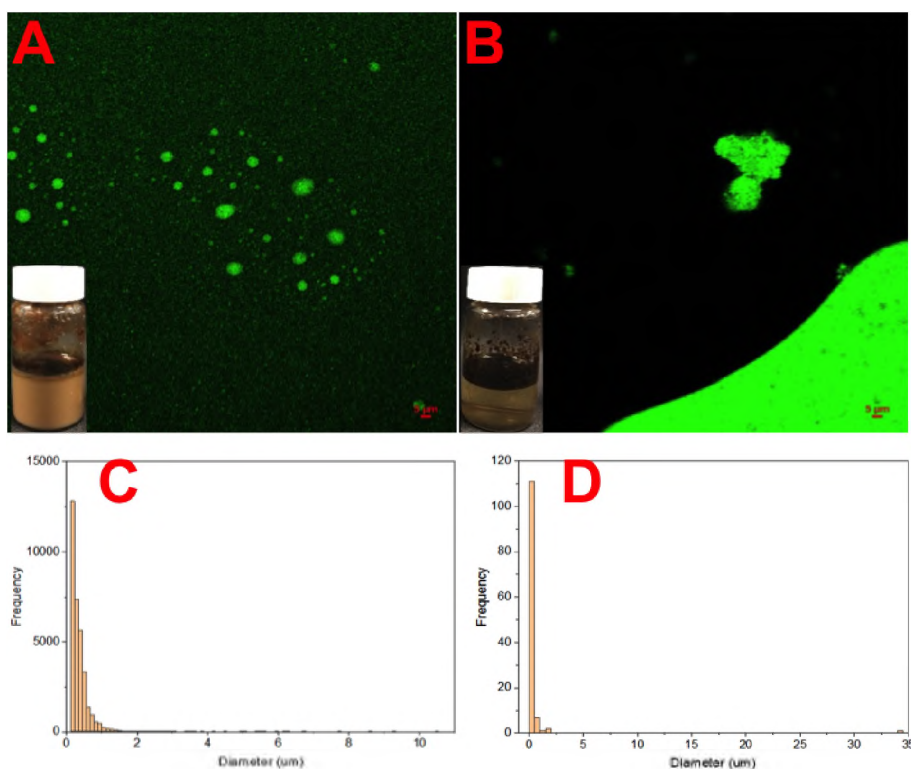


Figure 10. Confocal microscopy images of emulsions stabilized by 0.1 wt.% SDS dispersed in (A) 100-times diluted seawater, and (B) seawater. Emulsified oil drops are shown in green color. Scale bars are 5 μm . Particle size distribution of emulsified oil droplets stabilized by SDS in (C) 100-times diluted seawater, and (D) seawater.

conditions, as shown in Figure 11. The emulsified oil droplets tended to flocculate and coalescence within few hours under strong basic conditions, which remarkably reduced the stability of the Pickering emulsions. The coalescence of emulsified oil droplets was delayed under strong acidic conditions. In addition, emulsions stabilized by nanogel-Tween[®] 60 systems dispersed in lower brine salinity produced round-shaped oil droplets indicating that particles distributed evenly at the oil-brine interface. Figure 12 shows the confocal microscopy images of Pickering emulsions stabilized by nanogel-Tween[®] 60 systems dispersed in seawater under several pH. It was observed that the emulsion stability

reduced under strong basic and acidic conditions where emulsified oil droplets flocculated and coalesced within few hours, while the creaming process was noticeably delayed under neutral conditions.

Figure 13 illustrates confocal images of emulsion systems stabilized by nanogel-CTAB while dispersed in 100-times diluted seawater under several pH. It shows that the emulsion stability reduced under strong basic conditions. However, emulsions under all tested pH generated relatively larger emulsified oil droplets due to the synergy between nanogel and CTAB. Similar phenomena were observed in emulsions stabilized by nanogel-CTAB while dispersed in seawater, as shown in Figure 14. The opposite surface charges of nanogel and CTAB played an essential role on reducing the stability of these Pickering emulsions.

Confocal images of Pickering emulsions stabilized by nanogel-SDS while dispersed in 100-times diluted seawater are shown in Figure 15. It illustrates that the stability reduced under acidic conditions while the coalescence was delayed in strong basic samples. Under strong acidic conditions, the emulsified oil droplets tended to flocculate and coalesce which significantly reduced the stability of the Pickering emulsions. On the other hand, samples with pH of 7 and above showed good stability with an average emulsified oil droplet of $0.2 \mu\text{m}$. Figure 16 shows confocal images of emulsion systems stabilized by nanogel-SDS while dispersed in seawater and several pH. It illustrates that the emulsion stability reduced under strong basic and acidic conditions where emulsified oil droplets started to flocculate very quickly. It was also noted that Pickering emulsions stabilized by nanogel-SDS generated oil droplets with relatively round shape under pH of 5-7, however, droplets were smaller in size when dispersed in lower brine salinity.

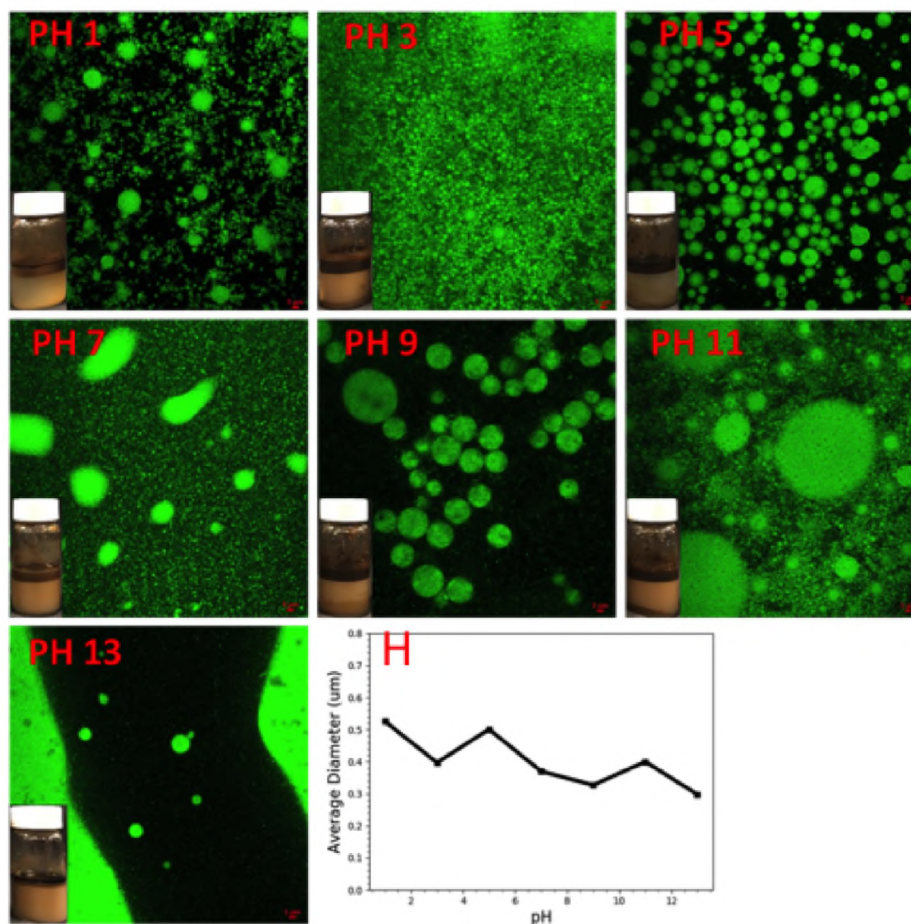


Figure 11. Confocal microscopy images of Pickering emulsions stabilized by 0.1 wt.% nanogel and Tween[®] 60 dispersed in 100-times diluted seawater at pH from 1 to 13. Scale bars are 5 μm . (H) the average diameter of emulsified oil droplets.

3.5. EFFECT OF HOMOGENIZING TIME ON NANOGEL - SURFACTANT PICKERING EMULSION

The shear between the formation fluids and the rock surface induces the in-situ oil emulsification. In general, in order to generate emulsion system, energy (shear) must be supplied to initiate emulsification. In this work, the effect of fragmentation energy on the behavior of Pickering emulsions stabilized by nanogel and several surfactants in different brine salinities was studied using ultrasound energy with multiple duration times in the range of 30-240 seconds. The stability of the emulsion systems exhibited a significant

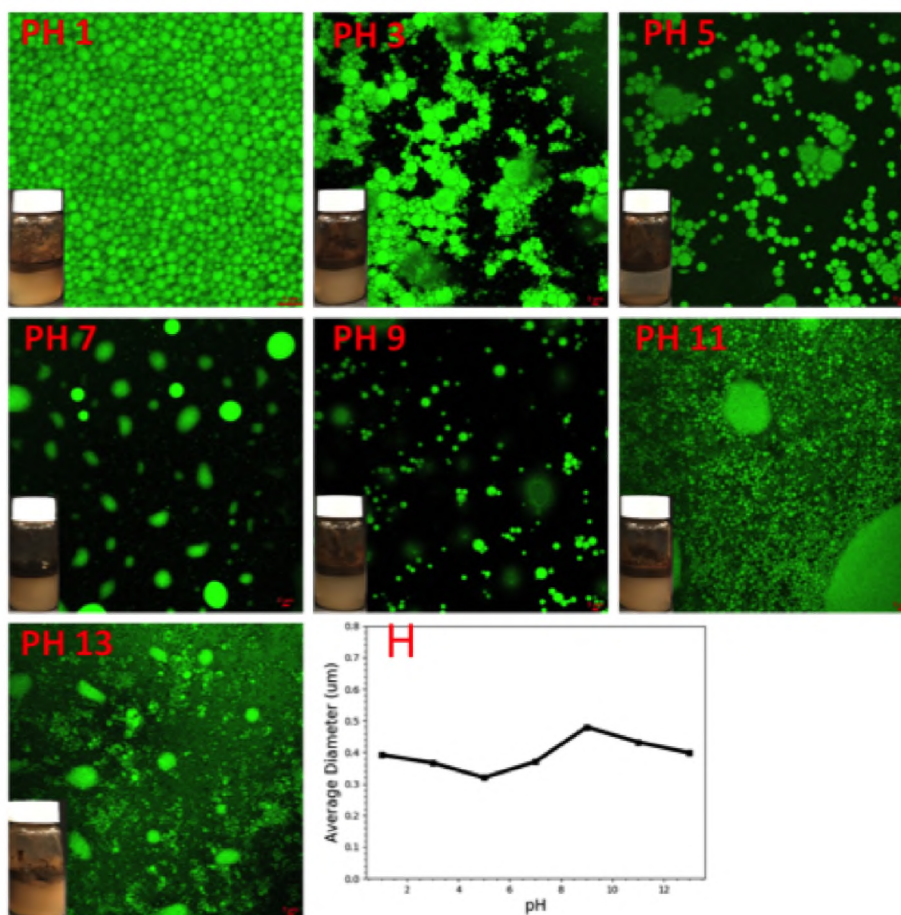


Figure 12. Confocal microscopy images of Pickering emulsions stabilized by 0.1 wt.% nanogel and Tween[®] 60 dispersed in seawater at pH from 1 to 13. Scale bars are 5 μm . (H) the average diameter of emulsified oil droplets.

dependence on the sonication duration. It was observed that the emulsion stability in nanogel-Tween[®] 60 systems dispersed in 100-times diluted seawater significantly reduced under 30-60 seconds of sonication which suggested that shorter times were not enough to produce stable emulsions, as shown in Figure 17. Longer sonication times were required to generate smaller and rounded emulsified oil droplets. Figure 18 illustrates that the stability of the nanogel-Tween[®] 60 emulsions dispersed in seawater at different sonication times was affected by the brine salinity. Here, higher brine salinity generated larger and less stable emulsified oil droplets.

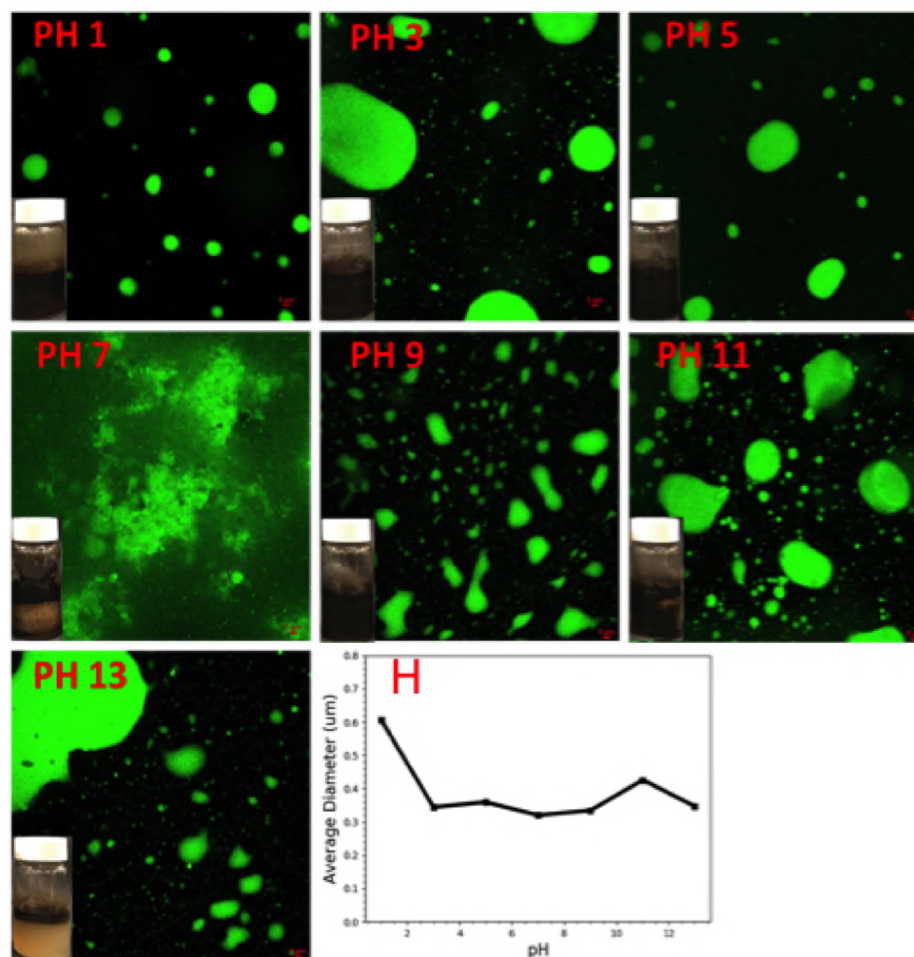


Figure 13. Confocal microscopy images of Pickering emulsions stabilized by 0.1 wt.% nanogel and CTAB dispersed in 100-times diluted seawater at pH from 1 to 13. Scale bars are 5 μm. (H) the average diameter of emulsified oil droplets.

The synergy between the employed anionic nanogel and cationic surfactant caused their Pickering emulsion systems not to be stable regardless of the sonication time and brine salinity, as shown in Figures 19 and 20. Emulsified oil droplets tended to flocculate with bigger oil drops without coalescence happening. These confocal images suggested that Pickering emulsions stabilized by nanogel combined with CTAB were not stable. Not only the long-term stability of these emulsion systems was poor under long sonication time, but emulsification failed since full dispersion of oil could not be achieved as oil-brine separation quickly took place due to the synergy between nanogel-CTAB particles.

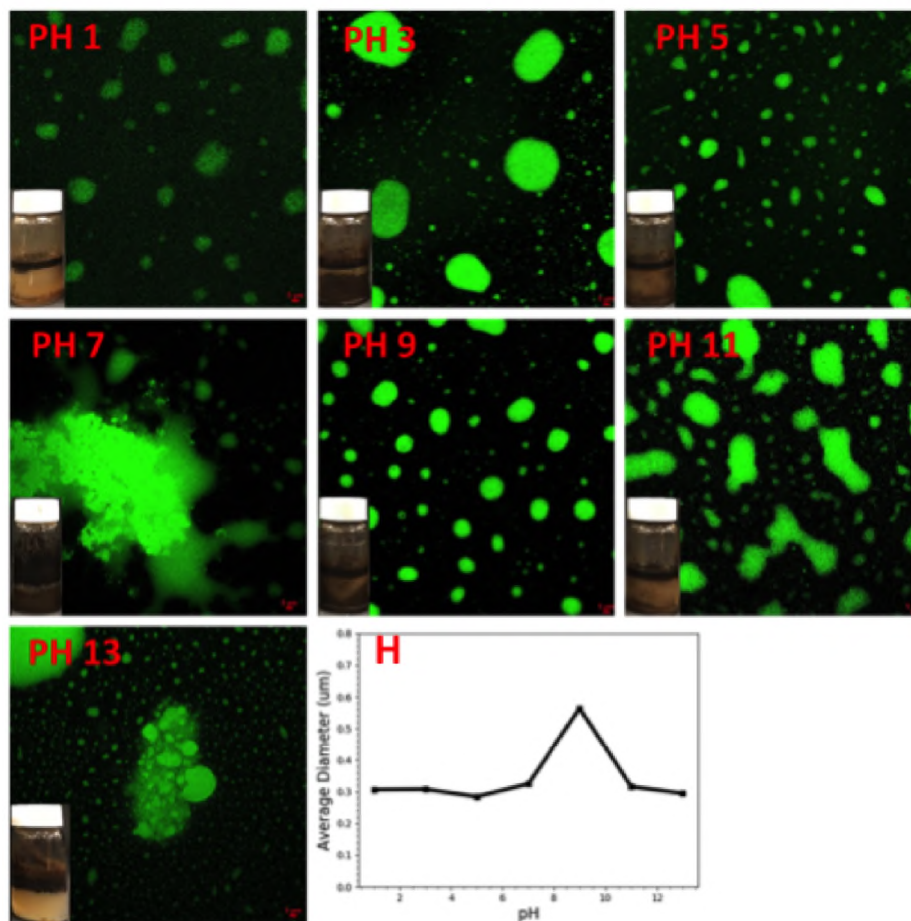


Figure 14. Confocal microscopy images of Pickering emulsions stabilized by 0.1 wt.% nanogel and CTAB dispersed in seawater at pH from 1 to 13. Scale bars are 5 μm . (H) the average diameter of emulsified oil droplets.

Figures 21 and 22 illustrate the confocal images of Pickering emulsions stabilized by nanogel combined with SDS in different brine salinities and under several sonication times. It was observed that little amount of energy was sufficient to produce stable emulsified oil droplets in lower brine salinity. However, longer periods of sonication were not sufficient enough to generate relatively stable emulsions in higher brine salinity. Here, emulsified oil droplets tended to flocculate with bigger drops.

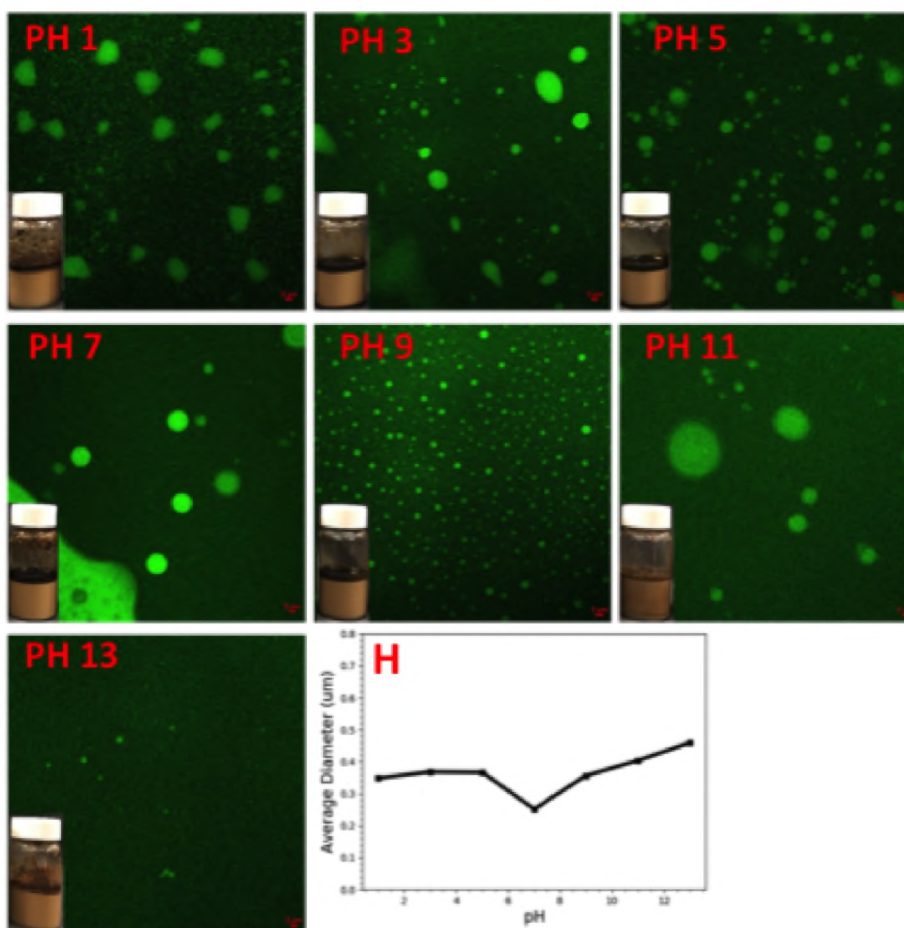


Figure 15. Confocal microscopy images of Pickering emulsions stabilized by 0.1 wt.% nanogel and SDS dispersed in 100-times diluted seawater at pH from 1 to 13. Scale bars are 5 μm . (H) the average diameter of emulsified oil droplets.

4. CONCLUSIONS

The stability against coalescence and flocculation of oil-in-water Pickering emulsions in the presence of polymeric nanogel combined with different surfactants in different brine salinities, pH and sonication times has been investigated. The size of the employed nanogel was found to be greatly influenced by the brine salinity. Furthermore, the ζ -potential measurements, which reflect the stability of the dispersions, were highly affected by brine salinity, especially when nanogel was combined with anionic surfactant. The use of surfactants, in the mixed O/W emulsion systems, resulted in improving the stability of

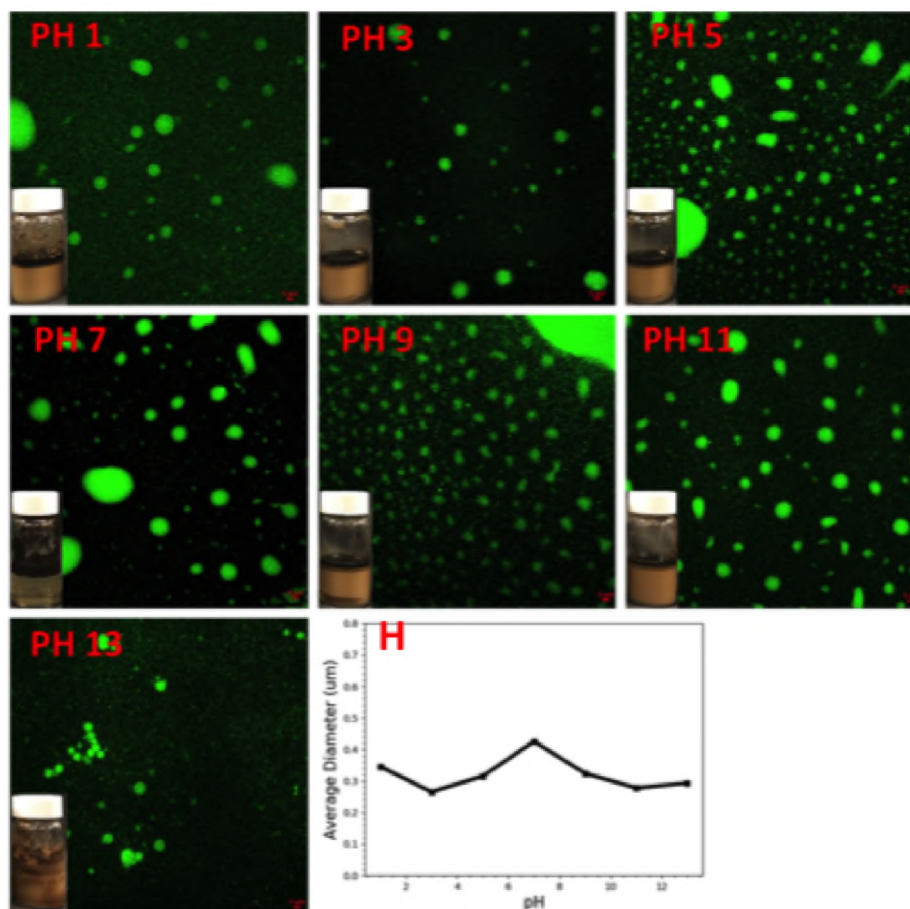


Figure 16. Confocal microscopy images of Pickering emulsions stabilized by 0.1 wt.% nanogel and SDS dispersed in seawater at pH from 1 to 13. Scale bars are 5 μm . (H) the average diameter of emulsified oil droplets.

Pickering emulsions. More specifically, nanogel particles, adsorbed at the oil-water interface when combined with anionic surfactant, were distributed evenly at oil-brine interface as brine salinity reduced. The synergy between nanogel and cationic surfactant lowered the stability of their emulsions as oil droplets tended to flocculate within few hours regardless of the brine salinity and sonication time. Stable Pickering emulsions were prepared by little amount of energy supplied by ultrasound power in the range of 30-240 seconds when nanogel was combined with anionic surfactant where emulsified oil droplets had an average particle size of 0.2 μm .

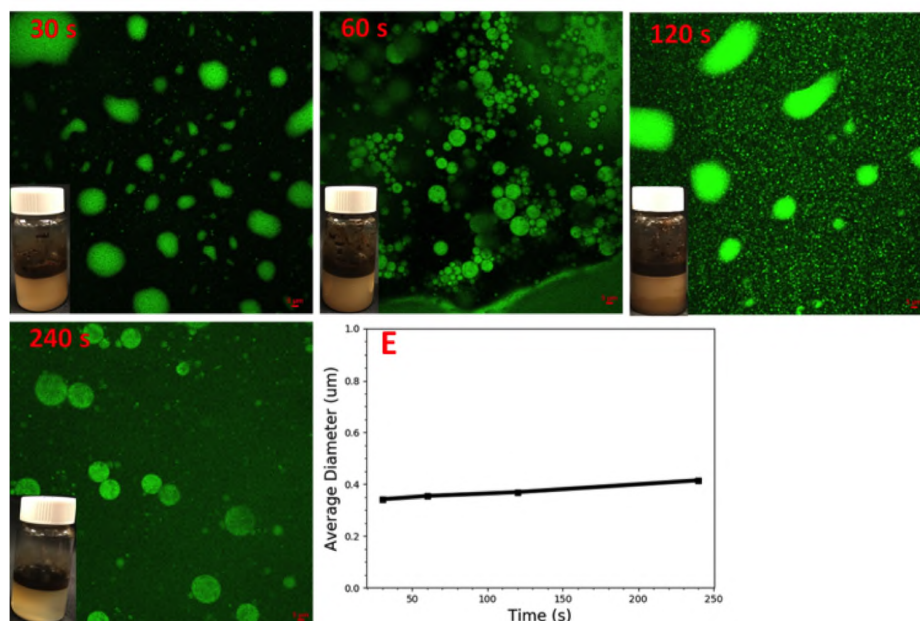


Figure 17. Confocal microscopy images of Pickering emulsions stabilized by 0.1 wt.% nanogel and Tween[®] 60 dispersed in 100-times diluted seawater at several homogenizing times from 30 to 240 seconds. Scale bars are 5 μm. (E) the average diameter of emulsified oil droplets.

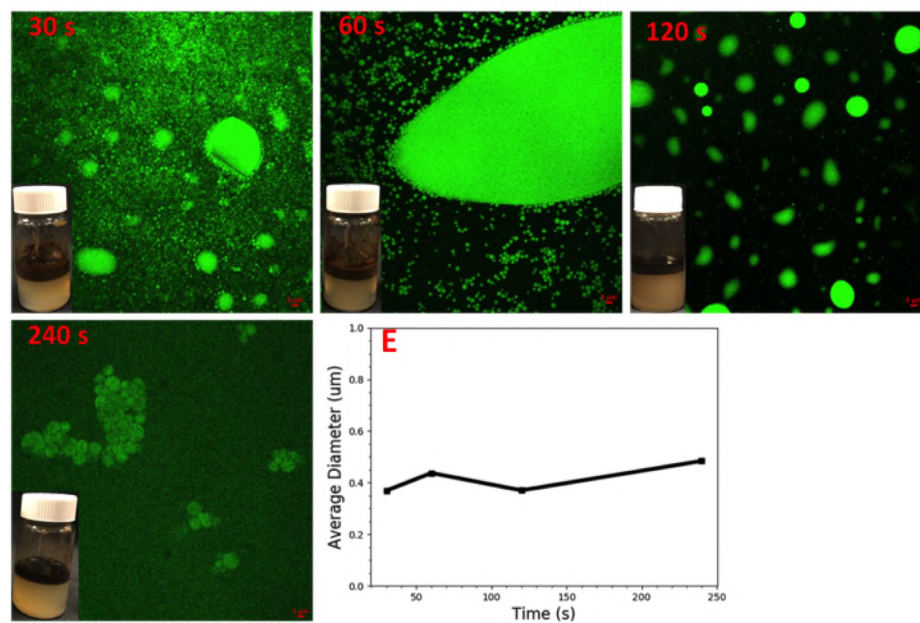


Figure 18. Confocal microscopy images of Pickering emulsions stabilized by 0.1 wt.% nanogel and Tween[®] 60 dispersed in seawater at several homogenizing times from 30 to 240 seconds. Scale bars are 5 μm. (E) the average diameter of emulsified oil droplets.

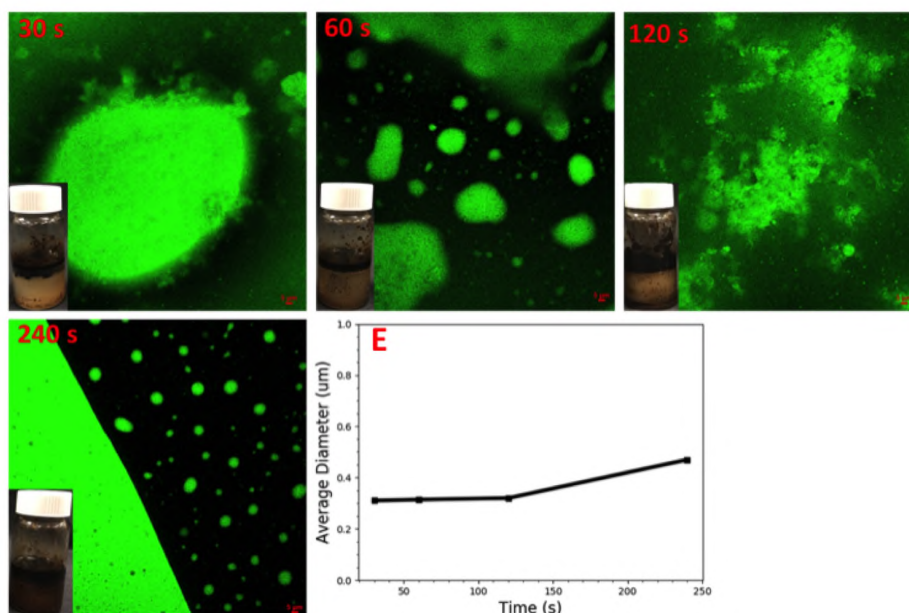


Figure 19. Confocal microscopy images of Pickering emulsions stabilized by 0.1 wt.% nanogel and CTAB dispersed in 100-times diluted seawater at several homogenizing times from 30 to 240 seconds. Scale bars are 5 μm. (E) the average diameter of emulsified oil droplets.

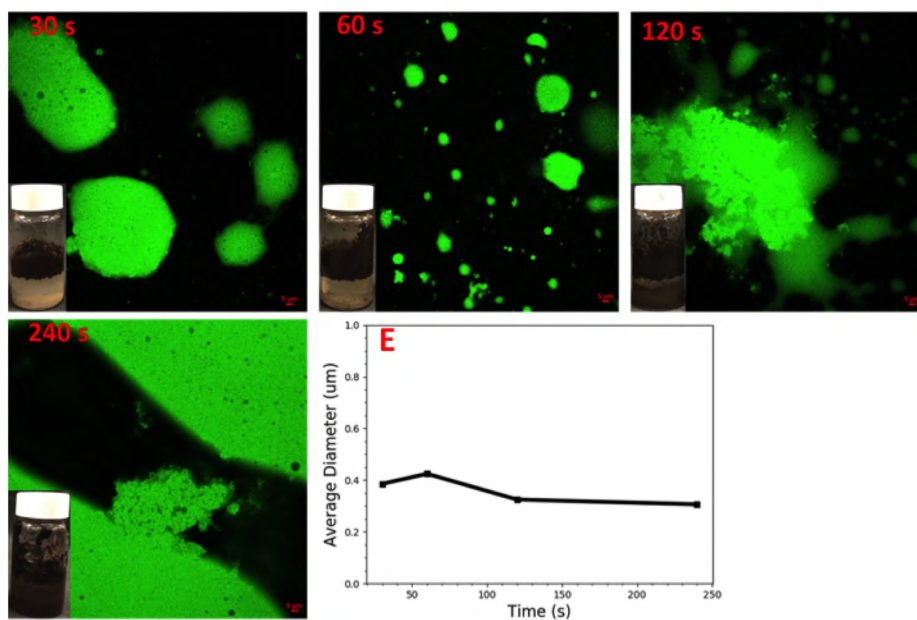


Figure 20. Confocal microscopy images of Pickering emulsions stabilized by 0.1 wt.% nanogel and CTAB dispersed in seawater at several homogenizing times from 30 to 240 seconds. Scale bars are 5 μm. (E) the average diameter of emulsified oil droplets.

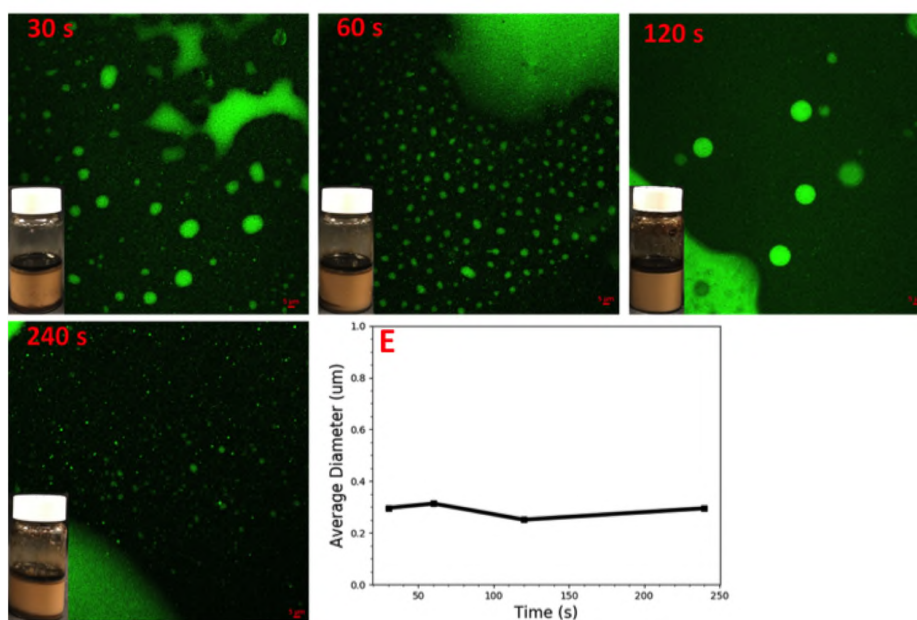


Figure 21. Confocal microscopy images of Pickering emulsions stabilized by 0.1 wt.% nanogel and SDS dispersed in 100-times diluted seawater at several homogenizing times from 30 to 240 seconds. Scale bars are 5 μm . (E) the average diameter of emulsified oil droplets.

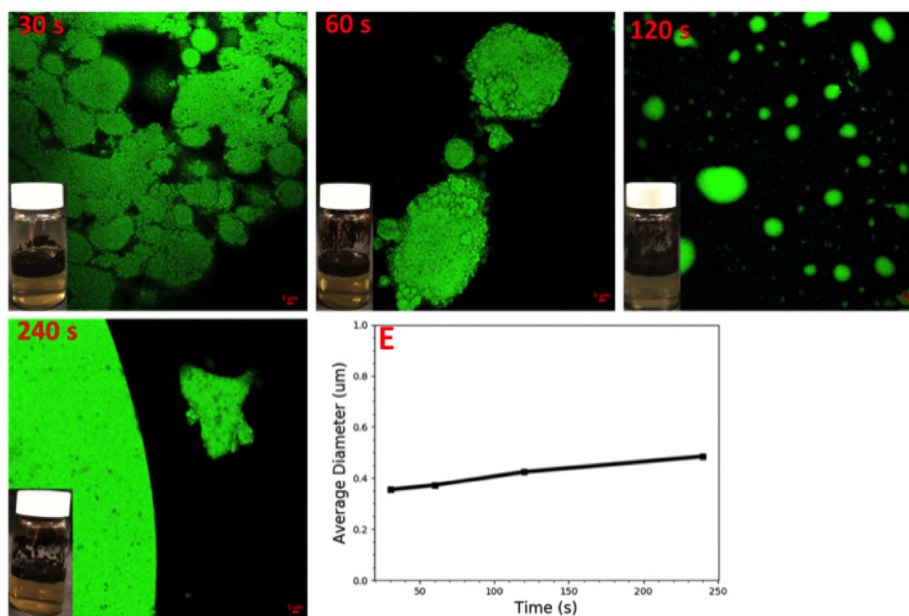


Figure 22. Confocal microscopy images of Pickering emulsions stabilized by 0.1 wt.% nanogel and SDS dispersed in seawater at several homogenizing times from 30 to 240 seconds. Scale bars are 5 μm . (E) the average diameter of emulsified oil droplets.

NOMENCLATURE

NG Nanogel.

SW Seawater.

10-DSW 10 times diluted seawater.

100-DSW 100 times diluted seawater.

ppm Parts per million.

SDS Sodium dodecyl sulfate.

PV Pore volume.

CMC Critical micelle concentration.

AMPS 2-acrylamido 2-methyl propane sulfonic acid monomer.

CTAB Cetyltrimethyl ammonium bromide.

TDS Total dissolved solids.

REFERENCES

- Achilleos, D. S. and Vamvakaki, M., 'End-grafted polymer chains onto inorganic nano-objects,' *Materials*, 2010, **3**(3), pp. 1981–2026.
- Almohsin, A., Alabdulmohsen, Z., Bai, B., Neogi, P., *et al.*, 'Experimental study of crude oil emulsion stability by surfactant and nanoparticles,' in 'SPE EOR Conference at Oil and Gas West Asia,' Society of Petroleum Engineers, 2018 .
- Aveyard, R., Binks, B. P., and Clint, J. H., 'Emulsions stabilised solely by colloidal particles,' *Advances in Colloid and Interface Science*, 2003, **100**, pp. 503–546.
- Becher, P., 'Encyclopedia of emulsion technology,' Basic theory, 1983, **1**, pp. 58–125.
- Binks, B. P., Murakami, R., Armes, S. P., and Fujii, S., 'Effects of ph and salt concentration on oil-in-water emulsions stabilized solely by nanocomposite microgel particles,' *Langmuir*, 2006, **22**(5), pp. 2050–2057.

- Binks, B. P. and Whitby, C. P., 'Nanoparticle silica-stabilised oil-in-water emulsions: improving emulsion stability,' *Colloids and Surfaces A: Physicochemical and Engineering Aspects*, 2005, **253**(1-3), pp. 105–115.
- Delmas, T., Piraux, H., Couffin, A.-C., Texier, I., Vinet, F., Poulin, P., Cates, M. E., and Bibette, J., 'How to prepare and stabilize very small nanoemulsions,' *Langmuir*, 2011, **27**(5), pp. 1683–1692.
- Goddard, E. D. and Vincent, B., *Polymer adsorption and dispersion stability*, ACS Publications, 1984.
- Griffith, N., Ahmad, Y., Daigle, H., Huh, C., *et al.*, 'Nanoparticle-stabilized natural gas liquid-in-water emulsions for residual oil recovery,' in 'SPE improved oil recovery conference,' Society of Petroleum Engineers, 2016 .
- Guzman, E., Orsi, D., Cristofolini, L., Liggieri, L., and Ravera, F., 'Two-dimensional dppc based emulsion-like structures stabilized by silica nanoparticles,' *Langmuir*, 2014, **30**(39), pp. 11504–11512.
- He, Y., Wu, F., Sun, X., Li, R., Guo, Y., Li, C., Zhang, L., Xing, F., Wang, W., and Gao, J., 'Factors that affect pickering emulsions stabilized by graphene oxide,' *ACS applied materials & interfaces*, 2013, **5**(11), pp. 4843–4855.
- Johansson, D., Bergenståhl, B., and Lundgren, E., 'Wetting of fat crystals by triglyceride oil and water. 1. the effect of additives,' *Journal of the American Oil Chemists' Society*, 1995, **72**(8), pp. 921–931.
- Kabanov, A. V. and Vinogradov, S. V., 'Nanogels as pharmaceutical carriers: finite networks of infinite capabilities,' *Angewandte Chemie International Edition*, 2009, **48**(30), pp. 5418–5429.
- Midmore, B., 'Preparation of a novel silica-stabilized oil/water emulsion,' *Colloids and Surfaces A: Physicochemical and Engineering Aspects*, 1998, **132**(2-3), pp. 257–265.
- Ngai, T., Auweter, H., and Behrens, S. H., 'Environmental responsiveness of microgel particles and particle-stabilized emulsions,' *Macromolecules*, 2006, **39**(23), pp. 8171–8177.
- Pichot, R., Spyropoulos, F., and Norton, I., 'O/w emulsions stabilised by both low molecular weight surfactants and colloidal particles: The effect of surfactant type and concentration,' *Journal of colloid and interface science*, 2010, **352**(1), pp. 128–135.
- Pyun, J., Jia, S., Kowalewski, T., Patterson, G. D., and Matyjaszewski, K., 'Synthesis and characterization of organic/inorganic hybrid nanoparticles: kinetics of surface-initiated atom transfer radical polymerization and morphology of hybrid nanoparticle ultrathin films,' *Macromolecules*, 2003, **36**(14), pp. 5094–5104.

- Samanta, A., Ojha, K., Sarkar, A., and Mandal, A., 'Surfactant and surfactant-polymer flooding for enhanced oil recovery,' *Advances in Petroleum Exploration and Development*, 2011, **2**(1), pp. 13–18.
- Sharma, S. and Sarangdevot, K., 'Nanoemulsions for cosmetics,' *IJARPB*, 2012, **1**(3), pp. 408–415.
- Van Boekel, M. and Walstra, P., 'Stability of oil-in-water emulsions with crystals in the disperse phase,' *Colloids and Surfaces*, 1981, **3**(2), pp. 109–118.
- Yousef, A. A., Al-Saleh, S. H., Al-Kaabi, A., Al-Jawfi, M. S., *et al.*, 'Laboratory investigation of the impact of injection-water salinity and ionic content on oil recovery from carbonate reservoirs,' *SPE Reservoir Evaluation & Engineering*, 2011, **14**(05), pp. 578–593.

SECTION

2. CONCLUSIONS AND RECOMMENDATIONS

2.1. CONCLUSIONS

This dissertation aimed at providing an understanding and evaluation of a novel EOR method consists of polymeric nanogel flooding when combined with two other promising technologies - surfactant and low salinity water flooding. The proposed novel combination is a promising technology in the oil industry. It has great potential in improving oil recovery from both sandstone and carbonate reservoirs. This dissertation consisted of five research papers that have been published or will be submitted for publication. The main conclusions drawn from each paper are listed below.

The main objective of the first paper was to provide an understanding of the recovery mechanisms associated with conventional nanoparticles when combined with surfactants. The recovery mechanisms associated with the combination are mainly classified into three categories: (1) modification of rock wettability towards water-wet, (2) interfacial tension reduction, and (3) oil viscosity reduction and conformance control. All these mechanisms can be achieved by introducing a disjoining pressure between oil-brine-rock and creating a wedge-like structure at the oil-brine interface. Different recovery mechanisms could be achieved by the employment of different sizes, types and concentrations of both nanoparticles and surfactants.

The second paper characterized several properties of a newly developed polymeric nanogel when combined with SDS surfactant. Nanogel showed narrow size distribution when dispersed in high salinity brine with one peak pointing to a predominant homogeneous droplet size. It also showed a good long-term structural stability for a period of two weeks.

The combined technology of nanogel and SDS effectively reduced the interfacial tension between oil-brine to low values. Lower IFT values were observed with increasing nanogel concentration from 0.1 to 1.0 wt%. The core flooding results suggested the ability of the proposed technology to enhance the oil recovery in sandstone reservoirs with permeability that ranged between 70-150 mD up to 15% beyond conventional seawater flooding.

The third paper discussed the potential of nanogel combined with surfactant and low salinity water flooding for sandstone reservoirs with relatively low permeability that ranged between 40-60 mD as a promising method to enhance oil recovery. The core flooding results revealed that the injection mode of nanogel and SDS played an essential role on the amounts of recovered oil. Sequential injections of nanogel and SDS, one after another, had a higher potential to recover additional incremental oil compared to one-slug injection mode. Combining nanogel and SDS with several brine salinities provided a significant increase in oil recovery up to 20% beyond conventional water flooding. It was also observed that the adsorption density of nanogel on sandstone surfaces was lower compared to carbonate rocks which reduced the plugging performance caused by nanogel.

The fourth paper evaluated the performance of nanogel combined with surfactant and low salinity water flooding for carbonate reservoirs with low permeability to improve oil recovery as a potential EOR method. The results revealed that altering the salinity of seawater has a significant impact on the size of nanogel. Lower seawater salinities caused nanogel particles to expand and further swell which increased the plugging performance. It was also observed that SDS injection did not affect the size of nanogel, however, it reduced its adsorption density from rock surfaces. The most substantial observation that needs to be highlighted in this study was the incremental oil recovery obtained by nanogel and SDS injections combined with several salinities of seawater. In general, varying the salinity of seawater after nanogel and SDS injections provided a significant increase in oil recovery up to 27% beyond conventional seawater flooding.

The fifth paper evaluated the stability improvement of oil-in-water emulsions caused by polymeric nanogel combined with several surfactants with different surface charges in several brine salinities, pH and sonication times. The ζ -potential measurements, which reflect the stability of the dispersions, were highly affected by brine salinity, especially when nanogel was combined with anionic surfactants. The combination of nanogel and surfactants in oil-in-water emulsion systems resulted in improving the stability of Pickering emulsions. More specifically, nanogel particles, adsorbed at the oil-water interface when combined with anionic surfactant, were distributed evenly at oil-brine interface as brine salinity reduced. The synergy between nanogel and cationic surfactant lowered the stability of their emulsions as oil droplets tended to flocculate within few hours regardless of the brine salinity and sonication time. Stable Pickering emulsions were prepared by little amount of energy supplied by ultrasound power in the range of 30-240 seconds when nanogel was combined with anionic surfactant where emulsified oil droplets had an average particle size of 0.2 μm .

2.2. RECOMMENDATIONS

Based on the experience and the laboratory knowledge gained from this dissertation, the following future work is recommended.

1. Core flooding experiments were conducted in ambient conditions. Introducing temperature to these experiments will help to identify their feasibility in field applications.
2. All cores used in this work were originally water-wet. Studying the effect of nanogel assisted surfactant flooding and LSWF on oil-wet cores will be beneficial.
3. Further investigation on nano emulsion flooding is suggested.
4. Nanogel flooding showed better results in low permeability cores. It is suggested to test EOR potential of NG in tight reservoirs.

APPENDIX

SYNTHESIS OF POLYMERIC NANOGEL

Na-AMPS nanogel is synthesized in our laboratory using a typical suspension polymerization process. The following materials have been used during the synthesis process. 2-Acrylamido-2-methylpropane sulfonic acid (99%, Sigma-Aldrich) is employed as the main monomer. Tween[®] 60 (CMC = 27 mg/l, Sigma-Aldrich) and Sorbitan monooleate (Span[®] 80, Alfa Aesar) are the two surfactants used during the synthesis. Also, n-decane (Alfa Aesar) is used as the oil phase. Sodium hydroxide (NaOH, 97%, Alfa Aesar) is used to neutralize the monomer solution. N,N'-methylene bis(acrylamide) (MBAA, 99%, Sigma-Aldrich) is the employed cross-linker. Ammonium persulfate ($\geq 98\%$, ACROS Organics) is used as an initiator. Deionized water is used as the water phase during the synthesis. All chemicals are used as received without further purification.

The preparation process could be summarized as follows (Figure 1): NaOH is added to a stirred solution of 15 grams of 2-Acrylamido-2-methylpropane sulfonic acid (AMPS) and 15 grams of deionized water at room temperature until the pH reaches exactly 7.0. Then, 0.1 gram of N,N'-methylene bis(acrylamide) (MBAA) is added to the solution while stirring. The solution is then added to n-decane (40 ml) containing Span[®] 80 (21 g) and Tween[®] 60 (9 g) in a three-neck flask and bubbled with nitrogen while kept in a water bath at 40° C for 15 minutes. After that, 0.2 ml of ammonium persulfate is added to the flask as an initiator. Stirring in the water bath is continued for 2 hours at 40° C. Then, the emulsion is precipitated and washed with acetone and separated by centrifugation. The process of washing the emulsion with acetone is repeated several times to ensure that all surfactants and unreacted monomers are washed out. The final isolated product is dried in the oven at 65° C for 24 hours. Figure 2 shows samples of the dried and dispersed Na-AMPS nanogel.

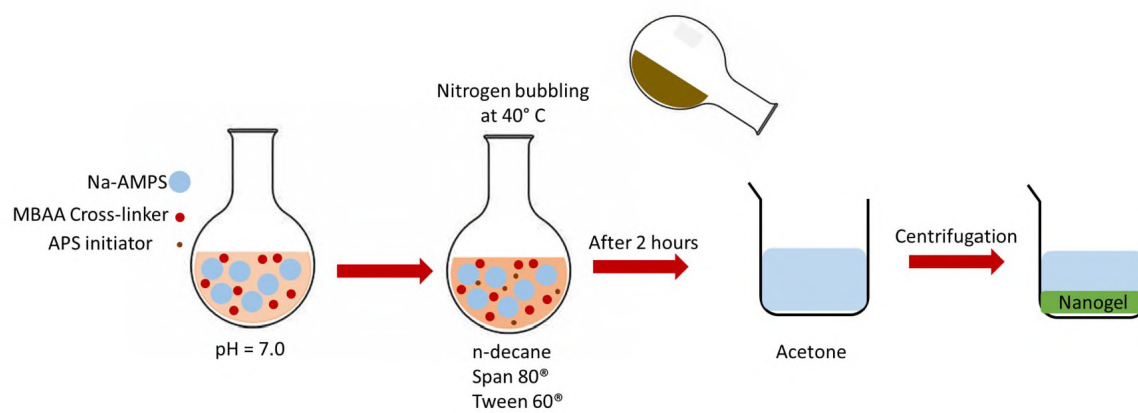


Figure 1. Nanogel synthesis process.

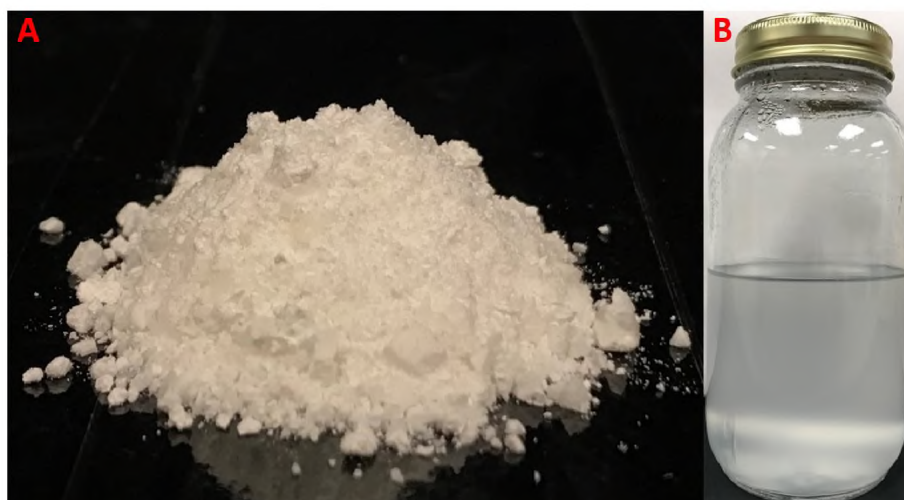


Figure 2. (A) Dried Na-AMPS nanogel. (B) Na-AMPS nanogel dispersed in seawater.

REFERENCES

- Achilleos, D. S. and Vamvakaki, M., 'End-grafted polymer chains onto inorganic nano-objects,' *Materials*, 2010, **3**(3), pp. 1981–2026.
- Afekare, D. A. and Radonjic, M., 'From mineral surfaces and coreflood experiments to reservoir implementations: Comprehensive review of low-salinity water flooding (lswf),' *Energy & fuels*, 2017, **31**(12), pp. 13043–13062.
- Ahmadall, T., Gonzalez, M. V., Harwell, J. H., Scamehorn, J. F., *et al.*, 'Reducing surfactant adsorption in carbonate reservoirs,' *SPE reservoir engineering*, 1993, **8**(02), pp. 117–122.
- Ahmadi, M. A., Shadizadeh, S. R., and , 'Adsorption of novel nonionic surfactant and particles mixture in carbonates: enhanced oil recovery implication,' *Energy & Fuels*, 2012, **26**(8), pp. 4655–4663.
- Ahmadi, M. A. and Shadizadeh, S. R., 'Induced effect of adding nano silica on adsorption of a natural surfactant onto sandstone rock: experimental and theoretical study,' *Journal of Petroleum Science and Engineering*, 2013, **112**, pp. 239–247.
- Ahmadi, Y., Eshraghi, S. E., Bahrami, P., Hasanbeygi, M., Kazemzadeh, Y., and Vahedian, A., 'Comprehensive water-alternating-gas (wag) injection study to evaluate the most effective method based on heavy oil recovery and asphaltene precipitation tests,' *Journal of Petroleum Science and Engineering*, 2015, **133**, pp. 123–129.
- Akbar, M., Vissapragada, B., Alghamdi, A. H., Allen, D., Herron, M., Carnegie, A., Dutta, D., Olesen, J.-R., Chourasiya, R., Logan, D., *et al.*, 'A snapshot of carbonate reservoir evaluation,' *Oilfield Review*, 2000, **12**(4), pp. 20–21.
- Al-Anazi, H. A., Sharma, M. M., *et al.*, 'Use of a ph sensitive polymer for conformance control,' in 'International Symposium and Exhibition on Formation Damage Control,' Society of Petroleum Engineers, 2002 .
- Al-Anssari, S., Barifcani, A., Wang, S., and Iglauer, S., 'Wettability alteration of oil-wet carbonate by silica nanofluid,' *Journal of colloid and interface science*, 2016, **461**, pp. 435–442.
- Almahfood, M. and Bai, B., 'The synergistic effects of nanoparticle-surfactant nanofluids in eor applications,' *Journal of Petroleum Science and Engineering*, 2018, **171**, pp. 196–210.
- Almahfood, M. and Bai, B., 'Characterization and oil recovery enhancement by a polymeric nanogel combined with surfactant for sandstone reservoirs,' submitted to *Journal of Petroleum Science*, 2020a.

- Almahfood, M. and Bai, B., 'Experimental evaluation of polymeric nanogel combined with surfactant and low salinity water flooding for carbonate reservoirs,' Submitted to Journal of Petroleum Science and Engineering, 2020b.
- Almahfood, M. and Bai, B., 'Potential oil recovery enhancement by a polymeric nanogel combined with surfactant for sandstone reservoirs,' in 'OTC 2020,' Offshore Technology Conference, 2020c .
- Almahfood, M., Bai, B., Zhang, Y., and Neogi, P., 'Stability of oil-in-water pickering emulsion in the presence of polymeric nanogels and surfactants,' Submitted to Nature Nanotechnology, 2020.
- Almohsin, A., Alabdulmohsen, Z., Bai, B., Neogi, P., *et al.*, 'Experimental study of crude oil emulsion stability by surfactant and nanoparticles,' in 'SPE EOR Conference at Oil and Gas West Asia,' Society of Petroleum Engineers, 2018 .
- Almohsin, A. M., Bai, B., Imqam, A. H., Wei, M., Kang, W., Delshad, M., Sepehrnoori, K., *et al.*, 'Transport of nanogel through porous media and its resistance to water flow,' in 'SPE Improved Oil Recovery Symposium,' Society of Petroleum Engineers, 2014 .
- Alomair, O. A., Matar, K. M., Alsaeed, Y. H., *et al.*, 'Nanofluids application for heavy oil recovery,' in 'SPE Asia Pacific Oil & Gas Conference and Exhibition,' Society of Petroleum Engineers, 2014 .
- Amanullah, M., Al-Tahini, A. M., *et al.*, 'Nano-technology-its significance in smart fluid development for oil and gas field application,' in 'SPE Saudi Arabia Section Technical Symposium,' Society of Petroleum Engineers, 2009 .
- Amott, E. *et al.*, 'Observations relating to the wettability of porous rock,' 1959.
- Ampian, S. G. and Virta, R. L., *Crystalline silica overview: Occurrence and analysis*, volume 9317, US Department of the Interior, Bureau of Mines, 1992.
- Anderson, W. G. *et al.*, 'Wettability literature survey-part 1: rock/oil/brine interactions and the effects of core handling on wettability,' Journal of petroleum technology, 1986, **38**(10), pp. 1–125.
- Arashiro, E. Y. and Demarquette, N. R., 'Use of the pendant drop method to measure interfacial tension between molten polymers,' Materials Research, 1999, **2**(1), pp. 23–32.
- Austad, T., Milter, J., *et al.*, 'Spontaneous imbibition of water into low permeable chalk at different wettabilities using surfactants,' in 'International Symposium on Oilfield Chemistry,' Society of Petroleum Engineers, 1997 .
- Austad, T., Shariatpanahi, S., Strand, S., Black, C., and Webb, K., 'Conditions for a low-salinity enhanced oil recovery (eor) effect in carbonate oil reservoirs,' Energy & fuels, 2011, **26**(1), pp. 569–575.

- Aveyard, R., Binks, B. P., and Clint, J. H., 'Emulsions stabilised solely by colloidal particles,' *Advances in Colloid and Interface Science*, 2003, **100**, pp. 503–546.
- Ayatollahi, S., Zerafat, M. M., *et al.*, 'Nanotechnology-assisted eor techniques: New solutions to old challenges,' in 'SPE international oilfield nanotechnology conference and exhibition,' Society of Petroleum Engineers, 2012 .
- Bai, B., Liu, Y., Coste, J.-P., Li, L., *et al.*, 'Preformed particle gel for conformance control: transport mechanism through porous media,' *SPE Reservoir Evaluation & Engineering*, 2007, **10**(02), pp. 176–184.
- Bai, B., Wei, M., Liu, Y., *et al.*, 'Field and lab experience with a successful preformed particle gel conformance control technology,' in 'SPE Production and Operations Symposium,' Society of Petroleum Engineers, 2013 .
- Baker, P., Kastner, M., Byerlee, J., and Lockner, D., 'Pressure solution and hydrothermal recrystallization of carbonate sediments—An experimental study,' *Marine Geology*, 1980, **38**(1-3), pp. 185–203.
- Bazazi, P., Gates, I. D., Sanati Nezhad, A., Hejazi, S. H., *et al.*, 'Silica-based nanofluid heavy oil recovery a microfluidic approach,' in 'SPE Canada Heavy Oil Technical Conference,' Society of Petroleum Engineers, 2017 .
- Becher, P., 'Encyclopedia of emulsion technology,' Basic theory, 1983, **1**, pp. 58–125.
- Bell, C. G., Breward, C. J., Howell, P. D., Penfold, J., and Thomas, R. K., 'Macroscopic modeling of the surface tension of polymer- surfactant systems,' *Langmuir*, 2007, **23**(11), pp. 6042–6052.
- Bera, A., Ojha, K., Kumar, T., and Mandal, A., 'Mechanistic study of wettability alteration of quartz surface induced by nonionic surfactants and interaction between crude oil and quartz in the presence of sodium chloride salt,' *Energy & Fuels*, 2012, **26**(6), pp. 3634–3643.
- Binks, B. and Lumsdon, S., 'Influence of particle wettability on the type and stability of surfactant-free emulsions,' *Langmuir*, 2000, **16**(23), pp. 8622–8631.
- Binks, B. P., 'Particles as surfactants—Similarities and differences,' *Current opinion in colloid & interface science*, 2002, **7**(1), pp. 21–41.
- Binks, B. P., Clint, J. H., Dyab, A. K., Fletcher, P. D., Kirkland, M., and Whitby, C. P., 'Ellipsometric study of monodisperse silica particles at an oil- water interface,' *Langmuir*, 2003, **19**(21), pp. 8888–8893.
- Binks, B. P., Desforges, A., and Duff, D. G., 'Synergistic stabilization of emulsions by a mixture of surface-active nanoparticles and surfactant,' *Langmuir*, 2007, **23**(3), pp. 1098–1106.

- Binks, B. P., Kirkland, M., and Rodrigues, J. A., 'Origin of stabilisation of aqueous foams in nanoparticle–surfactant mixtures,' *Soft Matter*, 2008, **4**(12), pp. 2373–2382.
- Binks, B. P., Murakami, R., Armes, S. P., and Fujii, S., 'Effects of pH and salt concentration on oil-in-water emulsions stabilized solely by nanocomposite microgel particles,' *Langmuir*, 2006, **22**(5), pp. 2050–2057.
- Binks, B. P. and Whitby, C. P., 'Nanoparticle silica-stabilised oil-in-water emulsions: improving emulsion stability,' *Colloids and Surfaces A: Physicochemical and Engineering Aspects*, 2005, **253**(1-3), pp. 105–115.
- Bolandtaba, S. F., Skauge, A., and Mackay, E., 'Pore scale modelling of linked polymer solution (Ips)—a new EOR process,' in 'IOR 2009-15th European Symposium on Improved Oil Recovery,' European Association of Geoscientists & Engineers, 2009 pp. cp-124.
- Bust, V. K., Oletu, J. U., Worthington, P. F., *et al.*, 'The challenges for carbonate petrophysics in petroleum resource estimation,' *SPE Reservoir Evaluation & Engineering*, 2011, **14**(01), pp. 25–34.
- Chang, H. L., Sui, X., Xiao, L., Guo, Z., Yao, Y., Yiao, Y., Chen, G., Song, K., Mack, J. C., *et al.*, 'Successful field pilot of in-depth colloidal dispersion gel (cdg) technology in daqing oilfield,' *SPE Reservoir Evaluation & Engineering*, 2006, **9**(06), pp. 664–673.
- Chengara, A., Nikolov, A. D., Wasan, D. T., Trokhymchuk, A., and Henderson, D., 'Spreading of nanofluids driven by the structural disjoining pressure gradient,' *Journal of colloid and interface science*, 2004, **280**(1), pp. 192–201.
- Craig, F. F., *The reservoir engineering aspects of waterflooding*, volume 3, HL Doherty Memorial Fund of AIME New York, 1971.
- Cui, Z.-G., Cui, Y.-Z., Cui, C.-F., Chen, Z., and Binks, B., 'Aqueous foams stabilized by in situ surface activation of CaCO₃ nanoparticles via adsorption of anionic surfactant,' *Langmuir*, 2010, **26**(15), pp. 12567–12574.
- Das, S. K., Choi, S. U., Yu, W., and Pradeep, T., *Nanofluids: science and technology*, John Wiley & Sons, 2007.
- Delmas, T., Piraux, H., Couffin, A.-C., Texier, I., Vinet, F., Poulin, P., Cates, M. E., and Bibette, J., 'How to prepare and stabilize very small nanoemulsions,' *Langmuir*, 2011, **27**(5), pp. 1683–1692.
- Diaz, D., Somaruga, C., Norman, C., Romero, J. L., *et al.*, 'Colloidal dispersion gels improve oil recovery in a heterogeneous Argentina waterflood,' in 'SPE Symposium on Improved Oil Recovery,' Society of Petroleum Engineers, 2008 .

- Ehtesabi, H., Ahadian, M., and Taghikhani, V., 'Investigation of diffusion and deposition of tio₂ nanoparticles in sandstone rocks for eor application,' in '76th EAGE Conference and Exhibition 2014,' 2014 .
- El-Diasty, A. I., Ragab, A. M. S., *et al.*, 'Applications of nanotechnology in the oil & gas industry: Latest trends worldwide & future challenges in egypt,' in 'North Africa Technical Conference and Exhibition,' Society of Petroleum Engineers, 2013 .
- El-Diasty, A. I. *et al.*, 'The potential of nanoparticles to improve oil recovery in bahariya formation, egypt: An experimental study,' in 'SPE Asia Pacific Enhanced Oil Recovery Conference,' Society of Petroleum Engineers, 2015 .
- Engeset, B., *The Potential of Hydrophilic Silica Nanoparticles for EOR Purposes: A literature review and an experimental study*, Master's thesis, Institutt for petroleumsteknologi og anvendt geofysikk, 2012.
- Eskandar, N. G., Simovic, S., and Prestidge, C. A., 'Interactions of hydrophilic silica nanoparticles and classical surfactants at non-polar oil–water interface,' *Journal of colloid and interface science*, 2011, **358**(1), pp. 217–225.
- Esmailzadeh, P., Hosseinpour, N., Bahramian, A., Fakhroueian, Z., and Arya, S., 'Effect of zro₂ nanoparticles on the interfacial behavior of surfactant solutions at air–water and n-heptane–water interfaces,' *Fluid Phase Equilibria*, 2014, **361**, pp. 289–295.
- Espinoza, D. A., Caldelas, F. M., Johnston, K. P., Bryant, S. L., Huh, C., *et al.*, 'Nanoparticle-stabilized supercritical co₂ foams for potential mobility control applications,' in 'SPE Improved Oil Recovery Symposium,' Society of Petroleum Engineers, 2010 .
- Fathi, S. J., Austad, T., and Strand, S., 'Water-based enhanced oil recovery (eor) by smart water: Optimal ionic composition for eor in carbonates,' *Energy & fuels*, 2011, **25**(11), pp. 5173–5179.
- Feng, Z. C., *Handbook of zinc oxide and related materials: volume two, devices and nano-engineering*, volume 2, CRC press, 2012.
- Fletcher, A., Davis, J., *et al.*, 'How eor can be transformed by nanotechnology,' in 'SPE Improved Oil Recovery Symposium,' Society of Petroleum Engineers, 2010 .
- Frampton, H., Morgan, J., Cheung, S., Munson, L., Chang, K., Williams, D., *et al.*, 'Development of a novel waterflood conformance control system,' in 'SPE/DOE Symposium on Improved Oil Recovery,' Society of Petroleum Engineers, 2004 .
- Friedheim, J. E., Young, S., De Stefano, G., Lee, J., Guo, Q., *et al.*, 'Nanotechnology for oilfield applications-hype or reality?' in 'SPE International Oilfield Nanotechnology Conference and Exhibition,' Society of Petroleum Engineers, 2012 .
- Gao, C., 'Factors affecting particle retention in porous media,' *Emirates Journal for Engineering Research*, 2007, **12**(3), pp. 1–7.

- Geng, J., Han, P., Bai, B., *et al.*, 'Experimental study on charged nanogels for interfacial tension reduction and emulsion stabilization at various salinities and oil types,' in 'SPE Asia Pacific Oil and Gas Conference and Exhibition,' Society of Petroleum Engineers, 2018a .
- Geng, J., Pu, J., Wang, L., and Bai, B., 'Surface charge effect of nanogel on emulsification of oil in water for fossil energy recovery,' *Fuel*, 2018b, **223**, pp. 140–148.
- Giraldo, J., Benjumea, P., Lopera, S., Cortes, F. B., and Ruiz, M. A., 'Wettability alteration of sandstone cores by alumina-based nanofluids,' *Energy & Fuels*, 2013, **27**(7), pp. 3659–3665.
- Goddard, E. D. and Vincent, B., *Polymer adsorption and dispersion stability*, ACS Publications, 1984.
- Gonzenbach, U. T., Studart, A. R., Tervoort, E., and Gauckler, L. J., 'Stabilization of foams with inorganic colloidal particles,' *Langmuir*, 2006, **22**(26), pp. 10983–10988.
- Green, D. W., Willhite, G. P., *et al.*, *Enhanced oil recovery*, volume 6, Henry L. Doherty Memorial Fund of AIME, Society of Petroleum Engineers Richardson, TX, 1998.
- Griffith, N., Ahmad, Y., Daigle, H., Huh, C., *et al.*, 'Nanoparticle-stabilized natural gas liquid-in-water emulsions for residual oil recovery,' in 'SPE improved oil recovery conference,' Society of Petroleum Engineers, 2016 .
- Gupta, P., Elkins, C., Long, T. E., and Wilkes, G. L., 'Electrospinning of linear homopolymers of poly (methyl methacrylate): exploring relationships between fiber formation, viscosity, molecular weight and concentration in a good solvent,' *Polymer*, 2005, **46**(13), pp. 4799–4810.
- Gupta, R., Smith, G. G., Hu, L., Willingham, T., Lo Cascio, M., Shyeh, J. J., Harris, C. R., *et al.*, 'Enhanced waterflood for carbonate reservoirs-impact of injection water composition,' in 'SPE Middle East oil and gas show and conference,' Society of Petroleum Engineers, 2011 .
- Guzman, E., Orsi, D., Cristofolini, L., Liggieri, L., and Ravera, F., 'Two-dimensional dppc based emulsion-like structures stabilized by silica nanoparticles,' *Langmuir*, 2014, **30**(39), pp. 11504–11512.
- Haroun, M. R., Alhassan, S., Ansari, A. A., Al Kindy, N. A. M., Abou Sayed, N., Kareem, A., Ali, B., Sarma, H. K., *et al.*, 'Smart nano-eor process for abu Dhabi carbonate reservoirs,' in 'Abu Dhabi International Petroleum Conference and Exhibition,' Society of Petroleum Engineers, 2012 .
- Hashemi, R., Nassar, N. N., and Almao, P. P., 'Nanoparticle technology for heavy oil in-situ upgrading and recovery enhancement: Opportunities and challenges,' *Applied Energy*, 2014, **133**, pp. 374–387.

- He, Y., Wu, F., Sun, X., Li, R., Guo, Y., Li, C., Zhang, L., Xing, F., Wang, W., and Gao, J., 'Factors that affect pickering emulsions stabilized by graphene oxide,' *ACS applied materials & interfaces*, 2013, **5**(11), pp. 4843–4855.
- Hendraningrat, L., Li, S., Torsaeter, O., *et al.*, 'Enhancing oil recovery of low-permeability berea sandstone through optimised nanofluids concentration,' in 'SPE Enhanced Oil Recovery Conference,' Society of Petroleum Engineers, 2013a .
- Hendraningrat, L., Li, S., Torsater, O., *et al.*, 'Effect of some parameters influencing enhanced oil recovery process using silica nanoparticles: An experimental investigation,' in 'SPE Reservoir Characterization and Simulation Conference and Exhibition,' Society of Petroleum Engineers, 2013b .
- Hendraningrat, L. and Torsæter, O., 'Metal oxide-based nanoparticles: revealing their potential to enhance oil recovery in different wettability systems,' *Applied Nanoscience*, 2015, **5**(2), pp. 181–199.
- Hendraningrat, L., Torsaeter, O., *et al.*, 'Unlocking the potential of metal oxides nanoparticles to enhance the oil recovery,' in 'Offshore Technology Conference-Asia,' Offshore Technology Conference, 2014 .
- Hornyak, G. L., Tibbals, H. F., Dutta, J., and Moore, J. J., *Introduction to Nanoscience and Nanotechnology*, CRC Press, Baton Rouge, 1 edition, 2009, ISBN 1420047795;9781420047790.
- Huang, T., Evans, B. A., Crews, J. B., Belcher, C. K., *et al.*, 'Field case study on formation fines control with nanoparticles in offshore applications,' in 'SPE Annual Technical Conference and Exhibition,' Society of Petroleum Engineers, 2010 .
- Huh, C., Nizamidin, N., Pope, G. A., Milner, T. E., and Bingqing, W., 'Hydrophobic paramagnetic nanoparticles as intelligent crude oil tracers,' 2014, uS Patent App. 14/765,426.
- Hunter, T. N., Wanless, E. J., Jameson, G. J., and Pugh, R. J., 'Non-ionic surfactant interactions with hydrophobic nanoparticles: Impact on foam stability,' *Colloids and Surfaces A: Physicochemical and Engineering Aspects*, 2009, **347**(1), pp. 81–89.
- Jadhunandan, P. and Morrow, N., 'Spontaneous imbibition of water by crude oil/brine/rock systems,' *In Situ*;(United States), 1991, **15**(4).
- Jadhunandan, P., Morrow, N. R., *et al.*, 'Effect of wettability on waterflood recovery for crude-oil/brine/rock systems,' *SPE reservoir engineering*, 1995, **10**(01), pp. 40–46.
- Jiang, L., Li, S., Yu, W., Wang, J., Sun, Q., and Li, Z., 'Interfacial study on the interaction between hydrophobic nanoparticles and ionic surfactants,' *Colloids and Surfaces A: Physicochemical and Engineering Aspects*, 2016, **488**, pp. 20–27.

- Jiang, L., Sun, G., Zhou, Z., Sun, S., Wang, Q., Yan, S., Li, H., Tian, J., Guo, J., Zhou, B., *et al.*, 'Size-controllable synthesis of monodispersed SnO_2 nanoparticles and application in electrocatalysts,' *The Journal of Physical Chemistry B*, 2005, **109**(18), pp. 8774–8778.
- Johannessen, A. M. and Spildo, K., 'Enhanced oil recovery (eor) by combining surfactant with low salinity injection,' *Energy & Fuels*, 2013, **27**(10), pp. 5738–5749.
- Johansson, D., Bergenståhl, B., and Lundgren, E., 'Wetting of fat crystals by triglyceride oil and water. 1. the effect of additives,' *Journal of the American Oil Chemists' Society*, 1995, **72**(8), pp. 921–931.
- Johnson, C. A. and Lenhoff, A. M., 'Adsorption of charged latex particles on mica studied by atomic force microscopy,' *Journal of colloid and interface science*, 1996, **179**(2), pp. 587–599.
- Ju, B., Dai, S., Luan, Z., Zhu, T., Su, X., Qiu, X., *et al.*, 'A study of wettability and permeability change caused by adsorption of nanometer structured polysilicon on the surface of porous media,' in 'SPE Asia Pacific Oil and Gas Conference and Exhibition,' Society of Petroleum Engineers, 2002 .
- Kabanov, A. V. and Vinogradov, S. V., 'Nanogels as pharmaceutical carriers: finite networks of infinite capabilities,' *Angewandte Chemie International Edition*, 2009, **48**(30), pp. 5418–5429.
- Kanj, M. Y., Rashid, M., Giannelis, E., *et al.*, 'Industry first field trial of reservoir nanoagents,' in 'SPE Middle East Oil and Gas Show and Conference,' Society of Petroleum Engineers, 2011 .
- Karimi, A., Fakhroueian, Z., Bahramian, A., Pour Khiabani, N., Darabad, J. B., Azin, R., and Arya, S., 'Wettability alteration in carbonates using zirconium oxide nanofluids: Eor implications,' *Energy & Fuels*, 2012, **26**(2), pp. 1028–1036.
- Kazemzadeh, Y., Eshraghi, S. E., Kazemi, K., Sourani, S., Mehrabi, M., and Ahmadi, Y., 'Behavior of asphaltene adsorption onto the metal oxide nanoparticle surface and its effect on heavy oil recovery,' *Industrial & Engineering Chemistry Research*, 2015, **54**(1), pp. 233–239.
- Kokal, S. and Al-Kaabi, A., 'Enhanced oil recovery: challenges & opportunities,' *World Petroleum Council: Official Publication*, 2010, **64**.
- Kothari, N., Raina, B., Chandak, K. B., Iyer, V., Mahajan, H. P., *et al.*, 'Application of ferrofluids for enhanced surfactant flooding in ior,' in 'SPE EUROPEC/EAGE Annual Conference and Exhibition,' Society of Petroleum Engineers, 2010 .
- Lake, L. W., 'Enhanced oil recovery,' 1989.

- Lan, Q., Yang, F., Zhang, S., Liu, S., Xu, J., and Sun, D., 'Synergistic effect of silica nanoparticle and cetyltrimethyl ammonium bromide on the stabilization of o/w emulsions,' *Colloids and Surfaces A: Physicochemical and Engineering Aspects*, 2007, **302**(1), pp. 126–135.
- Lau, H. C., Yu, M., and Nguyen, Q. P., 'Nanotechnology for oilfield applications: Challenges and impact,' *Journal of Petroleum Science and Engineering*, 2017, **157**, pp. 1160–1169.
- Le, N. Y. T., Pham, D. K., Le, K. H., and Nguyen, P. T., 'Design and screening of synergistic blends of SiO_2 nanoparticles and surfactants for enhanced oil recovery in high-temperature reservoirs,' *Advances in Natural Sciences: Nanoscience and Nanotechnology*, 2011, **2**(3), p. 035013.
- Legrand, J., Chamerois, M., Placin, F., Poirier, J., Bibette, J., and Leal-Calderon, F., 'Solid colloidal particles inducing coalescence in bitumen-in-water emulsions,' *Langmuir*, 2005, **21**(1), pp. 64–70.
- Lenchenkov, N. S., Slob, M., van Dalen, E., Glasbergen, G., van Kruijsdijk, C., *et al.*, 'Oil recovery from outcrop cores with polymeric nano-spheres,' in 'SPE Improved Oil Recovery Conference,' Society of Petroleum Engineers, 2016 .
- Li, R., Jiang, P., Gao, C., Huang, F., Xu, R., and Chen, X., 'Experimental investigation of silica-based nanofluid enhanced oil recovery: the effect of wettability alteration,' *Energy & Fuels*, 2016, **31**(1), pp. 188–197.
- Li, S., Genys, M., Wang, K., Torsæter, O., *et al.*, 'Experimental study of wettability alteration during nanofluid enhanced oil recovery process and its effect on oil recovery,' in 'SPE Reservoir Characterisation and Simulation Conference and Exhibition,' Society of Petroleum Engineers, 2015 .
- Li, S., Hendraningrat, L., , and Torsæter, O., 'A coreflood investigation of nanofluid enhanced oil recovery,' *Journal of Petroleum Science and Engineering*, 2013a, **111**, pp. 128–138.
- Li, S., Hendraningrat, L., and Torsaeter, O., 'Improved oil recovery by hydrophilic silica nanoparticles suspension: 2 phase flow experimental studies,' in 'IPTC 2013: International Petroleum Technology Conference,' 2013b .
- Ligthelm, D. J., Gronsveld, J., Hofman, J., Brussee, N., Marcelis, F., van der Linde, H., *et al.*, 'Novel waterflooding strategy by manipulation of injection brine composition.' in 'EUROPEC/EAGE conference and exhibition,' Society of Petroleum Engineers, 2009 .
- Limage, S., Kragel, J., Schmitt, M., Dominici, C., Miller, R., and Antoni, M., 'Rheology and structure formation in diluted mixed particle- surfactant systems,' *Langmuir*, 2010, **26**(22), pp. 16754–16761.

- Lyons, W. C. and Plisga, G. J., *Standard handbook of petroleum and natural gas engineering*, Elsevier, 2011.
- Ma, H., Luo, M., and Dai, L. L., 'Influences of surfactant and nanoparticle assembly on effective interfacial tensions,' *Physical Chemistry Chemical Physics*, 2008, **10**(16), pp. 2207–2213.
- Mahani, H., Sorop, T., Ligthelm, D. J., Brooks, D., Vledder, P., Mozahem, F., Ali, Y., *et al.*, 'Analysis of field responses to low-salinity waterflooding in secondary and tertiary mode in syria,' in 'SPE Europec/EAGE Annual Conference and Exhibition,' Society of Petroleum Engineers, 2011 .
- Mandal, A., Bera, A., Ojha, K., Kumar, T., *et al.*, 'Characterization of surfactant stabilized nanoemulsion and its use in enhanced oil recovery,' in 'SPE International Oilfield Nanotechnology Conference and Exhibition,' Society of Petroleum Engineers, 2012 .
- Martin, J. C. *et al.*, 'The effects of clay on the displacement of heavy oil by water,' in 'Venezuelan annual meeting,' Society of Petroleum Engineers, 1959 .
- Mcelfresh, P. M., Holcomb, D. L., Ector, D., *et al.*, 'Application of nanofluid technology to improve recovery in oil and gas wells,' in 'SPE International Oilfield Nanotechnology Conference and Exhibition,' Society of Petroleum Engineers, 2012a .
- Mcelfresh, P. M., Olguin, C., Ector, D., *et al.*, 'The application of nanoparticle dispersions to remove paraffin and polymer filter cake damage,' in 'SPE International Symposium and Exhibition on Formation Damage Control,' Society of Petroleum Engineers, 2012b .
- Metin, C., Bonnacaze, R., Nguyen, Q., *et al.*, 'The viscosity of silica nanoparticle dispersions in permeable media,' *SPE Reservoir Evaluation & Engineering*, 2013, **16**(03), pp. 327–332.
- Metin, C. O., Baran, J. R., and Nguyen, Q. P., 'Adsorption of surface functionalized silica nanoparticles onto mineral surfaces and decane/water interface,' *Journal of Nanoparticle Research*, 2012, **14**(11), p. 1246.
- Metin, C. O., Bonnacaze, R. T., and Nguyen, Q. P., 'Shear rheology of silica nanoparticle dispersions,' *Applied Rheology*, 2011a, **21**(1), p. 13146.
- Metin, C. O., Lake, L. W., Miranda, C. R., and Nguyen, Q. P., 'Stability of aqueous silica nanoparticle dispersions,' *Journal of Nanoparticle Research*, 2011b, **13**(2), pp. 839–850.
- Midmore, B., 'Preparation of a novel silica-stabilized oil/water emulsion,' *Colloids and Surfaces A: Physicochemical and Engineering Aspects*, 1998, **132**(2-3), pp. 257–265.

- Mohajeri, M., Hemmati, M., and Shekarabi, A. S., 'An experimental study on using a nanosurfactant in an eor process of heavy oil in a fractured micromodel,' *Journal of petroleum Science and engineering*, 2015, **126**, pp. 162–173.
- Mohebbifar, M., Ghazanfari, M. H., and Vossoughi, M., 'Experimental investigation of nano-biomaterial applications for heavy oil recovery in shaly porous models: A pore-level study,' *Journal of Energy Resources Technology*, 2015, **137**(1), p. 014501.
- Moraes, R. R., Garcia, J. W., Barros, M. D., Lewis, S. H., Pfeifer, C. S., Liu, J., and Stansbury, J. W., 'Control of polymerization shrinkage and stress in nanogel-modified monomer and composite materials,' *Dental Materials*, 2011, **27**(6), pp. 509–519.
- Muller, P., Sudre, G., and Theodoly, O., 'Wetting transition on hydrophobic surfaces covered by polyelectrolyte brushes,' *Langmuir*, 2008, **24**(17), pp. 9541–9550.
- Murray, B. S. and Ettelaie, R., 'Foam stability: proteins and nanoparticles,' *Current opinion in colloid & interface science*, 2004, **9**(5), pp. 314–320.
- Myint, P. C. and Firoozabadi, A., 'Thin liquid films in improved oil recovery from low-salinity brine,' *Current Opinion in Colloid & Interface Science*, 2015, **20**(2), pp. 105–114.
- Naje, A. N., Norry, A. S., and Suhail, A. M., 'Preparation and characterization of sno2 nanoparticles,' *International Journal of Innovative Research in Science, Engineering and Technology*, 2013, **2**(12).
- Nasralla, R. A., Bataweel, M. A., Nasr-El-Din, H. A., *et al.*, 'Investigation of wettability alteration and oil-recovery improvement by low-salinity water in sandstone rock,' *Journal of Canadian Petroleum Technology*, 2013, **52**(02), pp. 144–154.
- Nasralla, R. A., Sergienko, E., Masalmeh, S. K., van der Linde, H. A., Brussee, N. J., Mahani, H., Suijkerbuijk, B. M., Al-Qarshubi, I. S., *et al.*, 'Potential of low-salinity waterflood to improve oil recovery in carbonates: Demonstrating the effect by qualitative coreflood,' *SPE Journal*, 2016, **21**(05), pp. 1–643.
- Negin, C., Ali, S., and Xie, Q., 'Application of nanotechnology for enhancing oil recovery—a review,' *Petroleum*, 2016, **2**(4), pp. 324–333.
- Ng, W., Rana, D., Neale, G., and Hornof, V., 'Physicochemical behavior of mixed surfactant systems: petroleum sulfonate and lignosulfonate,' *Journal of applied polymer science*, 2003, **88**(4), pp. 860–865.
- Ngai, T., Auweter, H., and Behrens, S. H., 'Environmental responsiveness of microgel particles and particle-stabilized emulsions,' *Macromolecules*, 2006, **39**(23), pp. 8171–8177.

- Nguyen, P.-T., Do, B.-P. H., Pham, D.-K., Nguyen, Q.-T., Dao, D.-Q. P., Nguyen, H.-A., *et al.*, 'Evaluation on the eor potential capacity of the synthesized composite silica-core/polymer-shell nanoparticles blended with surfactant systems for the hpht offshore reservoir conditions,' in 'SPE International Oilfield Nanotechnology Conference and Exhibition,' Society of Petroleum Engineers, 2012 .
- Nwidee, L. N., Lebedev, M., Barifcani, A., Sarmadivaleh, M., and Iglauer, S., 'Wettability alteration of oil-wet limestone using surfactant-nanoparticle formulation,' *Journal of Colloid and Interface Science*, 2017.
- Ogolo, N., Olafuyi, O., Onyekonwu, M., *et al.*, 'Enhanced oil recovery using nanoparticles,' in 'SPE Saudi Arabia section technical symposium and exhibition,' Society of Petroleum Engineers, 2012 .
- Ogunberu, A. L. and Ayub, M., 'The role of wettability in petroleum recovery,' *Petroleum science and technology*, 2005, **23**(2), pp. 169–188.
- Parvazdavani, M., Masihi, M., and Ghazanfari, M. H., 'Monitoring the influence of dispersed nano-particles on oil–water relative permeability hysteresis,' *Journal of Petroleum Science and Engineering*, 2014, **124**, pp. 222–231.
- Pei, H., Zhang, G., Ge, J., Zhang, J., Zhang, Q., Fu, L., *et al.*, 'Investigation of nanoparticle and surfactant stabilized emulsion to enhance oil recovery in waterflooded heavy oil reservoirs,' in 'SPE Canada Heavy Oil Technical Conference,' Society of Petroleum Engineers, 2015 .
- Pichot, R., Spyropoulos, F., and Norton, I., 'O/w emulsions stabilised by both low molecular weight surfactants and colloidal particles: The effect of surfactant type and concentration,' *Journal of colloid and interface science*, 2010, **352**(1), pp. 128–135.
- Pourafshary, P., Azimpour, S., Motamedi, P., Samet, M., Taheri, S., Bargozin, H., Hendi, S., *et al.*, 'Priority assessment of investment in development of nanotechnology in upstream petroleum industry,' in 'SPE Saudi Arabia section technical symposium,' Society of Petroleum Engineers, 2009 .
- Purswani, P., Tawfik, M. S., and Karpyn, Z. T., 'Factors and mechanisms governing wettability alteration by chemically tuned waterflooding: A review,' *Energy & Fuels*, 2017, **31**(8), pp. 7734–7745.
- Pyun, J., Jia, S., Kowalewski, T., Patterson, G. D., and Matyjaszewski, K., 'Synthesis and characterization of organic/inorganic hybrid nanoparticles: kinetics of surface-initiated atom transfer radical polymerization and morphology of hybrid nanoparticle ultrathin films,' *Macromolecules*, 2003, **36**(14), pp. 5094–5104.
- Qiu, F., Mamora, D. D., *et al.*, 'Experimental study of solvent-based emulsion injection to enhance heavy oil recovery in alaska north slope area,' in 'Canadian Unconventional Resources and International Petroleum Conference,' Society of Petroleum Engineers, 2010a .

- Qiu, F. *et al.*, 'The potential applications in heavy oil eor with the nanoparticle and surfactant stabilized solvent-based emulsion,' in 'Canadian unconventional resources and international petroleum conference,' Society of Petroleum Engineers, 2010b .
- Ragab, A. M. S., Hannora, A. E., *et al.*, 'An experimental investigation of silica nano particles for enhanced oil recovery applications,' in 'SPE North Africa Technical Conference and Exhibition,' Society of Petroleum Engineers, 2015 .
- Rana, D., Neale, G., and Hornof, V., 'Surface tension of mixed surfactant systems: ligno-sulfonate and sodium dodecyl sulfate,' *Colloid and Polymer Science*, 2002, **280**(8), pp. 775–778.
- Rankin, K. and Nguyen, Q., 'Conformance control through in-situ gelation of silica nanoparticles,' in 'Nanotech Conference & Expo,' 2014 pp. 15–18.
- Ravera, F., Ferrari, M., Liggieri, L., Loglio, G., Santini, E., and Zanobini, A., 'Liquid–liquid interfacial properties of mixed nanoparticle–surfactant systems,' *Colloids and Surfaces A: Physicochemical and Engineering Aspects*, 2008, **323**(1), pp. 99–108.
- Reiter, P. K., *A water-sensitive sandstone flood using low salinity water*, Ph.D. thesis, University of Oklahoma, 1961.
- RezaeiDoust, A., Puntervold, T., Strand, S., and Austad, T., 'Smart water as wettability modifier in carbonate and sandstone: A discussion of similarities/differences in the chemical mechanisms,' *Energy & fuels*, 2009, **23**(9), pp. 4479–4485.
- Rousseau, D., Chauveteau, G., Renard, M., Tabary, R., Zaitoun, A., Mallo, P., Braun, O., Omari, A., *et al.*, 'Rheology and transport in porous media of new water shutoff/conformance control microgels,' in 'SPE international symposium on oilfield chemistry,' Society of Petroleum Engineers, 2005 .
- Roustaei, A. and Bagherzadeh, H., 'Experimental investigation of sio2 nanoparticles on enhanced oil recovery of carbonate reservoirs,' *Journal of Petroleum Exploration and Production Technology*, 2015, **5**(1), pp. 27–33.
- Roustaei, A., Moghadasi, J., Bagherzadeh, H., Shahrabadi, A., *et al.*, 'An experimental investigation of polysilicon nanoparticles' recovery efficiencies through changes in interfacial tension and wettability alteration,' in 'SPE International Oilfield Nanotechnology Conference and Exhibition,' Society of Petroleum Engineers, 2012 .
- Salem, A. M., Ragab, Hannora, A. E., *et al.*, 'A comparative investigation of nano particle effects for improved oil recovery–experimental work,' in 'SPE Kuwait Oil and Gas Show and Conference,' Society of Petroleum Engineers, 2015 .
- Salyer, I. O., 'Dry powder mixes comprising phase change materials,' 1993, uS Patent 5,211,949.

- Samanta, A., Ojha, K., Sarkar, A., and Mandal, A., 'Surfactant and surfactant-polymer flooding for enhanced oil recovery,' *Advances in Petroleum Exploration and Development*, 2011, **2**(1), pp. 13–18.
- Schmidt, G. and Malwitz, M. M., 'Properties of polymer–nanoparticle composites,' *Current opinion in colloid & interface science*, 2003, **8**(1), pp. 103–108.
- Shah, R. D. *et al.*, 'Application of nanoparticle saturated injectant gases for eor of heavy oils,' in 'SPE annual technical conference and exhibition,' Society of Petroleum Engineers, 2009 .
- Shahrabadi, A., Bagherzadeh, H., Roostaie, A., Golghanddashti, H., *et al.*, 'Experimental investigation of hlp nanofluid potential to enhance oil recovery: A mechanistic approach,' in 'SPE International Oilfield Nanotechnology Conference and Exhibition,' Society of Petroleum Engineers, 2012 .
- ShamsiJazeyi, H., Miller, C. A., Wong, M. S., Tour, J. M., and Verduzco, R., 'Polymer-coated nanoparticles for enhanced oil recovery,' *Journal of Applied Polymer Science*, 2014, **131**(15).
- Sharma, S. and Sarangdevot, K., 'Nanoemulsions for cosmetics,' *IJARPB*, 2012, **1**(3), pp. 408–415.
- Sharma, T., Iglauer, S., and Sangwai, J. S., 'Silica nanofluids in an oilfield polymer polyacrylamide: Interfacial properties, wettability alteration, and applications for chemical enhanced oil recovery,' *Industrial & Engineering Chemistry Research*, 2016, **55**(48), pp. 12387–12397.
- Sharma, T., Kumar, G. S., and Sangwai, J. S., 'Comparative effectiveness of production performance of pickering emulsion stabilized by nanoparticle–surfactant–polymer over surfactant–polymer (sp) flooding for enhanced oil recovery for brownfield reservoir,' *Journal of Petroleum Science and Engineering*, 2015, **129**, pp. 221–232.
- Sheng, J., *Enhanced oil recovery field case studies*, Gulf Professional Publishing, 2013.
- Shokrlu, Y. H., Babadagli, T., *et al.*, 'Transportation and interaction of nano and micro size metal particles injected to improve thermal recovery of heavy-oil,' in 'SPE Annual Technical Conference and Exhibition,' Society of Petroleum Engineers, 2011 .
- Singh, R., Mohanty, K. K., *et al.*, 'Foams stabilized by in-situ surface-activated nanoparticles in bulk and porous media,' *SPE Journal*, 2016, **21**(01), pp. 121–130.
- Skauge, T., Spildo, K., Skauge, A., *et al.*, 'Nano-sized particles for eor,' in 'SPE improved oil recovery symposium,' Society of Petroleum Engineers, 2010 .
- Song, E., Kim, D., Kim, B. J., and Lim, J., 'Surface modification of caco 3 nanoparticles by alkylbenzene sulfonic acid surfactant,' *Colloids and Surfaces A: Physicochemical and Engineering Aspects*, 2014, **461**, pp. 1–10.

- Soraya, B., Malick, C., Philippe, C., Bertin, H. J., Hamon, G., *et al.*, 'Oil recovery by low-salinity brine injection: laboratory results on outcrop and reservoir cores,' in 'SPE Annual Technical Conference and Exhibition,' Society of Petroleum Engineers, 2009 .
- Srinivasan, A., Shah, S. N., *et al.*, 'Surfactant-based fluids containing copper-oxide nanoparticles for heavy oil viscosity reduction,' in 'SPE Annual Technical Conference and Exhibition,' Society of Petroleum Engineers, 2014 .
- Standnes, D. C. and Austad, T., 'Wettability alteration in chalk: 1. preparation of core material and oil properties,' *Journal of Petroleum Science and Engineering*, 2000, **28**(3), pp. 111–121.
- Standnes, D. C. and Austad, T., 'Wettability alteration in carbonates: Interaction between cationic surfactant and carboxylates as a key factor in wettability alteration from oil-wet to water-wet conditions,' *Colloids and Surfaces A: Physicochemical and Engineering Aspects*, 2003, **216**(1-3), pp. 243–259.
- Suleimanov, B., Ismailov, F., and Veliyev, E., 'Nanofluid for enhanced oil recovery,' *Journal of Petroleum Science and Engineering*, 2011, **78**(2), pp. 431–437.
- Suleimanov, B. A. and Veliyev, E. F., 'Novel polymeric nanogel as diversion agent for enhanced oil recovery,' *Petroleum Science and Technology*, 2017, **35**(4), pp. 319–326.
- Sun, Q., Li, Z., Li, S., Jiang, L., Wang, J., and Wang, P., 'Utilization of surfactant-stabilized foam for enhanced oil recovery by adding nanoparticles,' *Energy & Fuels*, 2014, **28**(4), pp. 2384–2394.
- Sun, X., Zhang, Y., Chen, G., and Gai, Z., 'Application of nanoparticles in enhanced oil recovery: a critical review of recent progress,' *Energies*, 2017, **10**(3), p. 345.
- Tang, G., Morrow, N. R., *et al.*, 'Salinity, temperature, oil composition, and oil recovery by waterflooding,' *SPE Reservoir Engineering*, 1997, **12**(04), pp. 269–276.
- Tang, G.-Q. and Morrow, N. R., 'Influence of brine composition and fines migration on crude oil/brine/rock interactions and oil recovery,' *Journal of Petroleum Science and Engineering*, 1999, **24**(2-4), pp. 99–111.
- Tarek, M., El-Banbi, A. H., *et al.*, 'Comprehensive investigation of effects of nano-fluid mixtures to enhance oil recovery,' in 'SPE North Africa Technical Conference and Exhibition,' Society of Petroleum Engineers, 2015a .
- Tarek, M. *et al.*, 'Investigating nano-fluid mixture effects to enhance oil recovery,' in 'SPE Annual Technical Conference and Exhibition,' Society of Petroleum Engineers, 2015b .

- Tetteh, J. T., Rankey, E., Barati, R., *et al.*, 'Low salinity waterflooding effect: Crude oil/brine interactions as a recovery mechanism in carbonate rocks,' in 'OTC Brasil,' Offshore Technology Conference, 2017 .
- Thomas, S., 'Enhanced oil recovery-an overview,' Oil & Gas Science and Technology-Revue de l'IFP, 2008, **63**(1), pp. 9–19.
- Tian, H. and Wang, M., 'Electrokinetic mechanism of wettability alternation at oil-water-rock interface,' Surface Science Reports, 2017, **72**(6), pp. 369–391.
- Touhami, Y., Rana, D., Neale, G., and Hornof, V., 'Study of polymer-surfactant interactions via surface tension measurements,' Colloid and Polymer Science, 2001, **279**(3), pp. 297–300.
- Van Boekel, M. and Walstra, P., 'Stability of oil-in-water emulsions with crystals in the disperse phase,' Colloids and Surfaces, 1981, **3**(2), pp. 109–118.
- Vashisth, C., Whitby, C. P., Fornasiero, D., and Ralston, J., 'Interfacial displacement of nanoparticles by surfactant molecules in emulsions,' Journal of colloid and interface science, 2010, **349**(2), pp. 537–543.
- Vatanparast, H., Javadi, A., and Bahramian, A., 'Silica nanoparticles cationic surfactants interaction in water-oil system,' Colloids and Surfaces A: Physicochemical and Engineering Aspects, 2017, **521**, pp. 221–230.
- Vledder, P., Gonzalez, I. E., Carrera Fonseca, J. C., Wells, T., Ligthelm, D. J., *et al.*, 'Low salinity water flooding: proof of wettability alteration on a field wide scale,' in 'SPE Improved Oil Recovery Symposium,' Society of Petroleum Engineers, 2010 .
- Wagner, N. J. and Brady, J. F., 'Shear thickening in colloidal dispersions,' Physics Today, 2009, **62**(10), pp. 27–32.
- Wang, L., Zhang, G., Li, G., Zhang, J., Ding, B., *et al.*, 'Preparation of microgel nanospheres and their application in eor,' in 'International Oil and Gas Conference and Exhibition in China,' Society of Petroleum Engineers, 2010 .
- Wasan, D., Nikolov, A., and Kondiparty, K., 'The wetting and spreading of nanofluids on solids: Role of the structural disjoining pressure,' Current Opinion in Colloid & Interface Science, 2011, **16**(4), pp. 344–349.
- Wasan, D. T. and Nikolov, A. D., 'Spreading of nanofluids on solids,' Nature, 2003, **423**(6936), pp. 156–159.
- Worthen, A. J., Bryant, S. L., Huh, C., and Johnston, K. P., 'Carbon dioxide-in-water foams stabilized with nanoparticles and surfactant acting in synergy,' AIChE Journal, 2013, **59**(9), pp. 3490–3501.
- Wu, W., He, Q., and Jiang, C., 'Magnetic iron oxide nanoparticles: synthesis and surface functionalization strategies,' Nanoscale research letters, 2008a, **3**(11), p. 397.

- Wu, Y., Chen, W., Dai, C., Huang, Y., Li, H., Zhao, M., He, L., and Jiao, B., 'Reducing surfactant adsorption on rock by silica nanoparticles for enhanced oil recovery,' *Journal of Petroleum Science and Engineering*, 2017, **153**, pp. 283–287.
- Wu, Y., Shuler, P. J., Blanco, M., Tang, Y., Goddard, W. A., *et al.*, 'An experimental study of wetting behavior and surfactant eor in carbonates with model compounds,' *SPE Journal*, 2008b, **13**(01), pp. 26–34.
- XU, K., Zhu, P., Tatiana, C., Huh, C., Balhoff, M., *et al.*, 'A microfluidic investigation of the synergistic effect of nanoparticles and surfactants in macro-emulsion based eor,' in 'SPE Improved Oil Recovery Conference,' Society of Petroleum Engineers, 2016 .
- Yahya, N., Kashif, M., Nasir, N., Niaz Akhtar, M., and Yusof, N. M., 'Cobalt ferrite nanoparticles: an innovative approach for enhanced oil recovery application,' in 'Journal of Nano Research,' volume 17, Trans Tech Publ, 2012 pp. 115–126.
- Yi, Z., Sarma, H. K., *et al.*, 'Improving waterflood recovery efficiency in carbonate reservoirs through salinity variations and ionic exchanges: A promising low-cost" smart-waterflood" approach,' in 'Abu Dhabi International Petroleum Conference and Exhibition,' Society of Petroleum Engineers, 2012 .
- Yildiz, H. O. and Morrow, N. R., 'Effect of brine composition on recovery of moutray crude oil by waterflooding,' *Journal of Petroleum science and Engineering*, 1996, **14**(3-4), pp. 159–168.
- Yousef, A. A., Al-Saleh, S. H., Al-Kaabi, A., Al-Jawfi, M. S., *et al.*, 'Laboratory investigation of the impact of injection-water salinity and ionic content on oil recovery from carbonate reservoirs,' *SPE Reservoir Evaluation & Engineering*, 2011, **14**(05), pp. 578–593.
- Yu, H., Hermann, S., Schulz, S. E., Gessner, T., Dong, Z., and Li, W. J., 'Optimizing sonication parameters for dispersion of single-walled carbon nanotubes,' *Chemical Physics*, 2012, **408**, pp. 11–16.
- Yu, J., Berlin, J. M., Lu, W., Zhang, L., Kan, A. T., Zhang, P., Walsh, E. E., Work, S., Chen, W., Tour, J., *et al.*, 'Transport study of nanoparticles for oilfield application,' in 'SPE International Conference on Oilfield Scale,' Society of Petroleum Engineers, 2010 .
- Zargartalebi, M., Kharrat, R., and Barati, N., 'Enhancement of surfactant flooding performance by the use of silica nanoparticles,' *Fuel*, 2015, **143**, pp. 21–27.
- Zhang, P. and Austad, T., 'Wettability and oil recovery from carbonates: Effects of temperature and potential determining ions,' *Colloids and Surfaces A: Physicochemical and Engineering Aspects*, 2006, **279**(1-3), pp. 179–187.
- Zhang, P., Tweheyo, M. T., and Austad, T., 'Wettability alteration and improved oil recovery by spontaneous imbibition of seawater into chalk: Impact of the potential determining ions Ca^{2+} , Mg^{2+} , and SO_4^{2-} ,' *Colloids and Surfaces A: Physicochemical and Engineering Aspects*, 2007, **301**(1-3), pp. 199–208.

Zhang, T., Davidson, D., Bryant, S. L., Huh, C., *et al.*, 'Nanoparticle-stabilized emulsions for applications in enhanced oil recovery,' in 'SPE improved oil recovery symposium,' Society of Petroleum Engineers, 2010 .

VITA

Mustafa Almahfood received his Bachelor's degree from Missouri University of Science and Technology. Then, he joined Saudi Aramco as a reservoir engineer for two years. He received his Master's degree in Petroleum and Natural Gas Engineering from West Virginia University in 2016. He received his Ph.D. degree in Petroleum Engineering from Missouri University of Science and Technology in August 2020. Almahfood's research interest included conformance control gel treatments and nanogel evaluation.